

AD-A159 010

A DETERMINATION OF PARTICLE DENSITY DISTRIBUTIONS ABOVE
FLUIDIZED BEDS(U) MASSACHUSETTS INST OF TECH CAMBRIDGE
DEPT OF OCEAN ENGINEERING G A PIPER MAR 85

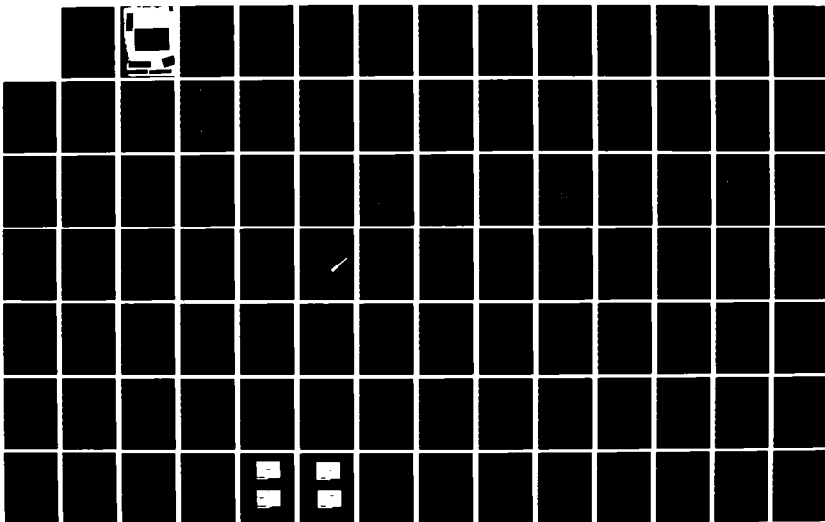
1/3

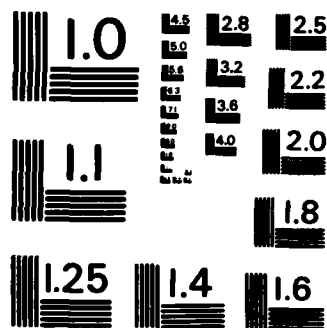
UNCLASSIFIED

N66314-70-A-0073

F/G 14/2

NL





MICROCOPY RESOLUTION TEST CHART
NATIONAL BUREAU OF STANDARDS-1963-A

DEPARTMENT OF OCEAN ENGINEERING

MASSACHUSETTS INSTITUTE OF TECHNOLOGY

CAMBRIDGE, MASSACHUSETTS 02139

*A DETERMINATION OF PARTICLE
DENSITY DISTRIBUTIONS ABOVE FLUIDIZED BEDS*

GLENN A. PIPER

XIII - A

N66314-70-A-0073 MAY 85.

A DETERMINATION OF PARTICLE DENSITY DISTRIBUTIONS

ABOVE FLUIDIZED BEDS

by

GLENN ALVAH PIPER III

B.S.M.E., University of Washington
(1980)

Submitted to the Department of Ocean Engineering in Partial
Fulfillment of the Requirements for the Degrees of

MASTER OF SCIENCE IN NAVAL ARCHITECTURE AND MARINE ENGINEERING

and

MASTER OF SCIENCE IN MECHANICAL ENGINEERING

at the

MASSACHUSETTS INSTITUTE OF TECHNOLOGY

MAY 1985

© Massachusetts Institute of Technology, 1985

Signature of Author: _____

Glenn A. Piper III

Department of Ocean Engineering
May 16, 1985

Certified by: _____

Leon R. Glicksman

Dr. Leon Glicksman, Thesis Supervisor
Senior Research Scientist, Department of Mechanical Engineering

Certified by: _____

A. Douglas Carmichael

A. Douglas Carmichael, Thesis Reader
Professor, Department of Ocean Engineering

Accepted by: _____

A. Douglas Carmichael

A. Douglas Carmichael
Chairman, Ocean Engineering Departmental Committee

Accepted by: _____

Ain A. Sonin

Ain A. Sonin
Chairman, Mechanical Engineering Departmental Committee

SEP 10 1985

A DETERMINATION OF PARTICLE DENSITY DISTRIBUTIONS
ABOVE FLUIDIZED BEDS

by

Glenn Alvah Piper III

Submitted to the Department of Ocean Engineering on May 16, 1985 in partial fulfillment of the requirements for the Degrees of Master of Science in Mechanical Engineering and Master of Science in Naval Architecture and Marine Engineering. The author hereby grants to the U.S. Government permission to reproduce and to distribute copies of this thesis document in whole or in part.

ABSTRACT

→ An experimental apparatus to measure the particle density distribution in the freeboard of an atmospheric fluidized bed was designed and constructed. The density versus height measured by the sampling apparatus gives a similar exponential decrease as previous investigations have found.

A particle trajectory model is developed which calculates the height and particle density distributions above the bed surface of an atmospheric fluidized bed. The parameters input to the model are the superficial velocity, initial particle velocity, gas jet velocity and duration, and the particle size distribution of the bed mass. The model was evaluated using the experimental data for jet velocity, duration, and particle size. The predicted slope of the particle density versus height in the freeboard agrees with the experimentally measured slope within 20%.

A sensitivity analysis, using the trajectory model, resulted in a determination of the particle distributions in the freeboard of a fluidized bed as affected by varying the input parameters to the trajectory model. The most significant effects were achieved when the jet velocity or duration was altered. (Thesis)

Thesis Supervisor: Dr. Leon Glicksman
Title: Senior Research Scientist

The authors hereby grants to M.I.T. and to the U.S. Government permission to reproduce and to distribute copies of this thesis document in whole or in part.

ACKNOWLEDGEMENTS

This thesis was prepared under the guidance and supervision of Dr. Leon Glicksman. His encouragement, patience, advice and understanding were all greatly appreciated, for without them, this work would not have been possible.

The help and support of Tom Yule, who freely gave his time, expert advice and assistance, is most strongly appreciated. I sincerely thank him for his efforts.

A special word of appreciation is given to the Tennessee Valley Authority for funding this research and making it all possible.

Most of all, I would like to thank my fiancée Heide, for her support, understanding, assistance and love during the entire project. She was always there when I needed her, even when her own work was laborsome.



| | |
|----------------------|---|
| Accession For | |
| THIS COPY | X |
| FILED | |
| Unrecorded | |
| For | |
| for Form 50 on file. | |
| A-1 | |

A DETERMINATION OF PARTICLE DENSITY DISTRIBUTIONS ABOVE FLUIDIZED BEDS

TABLE OF CONTENTS

| | |
|--|-----|
| ABSTRACT | 2 |
| ACKNOWLEDGEMENTS | 3 |
| TABLE OF CONTENTS | 4 |
| LIST OF FIGURES | 6 |
| LIST OF TABLES | 12 |
| CHAPTER I - INTRODUCTION | 14 |
| CHAPTER II - PARTICLE SAMPLING APPARATUS | 22 |
| Design Alternatives | 22 |
| Apparatus Requirements | 24 |
| Apparatus Design | 26 |
| Apparatus Testing | 37 |
| CHAPTER III - EXPERIMENTAL PROCEDURE | 40 |
| Fluidized Bed Configuration | 40 |
| Equipment Set-up | 43 |
| Sampling Procedure | 49 |
| Sample Analysis | 53 |
| CHAPTER IV - COMPUTER MODEL | 56 |
| Introduction | 56 |
| Model Theory | 56 |
| Testing of Program | 59 |
| CHAPTER V - EXPERIMENTAL RESULTS AND CONCLUSIONS | 68 |
| Minimum Fluidization Velocity | 68 |
| Entrainment Analysis | 68 |
| Particle Size Distribution | 80 |
| Oscilloscope Trace Analysis | 85 |
| Sample Weight vs Bed Activity Correlation | 89* |

| | |
|--|-----|
| CHAPTER VI - TRAJECTORY MODEL RESULTS AND DISCUSSION | 96 |
| Selection of Baseline Parameters | 96 |
| Typical Output Using Baseline Parameters | 99 |
| Model Sensitivity Analysis | 106 |
| variation of superficial velocity U_0 | 108 |
| variation of initial particle velocity U_{p0} | 115 |
| variation of jet velocity U_j | 121 |
| variation of jet duration t_j | 128 |
| variation of particle distribution in bed mass | 134 |
| Comparison of Model with Experimental Results | 140 |
| CHAPTER VII - CONCLUSIONS AND RECOMMENDATIONS | 145 |
| Conclusions | 145 |
| Recommendations | 146 |
| REFERENCES | 148 |
| APPENDIX A - MOMENT OF INERTIA CALCULATIONS FOR PADDLES | 150 |
| APPENDIX B - ERROR DETERMINATION OF VACUUM COLLECTION SYSTEM | 156 |
| APPENDIX C - SAMPLE TRAP CLOSURE TIME TEST | 158 |
| APPENDIX D - SOLENOID TORQUE AND DYNAMIC ANALYSIS | 162 |
| APPENDIX E - PARTICLE SIZE DISTRIBUTION ANALYSIS | 169 |
| APPENDIX F - MEAN BED FLOW VELOCITY DETERMINATION | 171 |
| APPENDIX G - COMPUTER PROGRAM FOR MEAN BED FLOW VELOCITY CALCULATION | 175 |
| APPENDIX H - PARTS LIST FOR APPARATUS | 178 |
| APPENDIX I - LISTING OF ALL SAMPLE DATA OBTAINED | 182 |
| APPENDIX J - IMAGE ANALYZER OUTPUT | 202 |
| APPENDIX K - OSCILLOSCOPE TRACES | 218 |
| APPENDIX L - COMPUTER PROGRAM FOR TRAJECTORY MODEL | 235 |
| APPENDIX M - ANEMOMETER CALIBRATION | 248 |

LIST OF FIGURES

| Figure | | Page |
|--------|---|------|
| 1 | Model of a fluidized bed. Particle Entrainment decreases exponentially with increasing freeboard height. | 15 |
| 2 | Side and top views of sampling apparatus. | 28 |
| 3 | Perspective view of sampling apparatus. | 29 |
| 4 | Top and side view of sample trap. | 31 |
| 5 | Design of closure paddles. | 32 |
| 6 | Torque output curve for rotary solenoid. | 34 |
| 7 | Schematic of solenoid power supply. | 35 |
| 8 | Schematic diagram for vacuum system. | 38 |
| 9 | Heat exchanger tube design showing the four (4) rows of 22 tubes. | 41 |
| 10 | Heat exchanger tube design. | 42 |
| 11 | Position of sample trap, bubble probe, and anemometer probe above heat exchanger tubes. | 44 |
| 12 | Position of bubble and Anemometer probe with respect to the sample trap and distributor. | 45 |
| 13 | Block diagram of the equipment used during the sampling operations. | 47 |
| 14 | Typical oscilloscope trace obtained during sampling operation. | 52 |
| 15 | Maximum particle height vs particle diameter obtained during increment sensitivity analysis. | 65 |
| 16 | Particle size distribution of bed mass used in increment sensitivity analysis. | 65 |
| 17 | Plots of relative particle density vs freeboard height showing the effect of varying the diameter interval and height interval. | 66 |

| | | |
|----|--|-----|
| 18 | Plot of pressure drop across bed vs U_o . The estimate of U_{mf} from this plot is 15.2 cm/s (0.5 ft/s). | 69 |
| 19 | Plot of particle density vs freeboard height as a function of U_o/U_{mf} . The data was obtained using the particle sampler. | 73 |
| 20 | Plot of P_o vs $(U_o/U_{mf} - 1)$ showing strong dependence of P_o on U_o . | 76 |
| 21 | Plot of $1/a$ vs U_o showing linear dependence of $1/a$ on U_o . | 79 |
| 22 | Particle size vs mass distribution and particle number of bed material from experimental data. | 81 |
| 23 | Analysis of variation of particle size vs freeboard height. | 84 |
| 24 | Oscilloscope trace of bubble probe, anemometer probe, and solenoid activation at low U_o . | 86 |
| 25 | Oscilloscope trace of bubble probe, anemometer probe, and solenoid activation at low U_o . | 86 |
| 26 | Oscilloscope trace of bubble probe, anemometer probe, and solenoid activation at higher U_o . | 87 |
| 27 | Oscilloscope trace of bubble probe, anemometer probe, and solenoid activation at higher U_o . | 87 |
| 28 | Typical oscilloscope trace during sampling procedure showing time before actuation. | 93 |
| 29 | Relative particle number distributions of bed material by sieve and image analyzer analysis. | 100 |
| 30 | Maximum particle height vs particle diameter for baseline conditions. | 100 |
| 31 | Relative particle number vs particle diameter for baseline conditions. Freeboard height of 4 cm. | 102 |
| 32 | Relative particle number vs particle diameter for baseline conditions. Freeboard height of 8 cm. | 102 |
| 33 | Relative particle number vs particle diameter for baseline conditions. Freeboard height of 12 cm. | 103 |

| | | |
|----|---|-----|
| 34 | Relative particle number vs particle diameter for baseline conditions. Freeboard height of 18 cm. | 103 |
| 35 | Relative particle number vs particle diameter for baseline conditions. Freeboard height of 22 cm. | 104 |
| 36 | Relative particle number vs particle diameter for baseline conditions. Freeboard height of 31 cm. | 104 |
| 37 | Particle density/unit volume vs freeboard height for baseline conditions. | 105 |
| 38 | ln particle density/unit volume vs freeboard height for baseline conditions. | 105 |
| 39 | Maximum particle height vs particle diameter as a function of U_0 . | 109 |
| 40 | Relative particle number vs particle diameter as a function of U_0 . Freeboard height of 4 cm. | 109 |
| 41 | Relative particle number vs particle diameter as a function of U_0 . Freeboard height of 8 cm. | 110 |
| 42 | Relative particle number vs particle diameter as a function of U_0 . Freeboard height of 12 cm. | 110 |
| 43 | Relative particle number vs particle diameter as a function of U_0 . Freeboard height of 18 cm. | 111 |
| 44 | Relative particle number vs particle diameter as a function of U_0 . Freeboard height of 22 cm. | 111 |
| 45 | Relative particle number vs particle diameter as a function of U_0 . Freeboard height of 31 cm. | 112 |
| 46 | Particle density/unit volume vs freeboard height as a function of U_0 . | 114 |
| 47 | ln Particle density/unit volume vs freeboard height as a function of U_0 . | 114 |
| 48 | Maximum particle height vs particle diameter as a function of U_0 . | 115 |
| 49 | Relative particle number vs particle diameter as a function of U_0 . Freeboard height of 4 cm. | 117 |
| 50 | Relative particle number vs particle diameter as a function of U_0 . Freeboard height of 8 cm. | 117 |

- 51 Relative particle number vs particle diameter as a 118
function of U_{po} . Freeboard height of 12 cm.
- 52 Relative particle number vs particle diameter as a 118
function of U_{po} . Freeboard height of 18 cm.
- 53 Relative particle number vs particle diameter as a 119
function of U_{po} . Freeboard height of 22 cm.
- 54 Relative particle number vs particle diameter as a 119
function of U_{po} . Freeboard height of 31 cm.
- 55 Particle density/unit volume vs freeboard height 120
as a function of U_{po} .
- 56 In particle density/unit volume vs freeboard 120
height as a function of U_{po} .
- 57 Maximum particle height vs particle diameter as a 122
function of U_j .
- 58 Relative particle number vs particle diameter as a 124
function of U_j . Freeboard height of 4 cm.
- 59 Relative particle number vs particle diameter as a 124
function of U_j . Freeboard height of 8 cm.
- 60 Relative particle number vs particle diameter as a 125
function of U_j . Freeboard height of 12 cm.
- 61 Relative particle number vs particle diameter as a 125
function of U_j . Freeboard height of 18 cm.
- 62 Relative particle number vs particle diameter as a 126
function of U_j . Freeboard height of 22 cm.
- 63 Relative particle number vs particle diameter as a 126
function of U_j . Freeboard height of 31 cm.
- 64 Particle density/unit volume vs freeboard height 127
as a function of U_j .
- 65 In Particle density/unit volume vs freeboard 127
height as a function of U_j .
- 66 Maximum particle height vs particle diameter as a 129
function of t_j .

- 67 Relative particle number vs particle diameter as a 130
function of t_j . Freeboard height of 4 cm.
- 68 Relative particle number vs particle diameter as a 130
function of t_j . Freeboard height of 8 cm.
- 69 Relative particle number vs particle diameter as a 131
function of t_j . Freeboard height of 12 cm.
- 70 Relative particle number vs particle diameter as a 131
function of t_j . Freeboard height of 18 cm.
- 71 Relative particle number vs particle diameter as a 132
function of t_j . Freeboard height of 22 cm.
- 72 Relative particle number vs particle diameter as a 132
function of t_j . Freeboard height of 31 cm.
- 73 Particle density/unit volume vs freeboard height 133
as a function of t_j .
- 74 ln Particle density/unit volume vs freeboard 133
height as a function of t_j .
- 75 Relative particle number vs particle diameter for 135
bed mass material.
- 76 Relative particle number vs particle diameter as a 136
function of bed mass. Freeboard height of 4 cm.
- 77 Relative particle number vs particle diameter as a 136
function of bed mass. Freeboard height of 8 cm.
- 78 Relative particle number vs particle diameter as a 137
function of bed mass. Freeboard height of 12 cm.
- 79 Relative particle number vs particle diameter as a 137
function of bed mass. Freeboard height of 18 cm.
- 80 Relative particle number vs particle diameter as a 138
function of bed mass. Freeboard height of 22 cm.
- 81 Relative particle number vs particle diameter as a 138
function of bed mass. Freeboard height of 31 cm.
- 82 Particle density/unit volume vs freeboard height 139
as a function of bed mass. The ln plot is also
shown as Fig. 82 b.

| | | |
|-----|--|-----|
| 83 | Particle density/unit volume vs freeboard height for baseline parameters. | 141 |
| 84 | ln Particle density/unit volume vs freeboard height for baseline parameters. | 141 |
| 85 | Comparison of slopes for the particle density distributions above the bed as derived from experimental data and computer model output. | 143 |
| A-1 | Constuction of paddles with aluminum interface cylinder shown. | 152 |
| A-2 | Diagram for moment of inertia calculation used for cylinder about Z axis. | 154 |
| A-3 | Diagram for moment of inertia calculation used for rectangular prisim about X axis. | 154 |
| C-1 | Diagram of closure time determination set up. | 159 |
| C-2 | Oscilloscope trace of paddle eclipsing electric eye. | 161 |
| D-1 | Torque output of rotary solenoid showing triangle approximation and spring constant determination. | 165 |
| M-1 | Calibration of anemometer probe. Oscilloscope voltage vs air velocity. | 249 |

LIST OF TABLES

| Table | | Page |
|-------|---|------|
| 1 | List of equipment used during particle sampling operations. | 48 |
| 2 | List of parameters used to check computer calculations against closed form solution. | 62 |
| 3 | Listing of input and resulting maximum particle heights with time to maximum height. These values were used during the increment sensitivity tests. | 64 |
| 4 | List of experimental data showing sample averages, standard deviations, heights, and velocity conditions measured. Density values are calculated by dividing the average sample weight by the sample trap volume. | 71 |
| 5 | Results of linear regression analysis for particle loading density (grams/cm) vs height above the bed surface (cm). | 75 |
| 6 | Comparison of least square fit relations for P_o as a function of U_o and U_{mf} . | 77 |
| 7 | Comparison of least square fit relations for $1/a$ as a function of U_o . | 78 |
| 8 | Statistical values for particle number distribution as a function of freeboard height. A complete listing of the data is given in Appendix J. | 83 |
| 9 | Average and standard deviation of jet velocity determined from oscilloscope traces in Appendix K. | 89 |
| 10 | List of transit times for particles traveling from the bed surface to the center of the trap. The time prior to actuation of the sample trap is also shown. | 91 |

| | | |
|-----|--|-----|
| 11 | List of samples and their correlation parameters. The resulting average for Q indicates that no correlation can be made from the data obtained to indicate by sample weight whether or not any bed activity occurred below the sample trap. | 95 |
| 12 | Effect of U_0 on the slope of the particle density distribution as a function of height for the distributions shown in Fig. 47. | 113 |
| 13 | Effect of U_{p0} on the slope of the particle density distribution as a function of height for the distributions shown in Fig. 56. | 121 |
| 14 | Effect of U_j on the slope of the particle density distribution as a function of height for the distributions shown in Fig. 65. | 123 |
| 15 | Effect of t_j on the slope of the particle density distribution as a function of height for the distributions shown in Fig. 74. | 134 |
| 16 | Baseline parameters used in computer model. | 140 |
| 17 | Comparison of slopes for the particle density distribution above the bed as derived from the experimental data and the computer model. | 142 |
| A.1 | Listing of paddle components and parameters. | 151 |
| A.2 | Calculated values for the moment of inertia of paddles and paddle components. | 155 |
| B.1 | Results of vacuum sample removal test. | 157 |
| C.1 | Sample trap closure data. | 160 |
| D.1 | Summary of dynamic analysis results. | 168 |
| E.1 | Average particle size distribution of bed material in grams and percentage of total weight using sieve analysis. | 170 |
| H.1 | List of components for sampling apparatus. | 179 |
| H.2 | Listing of components for solenoid power supply. | 180 |
| H.3 | Listing of components for vacuum system. distributions shown in Fig. 47. | 181 |

CHAPTER I

INTRODUCTION

Fluidized beds have been used in industry for many years. They have been used to mix and dry particulate materials and are the principle process in catalytic cracking plants. In the past decade or so, the use of fluidized bed combustors for power generation has become a source of major interest. Prototype coal burning beds have already been built which are comparable to existing coal plants. Fluidized bed combustors have the added benefit of low NO_x , SO_2 and hydrocarbon emissions and the flexibility of being able to burn a wide range of fuels ranging from refuse and high sulfur content coal to high grade fuels.

A fluidized bed [Fig 1] is composed of a distributor through which an air flow is introduced through thousands of small orifices. This air then passes through the dense zone of the bed which is comprised of a mass of particles. The air velocity through the dense zone is maintained above the minimum fluidization velocity (U_{mf}) during normal operations. At velocities equal to or greater than U_{mf} , the frictional force (Drag) of the air flowing past a particle is equal to the weight of the particle. Under these conditions, the particle mass behaves very much like a fluid. It will maintain a horizontal surface if the container is tilted, flow out of holes in the

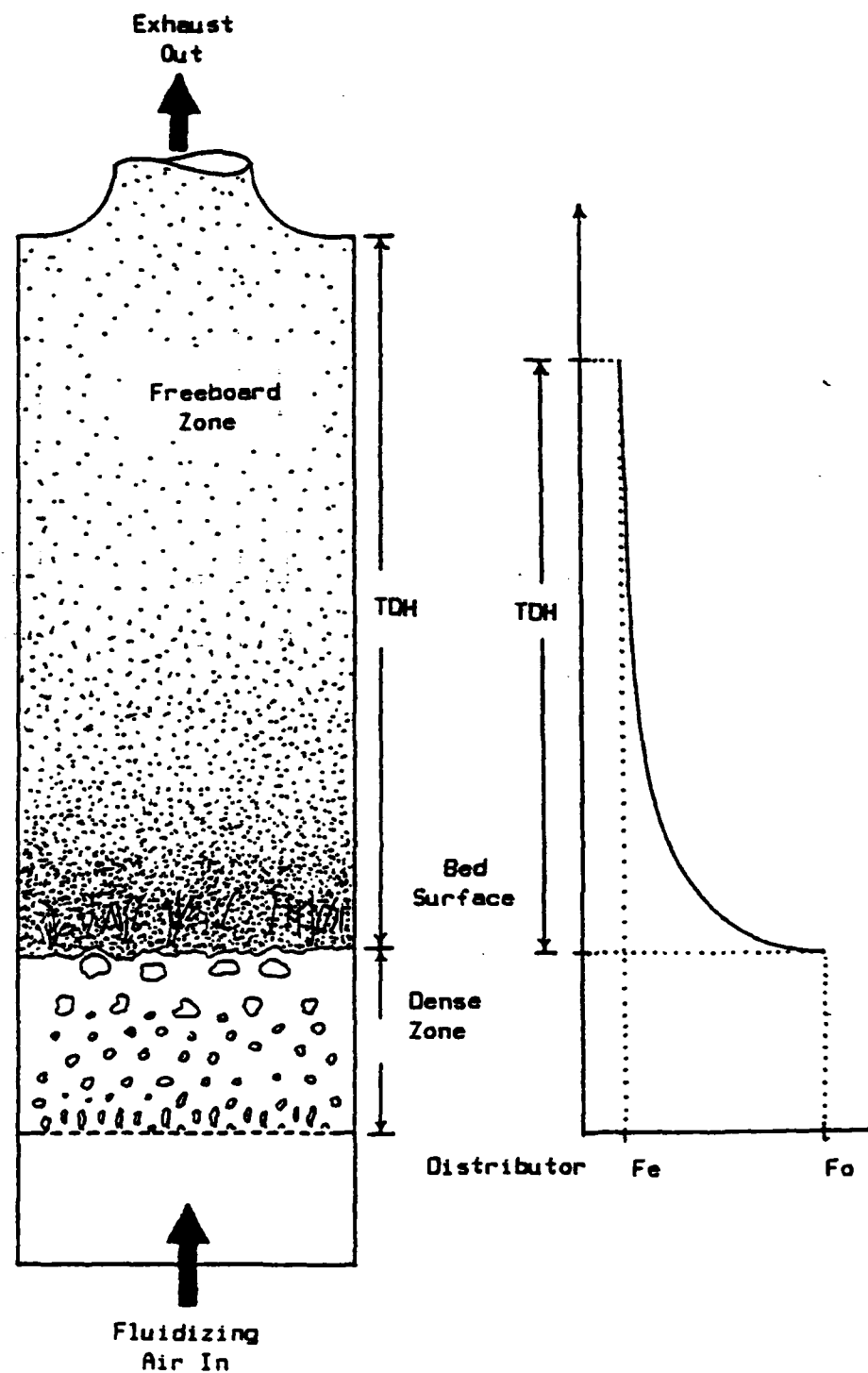


Fig. 1 Model of a fluidized bed. Particle entrainment decreases exponentially with increasing freeboard height.

container, and has a pressure drop across any section of the bed approximately equal to the weight of air and particles in the section [1]. At velocities above U_{mf} , the excess air will coalesce and form small voids or bubbles as it proceeds towards the surface of the fluidized bed.

As bubbles break at the surface of the bed, the solid particles are thrown up above the bed surface and are entrained by the upward flowing gas stream. This zone above the bed surface is the freeboard zone. In the freeboard, some particles are carried by the gas flow far above the bed surface and are removed from the fluidized bed (elutriated), while the remainder fall back to the bed. In general the amount of bed solids suspended in the freeboard (entrainment) decreases exponentially along the freeboard height. This distribution is similar to that of the Maxwell-Boltzmann distribution for the case of discrete energy states as it applies to the Law of Atmospheres [2].

$$N(z) = N_0 \exp(-mgz/kT) \quad (1)$$

Research in the area of entrainment by Lewis et al. [3], Zenz and Weil [4] and others has resulted in the following correlation for entrainment as a function of gas velocity and freeboard height for small-particle beds [1].

$$\frac{F}{At U_o} = B \exp\left(-\left[\left(\frac{b}{U_o}\right)^2 + a H\right]\right) \quad (2)$$

where:

F = Entrainment
 At = Area of bed
 Uo = Superficial velocity through bed
 B = Particle dependent constant
 b = Particle dependent constant
 a = Particle dependent constant
 H = Height of freeboard

At some point above the bed surface, the quantity of entrained particles becomes constant. At this point, the free fall velocity of the remaining particles is equal to or less than the uniform superficial operating velocity. The height at which the entrainment becomes constant is called the transport disengagement height (TDH) [1].

The particles that are thrown above the bed are affected in the freeboard region by hydrodynamic parameters such as: bubble size, bubble frequency, fluidizing velocity, height above the bed, particle size, particle density, column diameter [5], and baffles [6]. The intermittent high velocity bursts of gas which occurs when a bubble bursts, imposes a fluctuating and highly irregular time dependent velocity profile over the cross section of the bed surface. At successively higher levels above the bed surface, this velocity profile becomes more and more uniform until at the TDH, the flow is at the uniform superficial operating velocity (Uo) [4].

Until recently, little attention was paid to the understanding of the freeboard reactions for large particle beds. However, due to recent work in fluidized bed combustors, the extent of particle and fines loading in the freeboard has been shown to significantly affect the SO_2 absorption, NO_x reduction, CO emission. In general, the last 5 to 10% of the combustibles will burn in the freeboard. It was shown that the fine sorbent particles entrained into the freeboard will enhance sulphur capture and that entrained char particles will react with NO_x and reduce its emission [7]. Fines reinjection has been shown to significantly increases the fine particle concentration in the bed and in the freeboard with the consequence of further enhancing char oxidation. However, this can result in overheating in the freeboard region and excess SO_2 and NO_x emission [7]. The end result is that the potential for fluidized bed combustion power plants is enhanced by their ability to burn high sulphur content fuels and maintain low SO_2 emissions. Further research in the area directly above the bed surface is required to properly model the reactions occurring within the freeboard.

Extensive studies on entrainment rate and elutriation have been made with numerous correlations, some of which are proposed in [1, 3, 4, 5, 6, 7, 8]. However, most of the reported work on entrainment from fluidized beds has been carried out with either a closely sized fraction of particles or a mixture of two such fractions. Virtually all of this work has been conducted on bench scale or catalytic cracking fluidized beds. The results of these

studies have been shown to produce much lower entrainment rates than full sized beds or tend to operate in the slugging condition. Therefore, the entrainment rates and transport disengagement heights (TDH) for fluidized beds are generally estimated from empirical or semiempirical correlations obtained from this data and most of them show extreme discrepancies between different experimental results. Extrapolation of these empirical correlations usually leads to strange results [5] with discrepancies which can vary by two orders of magnitude.

The lack of good correlations stems mainly from the difficulty in obtaining accurate entrainment rate data. Most of the data is based on pressure measurements at incremental heights in fluidized cracking plant type beds [11]. The effect of wall loading by particles and the actual relation between pressure and particle concentration is considered to be major sources of error when using this method with large particles. As a result, none of the correlations are widely accepted as giving accurate predictions [8].

A complete model of the entrainment process from fluidized beds must take into account all the mechanisms involved within the process. The arrival of bubbles at the bed surface, ejection of particles from the dense-phased bed into the freeboard region as the bubbles erupt, particle-particle interactions, and the trajectories of ejected particles are all important [8]. Much work has been done concerning bubble growth, velocity, volume,

etc. and their behavior is fairly well understood.

The mechanism of solids ejection at the bubbling bed surface is still not well understood. The origin of ejected particles is reported to be primarily due to two sources. The particles which have been lifted by the bubble wake and thrown upwards following the bubble burst at the surface is the first source. This theory is supported by work done by George and Grace [8] who performed experiments which concluded that the vast majority of the ejected particles did not originate from the surface layers but from bubble wake pick up. Work done by Page and Harrison [6] also appears to agree with this. The second theory suggests that the ejected particles originate at the nose of the bursting bubbles and are thrown outward when the bubble breaks. Research by Rowe and Partridge [8] and Glicksman et al [12] have shown this second mechanism as being the dominate particle ejection source and thus supporting this second theory. Their work has also shown that under the conditions in which 2 bubbles coalesce just below the surface of the bed, the jet of gas produced can result in a significant amount of particles being ejected from the wake of the first bubble.

The effect of multiparticle interactions have been for the most part ignored except by Peters and Prybylowski [13]. The motion of any individual particle is influenced by the presence of other particles, i.e., through direct particle-particle interactions and deviations in the fluid drag force. The major

drawback of their work is that the paper compares their theory with only a single set of experimental results [3].

Studies to model the trajectories of particles in the freeboard have been conducted several times. The work of Walsh et al [7], George and Grace [8], and Peters and Prybylowski [13] name just a few of the latest efforts. All of these studies relied upon experimental data to develop their theories. However, to check the accuracy of their theories, more experimental data is required.

As of yet, none of the entrainment models available can be incorporated into fluidized bed combustion models with sufficient accuracy to warrant their use. This is due to a lack of experimental information on entrainment rate as a function of the complete fluidization parameters of the bed to test the models with. As a result, the purpose of this study has been to obtain particle density distributions above a cold atmospheric fluidized bed containing a continuous particle size distribution [Appendix E].

CHAPTER II

PARTICLE SAMPLING APPARATUS

Design Alternatives

There are many methods available for determining particle distributions in fluid flows. The more commonly used methods are:

- 1) Catching mechanisms
- 2) Trapping mechanisms
- 3) Radiation attenuation measurements
- 4) Optical measurements
- 5) Capacitance and Inductance measurements

Catching mechanisms are passive devices. That is, particles are captured merely by the presence of the catching mechanism in the fluid flow containing the particles to be sampled. The data obtained using this method is position dependent and produces average values for the particle flux loadings. These catching mechanisms are also limited in that they can only catch particles with particle fluxes traveling in a single direction. The device used by Walsh et al [10] only captured falling particles while the device used by George and Grace [8] required the upward moving particles to deflect off of a baffle surface and fall into a collecting trough.

Trapping mechanisms, unlike catching mechanisms, are active particle samplers. Their operation involves the trapping and isolation of a finite volume of the fluid flow at a specific period in time. This sampling technique produces time dependent as well as position dependent data. This will allow correlations between bubble eruption and particle density to be made using multiple bubble conditions rather than single bubble capture. As the number of random samples taken by this method increases, the average value of this data will approach that of the catching mechanism. Trapping mechanisms also capture particle fluxes traveling in multiple directions. This ability reduces the error inherent in measuring only the downward or only the upward particle flux. The apparatus used in this paper is a trapping mechanism.

Attenuation of nuclear particles from a radioactive source can be used to give average particle density distributions across a suspension. However, this method is not adaptable to density determinations at a point. An average time dependent density determination can be achieved with this method. Another draw-back of this method is the radiation hazards involved with the use of nuclear particles.

Optical density determinations consists of two separate methods. The first method uses a very small light beam which is eclipsed by the transition of a particle through it. A related

method uses the absorption and scattering of a somewhat larger light beam to correlate the change in light intensity with particle density. This method has been used frequently in the study of aerosols but requires complicated and intricate equipment [14]. The second method involves high speed photographs of a small volume of space. This method cannot be used when the particle density is so large that multiple particles eclipse each other frequently enough to produce unacceptable error. This is the case when the probe height above the bed is less than 7-15 cm (3-6 in).

Measurements at a point can also be made by inserting either a toroidal inductor or a parallel plate capacitor in the flow. The presence of the particles changes the permeability and thus the inductance of the inductor, or the dielectric strength and thus the capacitance of the capacitor. The draw-backs of these methods involves the unknown effects of particle velocity and external particles on the inductor and charge transfer to particles from the capacitor [14].

Apparatus Requirements

The goal of this study was to determine the density distribution of particles above an atmospheric fluidized bed with particle velocities of up to 10 meters per second. The particle size distribution of material ejected from bubbles is required for particle trajectory calculations. A correlation between the

average density and the density present immediately after a bubble bursts from the bed surface was also of interest. These requirements dictated that the method used for measuring densities have the following capabilities:

- 1) Measure densities with good spatial resolution.
- 2) Measure densities at specific moments in time.
- 3) Obtain particle size information.
- 4) Operate under extremely dirty conditions.
- 5) Easy sample removal from bed.
- 6) Remote operation of sampler.

The radiation attenuation and inductance/capacitance methods can not determine particle sizes. Therefore, these methods were no longer considered as possible measurement alternatives. Because the optical methods are either not reliable at small heights above the bed or their use is too complex, they were not used. Catching devices, although simple to use, do not have the ability to measure data at specific points in time and determine particle density loading in space. As a result, the determination to use a trapping mechanism as the method of measuring particle densities was made.

Apparatus Design

General Design Criteria

The following criteria was used in determining the design of the trapping device.

- 1) The closure time of the trap was chosen to be equal to the time for a particle with a velocity of 10 m/s to transit 1/10 the length of the sample container. This velocity is considered to be the upper limit of the particle velocity distribution present in the test bed, based on the work of George and Grace [8].
- 2) The apparatus must be capable of frequent sampling without requiring access to the sampling device itself.
- 3) The samples trapped, must be easily accessible from outside the fluidized bed without interrupting the bed conditions.
- 4) The apparatus must be able to operate in the high particle flux environment of the fluidized bed.

- 5) The actuation of the trapping device must be able to be accurately determined to allow correlation with other time resolved measurements.

General Design

The apparatus is shown in Figs. 2 and 3. A description and list of all components is given in Appendix H. The sample container is mounted on an extension arm to minimize the disturbance to the air flow around the sample trap caused by the rest of the mechanism. The sample container is closed using two (2) paddle arms, one above and the other below. These paddle arms are attached to aluminum interfaces which are used to connect them to a rotary solenoid. The solenoid is used to swing the paddles over the sample trap and shut it. Not shown in these figures are the power supply for the solenoid, the vacuum system used to remove the particles from the sample trap and the water-proof nylon shell used to keep the particles from interfering with the operation of the solenoid. All of these systems are described in greater detail in the following sections.

Sample Container

To ensure that the sampling device had minimal effect on the fluid flow, the cross sectional area presented to the flow had to be minimized. This constraint required that the sample container

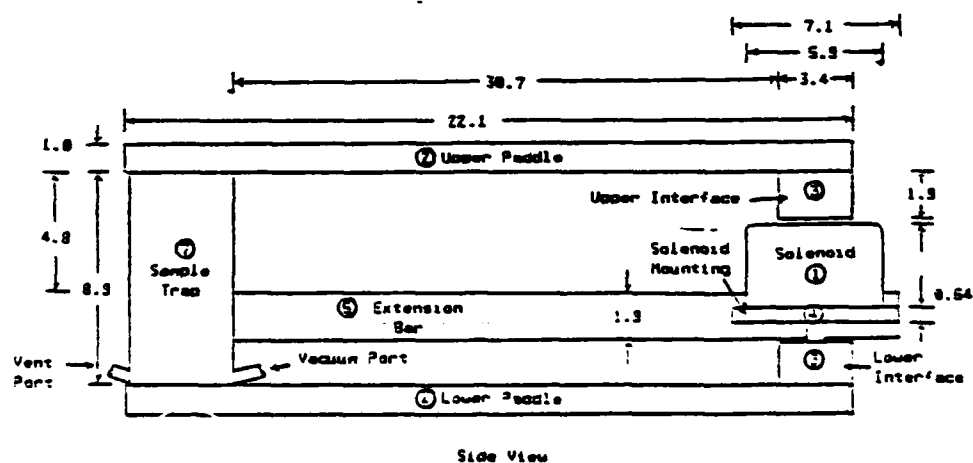
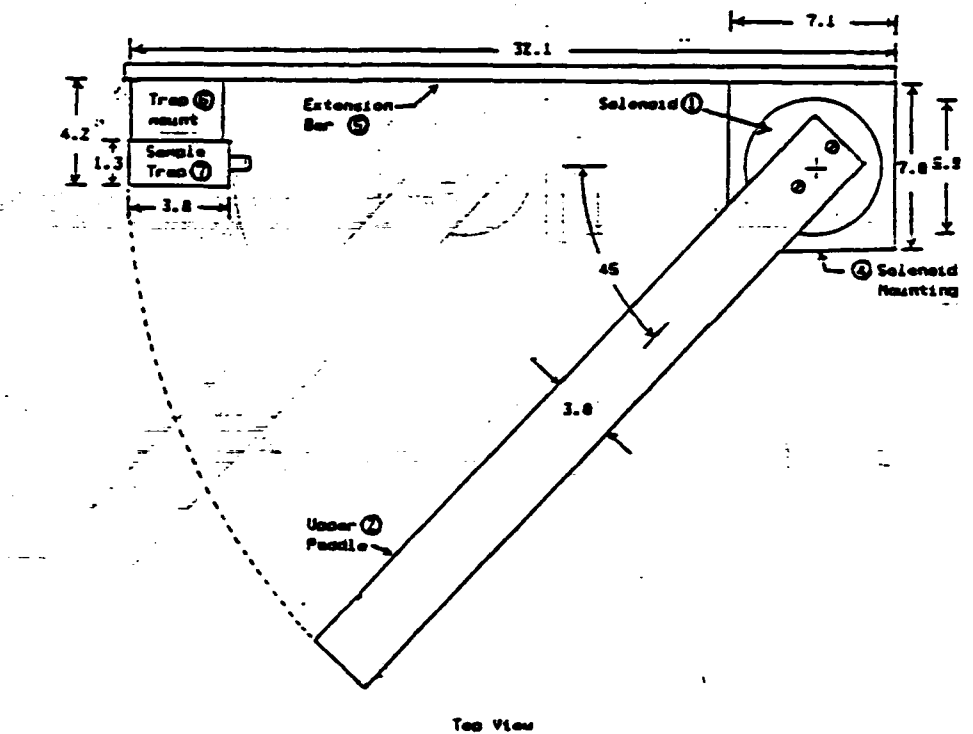


Fig. 2 Side and top views of sampling apparatus. All dimensions are in cm. ○ Reference number for component listed in Appendix M.

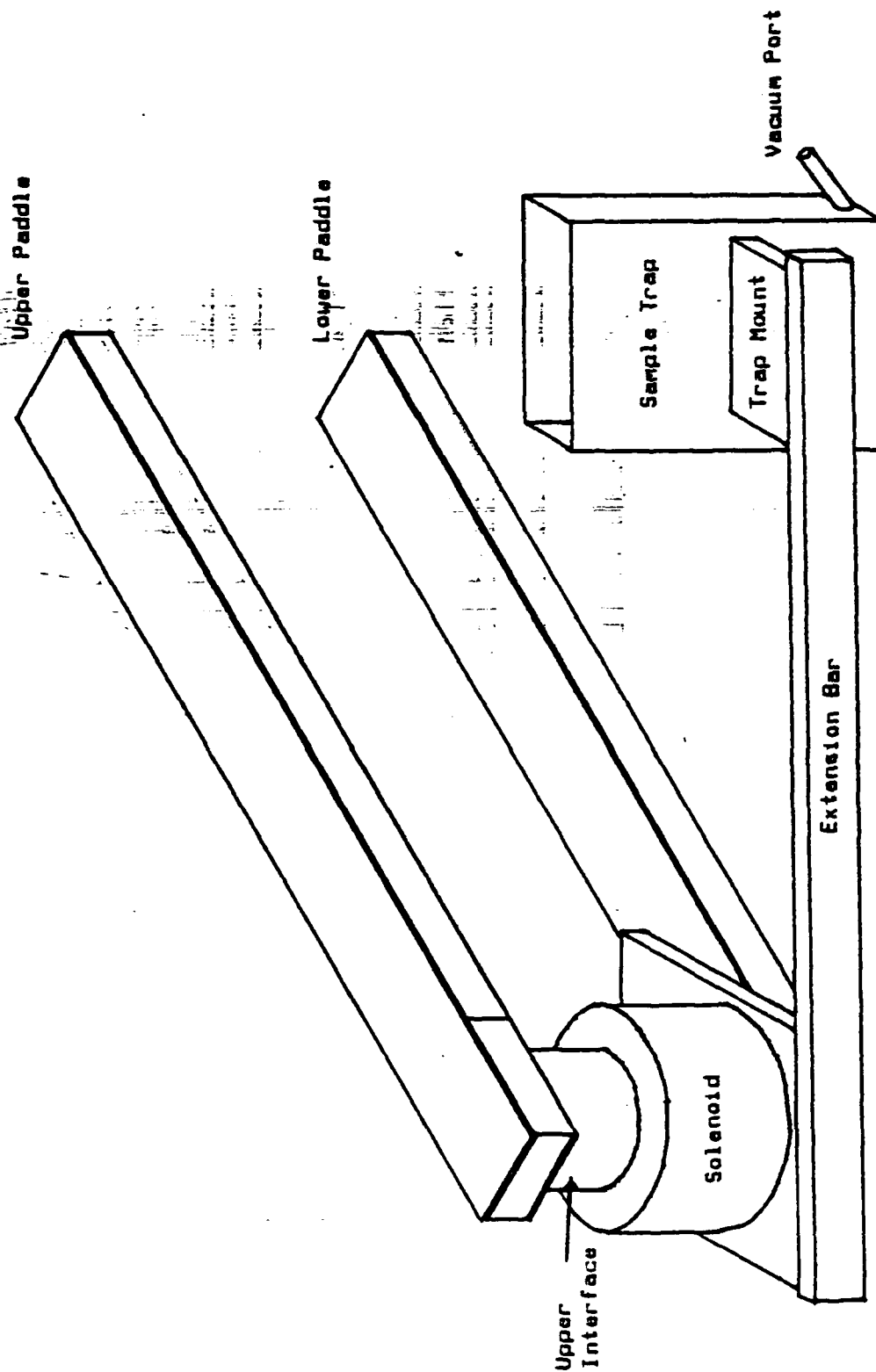


Fig. 3 Perspective view of sampling apparatus

be separated from the rest of the apparatus. This was beneficial in the final design because it helped to reduce the apparatus closure time.

To ensure a good seal was achieved when the trap was shut, felt was used as a gasket between the sample container and the closure paddles. Fig. 4 shows the final design used for the sampling mechanism. It is constructed of 1/16 inch aluminum with 1/4 inch square stock used for the frame and mounting structure. Epoxy is used to seal the sides of the container.

Closure Paddles

After several iterations on paddle designs, it was determined that the paddle construction which offered the greatest stiffness for the least weight was a composite laminate. The paddle, shown in Fig. 5, is made using a 0.4 in thick foam core with 1/32 inch thick Basswood laminations on the exterior. Hardwood (Maple) end pieces were used to provide a noncompressive connection between the foam paddles and the aluminum interfaces. The aluminum interfaces couple the solenoid shaft to the paddles. Epoxy was used to join the laminate materials.

Actuator

A rotating mechanism utilizing a rotary solenoid was chosen to shut the sample trap. A rotary solenoid was selected because

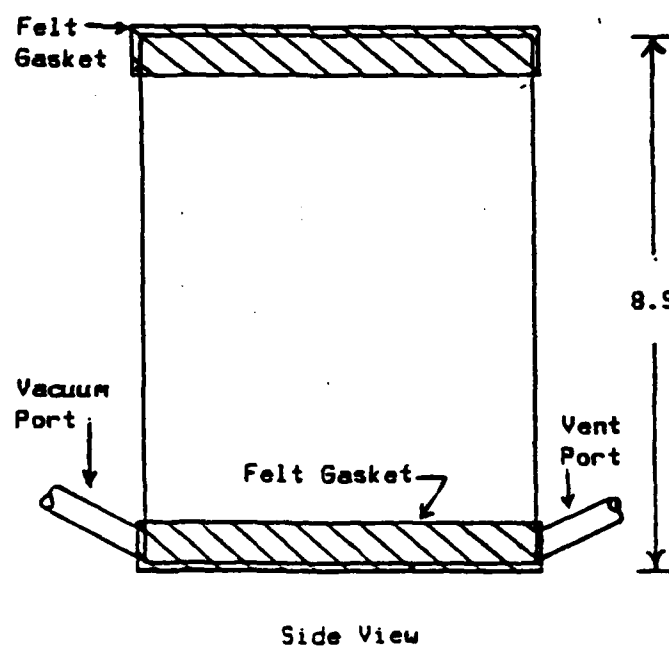
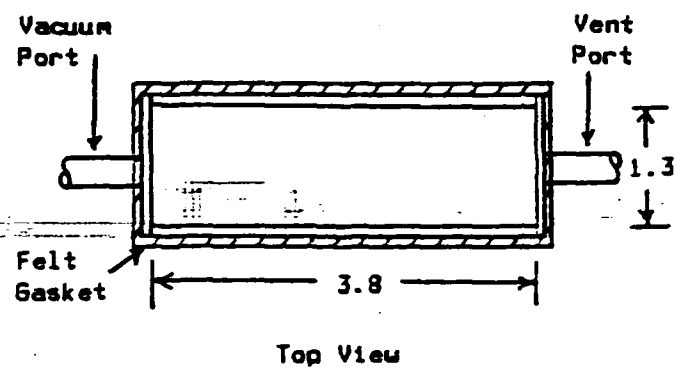


Fig. 4 Top and side view of sample trap.
Dimensions in cm.

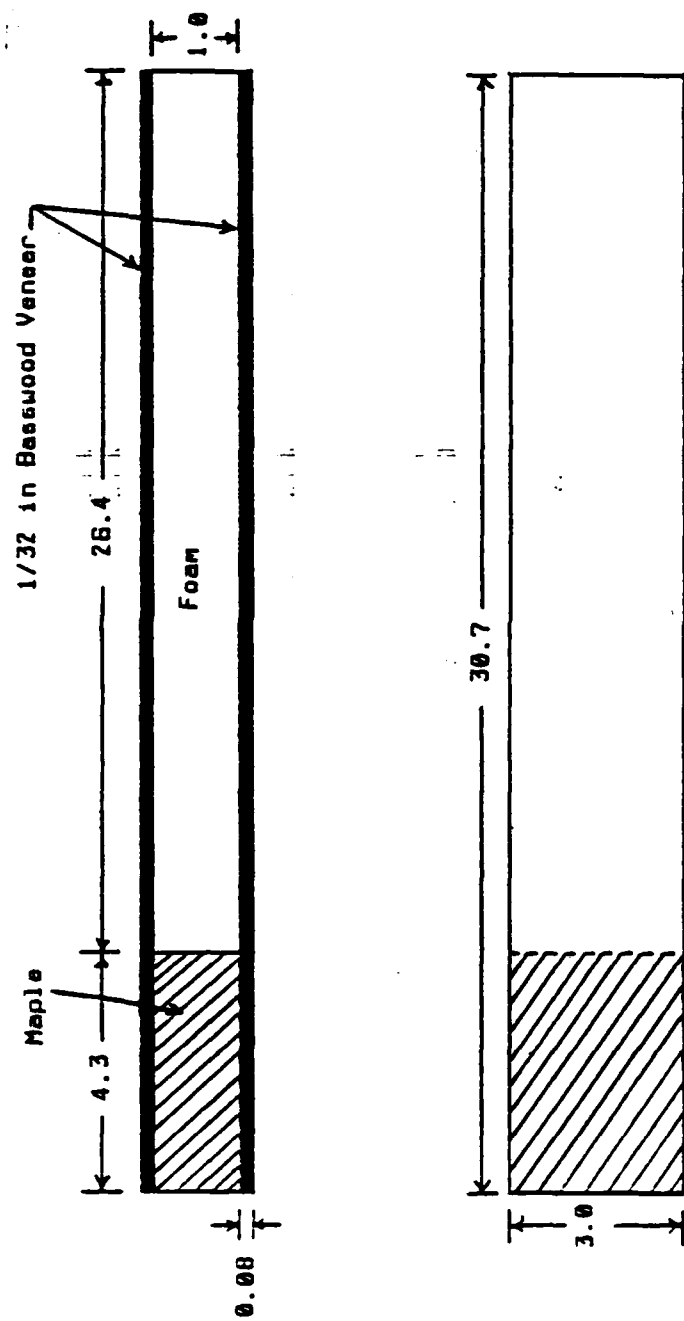


Fig. 5 Design of Closure Paddles. Dimensions in cm.

of the problems of maintaining low friction surfaces for sliding mechanisms in the presence of the particulate matter being sampled. This precluded the use of any sliding mechanism to shut the sample trap. The calculations found in Appendix A and Appendix C determined the size of the solenoid required to achieve the desired closure time.

The 45 degree stroke solenoid was chosen to place the paddle arms far enough away from the sample trap, such that when de-energized it prevents interference with the particle flow. This stroke also minimized the area which must be clear of obstructions to the travel of the paddles. The solenoid operates at a 1/10 duty cycle power rating when initially actuated, providing the torque output shown in Fig. 6. After the solenoid has shut the sample trap, the solenoid is operated at a lower power rating, providing a holding torque of 5.5 in-lbs. This decreased rating is necessary to prevent overheating of the solenoid. This assembly is encased within a nylon shell.

Power Supply

Fig. 7 is a schematic of the electrical system used to power the solenoid. Appendix H contains a list of all components used in the power supply. The power supply plugs directly into a standard 115 volt AC line source. Switch S1 is used to apply power to the solenoid M1. The full wave bridge rectifier assembly converts the AC line voltage to DC. The rectifier assembly is

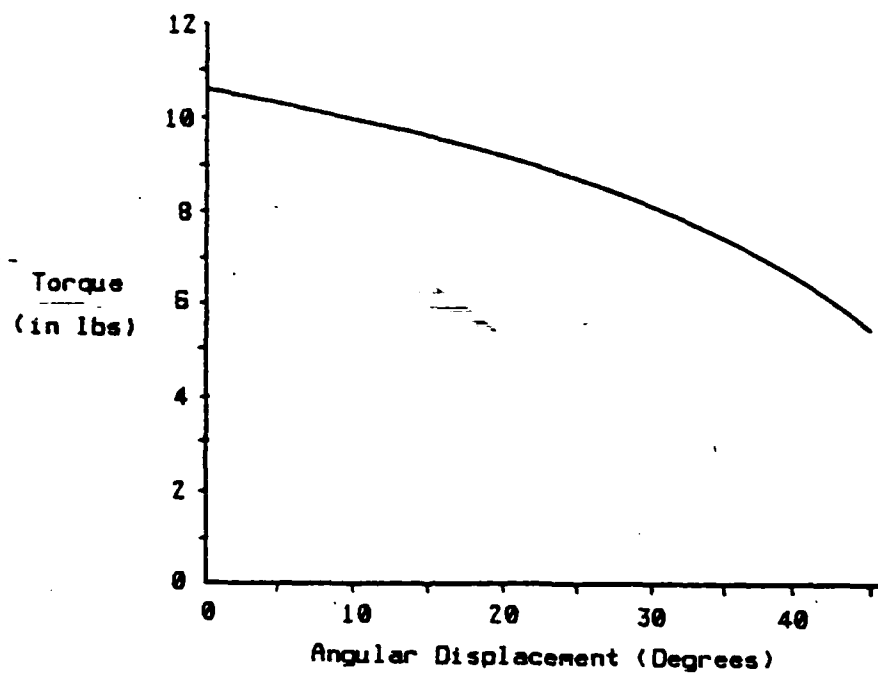


Fig. 6 Torque Output Curve for Rotary Solenoid.

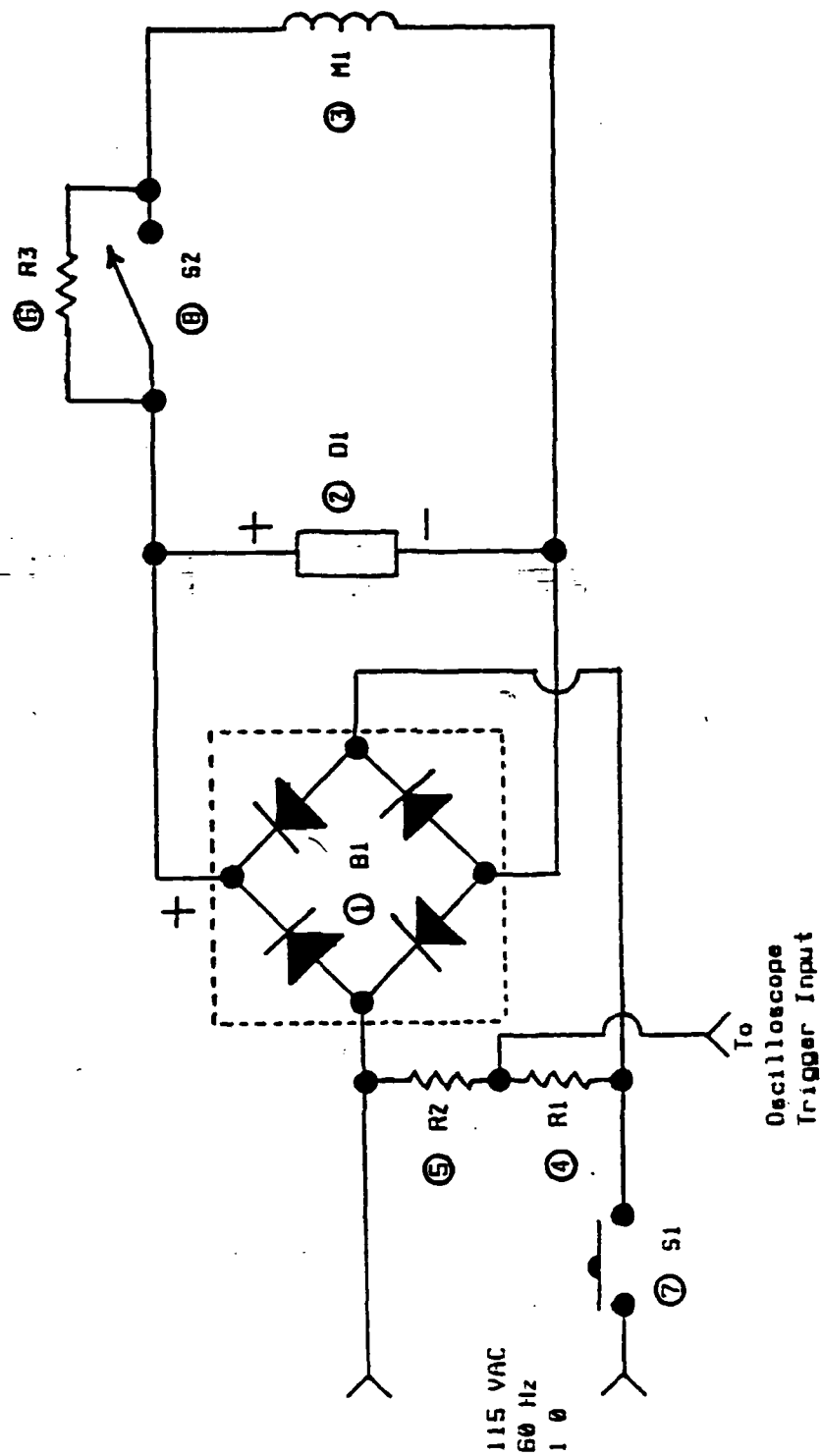


Fig. 7 Schematic of Solenoid Power Supply.
 ○ Reference number for component
 list in Appendix H.

protected by the arc suppresser D1 from the large voltage spike induced in the solenoid coil when the solenoid is actuated. Resistor R3 is used to reduce the current through the solenoid after the solenoid has been closed to prevent it from overheating. To initially shut the sample trap, full current is applied to the solenoid by shutting switch S2, which bypasses resistor R3. Resistors R1 and R2 form a voltage divider network to provide a low voltage (5.5 volts AC) trigger source for an oscilloscope.

Vacuum System

To remove the particles in the sample trap, a vacuum system was developed. This system is shown in Fig. 8 with a list of the components given in Appendix H. A vacuum is produced by allowing air from a 100 psi air source to flow through valve V1 into the venturi eductor P1. The vacuum places a suction on the sample container C2 via a fine mesh screen. The purpose of this screen is to prevent particles from escaping the sample container. The suction is applied to the sample trap C1 through 1/4 inch polyflow tubing. It is through this tube that the particles are removed from the sample trap and collected in the sample container. An equalization and agitation line is connected to the opposite side of the sample trap. This line serves two purposes. First, it ensures that the vacuum system does not pull in particles from outside of the sample trap. Second, it allows a flow of air to be introduced which stirs up the particles trapped inside. This helps push them into the suction line and reduce the remaining particles to a minimum.

Apparatus Testing

Two tests were run to determine the effectiveness of the system. The first test determined the closing time of the sample trap. The second evaluated the error from the loss of particles which were left in the sample trap by the vacuum system.

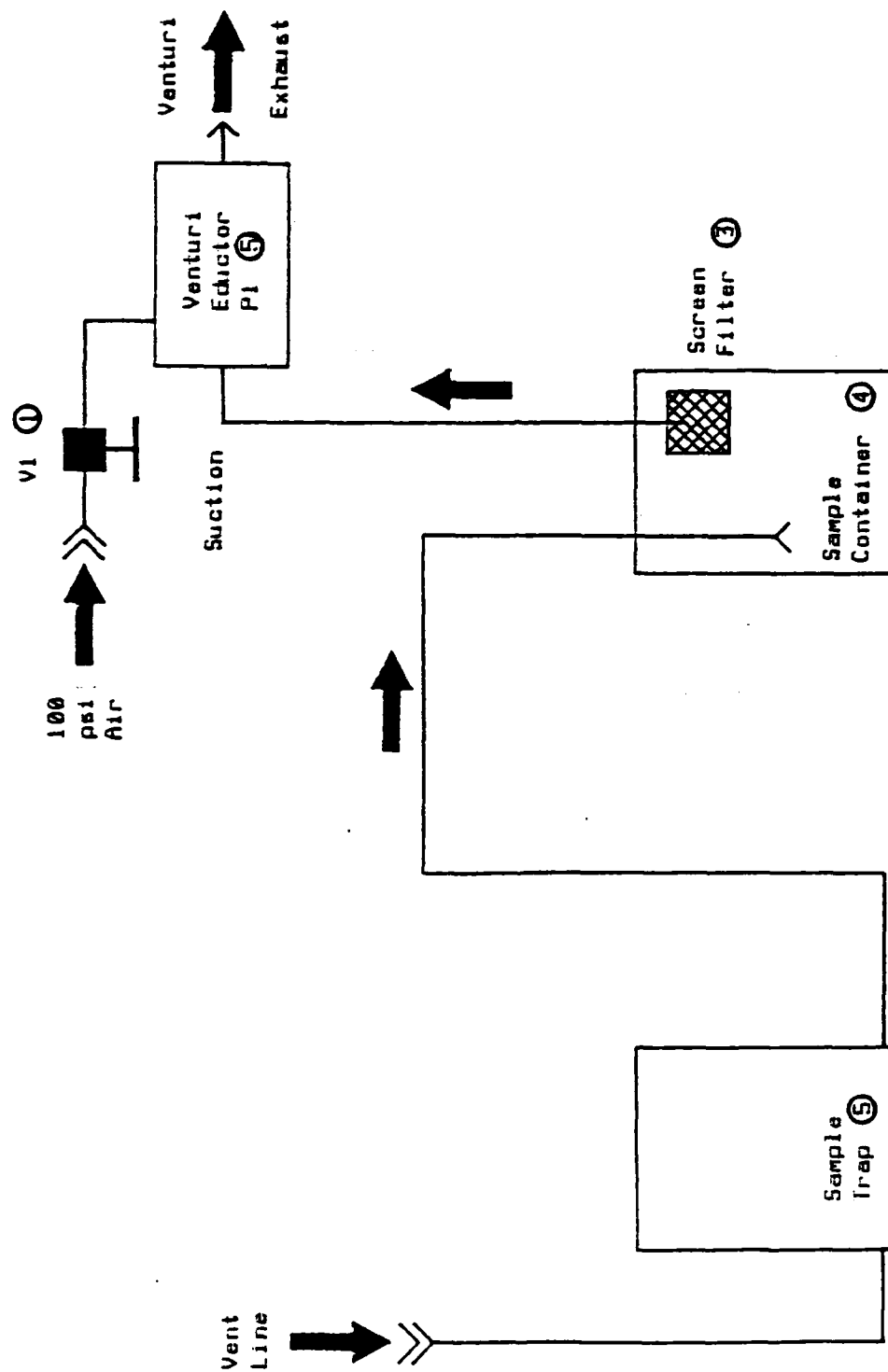


Fig. 8 Schematic Diagram For Vacuum System.
 ○ Reference number for component list in Appendix H.

The procedure and method used to determine closure time for the sample trap is given in Appendix C. From the results of these tests given in Appendix C, the closure time was determined to have an average value of 1.44 milliseconds. This is equal to a 10 m/s particle traveling 1.44 cm or approximately 16 % of the sample trap length. The average particle velocity will be less than 2 m/s and will therefore introduce an average error of less than 3 %.

Using the sample trap closure time, a dynamic analysis determined that the total time from initially applying power to the solenoid until it shut the sample trap is 42.6 milliseconds. These calculations are given in Appendix D. This actuation time is important for determining whether a specific bubble's debris was within the vicinity of the trap at the time of closure.

The procedure and results for the testing of the sample removal vacuum system are given in Appendix B. The average amount of particles lost by the vacuum system was determined to be 0.52 % of the initial sample placed in the trap. The maximum error was 0.93 %. The error from the vacuum system is therefore considered to have an insignificant effect on the data obtained.

CHAPTER III

EXPERIMENTAL PROCEDURE

Fluidized Bed Configuration

The M.I.T. atmospheric fluidized bed, in which the sampling device was used, is a model of the 20 MW atmospheric fluidized bed combustor prototype, jointly sponsored by the Tennessee Valley Authority and the Electric Power Research Institute. The fluidized bed model is described in Lord et al [15] and Jones et al [16]. While using the sampling apparatus, a different heat exchanger tube bundle configuration was used than is described in Jones et al [16]. The heat exchanger configuration used is shown in Figs. 9 and 10.

The heat exchanger used during this work is made of 1.26 cm (0.5 in) O.D. tubing arranged in 4 rows of 22 pipes each. The tubes are aligned as shown in Fig. 10. Each pipe is spaced with a vertical center to center distance of 5.08 cm (2 in) and a horizontal center to center distance of 3.91 cm (1.5 in). The distance from the distributor to the center of the upper most tube is 27.62 cm (10.875 in). A 5.08 cm (2 in) spacing separates the front and back walls of the fluidized bed from the end tubes of the bundle. The cross sectional area of the bed is 1.079 sq m (11.61 Sq Ft). The particulate material used in the bed is a

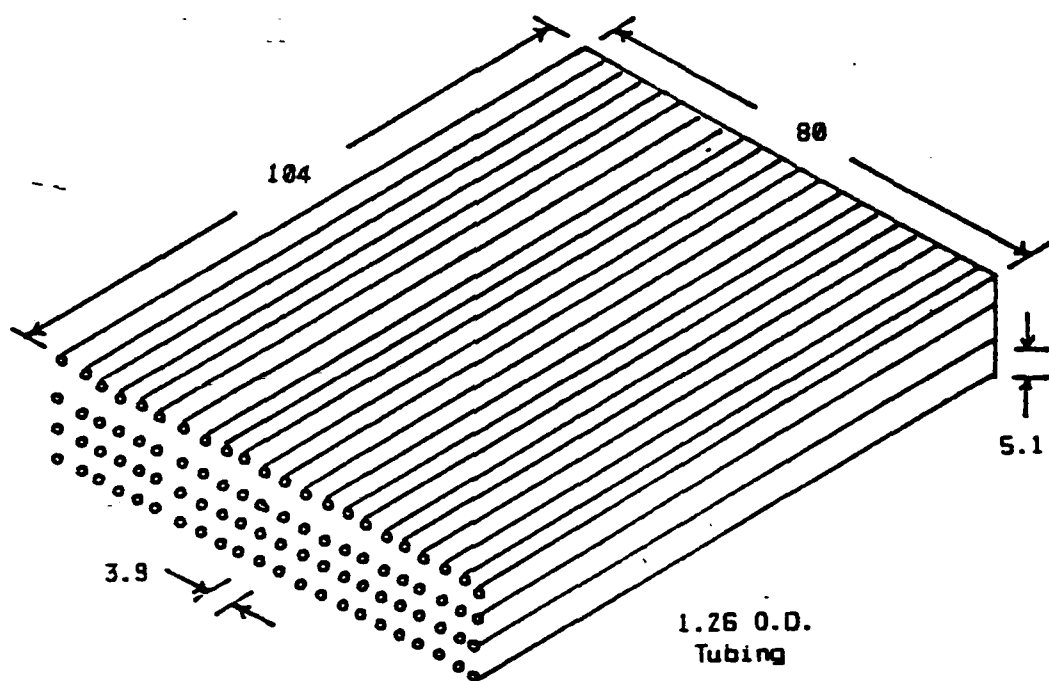


Fig. 9 Heat Exchanger Tube Design Showing The Four (4) Rows of 22 Tubes. All Dimensions in cm.

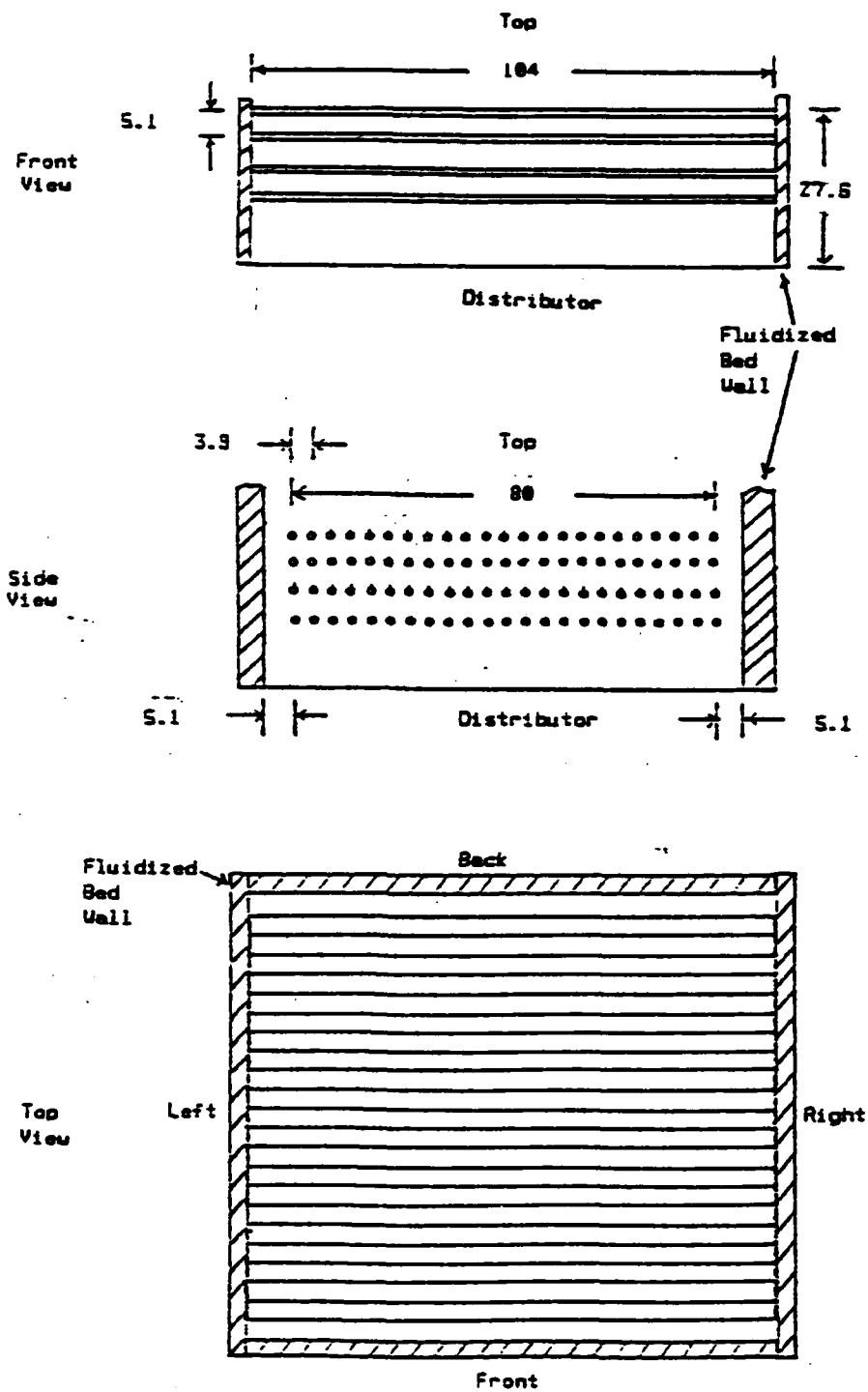


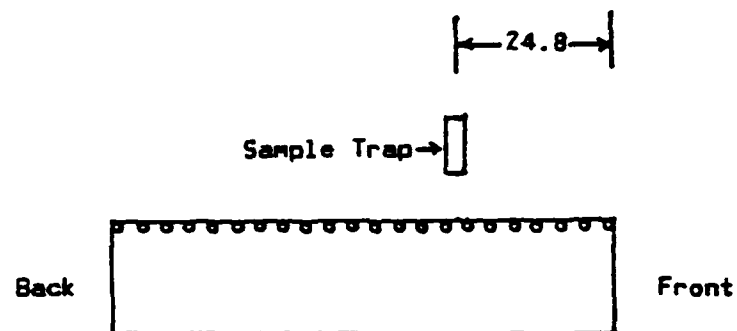
Fig. 10 Heat Exchanger Tube Design.
All Dimensions in cm.

mixture of steel grit abrasive having a specific gravity of 8.1. Appendix E lists the size distribution of the steel grit used during the sampling operation. The bed was operated without recycling the fines captured in the cyclones. The static bed height of the material was 22.54 cm (8.875 in) throughout the data collection period.

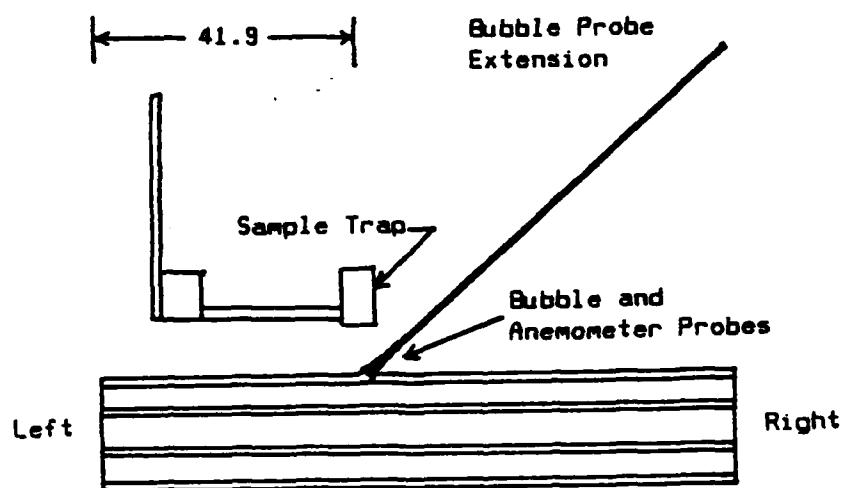
Equipment Set-up

Fig. 11 shows the placement of the sampling device inside the fluidized bed. The sample trap was positioned such that it was directly over a spacing between tubes [22.86 cm (9 in) from the center of the front-most tube] and 41.91 cm (16.5 in) from the left wall. The height of the sample trap above the distributor was varied during the sampling process as discussed in the section on sampling procedure.

Fig. 12 shows the placement of the bubble probe and the anemometer probe with respect to the sample trap. The bubble probe was placed directly below the sample trap and 26.67 cm (10.5 in) above the distributor. The probe extension was placed at an angle so as not to interfere with the sample trap operation. To protect the anemometer wire from particles impacting it, a special shield consisting of # 320 mesh screen and an aluminum frame was placed around it. The anemometer probe was attached to the bubble probe extension with the entrance to the anemometer probe 29.21 cm (11.5 in) above the distributor. This placed the entrance to the



(a) Right Side of Heat Exchanger Tubes



(b) Front of Heat Exchanger Tubes

Fig. 11 Position of Sample Trap, Bubble Probe, and Anemometer Probe Above Heat Exchanger Tubes. All Dimensions in cm.

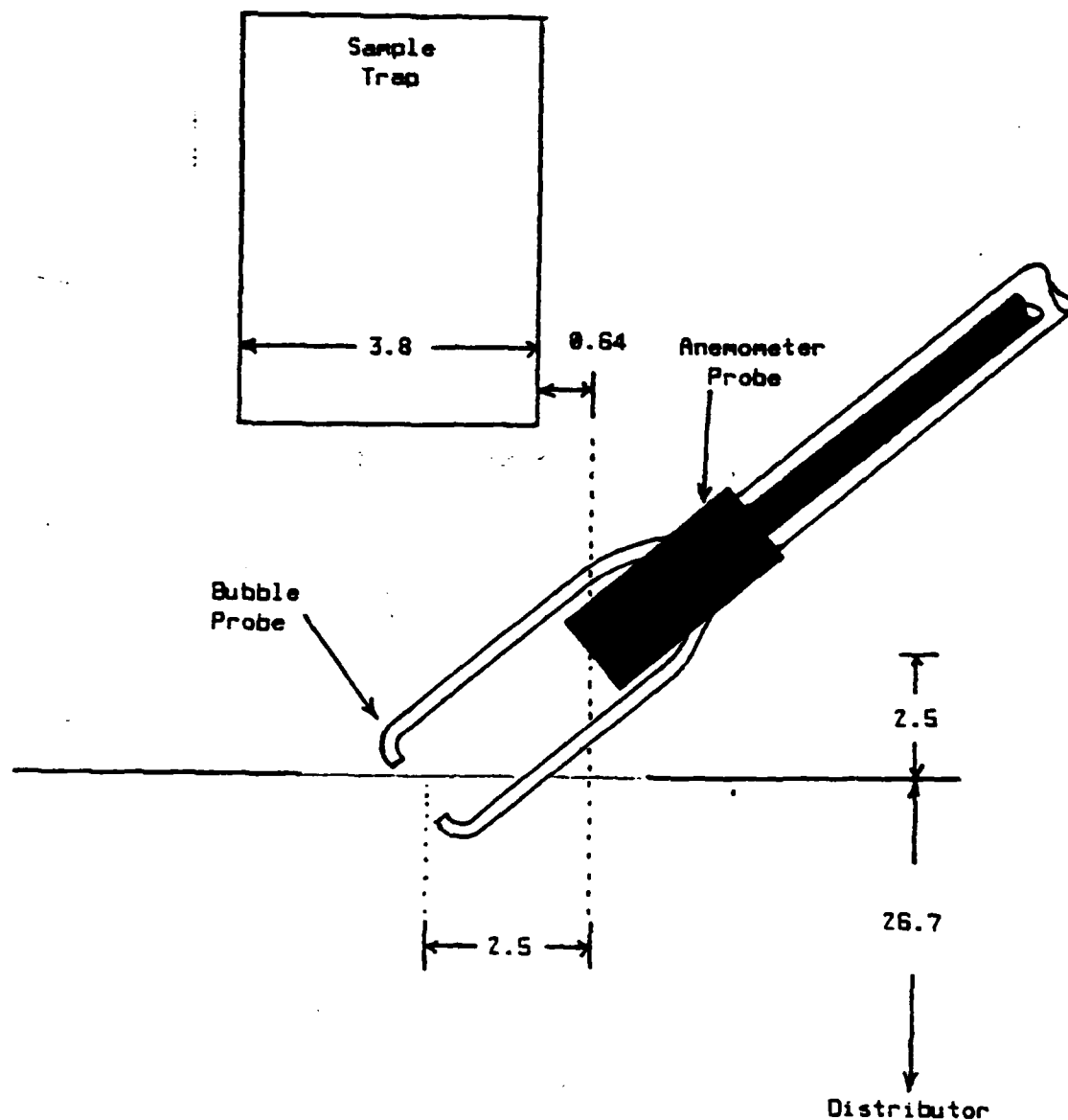


Fig. 12 Position of Bubble and Anemometer Probe with Respect to the Sample Trap and Distributor. All Dimensions are in cm.

anemometer probe 2.54 cm (1.0 in) away from the center of the sample trap and 0.64 cm (0.25 in) outside the area directly below the sample trap. As a result, the probe has a minimum effect on the air flow from the bed to the sample trap, but will only measure the gas velocity at the edge of the sample trap perimeter. The positioning of the two probes above the distributor remained constant throughout the sampling evolution.

Fig. 13 is a block diagram showing the equipment used during the sampling operations and their interconnections. Table 1 is a listing of the equipment used. The oscilloscope time base was set for MANUAL TRIGGER, SINGLE SWEEP mode and a sweep time of 50 ms/div. The channels of the dual trace amplifier were set at 5 volts per division for the bubble probe and 2 volts per division for the sample trap inputs. On the differential amplifier, one channel was not used and the second channel was set at 1 volt per division for the anemometer probe input.

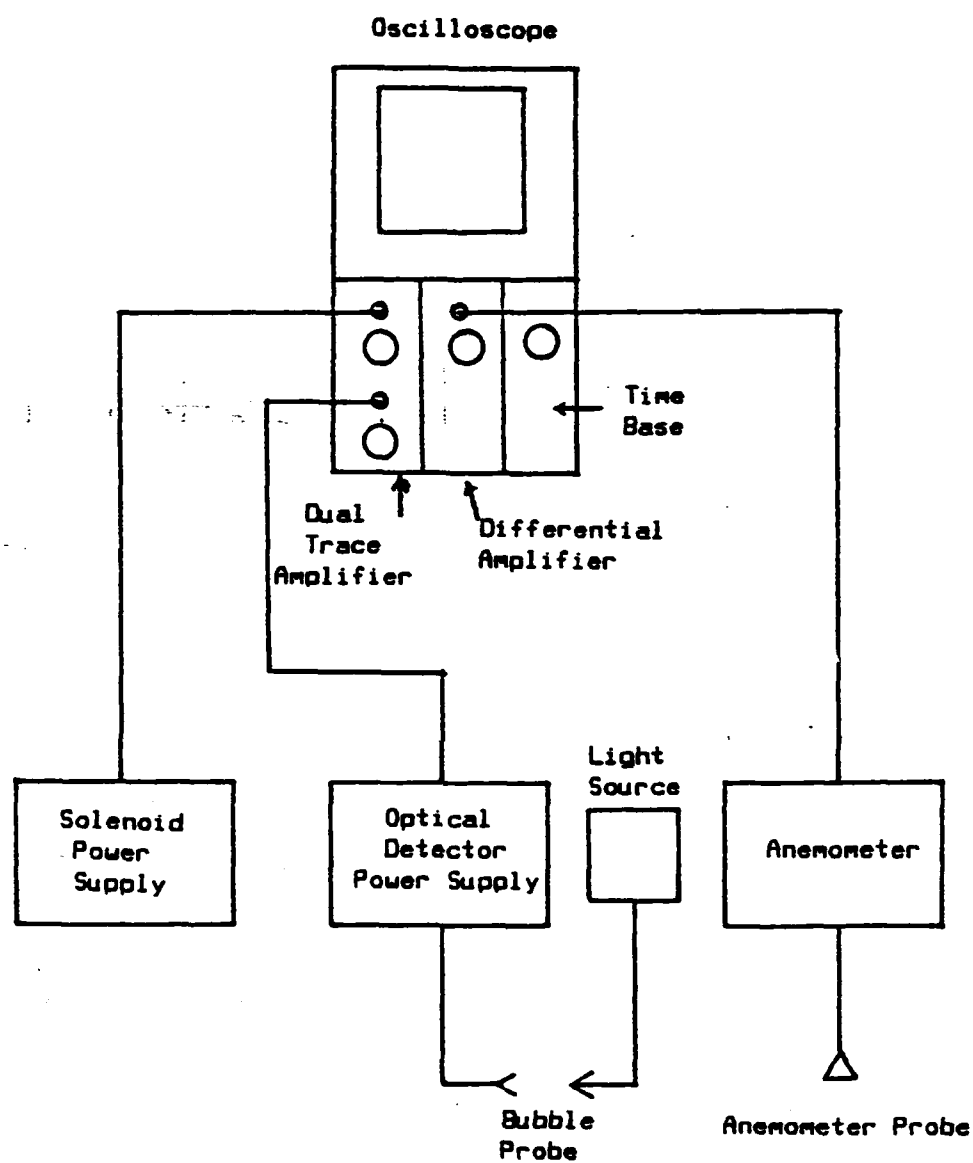


Fig. 13 Block Diagram of the Equipment Used During the Sampling Operations.

TABLE 1

| | |
|--------------------------------------|--|
| Oscilloscope | TEKTRONIX 5111 Storage Oscilloscope TEKTRONIX SA18N Dual Trace Ampl TEKTRONIX SA21N Differential Ampl TEKTRONIX SB10N Time Base |
| Anemometer | Thermal Systems Inc. 1051-2 Monitor and Power Supply 1054-A Linearized Anemometer Anemometer wire w/ #320 screen guard |
| Optical Signal Detector | |
| Optical Signal Detector Power Supply | |
| Optical Source and Power Supply | |
| Oscilloscope Camera | |

Listing of equipment used during particle sampling operations.

To determine the fluidization conditions within the bed, a set of manometers were used. These manometers measured pressures within the bed, at heights from 4.13 cm (1.62 in) to 37.15 cm (14.62 in) above the distributor, in 2.54 cm (1 in) increments. The pressure data corresponding to each trap position and bed velocity is listed in Appendix I.

To determine the gas flow conditions within the bed, an orifice flow meter with 1D - 1/2D taps was located upstream of the distributor. The computer program listed in Appendix G was used to convert the pressure tap data to mean air velocities within the bed.

Sampling Procedure

Data was collected for four (4) mean bed velocities at six (6) different sample heights. The sample trap was placed at a given sampling height (measured from the distributor to the bottom of the trap), and ten (10) samples were collected at each desired velocity. The trap position was then changed to a new height.

During certain sampling conditions, those which involved low sampling heights with the higher air velocities, the paddle arms would occasionally impact the sides of the sample trap and not close the sample trap completely. It is assumed that this occurred

when a large bubble erupted directly under the paddle arm and deflected the paddle arm into the side of the trap. Whenever this occurred, the trap was de-energized and the closure cycle repeated.

Each time the height or velocity was changed, a complete sampling cycle was conducted and this sample discarded. This was to prevent any accumulation of particles (in the entrance to the vacuum or purge lines on the sample trap) from being added to the first sample at the new height or velocity.

For each set of data at a given height and velocity the following information was recorded:

- 1) Fluidized bed height above the distributor
determined visually and by pressure measurements.
- 2) Pressure upstream of orifice plate (P1)
- 3) Pressure difference across orifice plate (ΔP)
- 4) Air temperature in bed
- 5) Pressure distribution in bed
- 6) Height of sample trap above distributor

The following procedure was used during sampling:

For each sample to be taken within a data set.

A. Initial conditions

- | | |
|----------------------------------|-------|
| 1) Vacuum air supply | OFF |
| 2) Sweep trigger on oscilloscope | RESET |

- | | |
|------------------------------------|----------|
| 3) O-scope memory | ON-CLEAR |
| 4) Solenoid power supply switch S1 | OFF |
| 5) Solenoid trigger switch S2 | ON |

B. Sampling Procedure

- 1) Trigger oscilloscope sweep and wait until sweep is at the center of the CRT.
- 2) Close the Solenoid power supply switch S1. When S1 is shut, the oscilloscope will show an additional trace. This third trace is used to determine the closure time relative to the presence of gas jets and bubble eruptions. An example of a typical oscilloscope trace is shown in Fig. 14.
- 3) Open the solenoid trigger switch S2. This reduces the current to the solenoid to prevent overheating. The maximum allowed time to let S2 remain closed is five (5) seconds.
- 4) Turn on the air supply to the vacuum system and leave on one (1) minute. The exhaust air from the venturi on the vacuum system must be directed into the purge line in an oscillatory manner. This will agitate the particles within the trap

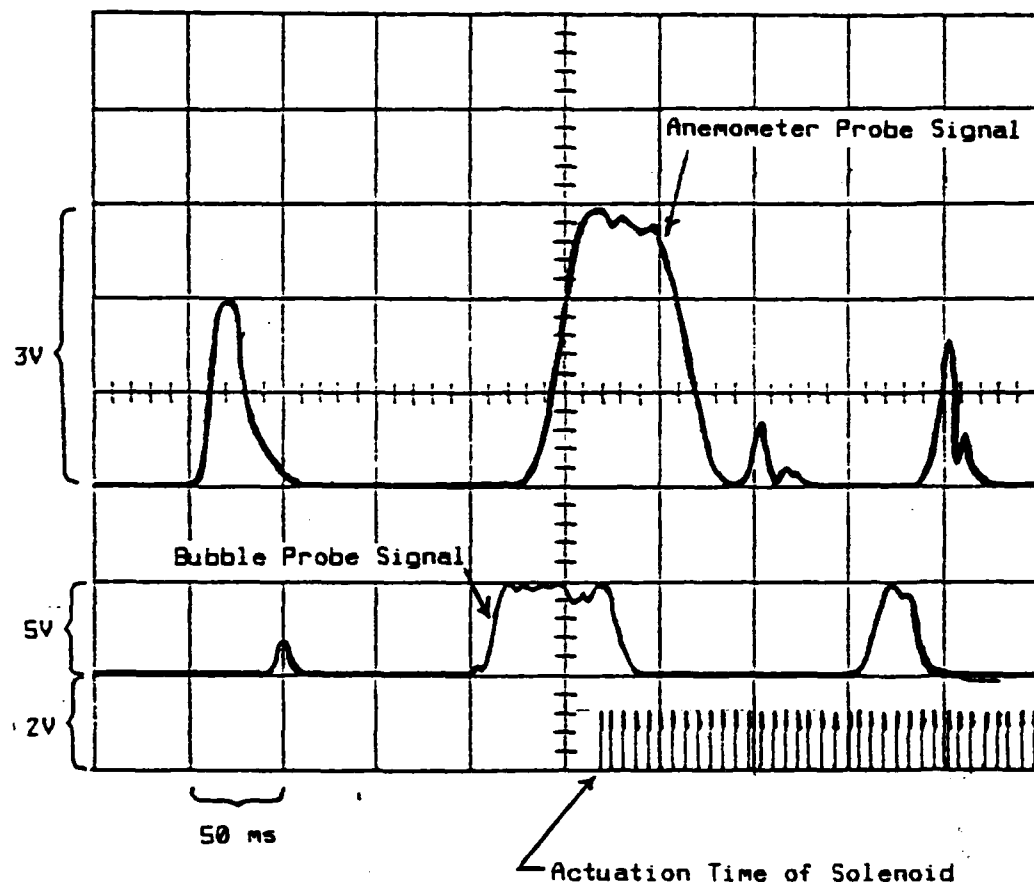


Fig. 14 Typical Oscilloscope Trace Obtained During Sampling Operation.

so as to move them into the vacuum line.

- 5) Turn off the vacuum air supply.
- 6) Turn off the solenoid power supply switch S1.
- 7) Remove sample from sample container and place in specimen bottle.
- 8) Photograph trace on oscilloscope.
- 9) Repeat from A.

Sample Analysis

Sample Weight Determination

Each sample obtained was weighed, using a Torsion Balance Co. TORBAL scale, to an accuracy of 0.01 grams. The average value and standard deviation was then determined for each set (specific height and velocity) of samples. The weight of particles in a completely filled sample trap was also determined for void determination. These results are listed in Appendix I.

Determination of Particle Size Distribution

To determine the particle size distribution which occurs at various heights for a specified gas velocity, three (3) samples from each set of data at a specified height and velocity, and from the bulk bed material were analyzed using a Zeiss Videoplan 2 Image analyzer. The software used was the "Image Analysis System MOP-Videoplan" distributed by KONTRON Electronics Group.

For each sample selected, a microscope slide was prepared using double sided adhesive tape on which a portion of the selected sample was placed. To ensure a sharp contrast was achieved, each slide was backed with white paper. The sample was then placed under a Zeiss microscope to which the image analyzer was connected via a videocon tube. The magnification used was 50X which provided an average view of about 8 particles at a time. The analyzer was then used to analyze the particles present on each slide of interest. The mode in which the image analyzer was used was the equivalent diameter mode. This mode determined the cross sectional area of each particle sampled and calculated the diameter of a circle with the same area. When a data set was completed, the data was analyzed for particle size distribution. The resulting output (Appendix J) consists of a particle count vs particle size histogram, a cumulative frequency plot and a classification data list. A gaussian distribution fit for the data is also plotted on the histogram and cumulative frequency

plots. The X axis of the plots are normalized with a range of zero (0) to four (4). To determine the actual diameter of the particle in microns for a given normalized value, the normalized value must be multiplied by the conversion factor 248.887.

CHAPTER IV

COMPUTER MODEL

Introduction

This chapter describes the theory, logic flow and testing of a particle trajectory computer model to predict the particle loading in the freeboard due to erupting bubbles. The program, listed in Appendix L, is written in HP BASIC 2.0 and was run on a Hewlett Packard 9816 microcomputer. The output from the model is discussed in chapter VI and compared with experimental results. An in depth analysis of the program logic and structure is given in Appendix L.

Model Theory

The model developed here, is based on calculating the trajectory of a single particle as it is ejected from the bed surface and is acted upon by gravitational and drag forces. The drag force is due to the difference in absolute particle and air velocities. The air velocity is a combination of the initial jet velocity produced when a bubble bursts, and the superficial bed velocity. To ensure that the particle drag is calculated accurately, the following drag coefficient correlation given by White [17] was used.

$$C_d = \frac{24}{Re} + \frac{6}{1 + \sqrt{Re}} + 0.4 \quad (3)$$

where:

C_d = Drag coefficient for sphere
 Re = Reynolds number

Eqn 3 is valid over the range $0 < Re < 10^5$. To calculate the particles position and velocity, the computer uses a forward difference method. Using Newton's Law ($\Sigma F = ma$) the acceleration of the particle due to gravity and drag is determined. Inserting this acceleration into Eqn 4, the particles new velocity is determined.

$$V = V_o + a t \quad (4)$$

where:

V = Particles new velocity
 V_o = Particles present velocity
 a = Acceleration of particle
 t = Time increment of calculation

To determine the particles new position, the velocity calculated in Eqn 4 is inserted into Eqn 5.

$$H = H_0 + \frac{(V_0 + V) t}{2} \quad (5)$$

where:

H = Particles new height
 H₀ = Particles present height
 V₀ = Particles present velocity
 V = Particles new velocity
 t = Time increment of calculation

Using Eqns 3,4,and 5, the trajectory of the particle is calculated from the time it initially leaves the bed until the time that it returns to the bed.

These calculations are repeated over a range of particle diameters from 80 to 570 microns. By determining the residence time of each particle within a specified height increment (ΔH) above the surface of the bed, a particle density distribution above the bed is determined. The height increment (ΔH) used in the program is 2 cm. At the end of each time step when the height calculation (Eqn 5) is completed, the counter representing the particular 2 cm height increment which the particle is in, is incremented by one. Each particle size has its own set of counters to allow individual particle analysis.

The calculated density distribution is then weighted with the particle size distribution of the bulk bed material since the

probability of a given size particle being present at a specified height is dependent upon the number of particles within the system. This is accomplished by multiplying each height counter of a given particle size with the number of particles for that given size present in the input bed distribution. By summing the density values for each set of particle diameters at a given height over the entire freeboard of the bed, the overall particle density above the bed surface is determined.

The model assumes that all the particles are ejected perpendicular to the surface of the bed and are initially at a uniform velocity. Because the model uses single particles for the analysis, the effects of multiparticle interactions are not included in the model.

Testing of Program

To evaluate the validity of the program, two tests were conducted. The first test compared the height solution produced by the computer with a closed form solution. The second test involved running the program with different particle diameter and particle distribution height intervals to ensure that a valid sample size was being used.

Closed Form Solution

To determine a closed form solution for particle height as a

function of initial particle velocity and superficial velocity U_0 , a force balance was used. The forces acting on a particle are gravitational and drag. The gravitational force, F_1 , is simply the volume of the particle multiplied by the particles density and the gravitational acceleration, and can be written as:

$$F_1 = - \frac{\rho_p \pi D^3}{6} g \quad (6)$$

where:

F_1 = Force due to gravity
 ρ_p = Density of particle
 D = Diameter of particle
 g = gravitational acceleration

In order to get a closed form solution that did not involve non-linear differential equations, Stokes flow was used for the closed form solution only. The computer model used the Stokes equation only to compare results with the closed form solution, afterward, Eqn 3 was used. Using the Stokes drag coefficient relation, the drag force on a particle can be determined as:

$$F_2 = 3 (U_0 - U_p) \mu D \quad (7)$$

where:

F_2 = Force due to drag
 U_0 = Superficial bed velocity
 U_p = Velocity of particle
 μ = Absolute viscosity of air
 D = Diameter of particle

By inserting Eqns 6 and 7 into Newton's Law ($\sum F=ma$) and simplifying, the following differential equation is obtained:

$$\ddot{X} + C1 \dot{X} = C2 \quad (8)$$

where:

\ddot{X} = Acceleration of particle

\dot{X} = Velocity of particle

$$C1 = \frac{18\mu}{P_p D^2}$$

$$C2 = C1 U_0 - g$$

boundary conditions:

- 1) $t=0 \quad \dot{X}=U_0$
- 2) $t=0 \quad X=0$

This second order linear differential equation can be solved using the given boundary conditions with the resulting closed form solution given as:

$$X = C3 + \frac{C2}{C1} t - C3 \exp(-C1 t) \quad (9)$$

where:

$$X = \text{Height of particle}$$

$$C3 = \left[U_0 - \frac{C2}{C1} \right] \frac{1}{C1}$$

Using the initial conditions listed in table 2, the solution obtained using the computer model (maximum height= 15.270 cm, time to maximum height= 0.275 sec) was identical to three decimal places with the solution obtained using Eqn 9.

TABLE 2

| | |
|---|------------------------|
| Superficial Velocity (U ₀): | 60.96 cm/s (2 ft/s) |
| Initial particle velocity (U _{po}): | 304.8 cm/s (10 ft/s) |
| Particle diameter: | 200 microns |
| Particle density: | 5000 kg/m ³ |
| Time increment (computer): | 0.001 sec |
| Jet velocity: | 0.0 cm/s |

List of parameters used to check computer calculations against closed form solution.

Sample Size Sensitivity Test

To ensure that appropriate sample sizes were used to minimize errors due to coarse sampling intervals, two sensitivity tests were run. One test involved changing the particle diameter interval from 10 microns to 5 microns. The second test changed the height sampling interval (ΔH) from 2 cm to 5 cm and then 1 cm. For each of the tests, the same initial conditions were input into the program. Table 3 shows the resulting output from the program listing the initial conditions and the resulting diameter versus maximum height data calculated. Fig. 15 shows a plot of the calculated maximum height vs particle diameter data listed in table 2. Fig. 16 shows the bed particle distribution used for each of the tests.

Fig. 17a shows the entrainment calculation using a diameter interval of 10 microns and a ΔH of 2 cm. Fig. 17b shows the same calculation using a diameter interval of 10 microns and a ΔH of 5 cm. The curve is not as smooth but still retains the same general shape. The peak of the curve shown in Fig. 17b occurs at a height of about 20 cm whereas the peak in Fig. 17a occurs at about 16 cm. A semi-log plot of these curves would show that the slope of the line to the right of the peak would be larger for the data represented by Fig. 17b. The effect of maintaining ΔH at 5 cm but decreasing the diameter interval to 5 microns is shown in Fig. 17c. There is no readily detectable difference between Fig.

Mean Bed Velocity= 57.912 cm/s
 Initial Particle Velocity= 97.2312
 Peak Jet Velocity= 609.6
 Gas Jet Duration= .02 s

| Diameter um | Maximum Height cm | Max Ht Time seconds | Diameter um | Maximum Height cm | Max Ht Time seconds |
|----------------|-------------------------|---------------------------|----------------|-------------------------|---------------------------|
| 80 | 56.1 | .282 | 90 | 57.0 | .290 |
| 100 | 57.2 | .297 | 110 | 56.8 | .302 |
| 120 | 55.8 | .305 | 130 | 54.4 | .307 |
| 140 | 52.7 | .307 | 150 | 50.8 | .305 |
| 160 | 48.8 | .303 | 170 | 46.8 | .299 |
| 180 | 44.7 | .295 | 190 | 42.7 | .290 |
| 200 | 40.7 | .285 | 210 | 38.8 | .280 |
| 220 | 37.0 | .275 | 230 | 35.3 | .270 |
| 240 | 33.7 | .264 | 250 | 32.2 | .259 |
| 260 | 30.8 | .254 | 270 | 29.5 | .249 |
| 280 | 28.2 | .245 | 290 | 27.1 | .240 |
| 300 | 26.1 | .236 | 310 | 25.1 | .232 |
| 320 | 24.2 | .228 | 330 | 23.3 | .224 |
| 340 | 22.5 | .220 | 350 | 21.8 | .217 |
| 360 | 21.1 | .213 | 370 | 20.4 | .210 |
| 380 | 19.8 | .207 | 390 | 19.2 | .204 |
| 400 | 18.7 | .201 | 410 | 18.2 | .199 |
| 420 | 17.7 | .196 | 430 | 17.3 | .194 |
| 440 | 16.9 | .191 | 450 | 16.5 | .189 |
| 460 | 16.1 | .187 | 470 | 15.7 | .185 |
| 480 | 15.4 | .183 | 490 | 15.1 | .181 |
| 500 | 14.8 | .179 | 510 | 14.5 | .178 |
| 520 | 14.2 | .176 | 530 | 14.0 | .174 |
| 540 | 13.7 | .173 | 550 | 13.5 | .171 |
| 560 | 13.2 | .170 | 570 | 13.0 | .168 |

Table 3 Listing of Input and Resulting Maximum Particle Heights with Time to Maximum Height. These Values Were Used During the Increment Sensitivity Tests.

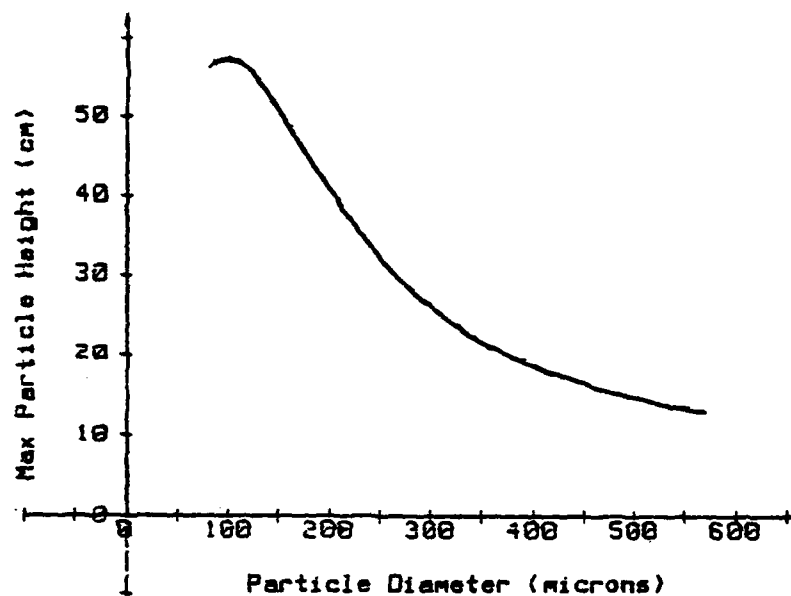


Fig. 15 Maximum Particle Height vs Particle Diameter

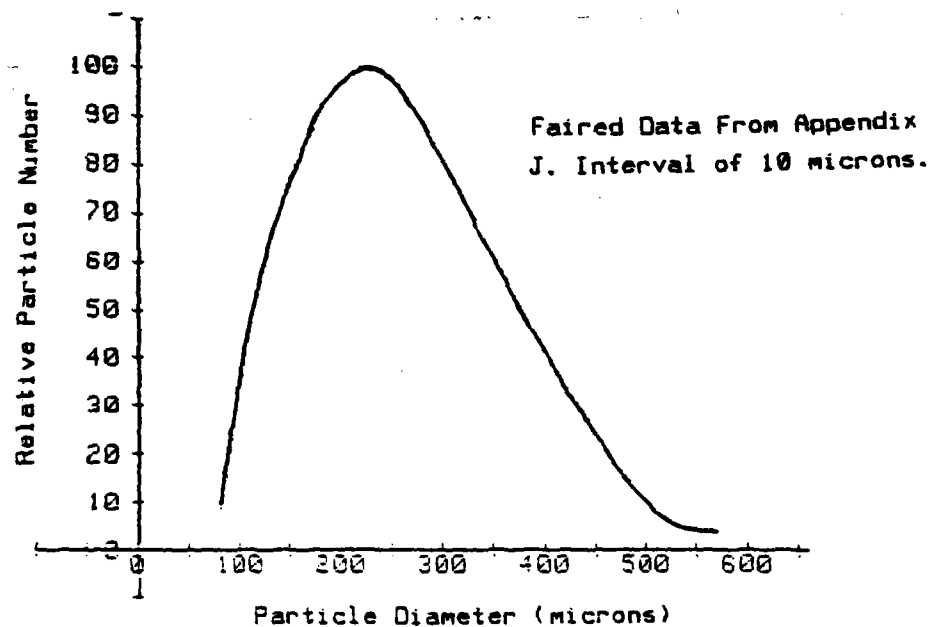
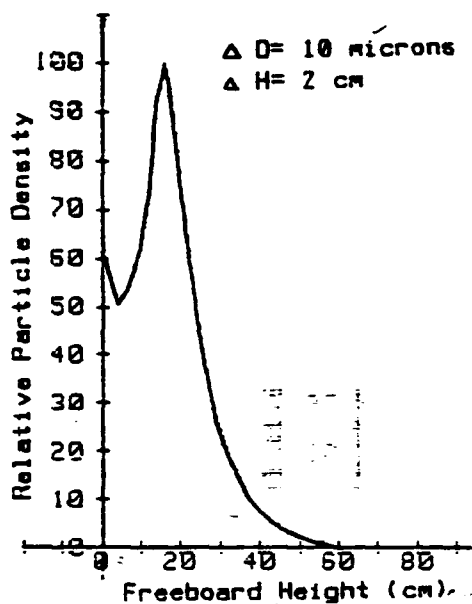
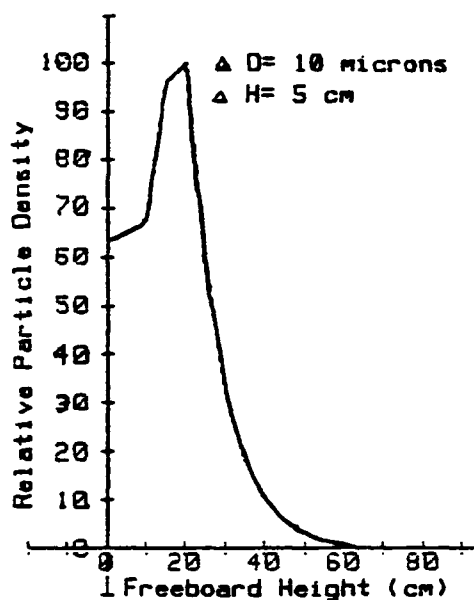


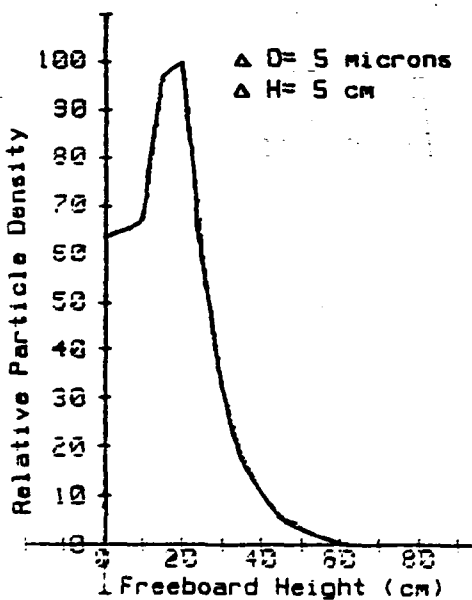
Fig. 16 Particle Size Distribution of Bed Mass Used in Increment Sensitivity Analysis.



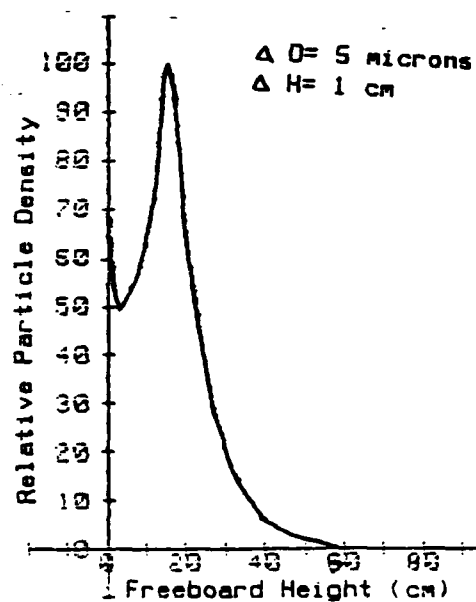
a



b



c



d

Fig. 17 Plots of Relative Particle Density vs Freeboard Height showing the effects of varying Diameter Interval and Height Interval.

17c and Fig. 17b. In Fig. 17d, the effect of changing ΔH to 1 cm and diameter spacing to 5 microns is shown. The difference between Fig. 17a and Fig. 17d is barely noticable and no detectable change in the slope to the right of the peaks is present. As a result of this analysis, the program was operated with a ΔH of 2 cm and a diameter interval of 10 microns. This reduced the calculation time to half of that required when using a diameter spacing of 5 microns when the same total diameter span was used and, as was seen in Figs. 17a and 17d, the difference in output does not require the finer increment.

CHAPTER V

EXPERIMENTAL RESULTS AND DISCUSSION

Minimum Fluidization Velocity

Fig. 18 is a plot of mean bed velocity (U_0) vs pressure drop through the bed (P_b). The velocity values were determined using the program in Appendix G and the pressure data listed in Appendix I. From this plot, the minimum fluidization velocity (U_{mf}) for the bed conditions used during this study is determined to be 0.15 m/s (0.5 Ft/sec).

Entrainment Analysis

Table 4 lists the averaged sample weights and their standard deviations for the samples (Appendix I) collected by the sampling apparatus. Looking at the standard deviation of the sample groups, the standard deviation is fairly large compared to the average values. However, visual observations of the fluidized bed in operation would suggest that a larger standard deviation would be expected. The short sample cycle (2 ms) and the bubble burst activity in the bed are the main reasons for this conclusion. The average standard deviation is 29 % of the average sample weight

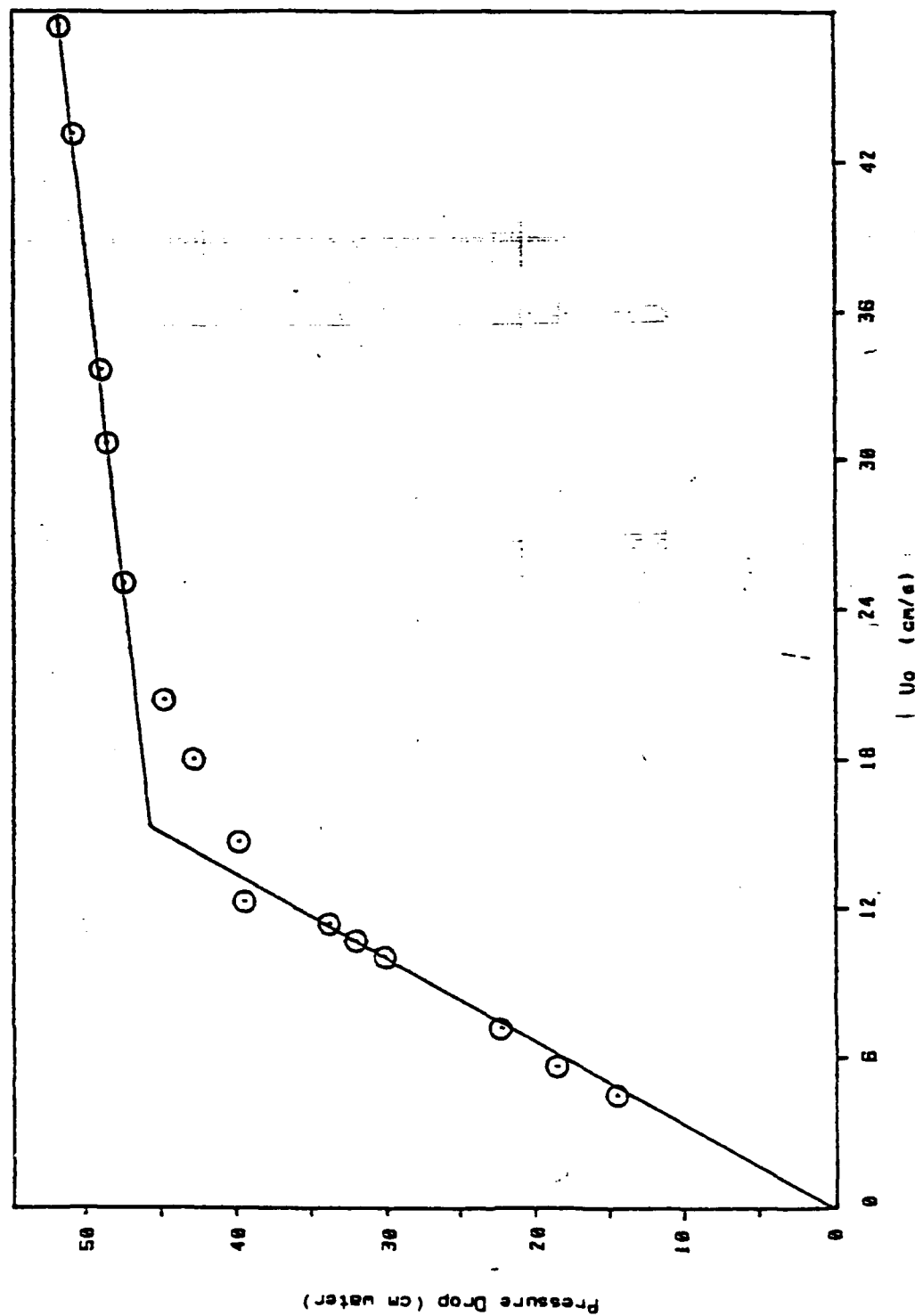


Fig. 18 Plot of Pressure Drop Across Bed vs U_o . The Estimate of U_{mf} from this Plot is 16.2 cm/s (0.5 ft/s).

and the range extends from 68 % of the average for the sample set numbers 106 thru 115 to only 7 % of the average for the samples 285 thru 295. This variation is believed to be due to the nature of the bubble activity within the bed. It would appear that when a bubble erupts at a time just prior to closure of the trap, a sample weight greater than the average would be obtained.

However, when no bubble has been present, the material caught by the trap should consist mainly of particles returning to the bed

and therefore be below the average weight caught. Table 4 also shows the density of each sample collected. These values were determined by dividing the averaged sample weights by the volume of the sample trap which is 43.02 cubic cm.

TABLE 4

Superficial Bed Velocity (U_o): 58.1 cm/s (1.905 ft/s)
 Non-dimensionalised velocity (U_o/U_{mf}): 3.81

| Sample Numbers | Height Above Bed (cm) | Average Weight (grams) | Standard Deviation (grams) | Average Density (grams/cm) |
|----------------|-----------------------|------------------------|----------------------------|----------------------------|
| 286-295 | 3.8 | 7.22 | 0.51 | 1.68 (-01) |
| 246-255 | 7.6 | 4.48 | 0.72 | 1.04 (-01) |
| 116-125 | 12.4 | 2.41 | 0.76 | 5.60 (-02) |
| 166-175 | 17.8 | 1.08 | 0.16 | 2.51 (-02) |
| 76-85 | 22.2 | 1.32 | 0.23 | 3.07 (-02) |
| 176-185 | 31.1 | 0.31 | 0.10 | 7.21 (-03) |

Superficial Bed Velocity (U_o): 48.3 cm/s (1.585 ft/s)
 Non-dimensionalised velocity (U_o/U_{mf}): 3.17

| Sample Numbers | Height Above Bed (cm) | Average Weight (grams) | Standard Deviation (grams) | Average Density (grams/cm) |
|----------------|-----------------------|------------------------|----------------------------|----------------------------|
| 276-285 | 5.1 | 4.35 | 1.05 | 1.01 (-01) |
| 236-245 | 8.9 | 1.88 | 0.22 | 4.37 (-02) |
| 96-105 | 13.6 | 1.36 | 0.32 | 3.16 (-02) |
| 156-165 | 19.1 | 0.60 | 0.12 | 1.39 (-02) |
| 56-65 | 24.1 | 0.92 | 0.36 | 2.14 (-02) |
| 186-195 | 31.8 | 0.18 | 0.04 | 4.18 (-03) |

Superficial Bed Velocity (U_o): 39.5 cm/s (1.297 ft/s)
 Non-dimensionalised velocity (U_o/U_{mf}): 2.59

| Sample Numbers | Height Above Bed (cm) | Average Weight (grams) | Standard Deviation (grams) | Average Density (grams/cm) |
|----------------|-----------------------|------------------------|----------------------------|----------------------------|
| 266-275 | 5.7 | 1.31 | 0.37 | 3.05 (-02) |
| 226-235 | 9.5 | 0.62 | 0.17 | 1.44 (-02) |
| 126-135 | 14.3 | 0.28 | 0.08 | 6.51 (-03) |
| 136-145 | 19.7 | 0.08 | 0.04 | 1.86 (-03) |
| 86-95 | 24.8 | 0.09 | 0.05 | 2.09 (-03) |
| 196-205 | 32.4 | 0.06 | 0.02 | 1.39 (-03) |

TABLE 4 (cont)

Superficial Bed Velocity (U_0): 35.4 cm/s (1.161 ft/s)
 Non-dimensionalised velocity (U_0/U_{mf}): 2.32

| Sample Numbers | Height Above Bed (cm) | Average Weight (grams) | Standard Deviation (grams) | Average Density (grams/cm ³) |
|----------------|-----------------------|------------------------|----------------------------|--|
| 256-265 | 6.4 | 0.63 | 0.13 | 1.46 (-02) |
| 216-225 | 10.2 | 0.32 | 0.04 | 7.44 (-03) |
| 106-115 | 14.9 | 0.22 | 0.15 | 5.11 (-03) |
| 146-155 | 20.3 | 0.02 | 0.01 | 4.65 (-04) |
| 66-75 | 26.0 | 0.12 | 0.04 | 2.79 (-03) |
| 206-215 | 33.0 | 0.01 | 0.004 | 2.32 (-04) |

List of experimental data showing sample averages, standard deviations, heights, and velocity conditions measured. Density values are calculated by dividing the average sample weight by the sample trap volume.

Fig. 19 shows the relationship between the average particle density caught in the sample trap and the sample trap height above the bed surface as a function of U_0/U_{mf} .

For the relatively low fluidization velocities used during the data measurements, (maximum $U_0/U_{mf} = 3.81$) the freeboard height can be assumed infinite. Using this assumption implies that all of the particles return to the bed and none are elutriated, ie complete reflux. Under these conditions, the following equation has been suggested by Lewis et al [3] and Kunii and Levenspiel [1] to model the particle loading within the freeboard.

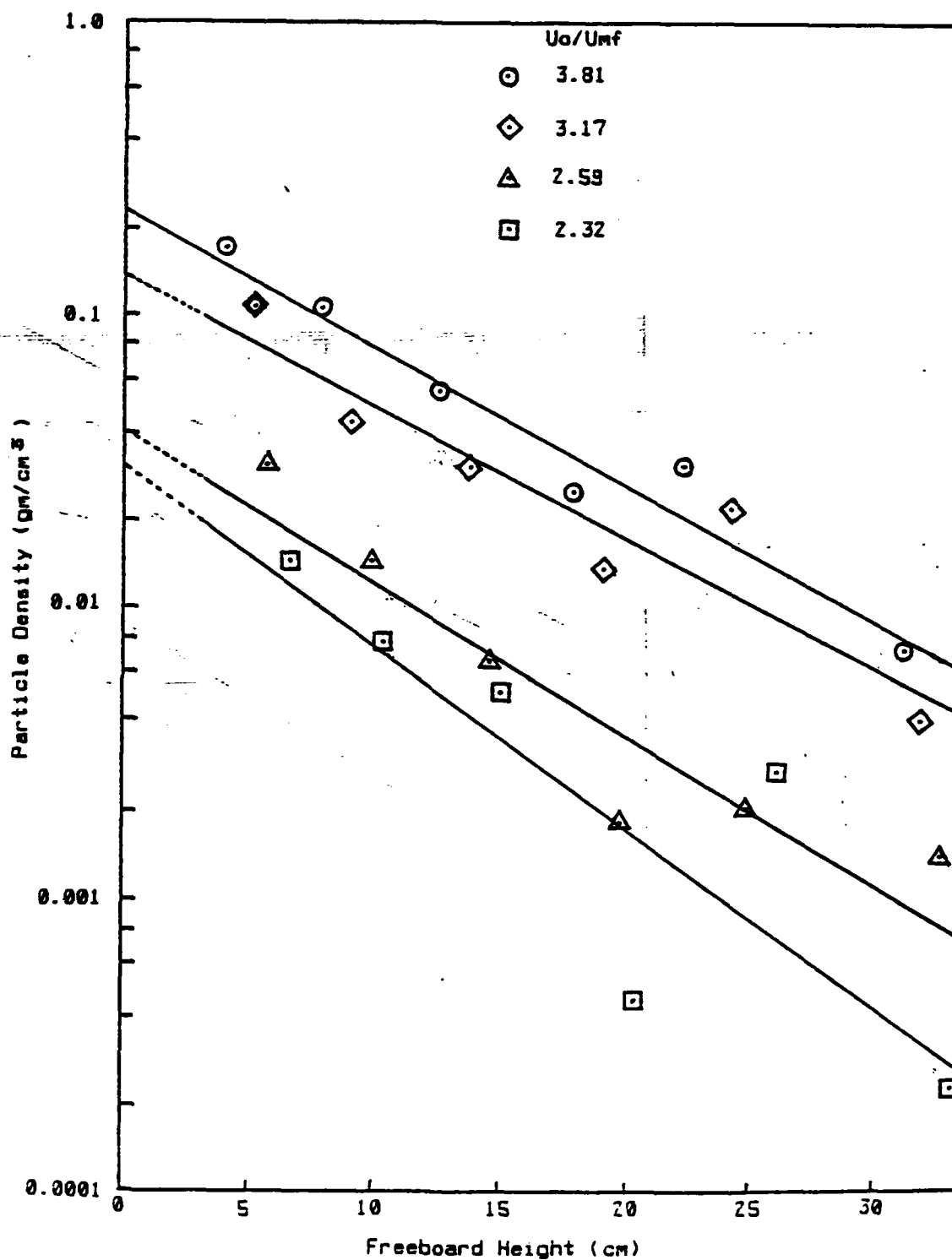


Fig. 19 Plot of Particle Density vs Freeboard Height as a Function of U_o/U_{mf} . This data was Obtained Using the Particle Sampler.

$$Pr = Po \exp(-a l) \quad (10)$$

where:

Pr = Particle density at height l
 Po = Particle density at (+)bed surface
 a = Characteristic particle decay length
 l = Height above bed surface

Table 5 shows the values for the parameters Po and a obtained by linear regression for the curves shown in Fig. 19.

TABLE 5

| Uo/Umf | Po | a | Correlation Coefficient |
|--------|-------|--------|----------------------------|
| 3.81 | 0.238 | 0.1097 | 0.979 |
| 3.17 | 0.137 | 0.1029 | 0.944 |
| 2.59 | 0.040 | 0.1181 | 0.937 |
| 2.32 | 0.031 | 0.1399 | 0.857 |

$$Pr = Po \exp(-a l)$$

Results of linear regression analysis for particle loading density (grams/cm) vs height above the bed surface (cm).

The parameter Po physically represents the particle loading density which would be obtained if the sample were taken at the surface of the bed. This is not necessarily the case as is indicated by the computer model which is discussed in chapter VI, but is only a parameter describing the particle loading distribution in the region of the data obtained. The dashed lines below freeboard heights of 4 cm indicate the region in question. The parameter a is a characteristic length of decay for the particle flux.

A correlation between the values for Po in table 5 and Uo/Umf is shown in Fig. 20. This plot shows that Po is closely related with Uo/Umf . Po varies with $(Uo/Umf - 1)$ approximately to the 2.9

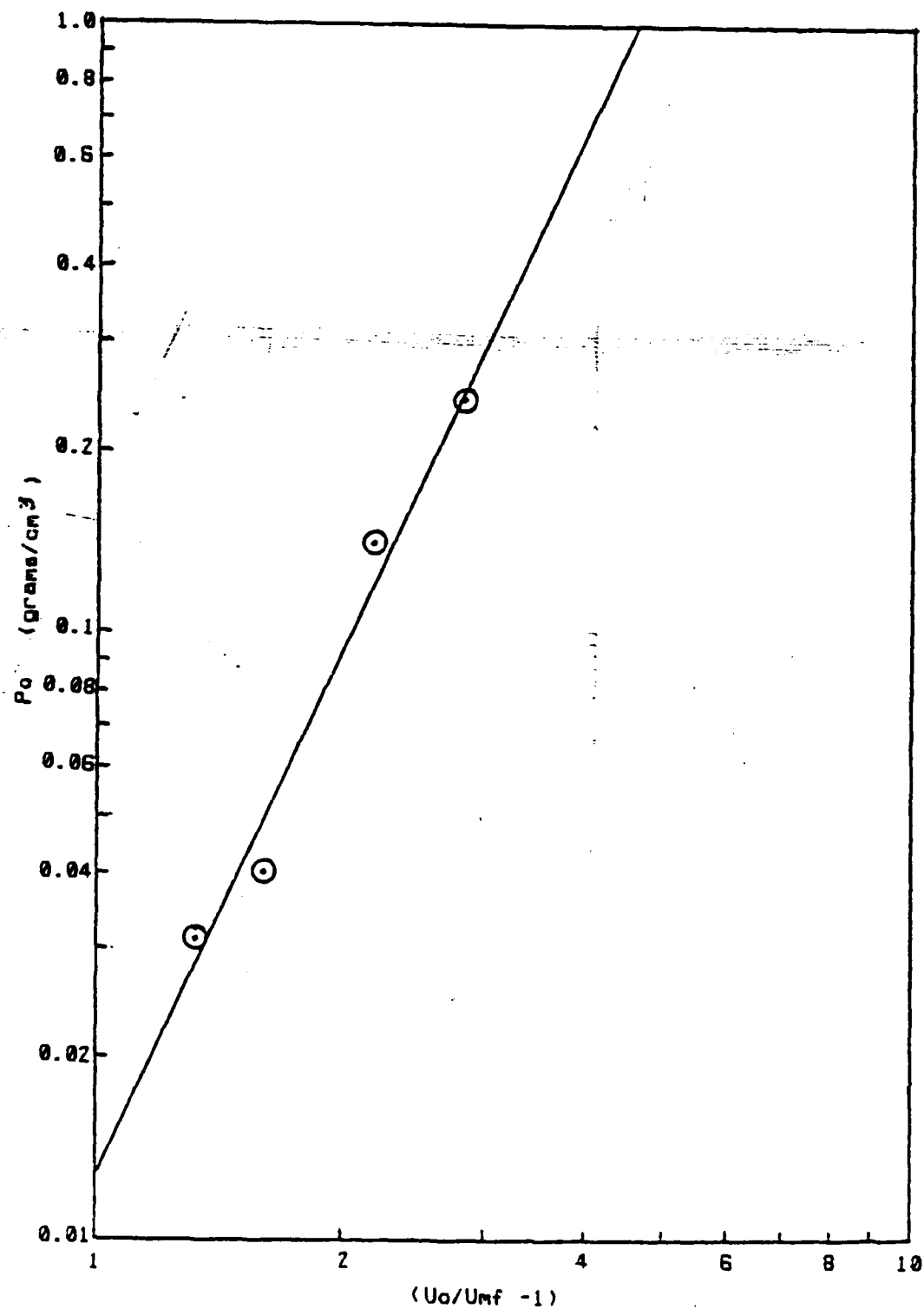


Fig. 20 Plot of P_o vs $(U_o/U_{mf} - 1)$ Showing Strong Dependence of P_o on U_o .

power, where as Walsh et al [10] determined the coefficient to be about 2.1. Wen and Chen [5] reported a correlation for particle flux which is proportional to bubble diameter and $(U_o/U_{mf} - 1)$ to the 5/2 power. These correlations are listed in table 6.

TABLE 6

| | | |
|--------------|--------------------------------|-----------|
| Present work | $B = 0.13 (U_o/U_{mf} - 1)$ | kg/ m sec |
| Wen and Chen | $B = 1.34 (04) (U_o - U_{mf})$ | kg/ m sec |
| Walsh et al | $B = 18 (U_o - U_{mf})$ | kg/ m sec |

Comparison of least square fit relations for P_o as functions of U_o and U_{mf} .

The differences in these correlations are due to the different bed configurations in which the data was taken and the measurement technique used. The present work utilized a bed with a relatively closely spaced tube configuration and steel grit (S.G. 8.1, median size 230 microns) for the bed mass. Both ascending and descending particle fluxes were captured in the sample. The work of Walsh et al [10], used a bed with two (2) widely spaced horizontal serpentine tubes and Ottawa sand (S.G. 2.6, median size 755 microns). Also, only descending particle flux was used in determining their relations. The correlations of Wen and Chen [5] are a result of studies conducted on previous research using cylindrical column beds and low mass bed materials

(S.G. 0.8 - 2.6). The data for these analysis is based mainly on pressure measurements.

It has been observed by Lewis et al [3] and Wen and Chen [5] that a is not a strong function of U_0 . Both of these studies recommend that the characteristic particle decay length, $1/a$, could be approximated by an expression of the form:

$$1/a = C U_0 \quad (11)$$

Table 7 is a list of correlations obtained by other studies and in the present work. The study by Lewis et al [3] was conducted with 75 micron glass spheres in a cylindrical bed. Fig. 21 shows the relationship between $1/a$ and U_0 in the present work.

TABLE 7

| | | |
|--------------|--------------------------------------|---|
| Present work | $1/a = (0.19 \pm 0.03 \text{ s})U_0$ | m |
| Lewis et al | $1/a = (1.42 \pm 0.14 \text{ s})U_0$ | m |
| Wen and Chen | $1/a = (0.25 \pm 0.09 \text{ s})U_0$ | m |
| Walsh et al | $1/a = (0.32 \pm 0.05 \text{ s})U_0$ | m |

Comparison of least square fit relations for $1/a$ as functions of U_0 (m/s).

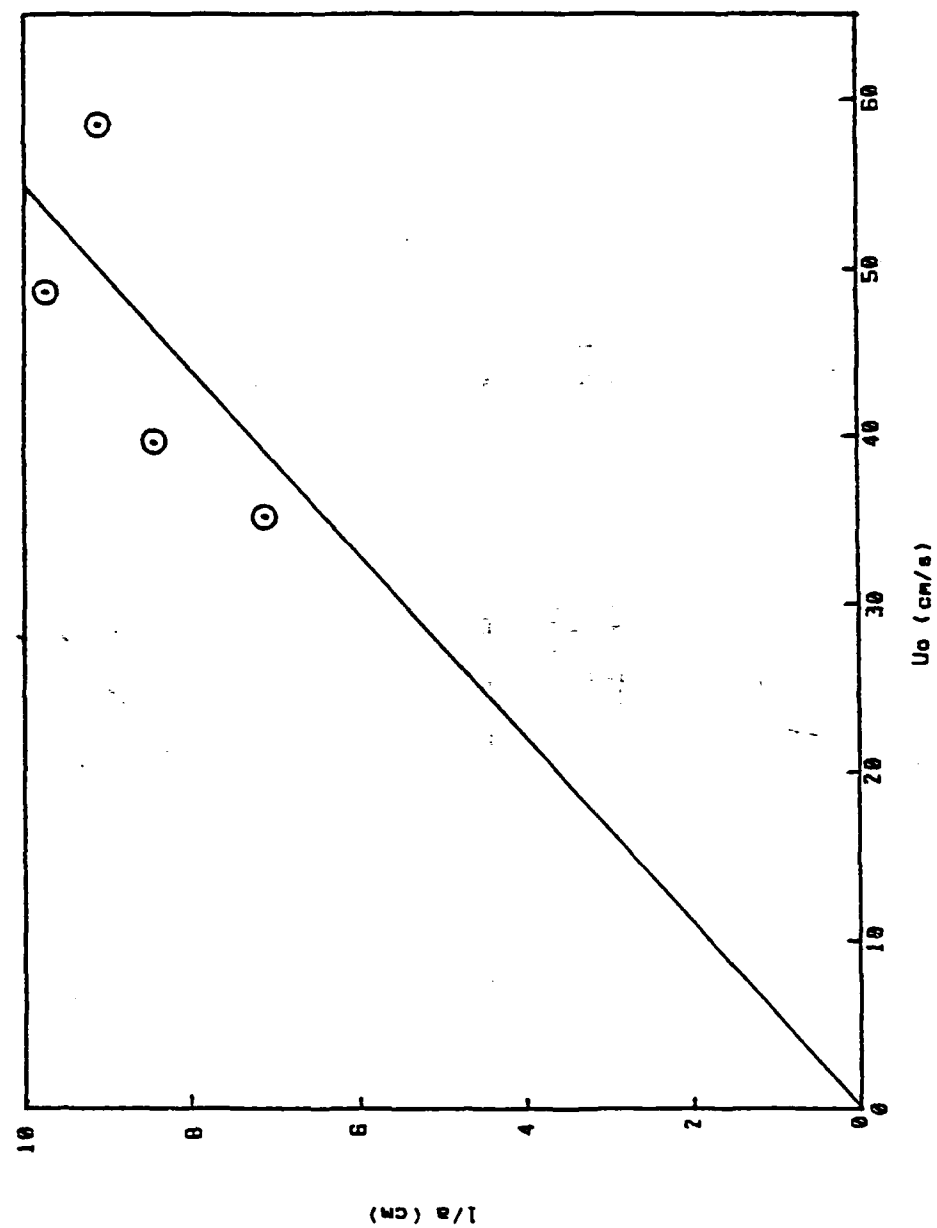


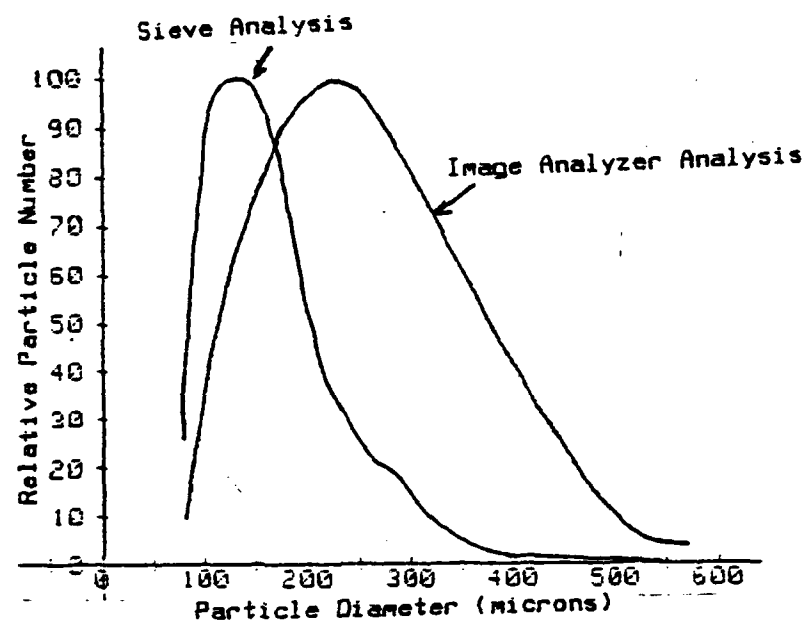
FIG. 21 Plot of $1/a$ vs U_0 Showing Linear Dependence of $1/a$ on U_0 .

Particle Size Distribution

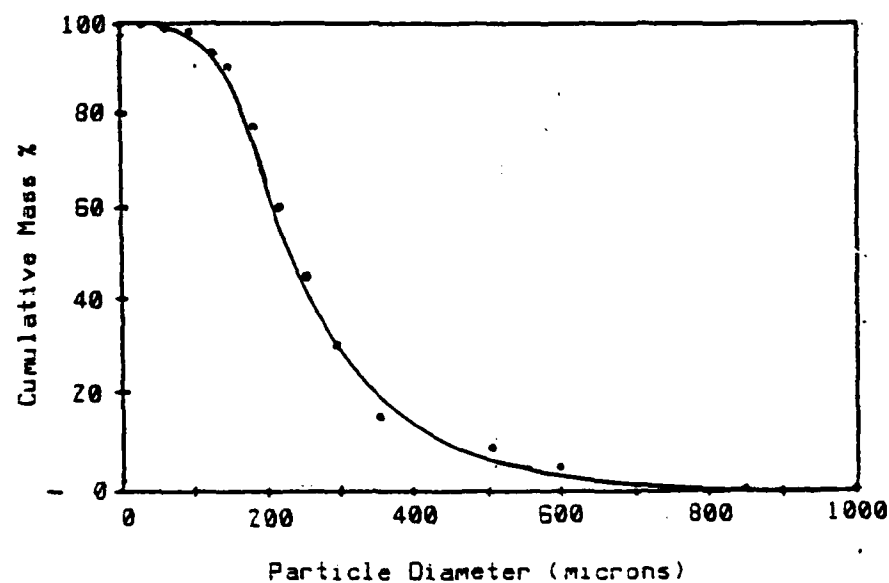
Two methods for determining particle size distribution were used. The sieve method, described in Appendix E, was used for bed material analysis only, due to the small sample sizes obtained from the trap. To analyze the small trap samples, an image analyzer was utilized. The procedure used with the image analyzer is described in the experimental procedure chapter.

The sieve data representing bed mass as a function of particle size, is listed in Appendix E. Fig. 22a shows the bed mass data converted to particle number as a function of particle diameter where the interval of particle diameter between successive measurements is 10 microns. These plots are faired from the data listed in Appendices E and J. Fig. 22b shows the bed mass distribution. The conversion from a mass distribution to a particle number distribution was calculated assuming that each particle was spherical in shape. The volume corresponding to a given particle diameter was multiplied by the particle density to get a unit particle mass. The mass fraction of the sieve analysis corresponding to the specified particle diameter was then divided by the unit particle mass to obtain the representative particle number. The overall resulting particle number distribution curve was then normalized with respect to a maximum value of 100.

The particle size distribution data obtained from the image



a) Particle Distributions



b) Mass Distribution

Fig. 22 Particle Size vs Mass distribution and Particle Number of Bed Material.

analyzer is listed in Appendix J. The image analyzer was used to analyze the bed mass and sample data from the $U_o/U_{mf} = 3.81$ data set. The bar graphs and the cumulative percentage plots show the number of particles viewed by the image analyzer plotted as a function of normalized particle diameter.

Fig. 22a shows a plot of the particle number distribution as a function of particle diameter as determined by the image analyzer. The data is normalized with respect to 100 and is compared with the data as determined by the sieve analysis. The discrepancy between the two plots can be explained by the methods used to determine the respective data. The analyzer first determines the cross sectional area of the viewed particle. A circle, having the same cross sectional area, is then calculated. This results in averaging the smaller minimum diameter with the larger maximum diameter of all particles with long cylindrical or ellipsoidal shapes. In the sieve however, a large portion of the particles will pass through the sieve screen by means of the small cross sectional area presented by their longitudinal direction. To be consistent in the following sections, the image analyzer data will be used to correlate all particle density distributions.

The particle size distribution as a function of height above the bed surface was evaluated using the data collected at $U_o/U_{mf} = 3.81$. The image analyzer was used to determine the distribution by viewing three (3) random samples from each of the six (6) height positions. Table 8 lists the various statistical values

for the particle size distribution data obtained (Appendix J).

TABLE 8

| Freeboard Height | Average Diameter | Median Diameter | Mode Diameter | Diameter at 50% of Cumulative Number Distribution |
|---------------------|---------------------|--------------------|------------------|---|
| (cm) | (microns) | (microns) | (microns) | (microns) |
| 3.8 | 199 | 192 | 142 | 159 |
| 7.6 | 219 | 214 | 187 | 203 |
| 12.3 | 204 | 189 | 162 | 167 |
| 17.8 | 179 | 164 | 154 | 179 |
| 22.2 | 197 | 179 | 152 | 177 |
| 31.1 | 212 | 197 | 194 | 190 |

Statistical values for particle number distribution as a function of freeboard height. A complete listing of the data is given in Appendix J.

Fig. 23 shows these values plotted against the bed height at which they were taken. The excursion of points at the 7.6 cm height is assumed to be due to analysis error. The linear regression lines for the average and median values show that they are weak functions of collection height. For the particle diameter values representing the mode and the 50% point on the cumulative percentage plot, the linear regression lines show a stronger dependence on collection height.

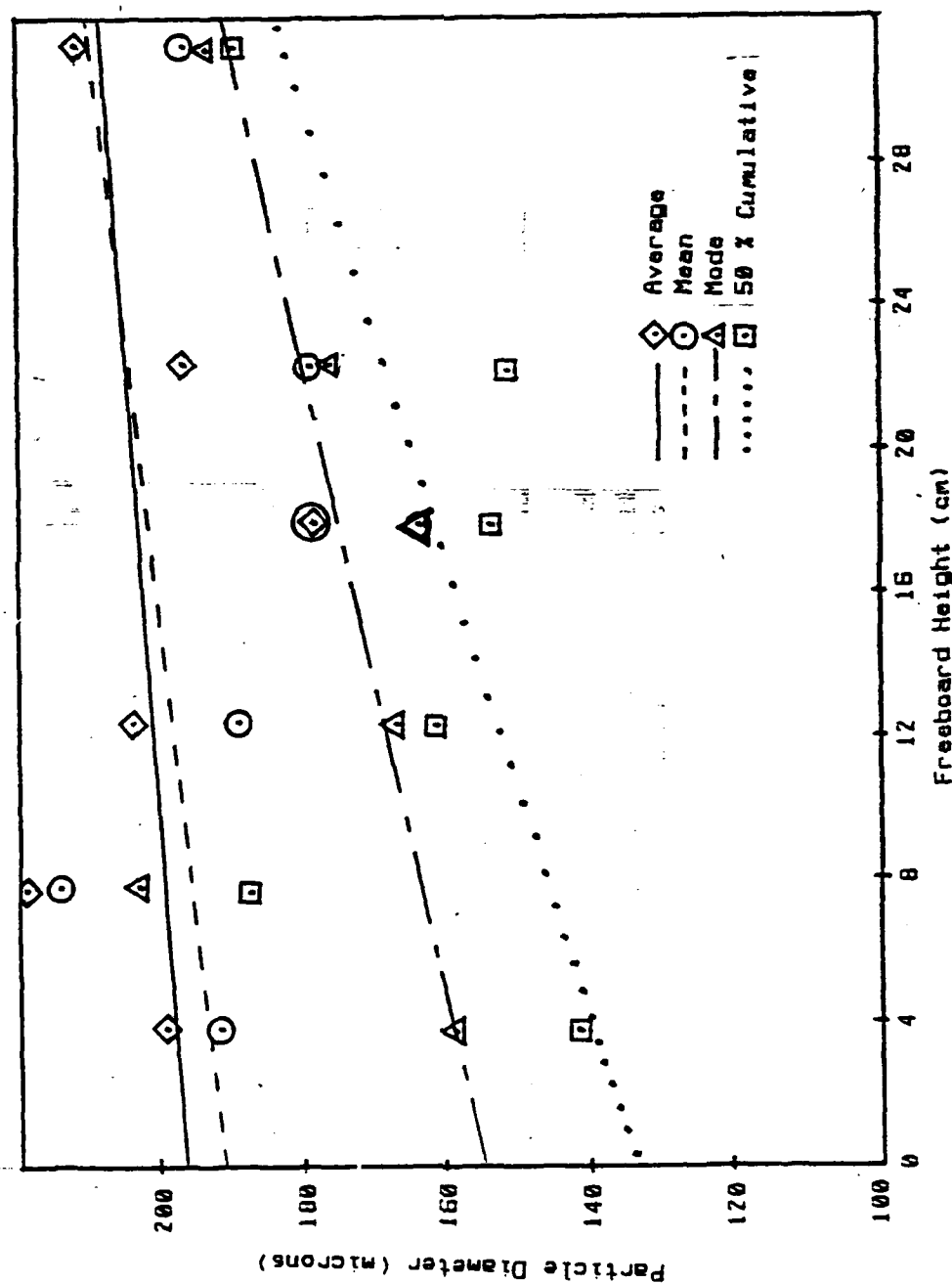


Fig. 23 Analysis of Variation of Particle Size vs Freeboard Height.

Oscilloscope Trace Analysis

Figs. 24 thru 27 show examples of the oscilloscope traces given in Appendix K. Figs. 24 and 25 represent the traces obtained during low U_0 conditions. Under these conditions, the normal bubble probe output is high (+ 5 volts dc). When a bubble erupts, particles are thrown from the surface of the bed and eclipse the light path at the tip of the probe (trace goes to zero). Figs. 26 and 27 represent the traces obtained at higher U_0 conditions when the bubble probe is normally eclipsed (bubble probe output is low, zero) by particles. The presence of a bubble is detected by a high output from the bubble probe due to the bubble creating a void through which the light beam can pass. The anemometer output just above the bubble probe is used to determine the velocity of the gas jet leaving the erupting bubble. As seen in the figures, there is not always a bubble associated with a gas jet and vice versa. This is due to the anemometer probe being slightly offset from the bubble probe as described in the experimental procedure section.

The gas jet in Fig. 24 is delayed 5 ms and the gas jet in Fig. 25 is delayed 35 ms from the point where the bubble traces begin their excursion to the zero (eclipsed) condition. Since the separation between the bubble probe and the anemometer is 1 cm, this results in an estimated jet velocity of 200 cm/s (Fig. 24)

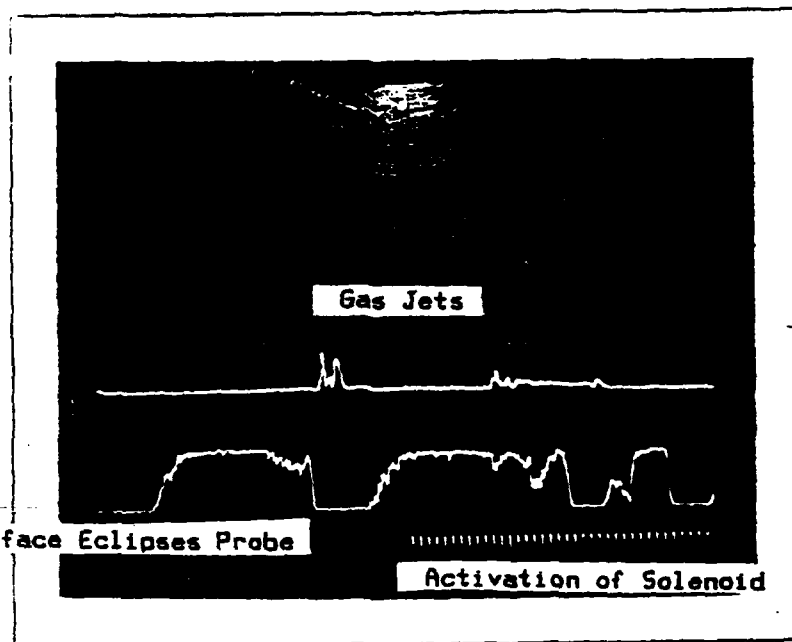


Fig. 24 Oscilloscope Trace of Bubble Probe, Anemometer Probe, and Solenoid Actuation at Low U_0 .

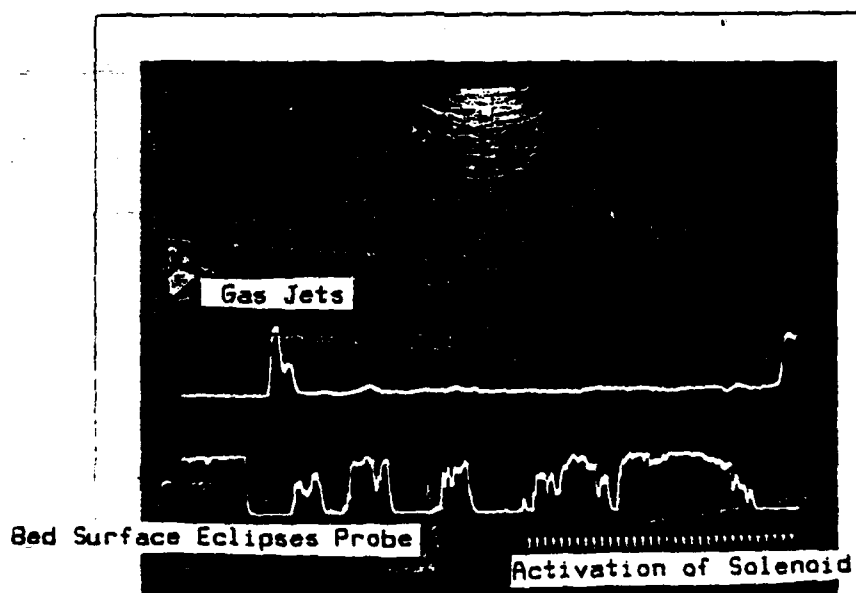


Fig. 25 Oscilloscope Trace of Bubble Probe, Anemometer Probe, and Solenoid Actuation at Low U_0 .

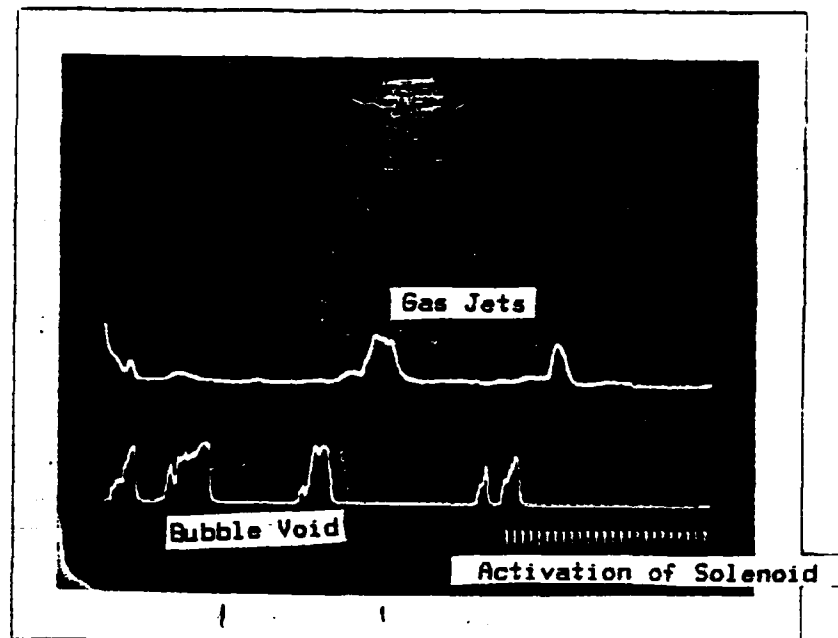


Fig. 26 Oscilloscope Trace of Bubble Probe, Anemometer Probe, and Solenoid Actuation at Higher U_0 .

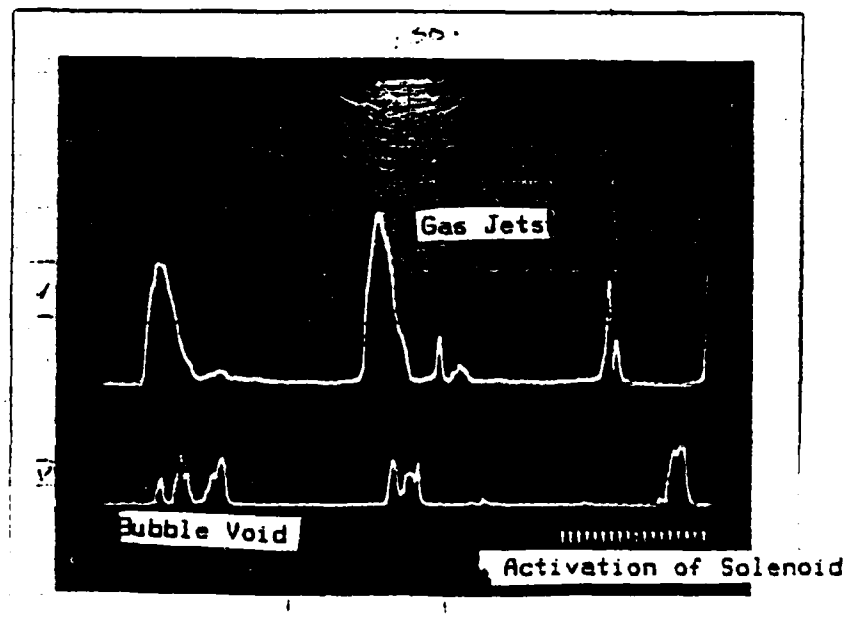


Fig. 27 Oscilloscope Trace of Bubble Probe, Anemometer Probe, and Solenoid Actuation at Higher U_0 .

and 28 cm/s (Fig. 25). Using the calibration curve in Appendix M, the velocities are determined to be 518 cm/s for the jet in Fig. 24 and 792 cm/s for the jet in Fig. 25. The large difference in these values could be due to a bulge in the bed surface from the bubble underneath eclipsing the bubble probe. If this is the case, there would be a delay between the time at which the bubble probe was eclipsed and the eruption of the bubble from the bed surface.

An analysis of Figs. 26 and 27 results in the same discrepancies between velocities calculated from delay times and measured by the anemometer probe. Fig. 27 shows another phenomena which occurs quite frequently. The gas jet appears before the bubble is detected. There are several possibilities which can explain these occurrences. First, the bubble occurs off center from the bubble probe. Under this condition, the bubble may erupt and initiate a jet which is registered by the anemometer. The bubble then continues to rise and the side of the bubble is registered by the bubble probe. This explanation can be altered to include bubbles coalescing below the surface. Under this condition, a bubble may be pulled into the vortex of an already erupting bubble and it eclipses the bubble probe.

An analysis of the jet velocities and durations for all the oscilloscope traces in Appendix K, resulted in the data listed in table 9. In later calculations, the values to be used for the jet velocity and duration will be 609.6 cm/s (20 ft/s) and 20 ms

respectively.

TABLE 9

| | Average | | Stnd Dev | |
|--------------|---------|------|----------|------|
| Jet Velocity | 689 | cm/s | 533 | cm/s |
| | 22.5 | ft/s | 18. | ft/s |
| Jet duration | 21.25 | ms | 13.22 | ms |

Average and standard deviation of jet velocity determined from oscilloscope traces in Appendix K.

Sample Weight Versus Bed Activity Correlation

The main purpose of inserting the bubble and anemometer probe beneath the sampling apparatus was to determine whether a correlation exists between the sample weight collected and the presence of bubble eruptions and gas jets. To evaluate the photographs taken of the oscilloscope traces (Appendix K), the following information was required:

- A. The average velocity of the particles as they travel from the bed surface to the trap.
- B. The distance the particle must travel to reach the trap.
- C. The closure time of the trap relative to the bubble eruptions and gas jets.

The average particle velocity was calculated by determining the average particle size and using the height output from the computer trajectory model. The average particle size as determined by the image analyzer was 180 microns. To determine the average velocity using the model, the following initial conditions were input to the program:

Superficial velocity (U_0) = 57.9 cm/s (1.9 ft/s)

This was the actual velocity measured during sampling.

Jet velocity (U_j) = 609.6 cm/s (20 ft/s)

This value was determined from the anemometer data.

Jet duration (t_{jet}) = 20 ms

This value was determined from the oscilloscope traces.

The height attained by a 180 micron particle, as determined by the model with the above conditions is 44.7 cm in 0.295 seconds. This results in an average velocity of $44.7/0.295 = 151.5$ cm/s (4.97 ft/s).

The distance a particle must travel to reach the center of the trap from the bed surface is obtained from the data listed in Appendix I. Since trap height is measured from the bed surface to the bottom of the trap, 4 cm (0.13 ft) must be added to the trap

heights to obtain the distance to the center of the trap. The total time required for the particles to leave the bed surface and arrive at the center of the trap can now be determined. Table 10 shows the transit time for each set of data for which the oscilloscope traces were photographed (Appendix K).

TABLE 10

| Data set Number | Trap Height Bottom (cm) | Trap Height Center (cm) | Total Transit Time (ms) | Time Before Actuation (ms) |
|-----------------------|----------------------------------|----------------------------------|----------------------------------|-------------------------------------|
| 56-65 | 24.13 | 27.13 | 179 | 136 |
| 66-75 | 26.03 | 30.03 | 198 | 155 |
| 76-85 | 22.23 | 26.23 | 173 | 130 |
| 86-95 | 24.76 | 28.76 | 190 | 147 |
| 96-105 | 13.65 | 17.65 | 116 | 73 |

List of transit times for particles traveling from the bed surface to the center of the trap. The time prior to actuation of the sample trap is also shown (Total time - 42.6 ms).

The total closure time of the sampling apparatus (closure of solenoid power supply switch S1 until trap is shut) is determined in Appendix D to be 42.6 ms. This value is subtracted from the particle transit time to obtain the time before actuation in which particles leaving the bed surface will be caught in the trap.

To determine whether or not a correlation exists between the

weight of a sample and the amount of bed activity present in the bed, a weighted analysis was used. Each sample was evaluated three ways. First, if the sample weight was less than the average sample weight, a weight factor (W) of -1 was assigned to it. If the sample weight was greater than the average, a weight factor of +1 was assigned. Second, the oscilloscope trace was analyzed at the point corresponding to the "time before actuation" listed in Table 10. This position is the time before the solenoid power supply trace is present (Fig. 28). If the trace showed signs of a bubble eruption or a gas jet at this point, the position factor (p) was assigned a value of +1. If no activity was present, the position factor was assigned a value of -1. Third, each trace was analyzed again at the "before actuation time" but bed activity within a ± 25 ms region was counted. If there was bed activity within this region, the region factor (r) was assigned the value of +1. If no activity was present, the region factor was assigned the value of -1. The following equation was used to assign a correlation factor to each sample:

$$Q = W p + W r \quad (10)$$

where:

Q = Correlation factor

W = +1 if sample is $>$ average of data set
 -1 if sample is $<$ average of data set

p = -1 if no activity is present in bed
 +1 if bubble or gas jet activity present

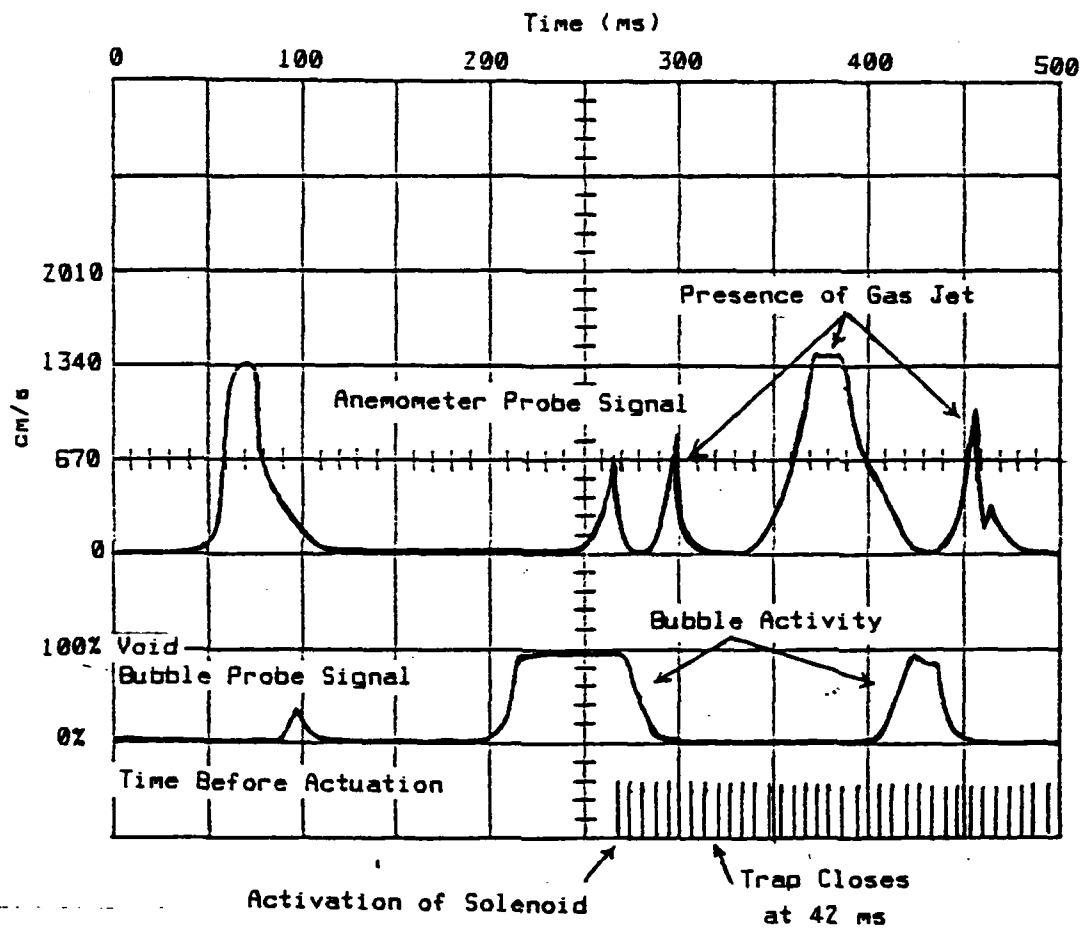


Fig. 28 Typical Oscilloscope Trace During Sampling Procedure.

$r = -1$ if no activity is present ± 25 ms
 $+1$ if activity is present ± 25 ms

Table 11 shows the correlation factor for each sample. The resulting average correlation factor for all samples is 0.32. This value suggests that no correlation can be made between the sample weight and bed activity. There are several explanations for this. Bubbles not detected by the bubble probe or debris from previous bubbles returning to the bed surface can influence the sample weight by increasing the amount of particles collected. Also, bubbles of smaller size have a smaller velocity and would therefore produce a particle stream which is either slower or just delayed in leaving the bed surface. This would result in lower sample weights than expected.

TABLE 11

| Sample Number | W | p | r | Q |
|---------------|----|----|----|----|
| 56 | 1 | 1 | 1 | 2 |
| 57 | -1 | 1 | 1 | -2 |
| 58 | 1 | 1 | 1 | 2 |
| 59 | -1 | -1 | -1 | 2 |
| 60 | 1 | -1 | -1 | -2 |
| 62 | -1 | 1 | 1 | -2 |
| 63 | 1 | 1 | 1 | 2 |
| 64 | -1 | -1 | -1 | 2 |
| 66 | -1 | -1 | 1 | 0 |
| 67 | 1 | 1 | 1 | 2 |
| 69 | -1 | 1 | 1 | -2 |
| 70 | -1 | 1 | 1 | -2 |
| 77 | 1 | 1 | 1 | 2 |
| 79 | -1 | 1 | 1 | -2 |
| 83 | 1 | 1 | 1 | 2 |
| 84 | 1 | 1 | 1 | 2 |
| 86 | -1 | -1 | 1 | 0 |
| 88 | 1 | 1 | 1 | 2 |
| 89 | -1 | 1 | 1 | -2 |
| 90 | -1 | -1 | 1 | 0 |
| 92 | -1 | -1 | 1 | 0 |
| 93 | 1 | 1 | 1 | 2 |
| 94 | -1 | -1 | 1 | 0 |
| 95 | 1 | 1 | 1 | 2 |
| 96 | -1 | -1 | 1 | 0 |
| 97 | -1 | -1 | -1 | 2 |
| 98 | 1 | -1 | 1 | 0 |
| 99 | 1 | -1 | -1 | -2 |
| 100 | 1 | -1 | -1 | -2 |
| 101 | 1 | 1 | 1 | 2 |
| 102 | -1 | -1 | 1 | 0 |

Average = 0.32

List of samples and their correlation parameters. The resulting average value for Q indicates that no correlation can be made from the data obtained to indicate by sample weight whether or not any bed activity occurred below the sample trap.

AD-A159 010

A DETERMINATION OF PARTICLE DENSITY DISTRIBUTIONS ABOVE
FLUIDIZED BEDS(U) MASSACHUSETTS INST OF TECH CAMBRIDGE
DEPT OF OCEAN ENGINEERING G A PIPER MAR 85

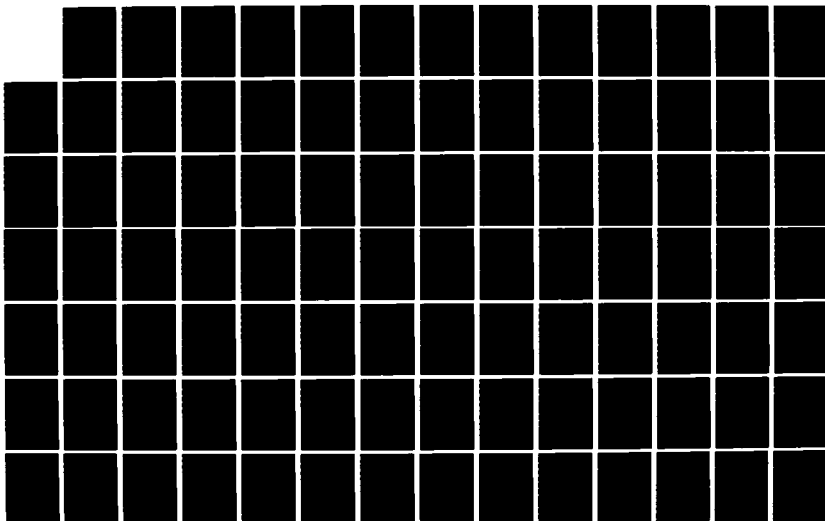
2/3

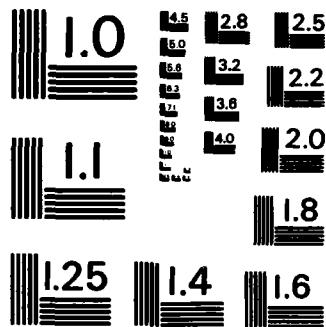
UNCLASSIFIED

N66314-70-A-0073

F/G 14/2

NL





MICROCOPY RESOLUTION TEST CHART
NATIONAL BUREAU OF STANDARDS-1963-A

CHAPTER VI

TRAJECTORY MODEL RESULTS AND DISCUSSION

Selection of Baseline Parameters

The input to the model consists of the following five (5) parameters:

- 1) Superficial bed velocity (U_o)
- 2) Initial particle velocity (U_{po})
- 3) Peak gas jet velocity (U_j)
- 4) Gas jet duration (t_j)
- 5) Particle distribution of the bed mass

The baseline values for each of these inputs was determined to be as close to the actual experimental bed conditions as possible.

Superficial Bed Velocity

The superficial bed velocity was determined directly from the experimental data. For the bed conditions discussed in this section, the superficial velocity used is the same as the highest velocity condition under which the particle sampler was used. The superficial velocity within the bed for these samples was

calculated to be 57.9 cm/s (1.9 ft/s).

Initial Particle Velocity

To determine the initial velocity of the particle, it was assumed that the particle was located at the nose of a bubble and would therefore have the bubbles velocity. To determine the bubble velocity, Kunii and Levenspiel [1] give the following equation:

$$U_b = 0.711 [g D_b]^{1/2} + U_o - U_{mf} \quad (11)$$

where:

U_b = Bubble velocity

U_o = Superficial bed velocity

U_{mf} = Minimum fluidization velocity

D_b = Bubble diameter

g = gravitational acceleration

Observations of the bed material during the sampling operation suggests that the average bubble diameter present in the bed is approximately 5 cm (2.4 in). For $U_o = 57.9$ cm/s, $U_{mf} = 15.2$ cm/s and $D_b = 5$ cm, the bubble velocity is calculated to be 97.2 cm/s (3.19 ft/s). This value was used as the initial particle velocity for the base line data.

Peak Gas Jet Velocity

To determine an average peak jet velocity, the anemometer output on the oscilloscope traces (Appendix K) were analyzed. To determine the relationship between the voltage output from the anemometer (which is displayed on the oscilloscope) and the actual gas jet velocity, the anemometer was calibrated in a wind tunnel. The resulting calibration curve for the anemometer output, as displayed on the oscilloscope trace, is given in Appendix M. The average peak velocity of the anemometer traces analyzed in chapter V was determined to be approximately 609.6 cm/s (20 ft/s).

Gas Jet Duration

To determine an average gas jet duration time to use as a baseline, the anemometer traces in Appendix K were used. The time duration of each gas jet analyzed is determined directly from the oscilloscope trace. The average duration of a gas jet was determined to be approximately 20 ms in chapter V.

Particle Distribution of the Bed Mass

Two particle distributions for the bed mass were available for use as the baseline data. Both particle distributions were determined using the same sample but analyzed using different analysis techniques. The two methods used are the sieve method and the image analyzer method, both of which are described earlier

in chapter V. The two distributions are shown in Fig. 29.

The bed distribution determined by the image analyzer was used to be consistent with the particle distributions measured at various freeboard heights.

Typical Output Using Baseline Parameters

Fig. 30 shows the resulting maximum particle height obtained as a function of particle diameter for the baseline conditions. The general shape of the curve is determined by the dominating force acting on the particle. For large particles, the dominating force at these air velocities is gravity. Therefore, momentum (initial particle velocity) is the controlling factor determining the maximum height attained by the particle. As the particle size decreases, the proportion of drag force to gravitational force becomes larger. For the smaller particles, the drag force becomes the dominate force. The result is that the maximum height attained by a particle continues to increase as particle size decreases. This continues until the value of U_0 approaches the terminal velocity of the smaller particles. At this point, the particle is totally dominated by the air flow in the bed. This is seen in the small decrease in height attained by particles less than 110 microns as a result of the particles rapid deacceleration to U_0 after the gas jet has stopped while the larger particles continue a little higher due to momentum. The particle height continues to decrease for a short time until U_0 becomes equal to

Faired Data From Appendix E and J. Interval of 10 microns.

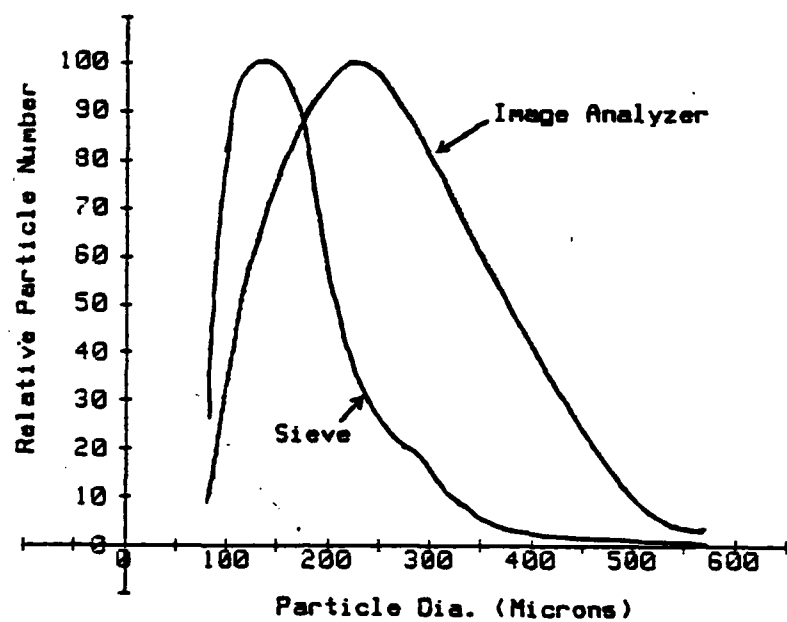


Fig. 29 Relative Particle Number Distributions of Bed Material by Sieve and Image Analyzer Analysis.

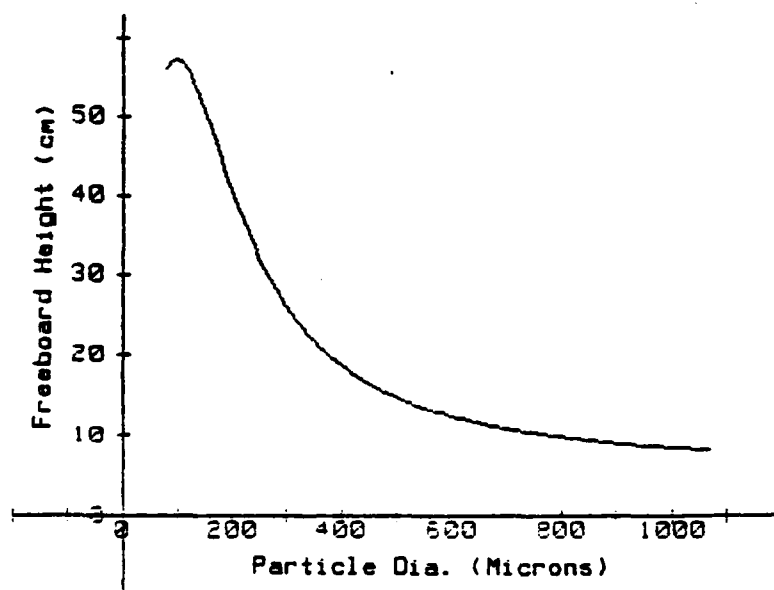


Fig. 30 Maximum Particle Height vs Particle Diameter for Baseline Conditions.

or greater than the terminal velocity for the remaining particles. These particles would be elutriated from the system.

Figs. 31 thru 36 show the individual particle densities at different heights above the bed. All of the heights show an increase in particle density for the smaller diameter particles. This is the result of the smaller particles falling at their respective terminal velocities which is slower than for the larger particles. The result is that the smaller the particle velocity, the longer the particle exists within a given height region and thus, the larger the particle density. It is also due to the larger number of smaller particles present within the system.

Fig. 37 shows the particle density distribution above the bed. The two curves represent the effect of varying the range of particle diameters used in the model. The two ranges are 80 - 570 microns and 80 - 1070 microns. The peak of the 80 - 570 micron distribution is at about 18 cm of bed height whereas the other distribution peaks at about 11 cm. The region shown on the graph below these heights is the area known as the splash zone. The shape of this part of the curve is due to the initial acceleration of the particles leaving the surface of the bed by the gas jet. The particles then begin to slow down due to drag and gravity resulting in an increase in particle density. The peak on this curve coincides with the maximum height attained by the largest particles, and therefore, it can be assumed that the change in slope is due to the loss of particles as they return to the bed.

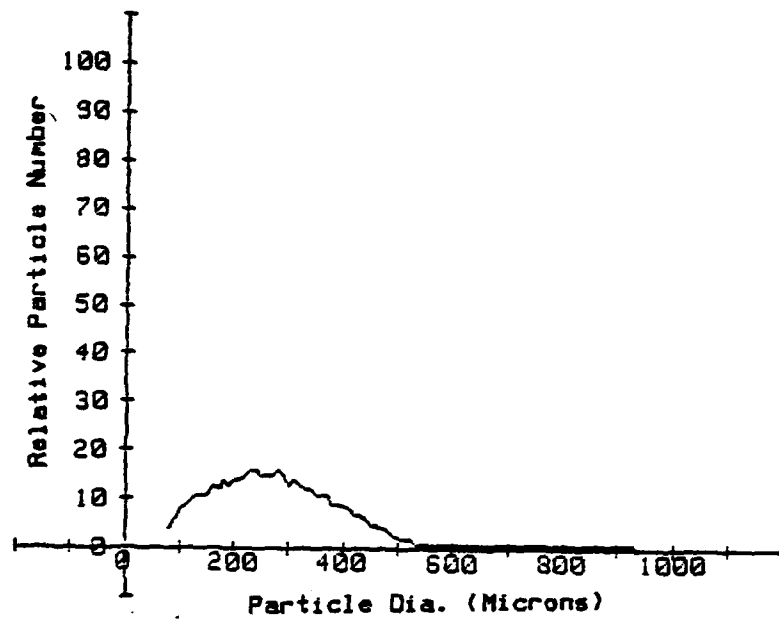


Fig. 31 Relative Particle Number vs Particle Diameter for Baseline Conditions. Freeboard Height of 4 cm.

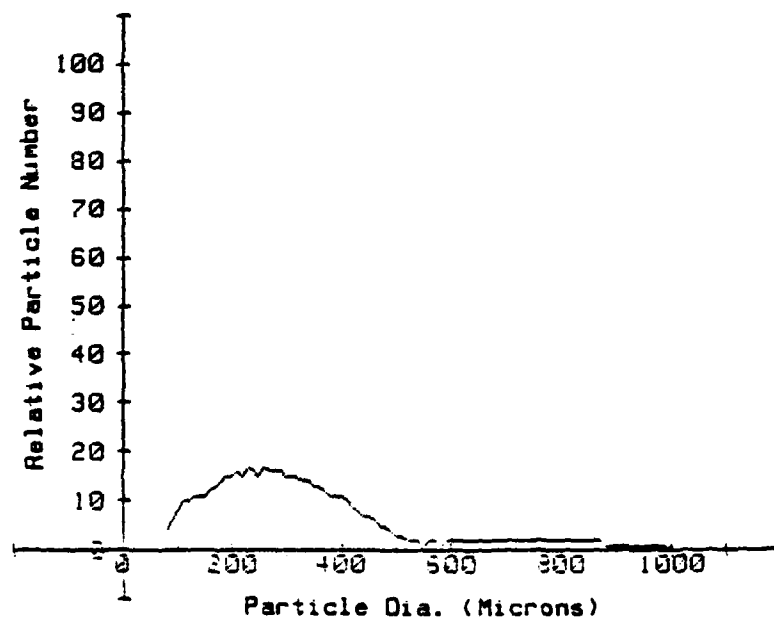


Fig. 32 Relative Particle Number vs Particle Diameter for Baseline Conditions. Freeboard Height of 8 cm.

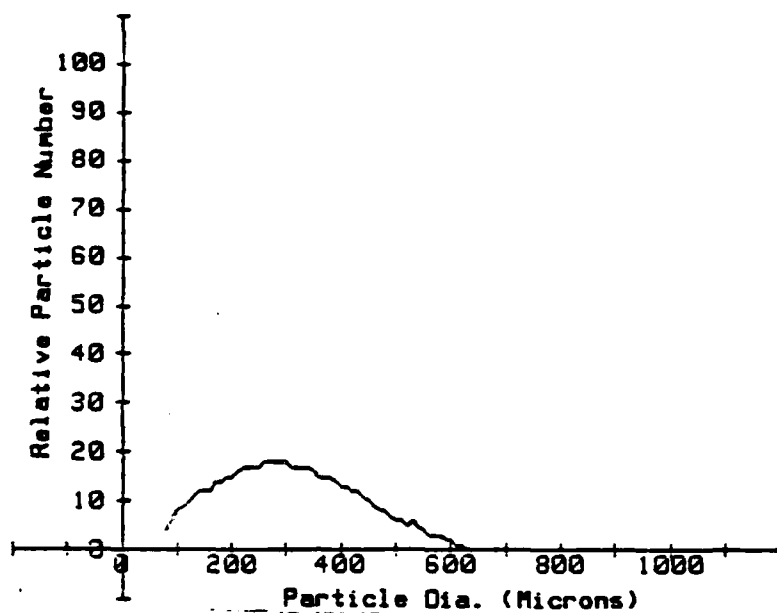


Fig. 33 Relative Particle Number vs Particle Diameter for Baseline Conditions. Freeboard Height of 12 cm.

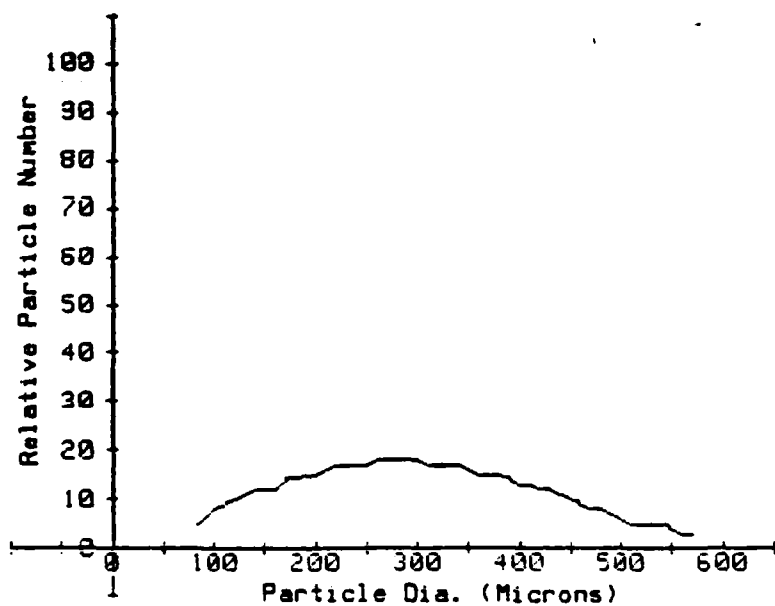


Fig. 34 Relative Particle Number vs Particle Diameter for Baseline Conditions. Freeboard Height of 18 cm.

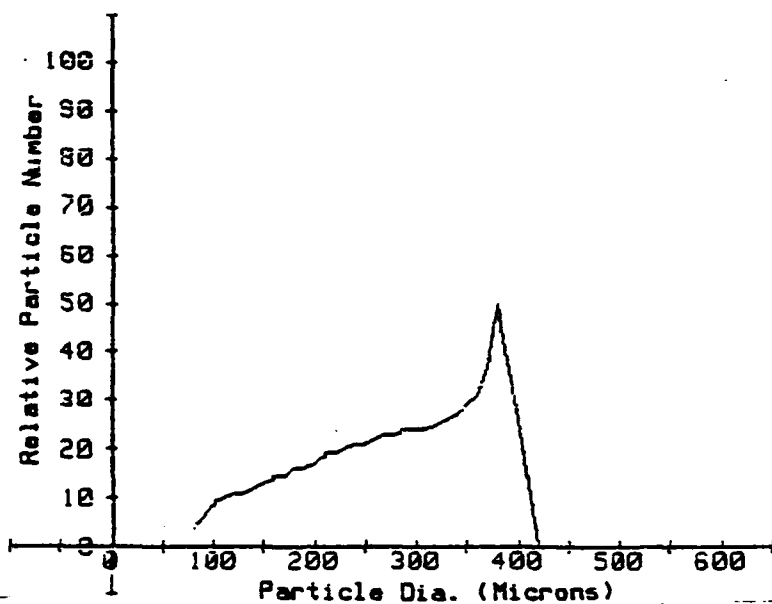


Fig. 35 Relative Particle Number vs Particle Diameter for Baseline Conditions.
Freeboard Height of 22 cm.

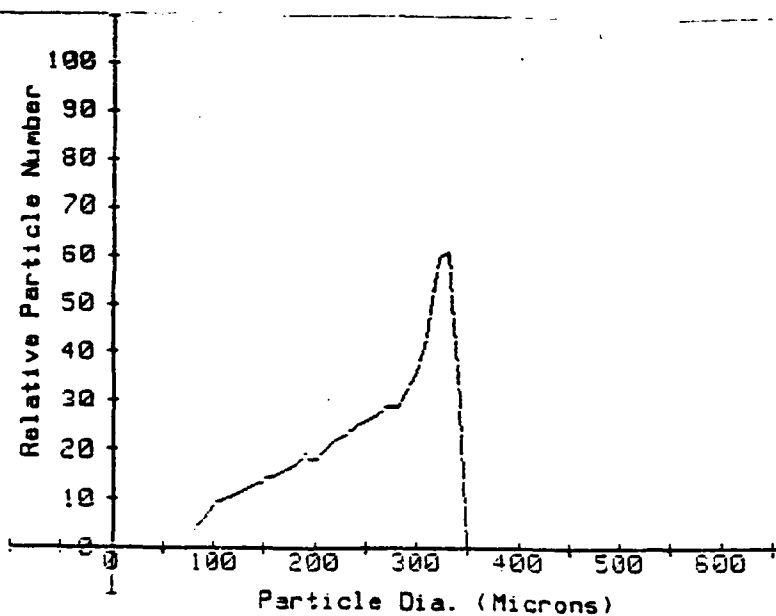


Fig. 36 Relative Particle Number vs Particle Diameter for Baseline Conditions.
Freeboard Height of 31 cm.

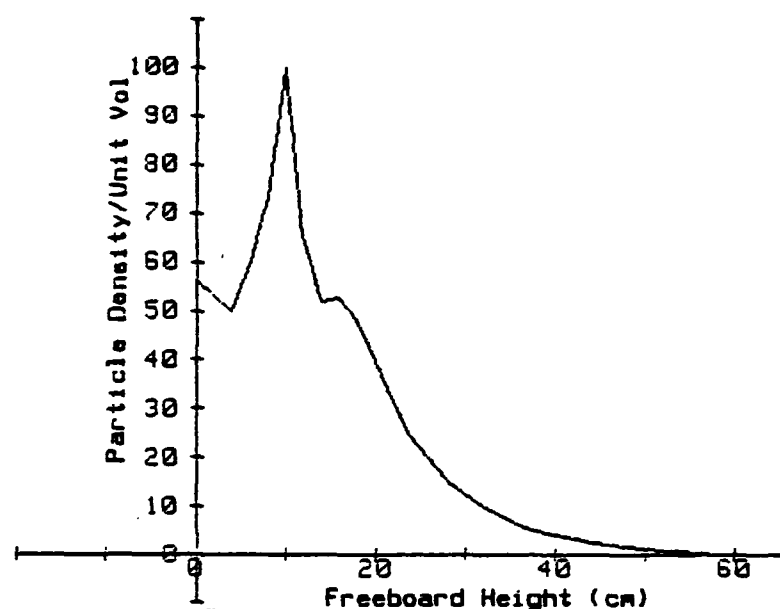


Fig. 37 Particle Density/Unit Volume vs Freeboard height for Baseline Conditions.

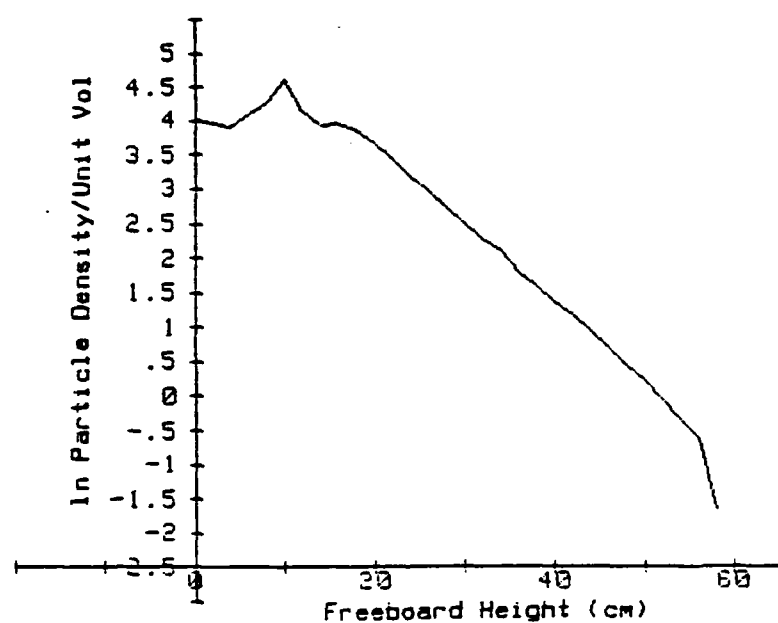


Fig. 38 ln Particle Density/Unit Volume vs Freeboard height for Baseline Conditions.

Fig. 38 is a semi-ln plot of the same data as plotted in Fig. 37. The sharp drop at the right end of the plot is due to analyzing particles with a minimum diameter of 80 microns. Had smaller particles been included, the slope would have approached zero instead of infinity which would model the elutriation of particles. The slope of the line to the right of the peaks shown in Fig. 38, which are located at 11 and 18 cm of height above the bed surface are the same and are approximately -0.117 grams/cm. To decrease computation time, the 80 - 570 micron particle distribution was used in the following sensitivity analysis as the decay slopes are equal.

Model Sensitivity Analysis

An analysis of the change in bed characteristics due to a change in one of the five model input parameters was conducted.

The parameters changed and the values used are as follows:

Superficial velocity (U_o):

Baseline U_o : 57.9 cm/s (1.9 ft/s)

1. 30.5 cm/s (1 ft/s)
2. 91.4 cm/s (3 ft/s)

Initial particle velocity (U_{po}):

Baseline U_{po} : 119.2 cm/s (3.19 ft/s)

1. 61.0 cm/s (2 ft/s)
2. 152.4 cm/s (5 ft/s)

3. 305.0 cm/s (10 ft/s)

Gas Jet velocity (U_j):

Baseline U_j : 609.6 cm/s (20 ft/s)

1. 305.0 cm/s (10 ft/s)
2. 457.2 cm/s (15 ft/s)

Gas jet duration (t_j):

Baseline t_j : 20 ms

1. 10 ms
2. 30 ms

Particle distribution of bed mass:

Baseline distribution: Image Analyzer

1. Sieve analysis data

The bed characteristics which are evaluated against the baseline characteristics are:

1. The maximum height attained by each particle from 80 to 570 microns.
2. The density of each particle size (80 - 570 microns) at freeboard heights of:

- a. 4 cm (1.5 in)
- b. 8 cm (3.1 in)

- c. 12 cm (4.7 in)
- d. 18 cm (7.1 in)
- e. 22 cm (8.7 in)
- f. 31 cm (12.2 in)

3. The particle density distribution in the freeboard.

Variation of Superficial Velocity (U_o)

Fig. 39 shows the influence of U_o on the maximum height attained by the particles. As was described in the previous section, the larger particles are dominated by momentum and not drag. This is shown in Fig. 39 by the small change in maximum height attained by the large particles due to a change in U_o . As the particle size decreases, the drag force becomes the dominant force and the effect of U_o on particle height increases. As seen in Fig. 39, a change in U_o produces a moderate change in the maximum height attained by the small particles.

Figs. 40 thru 45 show the effect of U_o on individual particle densities at different heights above the bed. All of the heights show an increase in particle density for the smaller diameter particles as U_o is increased. This is the result of the smaller particles falling at their respective relative terminal velocities which is slower for smaller particles. A decrease in the maximum particle diameter present at a given freeboard height as U_o is decreased can be observed in Figs. 40 thru 45. This

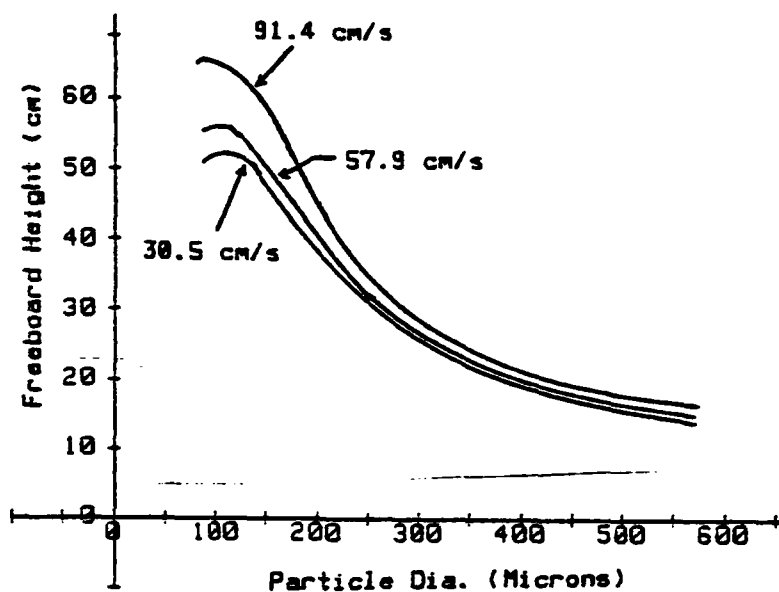


Fig. 39 Maximum Particle Height vs Particle Diameter as a Function of U_o .

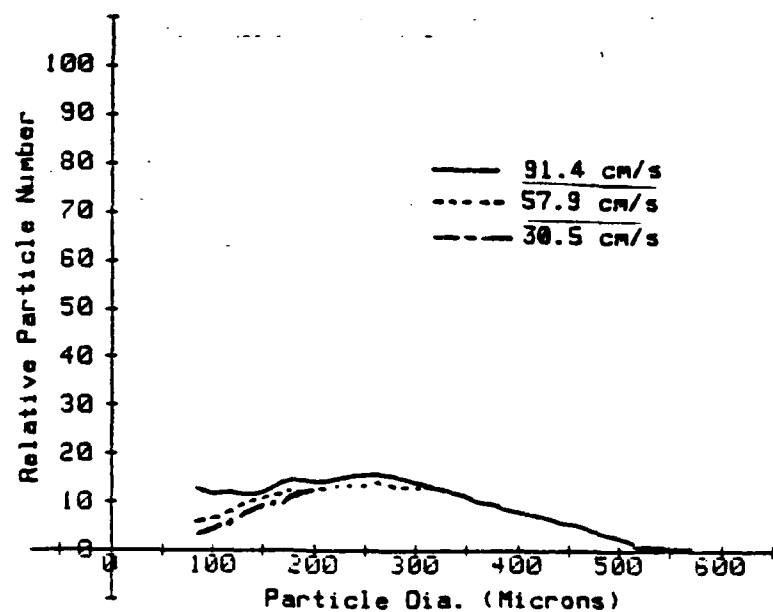


Fig. 40 Relative Particle Number vs Particle Diameter as a Function of U_o . Freeboard Height of 4 cm.

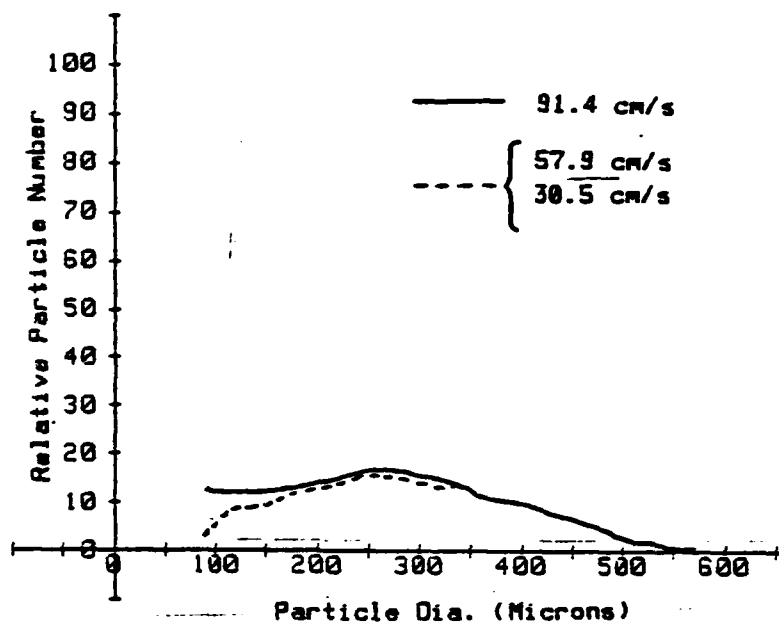


Fig. 41 Relative Particle Number vs Particle Diameter as a function of U_0 . Freeboard Height of 8 cm.

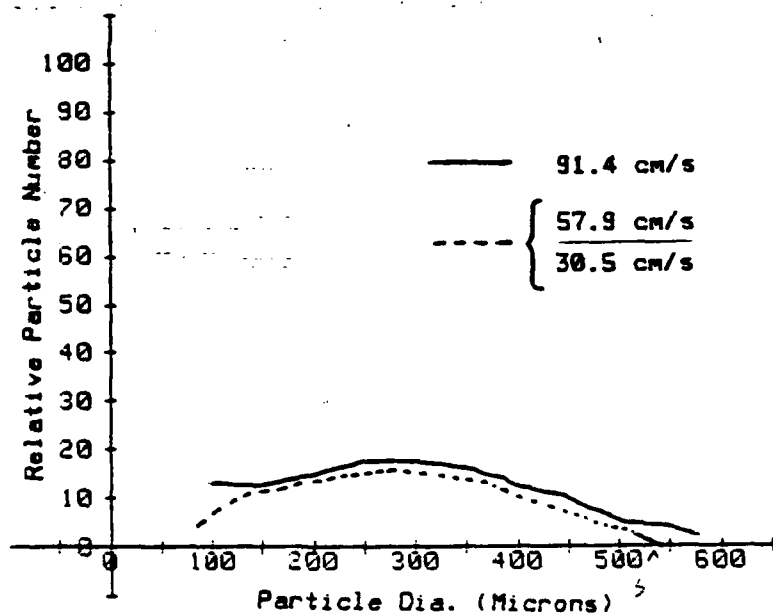


Fig. 42 Relative Particle Number vs Particle Diameter as a function of U_0 . Freeboard Height of 12 cm.

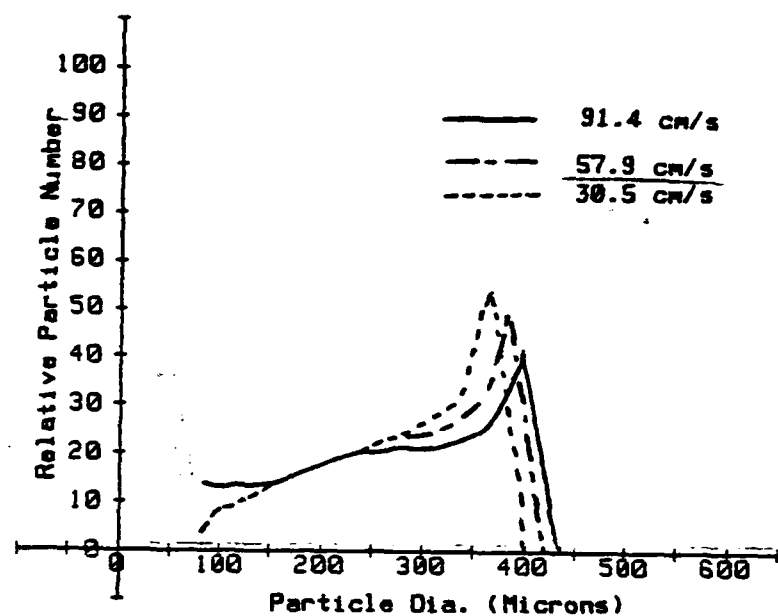


Fig. 43 Relative Particle Number vs Particle Diameter as a Function of U_o . Freeboard Height of 18 cm.

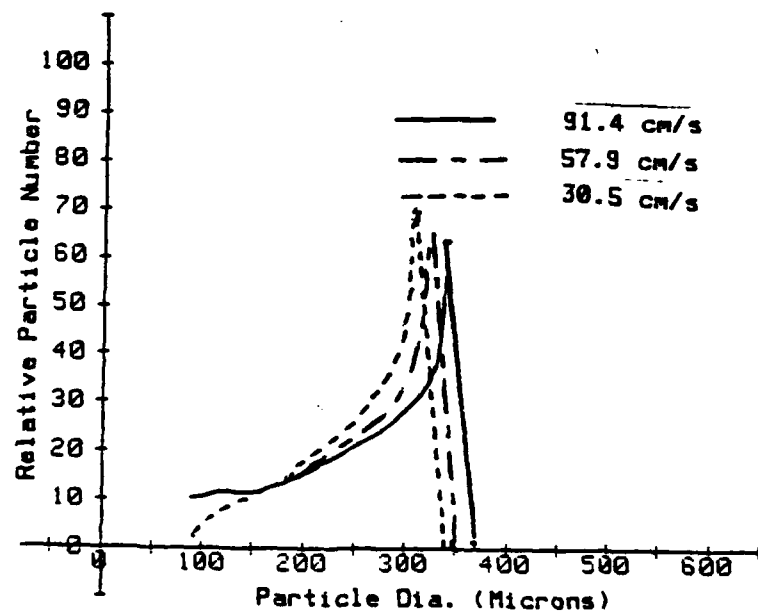


Fig. 44 Relative Particle Number vs Particle Diameter as a Function of U_o . Freeboard Height of 22 cm.

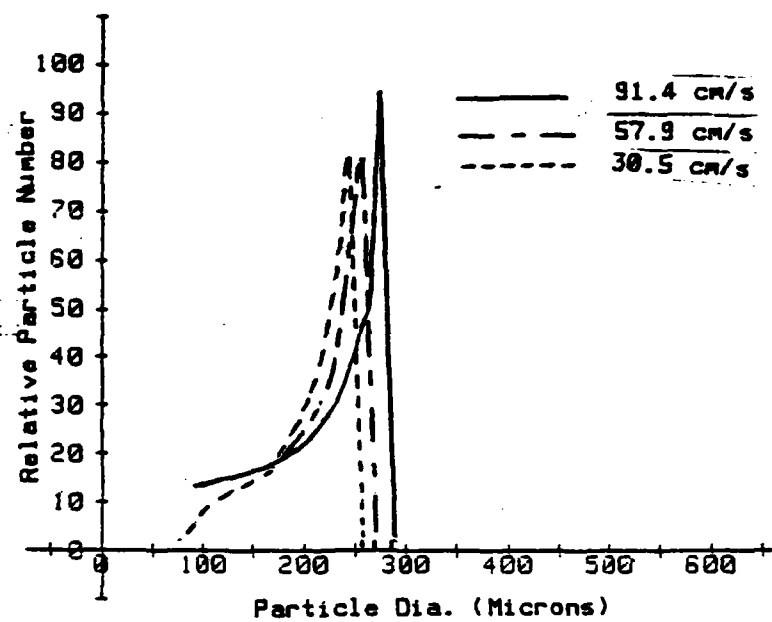


Fig. 45 Relative Particle Number vs Particle Diameter as a Function of U_o . Freeboard Height of 31 cm.

decrease is due to the decrease in lift given to the ascending particle as U_0 is decreased. As a result, all particles achieve a lower maximum height when U_0 is decreased.

Fig. 46 shows the effect of U_0 on the particle density distribution above the bed. There is a slight increase in overall particle density with an increase in U_0 . As expected, there is also an increase in the maximum height attained by the particles with an increase in U_0 . Fig. 47 is a semi-ln plot of the same data plotted in Fig. 46. Table 12 lists the slopes of the lines to the right of the peak shown in Fig. 47 which is located at about 18 cm of height above the bed surface. This table shows an increase in the particle distribution slope as U_0 is decreased.

TABLE 12

| U_0 cm/s | Slope gms/cm | Intercept gms/cm |
|---------------|-----------------|---------------------|
| 30.5 | -0.136 | 7.036 |
| 57.9 | -0.117 | 6.758 |
| 91.4 | -0.098 | 6.473 |

Effect of U_0 on the slope of the particle density distribution as a function of height for the distributions shown in Fig. 47.

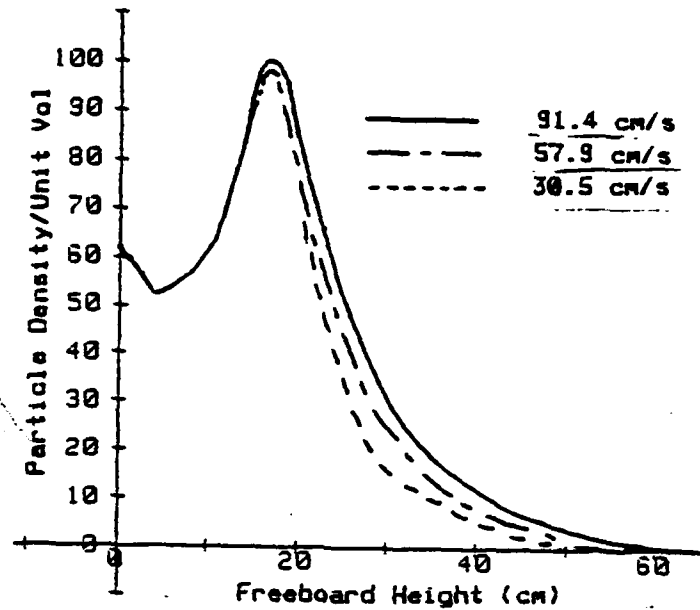


Fig. 46 Particle Density/Unit Volume vs Freeboard height as a Function of U_o .

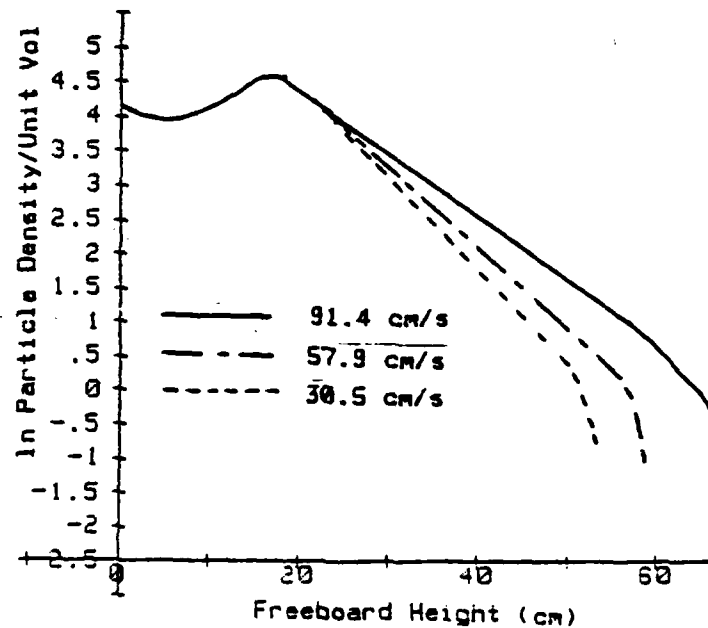


Fig. 47 \ln Particle Density/Unit Volume vs Freeboard height as a Function of U_o .

Variation of Initial Particle Velocity (U_{po})

Fig. 48 shows the relation between initial particle velocity (U_{po}) and the maximum height attained by particles of different size. This figure also shows that the larger particles are mainly momentum dependent while the smaller particles are drag dependent. If U_{po} were increased further, the larger particles would continue to increase their maximum height. The smaller particles would approach a height limit which is dependent upon the superficial velocity in the bed.

Figs. 49 thru 54 show the effects of increasing U_{po} on the individual particle densities for increasing heights. In general, the individual particle distributions undergo the same relative changes from the bed surface to the maximum height position. The difference being the height above the bed surface at which the particular distribution is present.

Fig. 55 shows the effect of varying U_{po} on the particle density distribution in the freeboard. As was noted previously, the peak density occurs at the point where the largest particles attain their maximum height above the bed. As U_{po} is increased, the curve to the right of the peak becomes shorter and steeper. This trend will continue until the the effect of the smaller particles returning to the bed cause the slope to decrease. Fig.

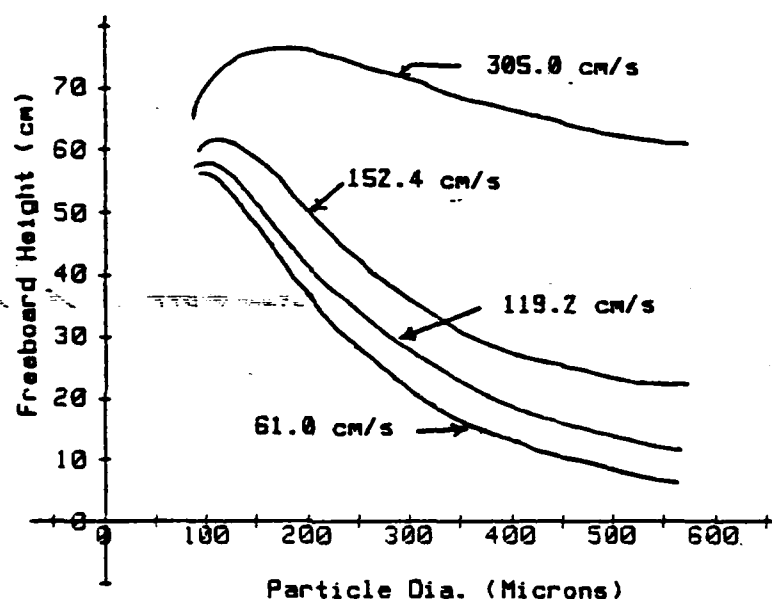


Fig. 48 Maximum Particle Height vs Particle Diameter as a Function of Upo.

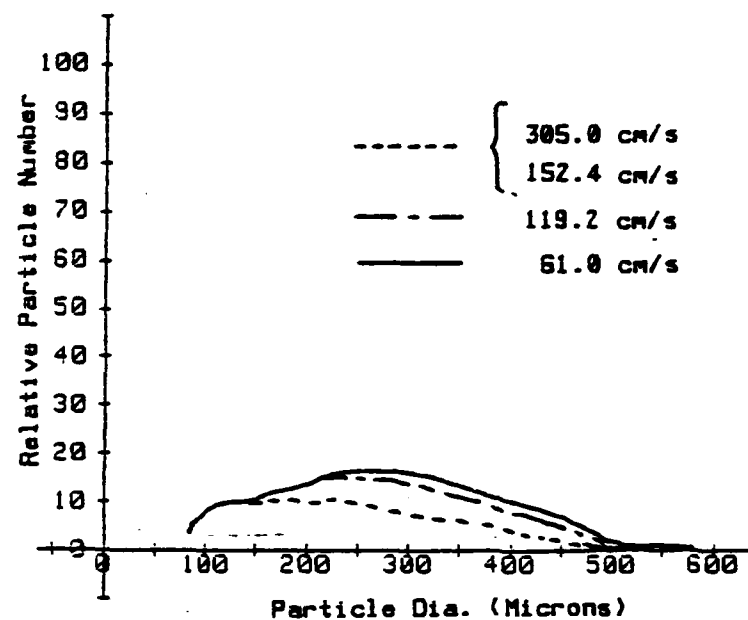


Fig. 49 Relative Particle Number vs Particle Diameter as a Function of Upo. Freeboard Height of 4 cm.

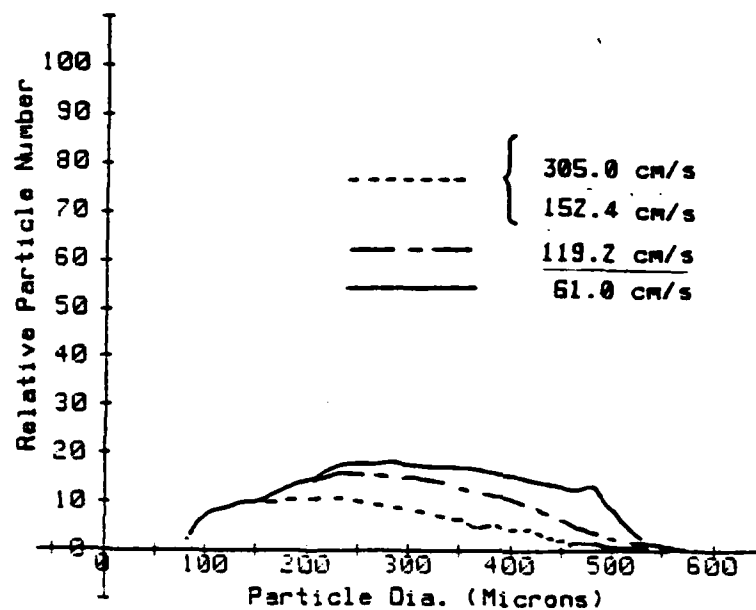


Fig. 50 Relative Particle Number vs Particle Diameter as a Function of Upo. Freeboard Height of 8 cm.

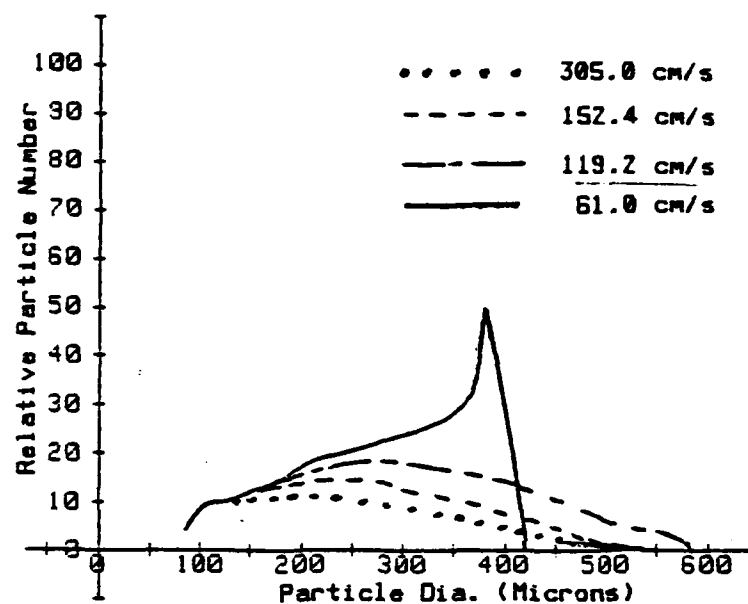


Fig. 51 Relative Particle Number vs Particle Diameter as a Function of Upo. Freeboard Height of 12 cm.

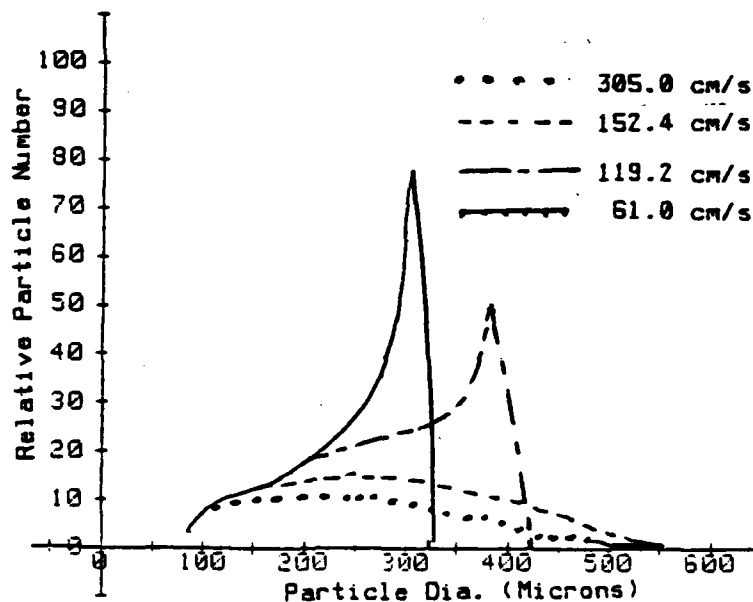


Fig. 52 Relative Particle Number vs Particle Diameter as a Function of Upo. Freeboard Height of 18 cm.

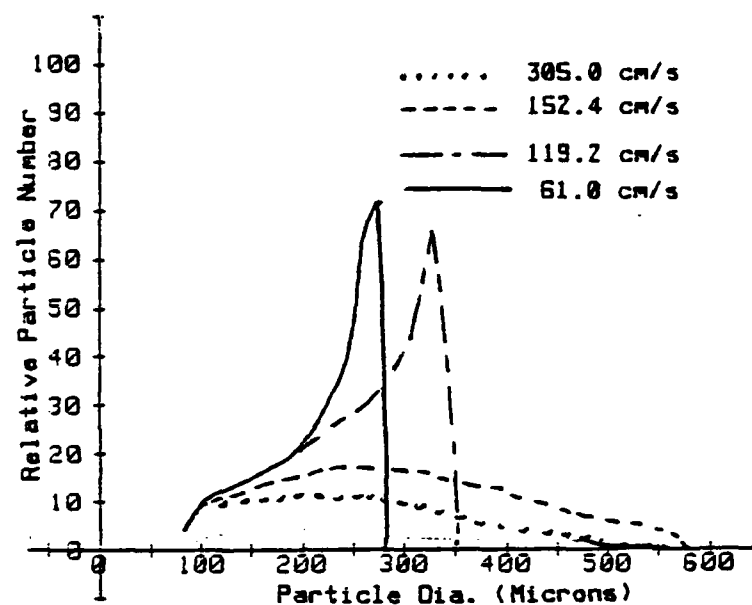


Fig. S3 Relative Particle Number vs Particle Diameter as a Function of Upo. Freeboard Height of 22 cm.

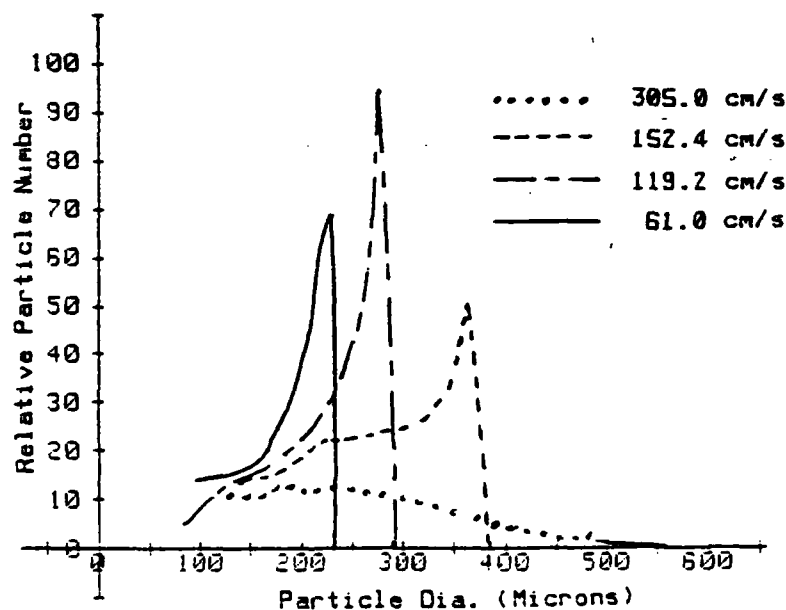


Fig. S4 Relative Particle Number vs Particle Diameter as a Function of Upo. Freeboard Height of 31 cm.

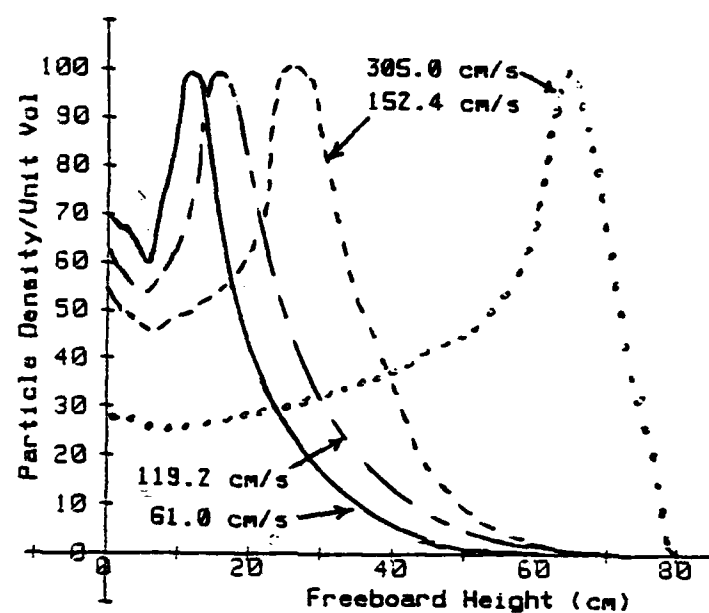


Fig. 55 Particle Density/Unit Volume vs Freeboard height as a Function of Upo.

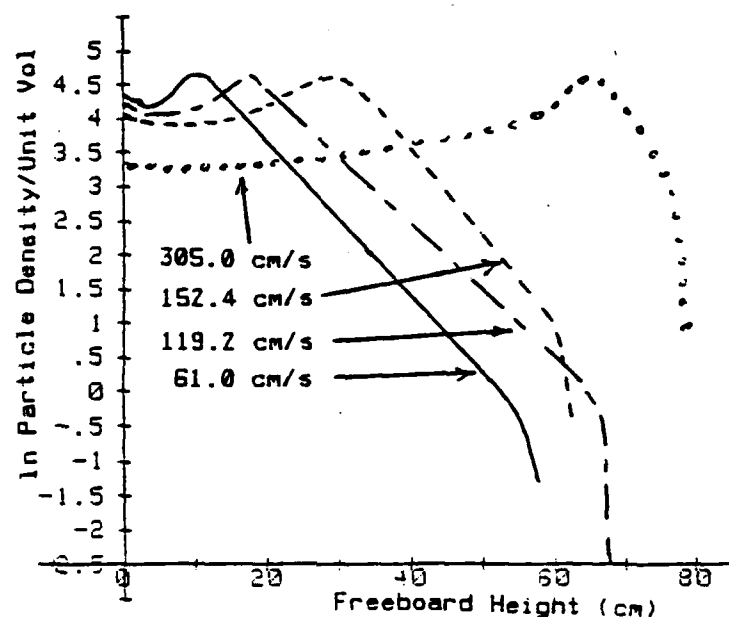


Fig. 56 ln Particle Density/Unit Volume vs Freeboard height as a Function of Upo.

56 is a semi-ln plot of the data in Fig. 55. Table 13 confirms that the slope is becoming steeper as U_{po} is increased although the influence of initial particle velocity on the slope of the density vs height curve is moderate.

TABLE 13

| U_{po} cm/s | Slope gms/cm | Intercept gms/cm |
|------------------|-----------------|---------------------|
| 61.0 | -0.118 | 6.058 |
| 97.2 | -0.117 | 6.758 |
| 152.4 | -0.125 | 8.500 |
| 304.8 | -0.200 | 18.20 |

Effect of U_{po} on the slope of the particle density distribution as a function of height for the distributions shown in Fig. 56.

Variation of Jet Velocity (U_j)

Fig. 57 shows the effect on maximum particle height when U_j is varied. As in the two previous analysis', the influence of momentum and drag on the different particle sizes is apparent. A decrease in jet velocity from the baseline value results in a large drop in small particle height and a small change in large particle height. This suggests that jet velocity has a strong effect on the dispersion, or separation of particles of different sizes at increasing freeboard heights. Increasing U_j results in a stretching effect of the particle size distributions above the

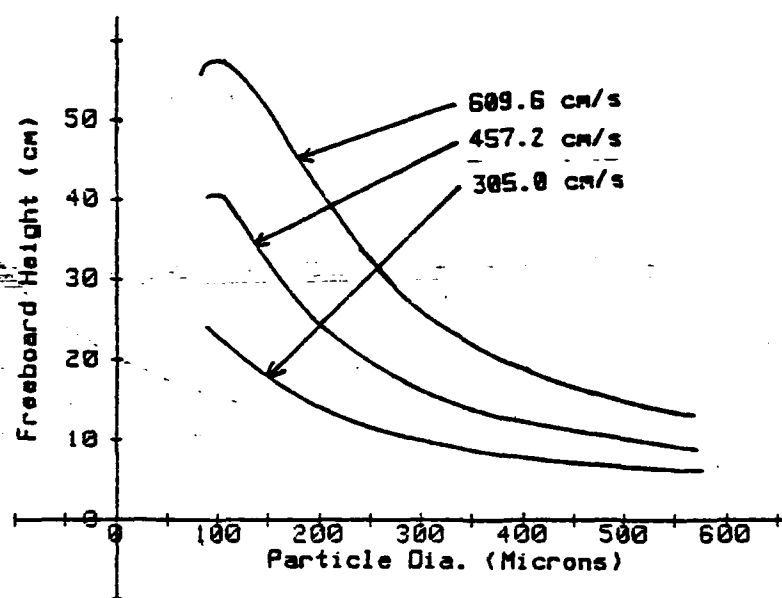


Fig. 57 Maximum Particle Height vs Particle Diameter as a Function of U_j .

bed. One interesting point to note is the loss of the rounded edge at the heights corresponding to the smaller particles. This shows the extremely large effect that drag plays when the air velocity is very close to the terminal velocity of the particle.

Figs. 58 thru 63 show the effect of varying U_j on the individual particle densities at varying heights above the bed. Again, as in the previous parameter analysis, the same distribution shapes can be seen for each value of U_j , the only difference being the height at which it occurs.

Fig. 64 shows the change in particle density distribution as U_j is varied. Fig. 65 is a semi-ln plot of this data showing that as U_j is decreased, the slope of the distribution changes substantially. Table 14 also shows this effect.

TABLE 14

| U_j cm/s | Slope gms/cm | Intercept gms/cm |
|---------------|-----------------|---------------------|
| 609.6 | -0.117 | 6.758 |
| 457.2 | -0.207 | 7.380 |
| 304.8 | -0.400 | 7.800 |

Effect of U_j on the slope of the particle density distribution as a function of height for the distributions shown in Fig. 65.

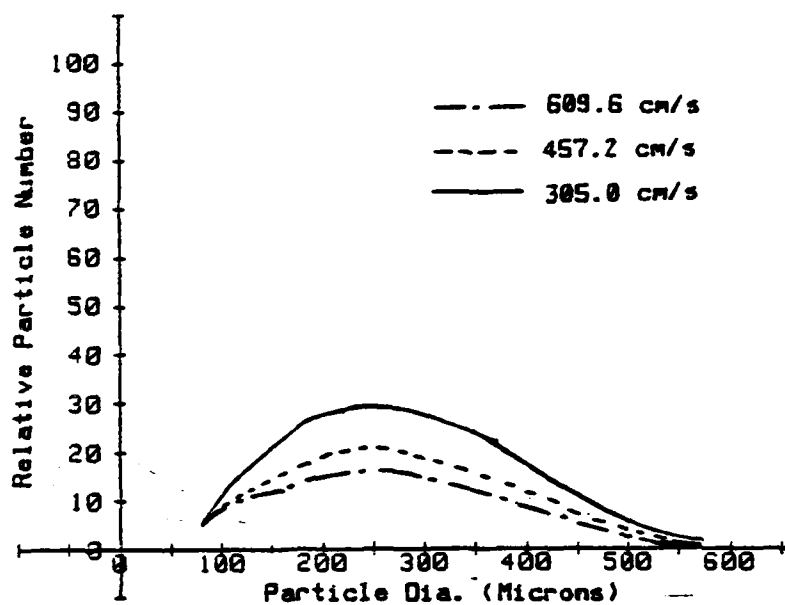


Fig. 58 Relative Particle Number vs Particle Diameter as a Function of U_j . Freeboard Height of 4 cm.

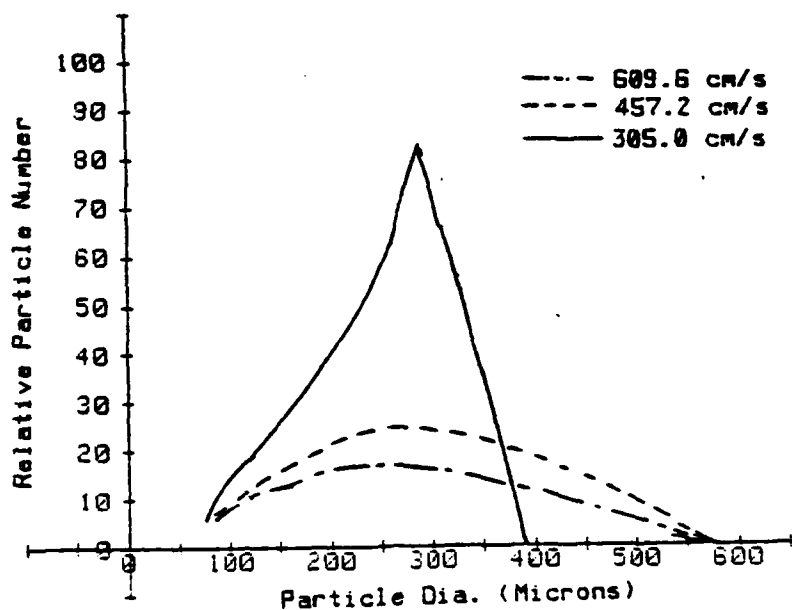


Fig. 59 Relative Particle Number vs Particle Diameter as a Function of U_j . Freeboard Height of 8 cm.

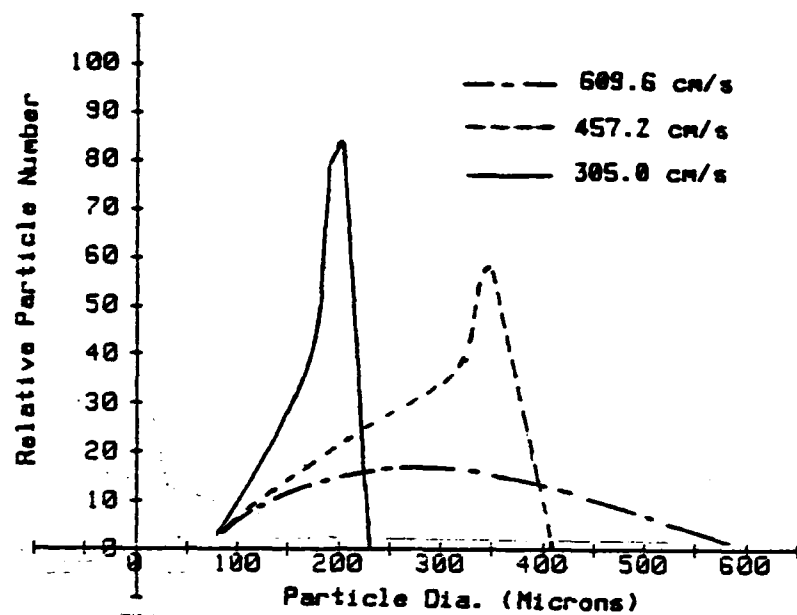


Fig. 60 Relative Particle Number vs Particle Diameter as a Function of U_j .
Freeboard Height of 12 cm.

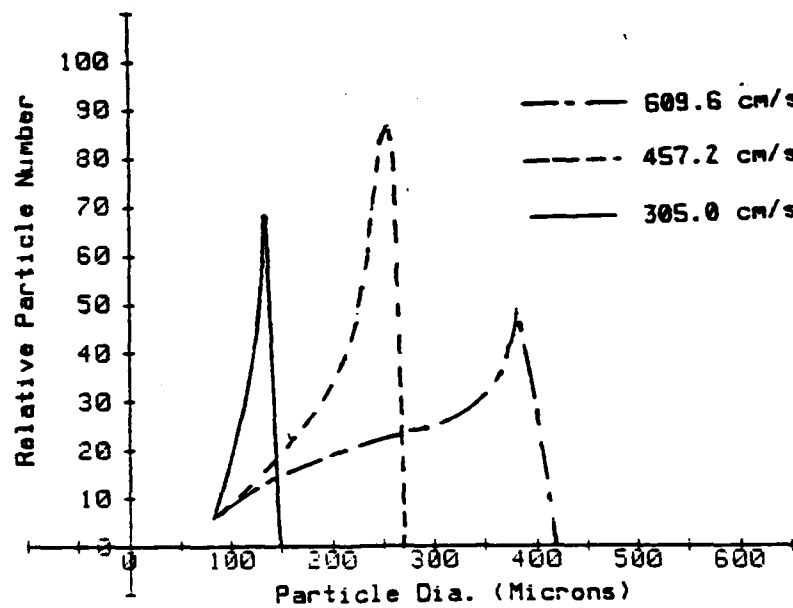


Fig. 61 Relative Particle Number vs Particle Diameter as a Function of U_j .
Freeboard Height of 18 cm.

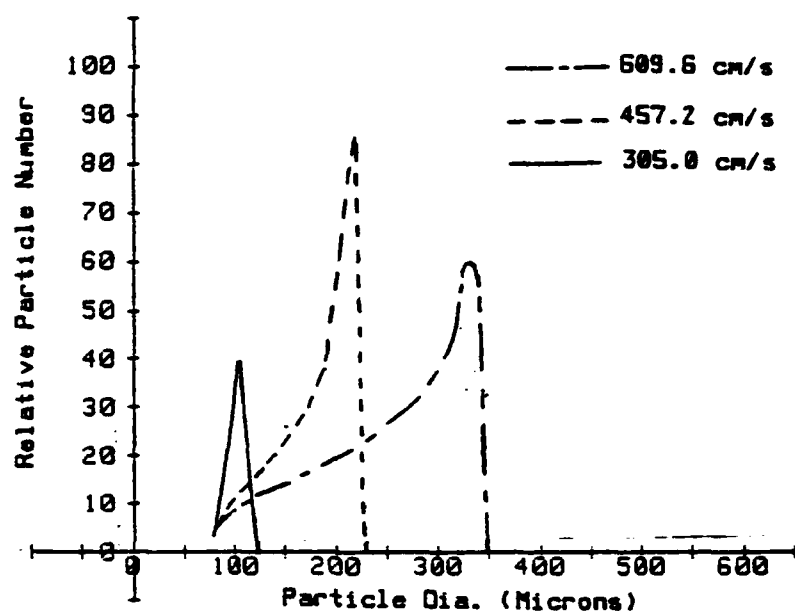


Fig. 62 Relative Particle Number vs Particle Diameter as a Function of U_j . Freeboard Height of 22 cm.

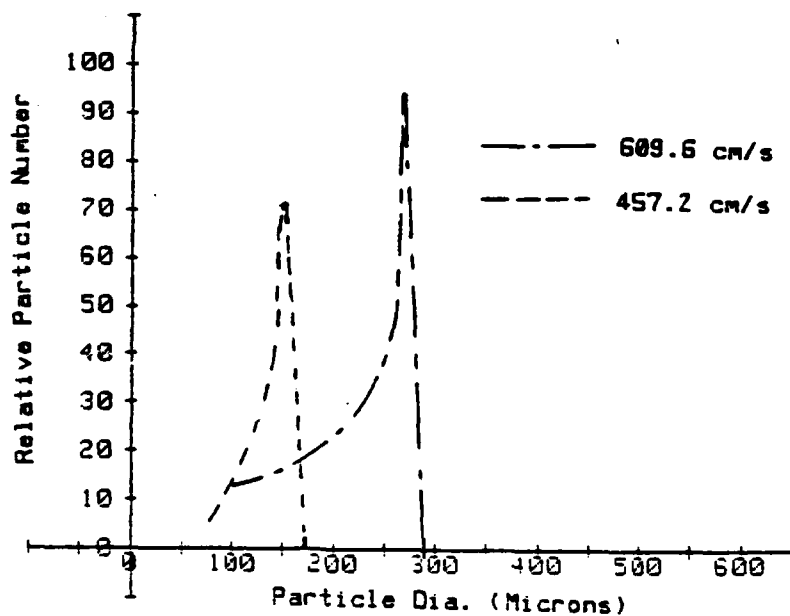


Fig. 63 Relative Particle Number vs Particle Diameter as a Function of U_j . Freeboard Height of 31 cm.

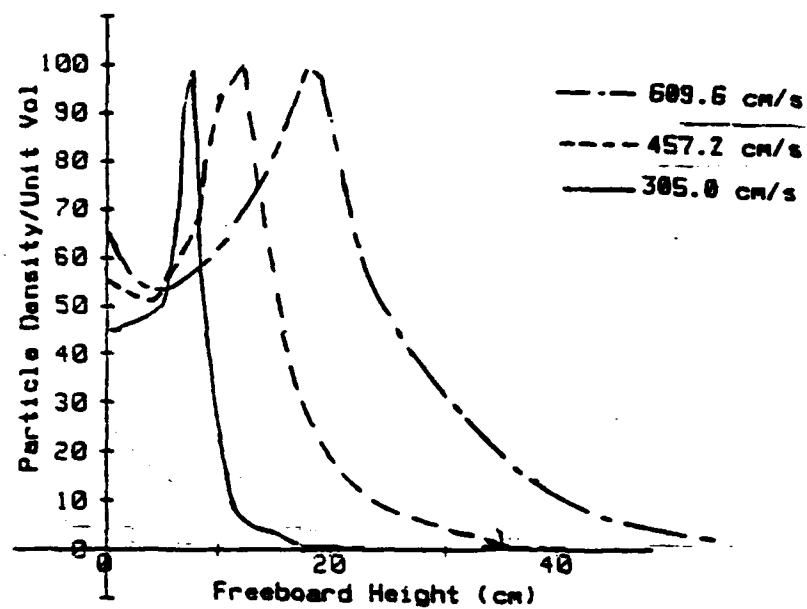


Fig. 64 Particle Density/Unit Volume vs Freeboard height as a Function of U_j .

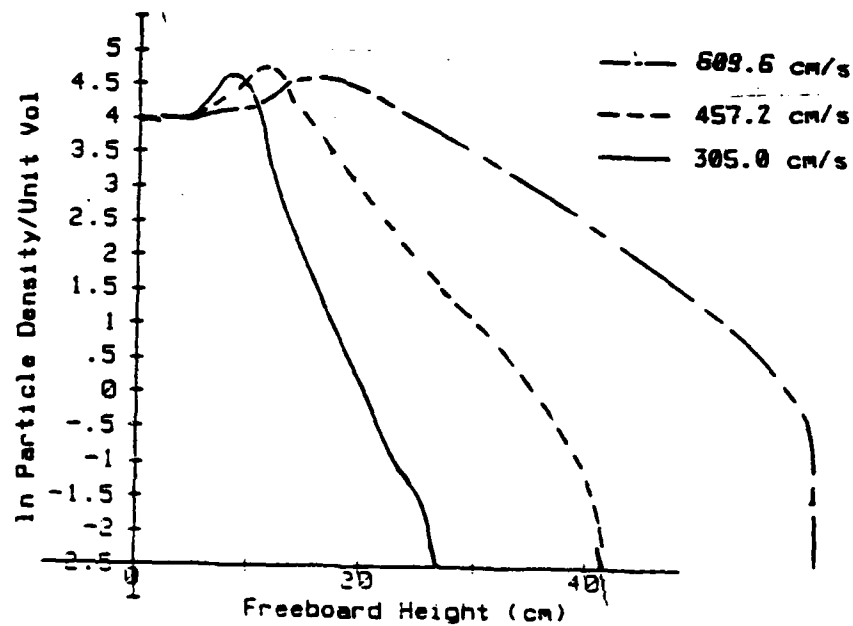


Fig. 65 ln Particle Density/Unit Volume vs Freeboard height as a Function of U_j .

Variation of Jet Duration (t_j)

Fig. 66 is a graph showing the effect of varying jet duration on the maximum heights attained by the particles. It is easily seen that a small change in jet duration results in a substantial change in particle height. This effect indicates that the distribution present in an actual fluidized bed is probably a statistical average of a rapidly fluctuating particle distribution which is controlled by the durations of the jets from the neighboring bubble eruptions as well as local eruptions.

Figs. 67 thru 72 show the effects on the individual particle density distributions, at different freeboard heights, as a function of jet duration. These figures also show the drastic change in density distributions caused by changes in jet duration.

Fig. 73 shows the particle density distributions above the bed as affected by jet duration. Fig. 74, which is a semi-ln plot of the data, shows the drastic changes in the decay slopes. Table 15 also shows this drastic variation in slope.

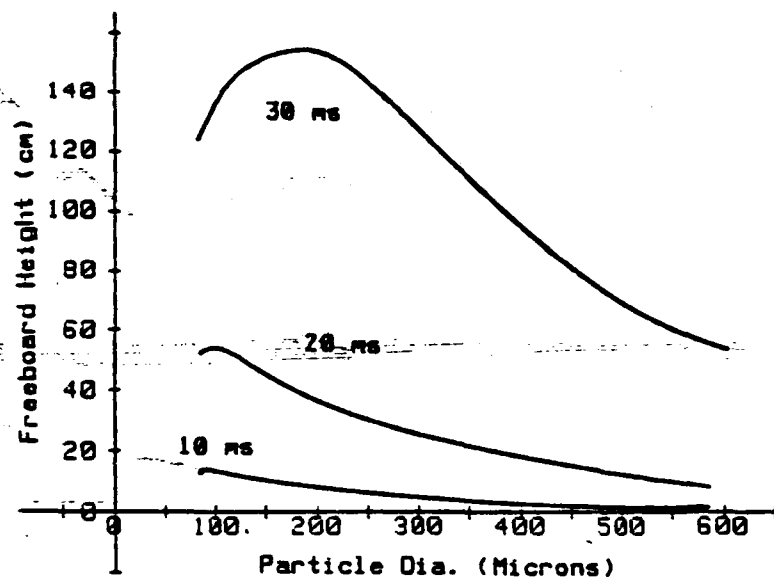


Fig. 66 Maximum Particle Height vs Particle Diameter as a Function of t_j .

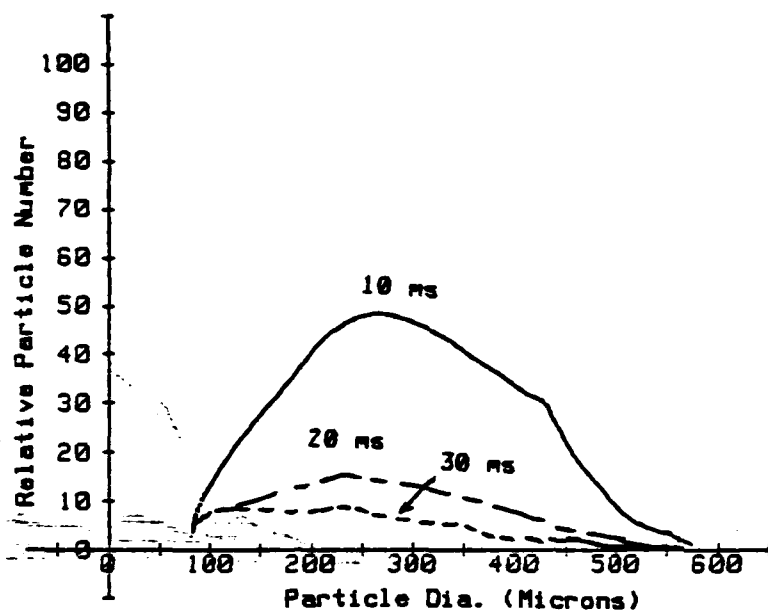


Fig. 67 Relative Particle Number vs Particle Diameter as a Function of t_j . Freeboard Height of 4 cm.

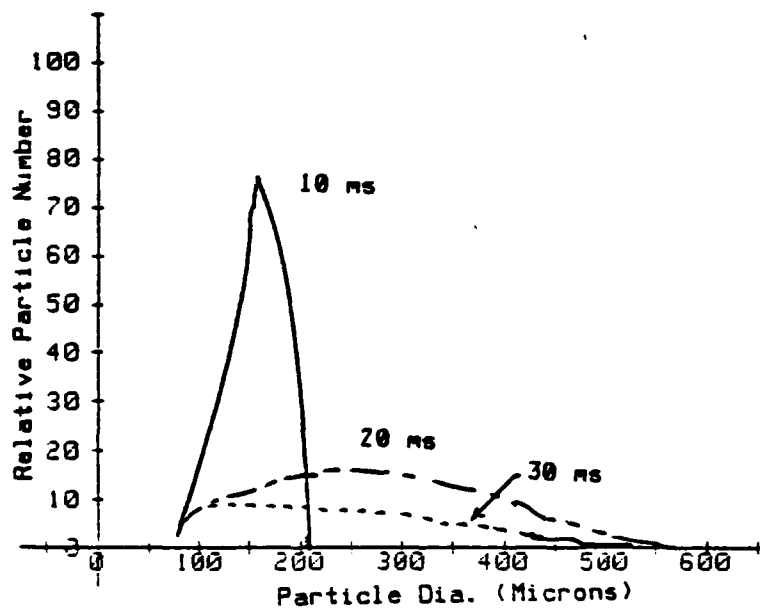


Fig. 68 Relative Particle Number vs Particle Diameter as a Function of t_j . Freeboard Height of 8 cm.

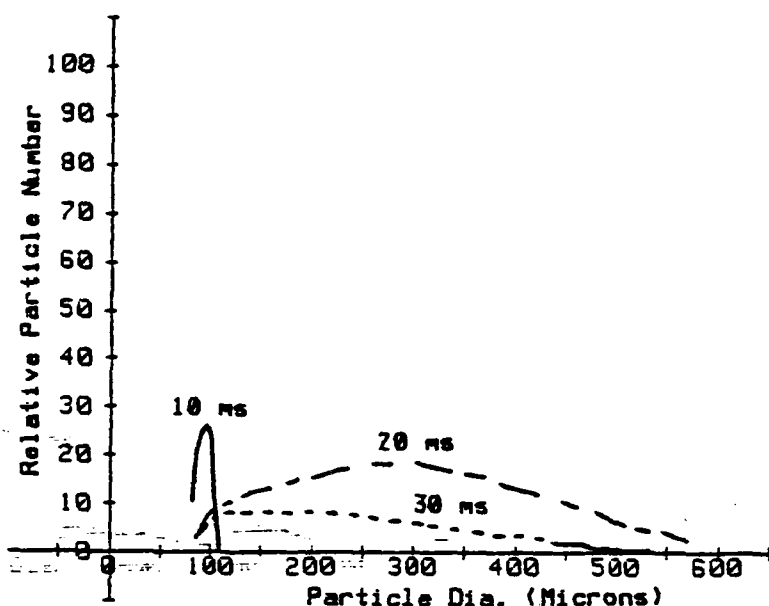


Fig. 69 Relative Particle Number vs Particle Diameter as a Function of t_j . Freeboard Height of 12 cm.

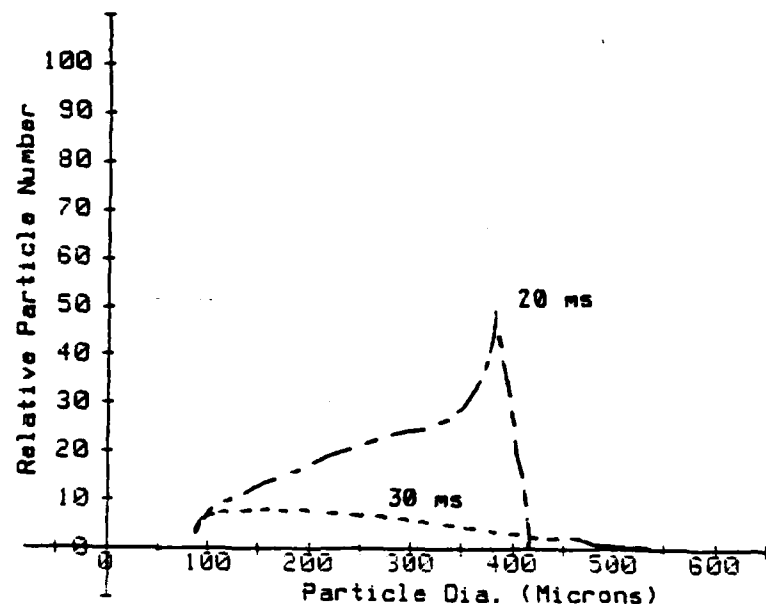


Fig. 70 Relative Particle Number vs Particle Diameter as a Function of t_j . Freeboard Height of 18 cm.

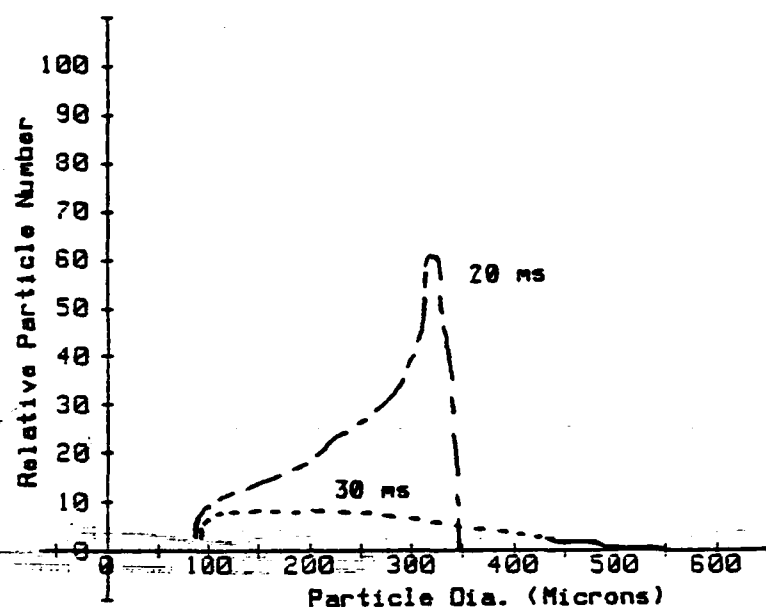


Fig. 71 Relative Particle Number vs Particle Diameter as a Function of t_j . Freeboard Height of 22 cm.

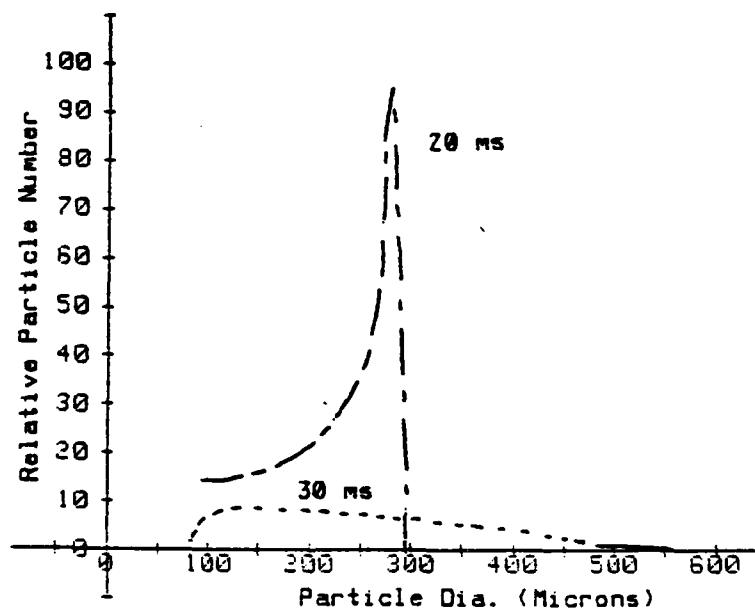


Fig. 72 Relative Particle Number vs Particle Diameter as a Function of t_j . Freeboard Height of 31 cm.

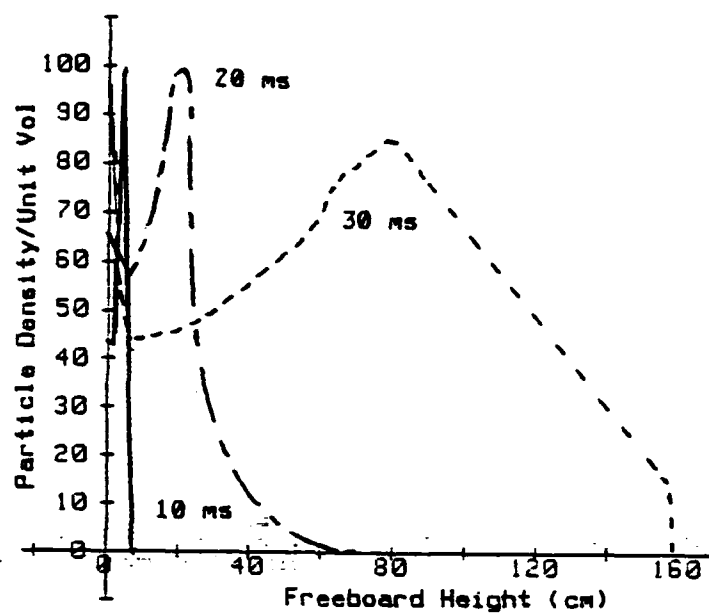


Fig. 73 Particle Density/Unit Volume vs Freeboard height as a Function of t_j .

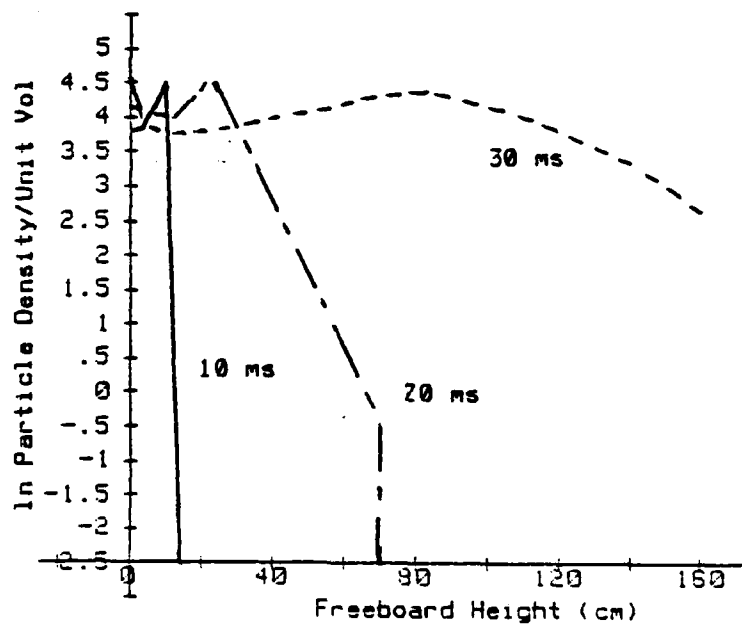


Fig. 74 \ln Particle Density/Unit Volume vs Freeboard height as a Function of t_j .

TABLE 15

| tj cm/s | Slope gms/cm | Intercept gms/cm |
|------------|-----------------|---------------------|
| 10.0 | -1.071 | 12.50 |
| 20.0 | -0.117 | 6.758 |
| 30.0 | -0.020 | 6.234 |

Effect of tj on the slope of the particle density distribution as a function of height for the distributions shown in Fig. 74.

Variation of Particle Distribution in Bed Mass

Fig. 75 shows the two bed particle distributions used in this analysis. The determination of these distributions is described earlier in this work.

Figs. 76 thru 81 show the effects of varying the bed particle distribution on the individual particle distributions at different heights above the bed surface. Using the sieve particle distribution instead of the image analysis distribution produces a shift in the mean particle distribution towards the smaller particles. The distributions resulting from the sieve data do not shift as much as the image analyzer data when the freeboard height is increased. The small shift in mean diameter exhibited by these plots is consistent with the distributions listed in Appendix J.

Fig. 82 shows the particle density distributions in the

Faired Data From Appendix E and J. Interval of 10 microns.

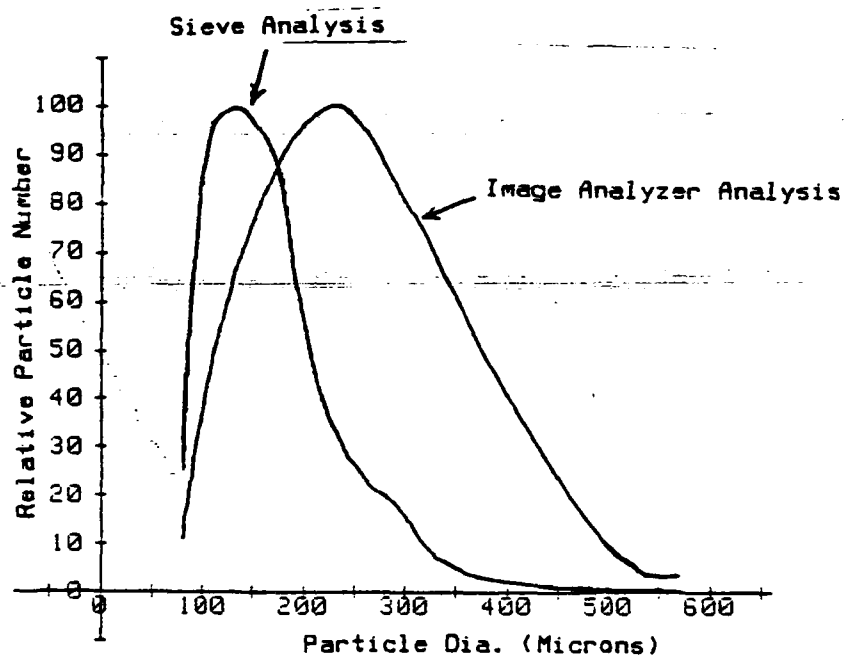


Fig. 75 Relative Particle Number vs Particle Diameter for Bed Mass Material.

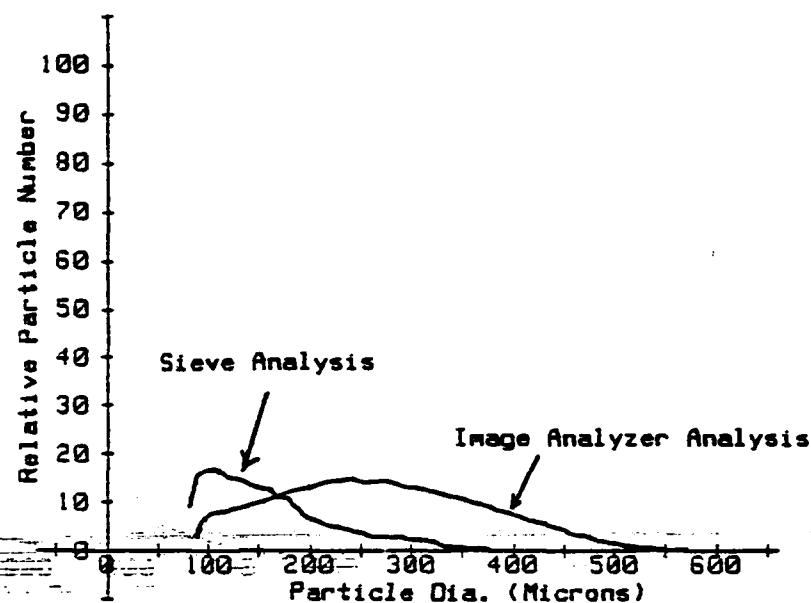


Fig. 76 Relative Particle Number vs Particle Diameter as a Function of Bed Mass.

Freeboard Height of 4 cm

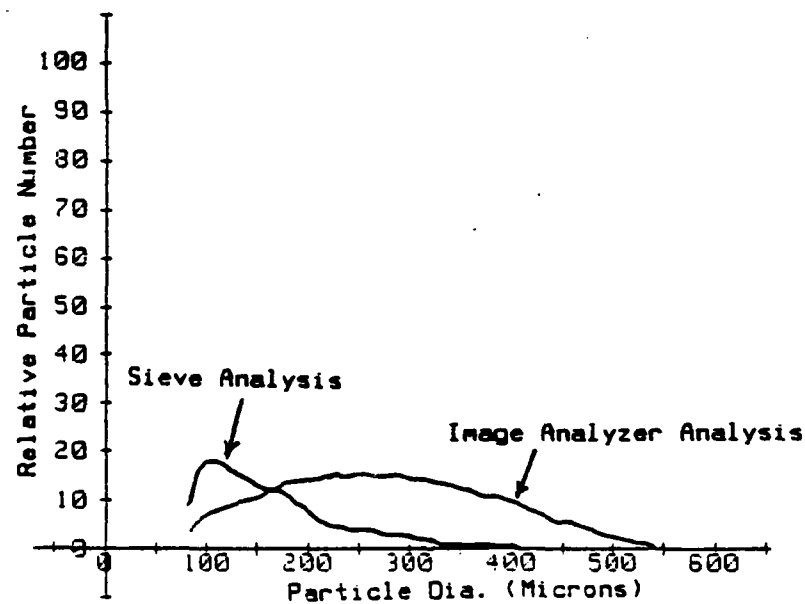


Fig. 77 Relative Particle Number vs Particle Diameter as a Function of Bed Mass.

Freeboard Height of 8 cm.

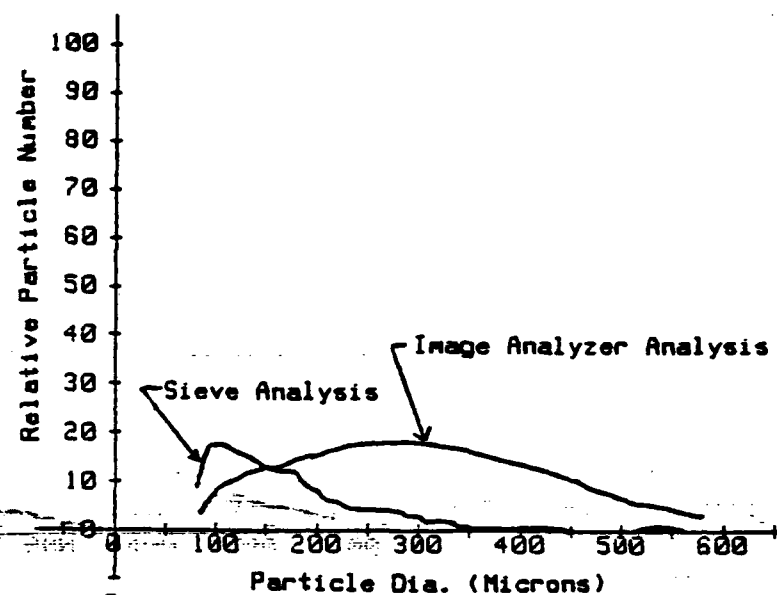


Fig. 78 Relative Particle Number vs Particle Diameter as a Function of Bed Mass. Freeboard Height of 12 cm.

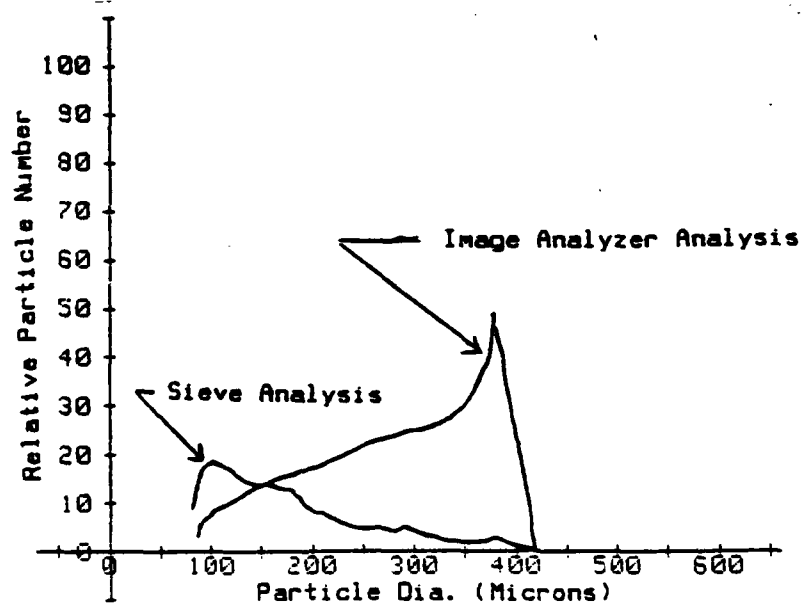


Fig. 79 Relative Particle Number vs Particle Diameter as a Function of Bed Mass. Freeboard Height of 18 cm.

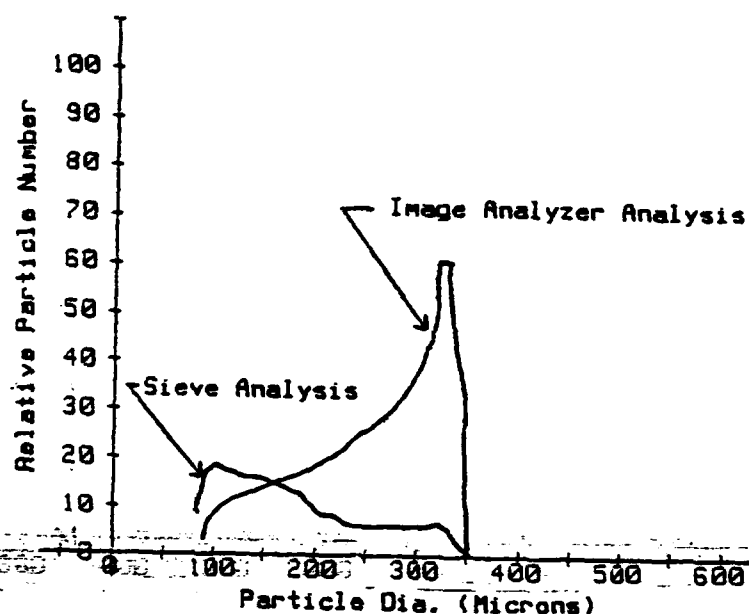


Fig. 80 Relative Particle Number vs Particle Diameter as a Function of Bed Mass. Freeboard Height of 22 cm.

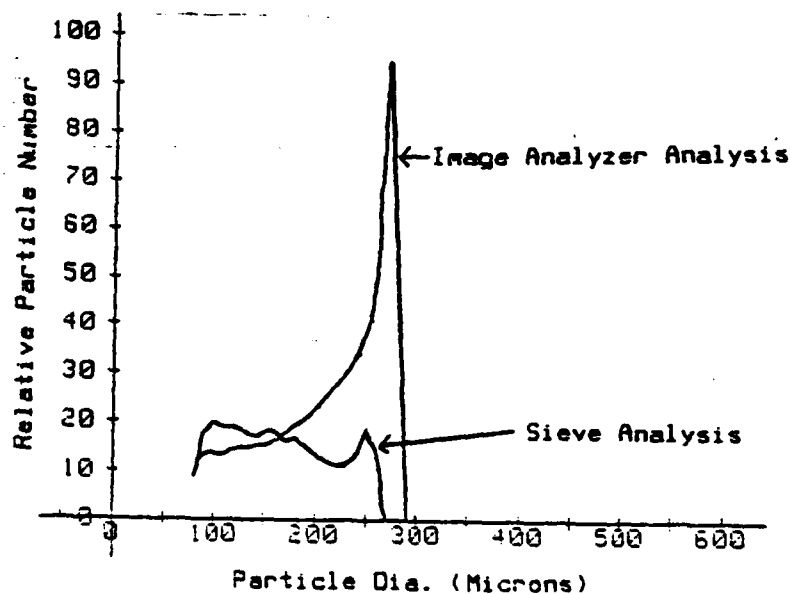


Fig. 81 Relative Particle Number vs Particle Diameter as a Function of Bed Mass. Freeboard Height of 31 cm.

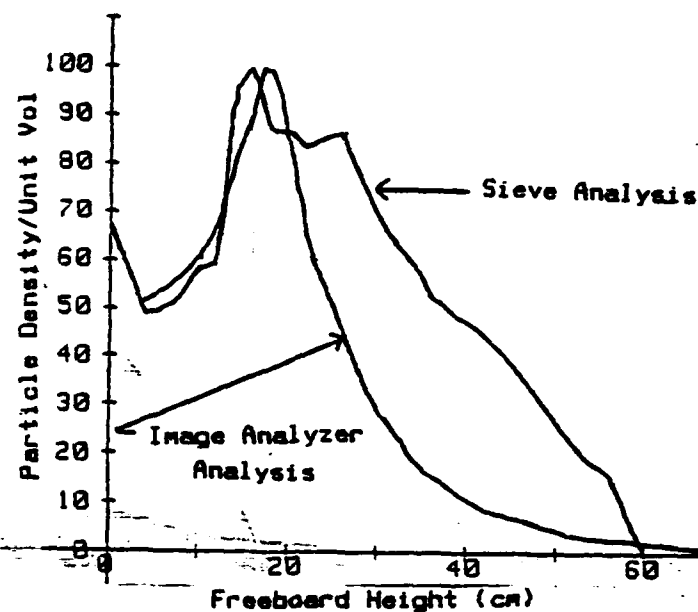


Fig. 82 a Particle Density/Unit Volume vs Freeboard height as a Function Bed Mass.

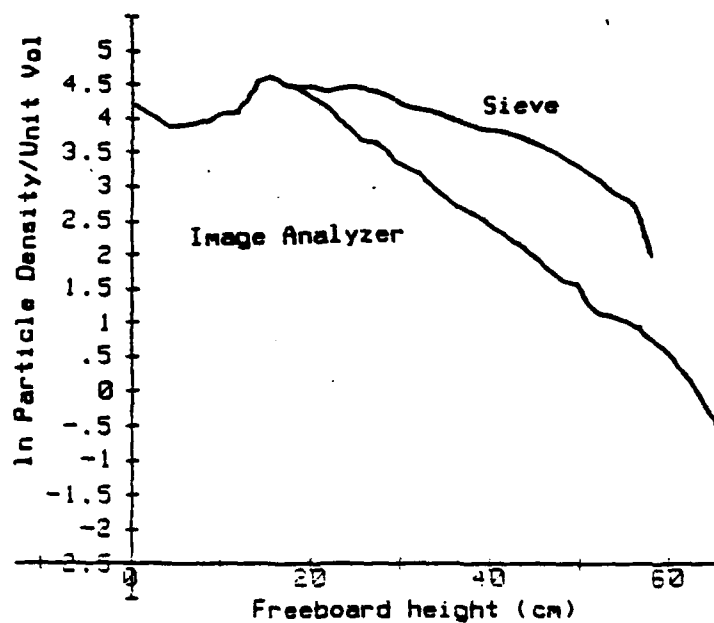


Fig. 82b

freeboard for the two bed mass conditions. The effect of the sieve distribution (which has a much lower average particle diameter) is to decrease the initial rate at which particle mass returns to the bed. This is due to the smaller particles having a much smaller terminal velocity. This will not only raise the bulk of the particles to a higher height, but will also increase the time required for the particles to return to the bed.

Comparison of Model with Experimental Results

As discussed in the previous section, the baseline parameters were selected as the experimental conditions present in the bed when sampling at the highest U_0 setting. Table 16 lists these baseline parameters again for review.

TABLE 16

U_0 = 57.9 cm/s (1.9 ft/s)
 U_{p0} = 97.2 cm/s (3.19 ft/s)
 U_j = 609.6 cm/s (20 ft/s)
 t_j = 20 ms

Baseline parameters used in computer model.

Fig. 83 shows the particle density distribution predicted by the model using the baseline conditions. Fig. 84 is a semi-log plot of this same data. A comparison of the slope of the

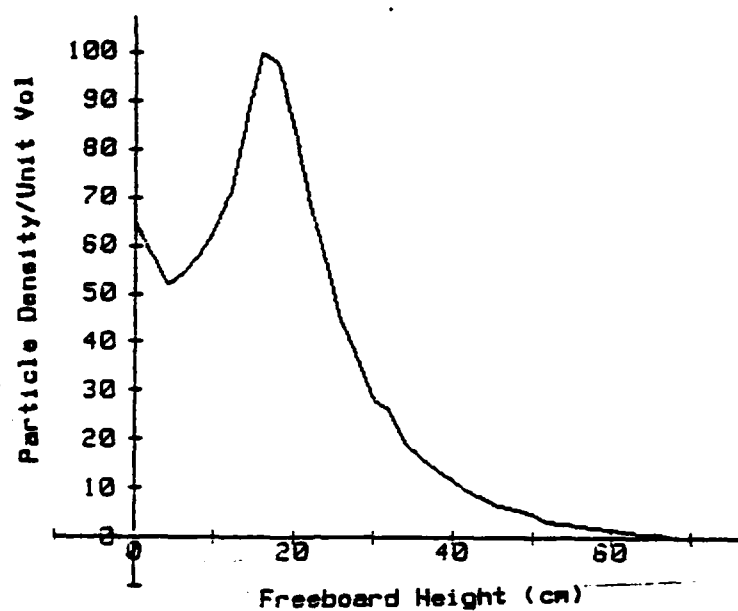


Fig. 83 Particle Density/Unit Volume vs Freeboard height for Baseline Conditions.

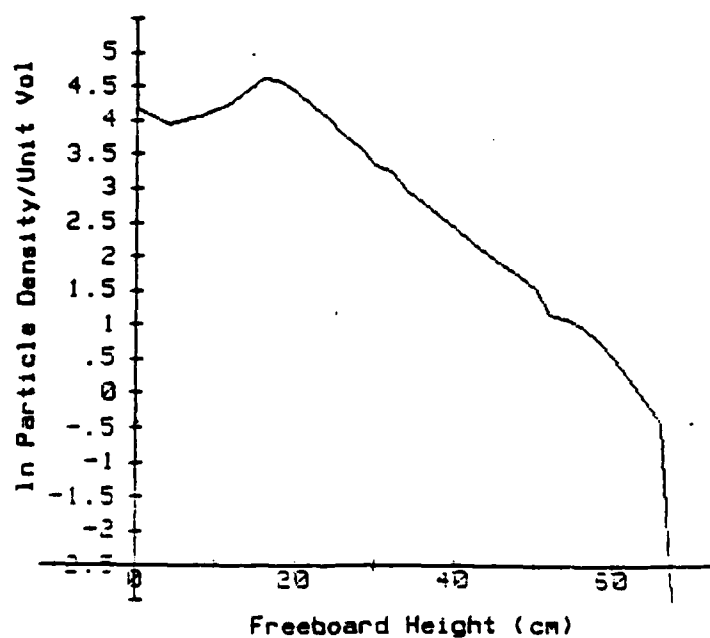


Fig. 84 ln Particle Density/Unit Volume vs Freeboard height for Baseline Conditions.

distribution line after the peak value in Fig. 84 with the slope obtained from the experimental data shows very good agreement between the two. This data is also given in Table 17 along with the data obtained for the other experimental data sets and is shown plotted in Fig. 85. The slopes for the model data show a steady increase in slope as U_o/U_{mf} is decreased. This trend is also followed by the experimental data but is not as smooth. The slope of the experimental data is also changing faster than the slope of the model data. One reason for this is that all the model calculations were performed using the same value for jet velocity and duration of 609.6 cm/s and 20 ms respectively. The magnitudes of these values should decrease with decreasing U_o/U_{mf} , but the values to be used for these different conditions could not be determined.

TABLE 17

| U_o/U_{mf} | Experimental Slope gms/cm | Model Slope gms/cm | Diff % |
|--------------|---------------------------------|--------------------------|-----------|
| 3.81 | -0.1097 | -0.117 | 6.6 |
| 3.17 | -0.1029 | -0.123 | 19.5 |
| 2.59 | -0.1181 | -0.129 | 9.2 |
| 2.32 | -0.1399 | -0.132 | 5.6 |

Comparison of slopes for the particle density distributions above the bed as derived from the experimental data and the computer model.

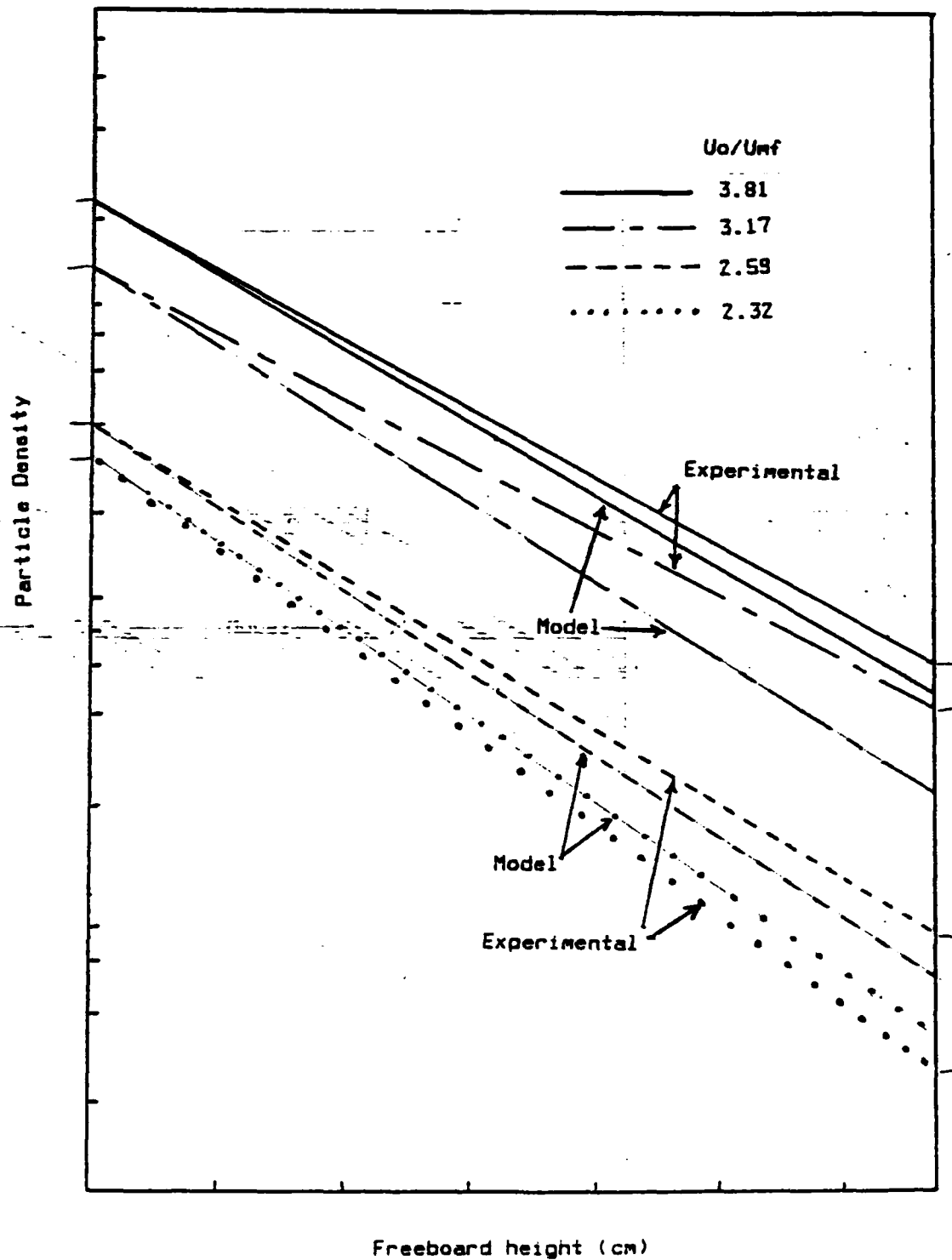


Fig. 85 Comparison of slopes for the particle density distribution above the bed as derived for experimental data and computer model output.

The slope shown in Fig. 84 for heights between approximately 4 and 18 cm is totally different from the slopes listed in table 17. This is also the lower range in which the experimental data was collected. As was shown earlier, when the particle distribution analyzed included particles from 80 - 1070 microns, the peak was located at 11 cm. This is the height where the largest particles attain their maximum height and begin to fall back to the bed. It does not seem likely that including the few particles present above 1070 microns would totally account for this discrepancy. Other factors which the model has not accounted for which may explain these discrepancies is the effect of varying ~~averages and time~~ jet velocities and durations which were shown in chapter V to vary greatly, and the effect of particles whose velocity vector is not ~~perpendicular to the bed surface.~~ perpendicular to the bed surface.

CHAPTER VII

CONCLUSIONS AND RECOMMENDATIONS

Conclusions

Several important conclusions can be made concerning the particle trajectory computer model and the experimental data.

1. A particle trajectory model, even as simple as the one discussed in this work, produces results which closely predict several aspects of particle activity within a fluidized bed. The more important predictions include the particle density distribution in the freeboard and the height distribution of particles. The results obtained with the current model indicate that further work on improving the particle trajectory model to include particle-particle interactions and particle velocities not perpendicular to the bed surface is very desirable.

2. The sensitivity analysis indicates that the jet duration and jet velocity are critical parameters in determining particle loading conditions in the freeboard. Since these are constantly changing from one bubble eruption to the next, a statistical distribution will be required to accurately model freeboard particle activity. The development of a basic model to predict

the jet duration and velocity as a function of bubble size, U_0 , U_{mf} , etc is therefore needed.

3. Particle distribution analysis of experimental samples at increasing heights above the bed, show the presence of large particles. Many of these are above the maximum calculated trajectory heights for these particle sizes. This indicates that either the jet velocity or jet duration carried these particles to these heights, or, particle-particle collisions are present in numbers great enough to be important in the analysis.

4. The sampling apparatus designed and built for this study appears to operate satisfactory. The data obtained correlates with work done by other researchers and with the computer model. However, additional work is needed to correlate sample size and particle size distribution with freeboard height.

Recommendations

1. Further experimental data is needed at higher velocities and higher heights above the bed using the sampling apparatus designed in this work. This will provide additional data to evaluate the operation of the sampling apparatus and the computer model. Also, a scale capable of measuring quantities of samples less than 0.01 grams and a particle removal system which removes the particles with less error from the sample trap is necessary for accurate work.

2. A sampling device which has a shorter trap height should be designed. The present sample trap is very direction oriented and samples particles traveling only in a narrow range from the vertical. This would allow more accurate work to be done in the splash zone where particles are more likely to be traveling in directions other than vertical.

3. The computer model needs to have incorporated in it, a statistical distribution model for jet velocity and jet duration. This will allow the determination of the effects of varying jet velocity and duration on particle distributions in the freeboard.

4. A correlation for jet velocity and duration as functions of bubble diameter, U_0 , and U_{mf} should be determined and included in the model.

REFERENCES

- [1] D. Kunii and O. Levenspiel, Fluidization Engineering, Robert E. Krieger Pub Co., Huntington, NY, 1977.
- [2] P.A. Tipler, Modern Physics, Worth Publishers Inc, New York, NY, 1978, p74.
- [3] W.K. Lewis, E.R. Gilliland and Peter M. Lang, "Entrainment From Fluidized Beds", Fluidization, AIChE Symposium Series, No. 38, Vol. 58, 1962, p65.
- [4] F.A. Zenz and N.A. Weil, "The Theoretical-Empirical Approach to the Mechanism of Particle Entrainment from Fluidized Beds", AIChE Journal, No. 4, Vol. 4, 1958, p472.
- [5] C.Y. Wen and L.H. Chen, "Fluidized Bed Freeboard Phenomena: Entrainment and Elutriation", Chemical Engineering Research and Development, AIChE Journal, Vol. 28, No. 1, January 1982, p117.
- [6] R.E. Page and D. Harrison, "Particle Entrainment from a Three-Phase Fluidized Bed", Fluidization and its Applications, Proceedings of the International Symposium, 1974, p393.
- [7] P.M. Walsh, T.Z. Chung, A. Dutta, J.M. Beer, and A.F. Sarofim, "Particle Entrainment and Nitric Oxide Reduction in the Freeboard of a Fluidized Coal Combustor", American Chemical Society Division of Fuel Chemistry, No. 1, Vol. 27, 1982, p243.
- [8] S.E. George and J.R. Grace, "Entrainment of Particles from Aggregative Fluidized Beds", Fluidization: Application to Coal Conversion Processes, AIChE Symposium Series, No. 176, Vol. 74, 1978, p67.
- [9] T.P. Chen and S.C. Saxena, "A Theory of Solids Projection from a Fluidized Bed Surface as a First Step in the Analysis of Entrainment Processes", Fluidization, Proceedings, Cambridge University Press, 1978, p151.
- [10] P.M. Walsh, J.E. Mayo, and J.M. Beer, "Refluxing Particles in the Freeboard of a Fluidized Bed", Fluidization and Fluid-particle Systems: Theories and Applications, AIChE Symposium Series, No. 234, Vol. 80, 1984, p119.
- [11] A. Nazemi, M.A. Bergougnou, and C.G.J. Baker, "Dilute Phase Hold-up in a Large Gas Fluidized Bed", Fluidization and Fluid-particle Systems: Theories and Applications, AIChE Symposium Series, No. 141, Vol. 70, 1974, p98.

- [12] L. R. Glicksman, W. K. Lord, G. McAndrews, M. Sakagami,
"Measurement of Bubble Properties in Fluidized Beds",
Proceedings of the Seventh International Conference on Fluidized
Beds, 1982.
- [13] M.H. Peters and D.L. Prybylowski, "Particle Motion Above the
Surface of a Fluidized Bed: Multiparticle Effects",
Fluidization and Fluid-particle Systems: Theories and
Applications, AIChE Symposium Series, No. 222, Vol. 79, 1983,
p83.
- [14] R.G. Boothroyd, Flowing Gas-Solids Suspensions,
Chapman and Hall LTD, London, 1971.
- [15] W.K Lord, "Bubbly Flow in Fluidized Beds of Large Particles",
Sc.D. Thesis, M.I.T., Department of Mechanical Engineering,
1983.
- [16] H.S. Bean, "Fluid Meters Their Theory and Application", Report
of ASME research committee on fluid meters, sixth edition,
The American Society of Mechanical Engineers, New York, NY,
1971.
- [17] Frank M. White, Viscous Fluid Flow, McGraw-Hill, 1974,
p209.

APPENDIX A

Moment of Inertia Calculations for Paddles

The calculation of the total Moment of inertia (I) of the paddles can be broken up into three separate calculations. First, the moment of inertia (I1) of the two aluminum cylinders used to mount the paddle arms to the solenoid shaft is calculated. The second calculation (I2), accounts for the moment of inertia of the paddles themselves, which are constructed of a foam, basswood and epoxy laminate (Figure A-10). Finally, the moment of inertia (I3) of the hardwood mounting ends on the paddles is calculated.

The following equations were used to calculate the mass moments of inertia:

$$I1 = \frac{P H r^4}{2} \quad (A1)$$

$$I2 = \frac{L W (L^2 + W^2) (P1 t1 + P2 t2)}{12} \quad (A2)$$

$$I3 = \frac{2 L W t + P (L^2 + W^2)}{12} \quad (A3)$$

Table A.1 is a listing of parameters required for the moment calculations.

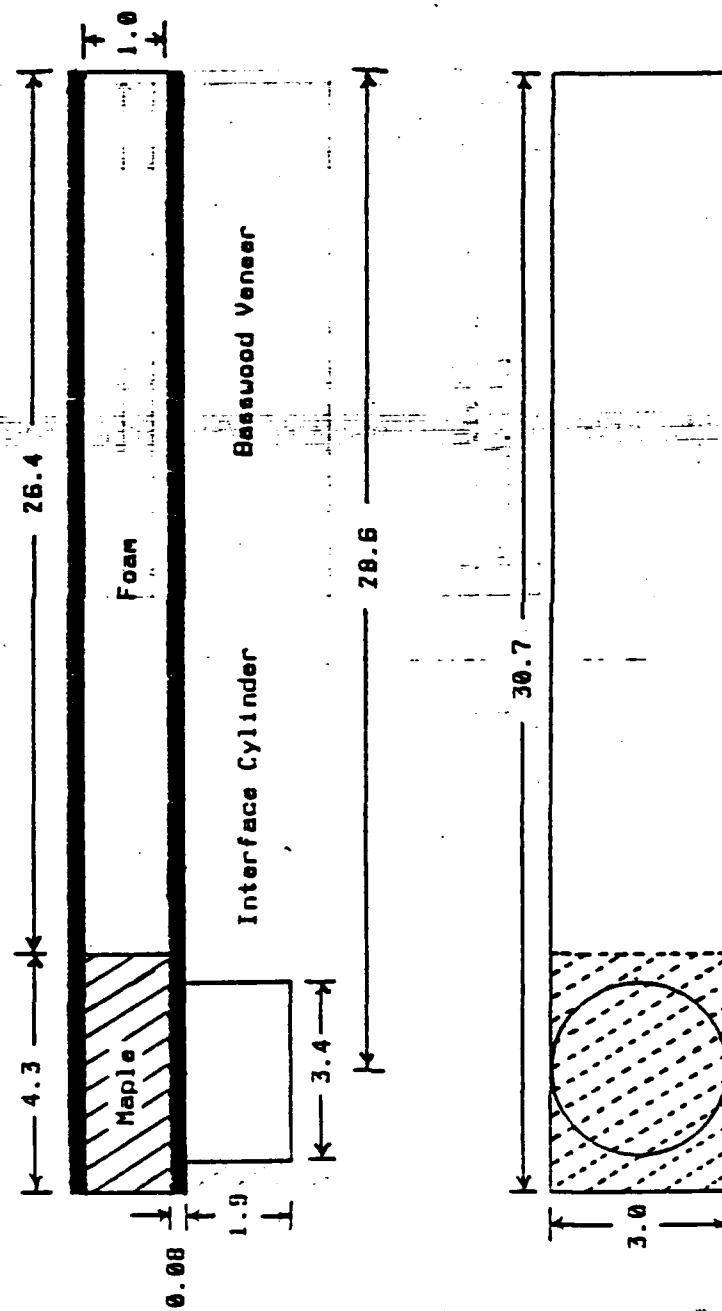


Fig. A-1 Construction of Paddles with Aluminum Interface Cylinder Shown. All Dimensions in cm.

TABLE A.1

| Component | MKS units | | English units | |
|--------------------------|-----------|-------------------|---------------|---------------------|
| <u>Aluminum Cylinder</u> | | | | |
| Density Al [P1] | 2780 | kg/m ³ | 0.1004 | lbf/in ³ |
| Radius [r] | 0.0171 | m | 0.675 | in |
| Height [H] | 0.0381 | m | 1.5 | in |
| <u>Paddles</u> | | | | |
| Density Foam [P1] | 50 | kg/m ³ | 0.00181 | lbf/in ³ |
| Density Basswood [P2] | 400 | kg/m ³ | 0.0144 | lbf/in ³ |
| Thickness Foam [t1] | 0.0102 | m | 0.4 | in |
| Thickness Basswood [t2] | 0.00159 | m | 0.0625 | in |
| Length Foam [L1] | 0.5842 | m | 23.0 | in |
| Length Basswood [L2] | 0.5842 | m | 23.0 | in |
| Width Foam [W1] | 0.0305 | m | 1.2 | in |
| Width Basswood [W2] | 0.0305 | m | 1.2 | in |
| <u>Hardwood</u> | | | | |
| Density Maple [P1] | 650 | kg/m ³ | 0.0235 | lbf/in ³ |
| Thickness Maple [t] | 0.0102 | m | 0.4 | in |
| Length Maple [L] | 0.0432 | m | 1.7 | in |
| Width Maple [W] | 0.0348 | m | 1.2 | in |

Listing of paddle components and parameters.

Equation (A.1) is used to calculate the mass moment of inertia for a right circular cylinder rotating about its Z axis (Fig. A-2). The height H, accounts for both the upper and the lower solenoid shaft cylinders. Equations (A.2) and (A.3) determine the mass moment of inertia for a rectangular prism

rotating about its X-Y axis rotating about its X-Y centroidal axis (Fig. A-3). The length L

in equation A2 accounts for both the upper and lower paddle

lengths. The factor of 2 in equation (A.3) is because both the upper and lower hardwood sections are identical and can be

combined. By inserting the respective values from Table A.1 into

equations (A.1), (A.2), and (A.3), the value for each inertia

component can be calculated. Adding these components, the total

mass moment of inertia applied to the solenoid by the paddles is

determined. These results are listed in Table A.2.

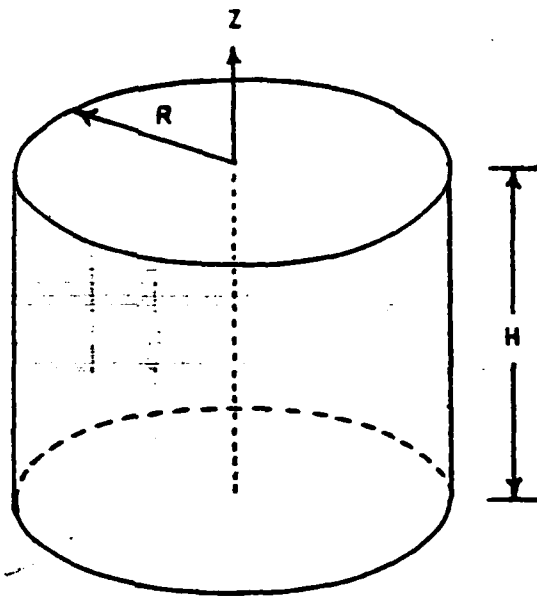


Fig. A-2 Diagram for Moment of Inertia Calculation
Used for Cylinder About Z Axis.

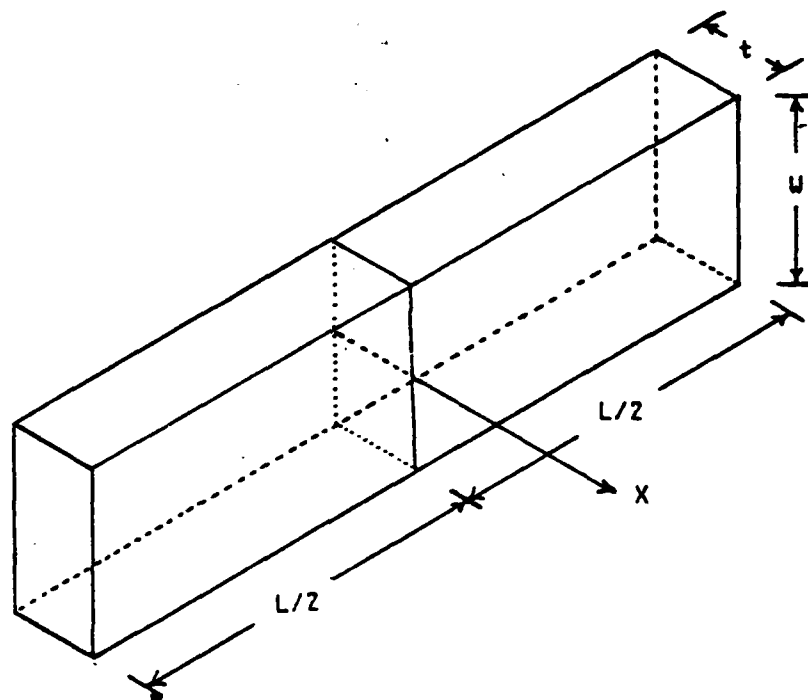


Fig. A-3 Diagram for Moment of Inertia Calculation
Used for Rectangular Prism About X Axis.

TABLE A.2

Moment of inertia components:

| MKS units | English units |
|-------------------------------------|--------------------------------|
| $I_1 = 1.422 (-05) \text{ kg m}^2$ | $4.911 (-02) \text{ lbf in}^2$ |
| $I_2 = 5.823 (-04) \text{ kg m}^2$ | $1.982 (00) \text{ lbf in}^2$ |
| $I_3 = 2.556 (-06) \text{ kg m}^2$ | $6.919 (-03) \text{ lbf in}^2$ |
| Total moment: $I = I_1 + I_2 + I_3$ | |
| $I = 5.991 (-04) \text{ kg m}^2$ | $2.037 (00) \text{ lbf in}^2$ |

Calculated values for mass moment of inertia of paddles and paddle components. I_1 is inertia value for the aluminum cylinders. I_2 is the inertia value for the paddles themselves and I_3 is for the hardwood end pieces.

APPENDIX B

Error Determination of Vacuum Collection System

Tests of the vacuum sample removal system indicated that some particles remained in the sample trap. These particles were located in the corners of the trap where the equalizing air stream could not agitate them enough to move them into the vacuum stream. As a result, it became necessary to determine to what extent these remaining particles affected the accuracy of the sample attained.

The procedure used involved placing samples of known weight and particle size distribution (equivalent to the bed material) inside the sample trap. Sample sizes of 10, 15, 20, and 25 grams were used. The sample particles were then vacuumed out and their weight determined. The difference in weights of the samples were then calculated along with the percentage differences. These results are listed in Table B.1.

An analysis of the results listed in Table B.1 indicates that the average difference between the two sample weights is only 0.52 % while the maximum difference observed was 0.93 %. It can therefore be concluded that the particles remaining in the sample trap do not significantly affect the accuracy of the sample attained.

TABLE 8.1

| SAMPLE No. | Initial Weight grams | Sample Weight grams | Weight Difference grams | Weight Difference Percent |
|---------------|----------------------------|---------------------------|-------------------------------|---------------------------------|
| 1 | 10 | 9.95 | 0.05 | 0.50 |
| 2 | 10 | 9.92 | 0.08 | 0.80 |
| 3 | 10 | 9.95 | 0.05 | 0.50 |
| 4 | 10 | 9.98 | 0.02 | 0.20 |
| 5 | 15 | 15.03 | -0.03 | -0.20 |
| 6 | 15 | 15.02 | -0.02 | -0.13 |
| 7 | 15 | 14.86 | 0.14 | 0.93 |
| 8 | 15 | 14.87 | 0.13 | 0.87 |
| 9 | 15 | 14.97 | 0.03 | 0.20 |
| 10 | 20 | 19.93 | 0.07 | 0.35 |
| 11 | 20 | 19.86 | 0.14 | 0.70 |
| 12 | 20 | 19.90 | 0.10 | 0.50 |
| 13 | 20 | 19.93 | 0.07 | 0.35 |
| 14 | 20 | 19.94 | 0.06 | 0.30 |
| 15 | 25 | 24.83 | 0.17 | 0.68 |
| 16 | 25 | 24.80 | 0.20 | 0.80 |
| 17 | 25 | 24.78 | 0.22 | 0.88 |
| 18 | 25 | 24.83 | 0.17 | 0.68 |
| 19 | 25 | 24.77 | 0.23 | 0.93 |
| AVG= | | | 0.10 | 0.52 |
| STNDV= | | | 0.08 | 0.34 |

Results of vacuum sample removal test.

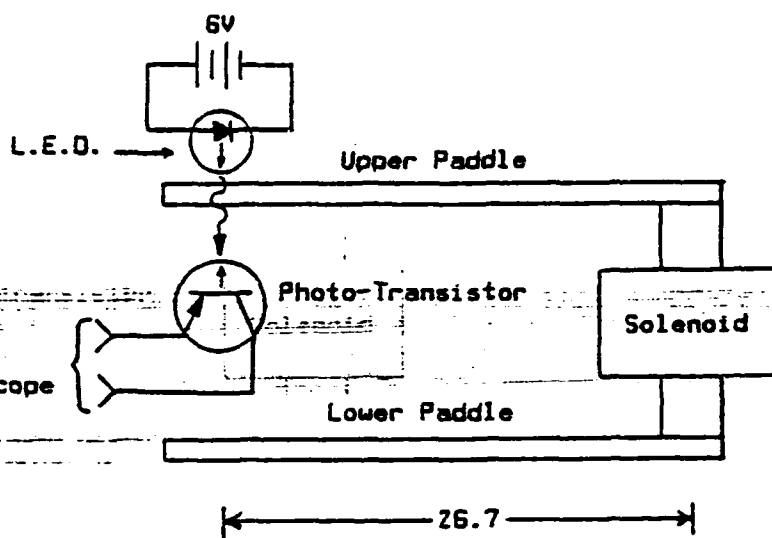
APPENDIX C

Sample Trap Closure Time Test

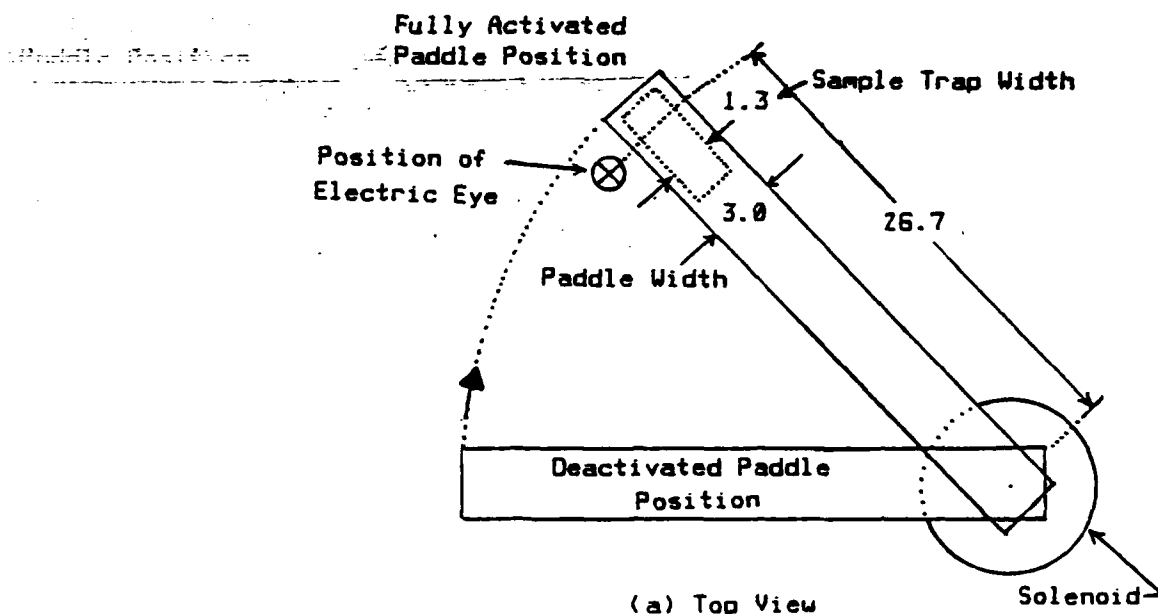
Due to the high velocity of the particles with respect to the size of the sample trap, it was important to ensure that the sample trap was closed in a very short period of time. To measure the closure time, the set-up shown in Fig. C-1 was used.

An electric eye, consisting of a light emitting diode and a photo transistor, was used. The diode was powered by a 6 volt battery and the photo transistor was wired directly to an oscilloscope. The electric eye circuit was then placed at a distance of 0.267 m (10.5 in) from the pivot point of the paddles. At this position, the closing time calculation involves only a simple proportion relationship between the paddle and the sample trap widths. The eye was also positioned as close to the trailing edge of the fully closed paddle as possible to minimize error.

The oscilloscope sweep was set to trigger off of the initial change of state from the photo transistor when the paddle first eclipsed the light beam. The resultant traces were then analysed to determine closure time. Time $t=0$ was set equal to the initiation of the trace on the oscilloscope. Time $t=t_1$ was defined as the point at which the trace begins its excursion back



(b) Side View



(a) Top View

Fig. C-1 Diagram of Closure Time Determination Set Up.
All Dimensions in cm.

to the base voltage as shown in Fig. C-2. By using the ratios:

$$\frac{W_1}{t_1} = \frac{W_2}{t_2} \quad (C.1)$$

Where:

W_1 = width of the paddle

W_2 = width of sample trap

t_1 = time delay measured on oscilloscope

t_2 = closure time of sample trap

the closure time of the sample trap can be determined. Several

trials were run with the resulting data listed in Table C-1. All

of the trials were very consistent. The resultant determination

for the average closure time was 1.44 ms.

TABLE C-1

$W_1 = 0.0305 \text{ m}$ (1.2 in)
 $W_2 = 0.0127 \text{ m}$ (0.5 in)

| Trial No. | t_1 ms | t_2 ms |
|-----------|----------|----------|
| 1 | 3.4 | 1.42 |
| 2 | 3.4 | 1.42 |
| 3 | 3.55 | 1.48 |
| 4 | 3.5 | 1.46 |
| 5 | 3.5 | 1.46 |
| Avg | 3.47 | 1.44 |

Sample trap closure data: W_1 is the width of the paddle, W_2 is the width of the sample trap and time t_1 is eclipse time of paddle through light beam. Time t_2 is closure time of Sample trap as calculated using equation (C.1).

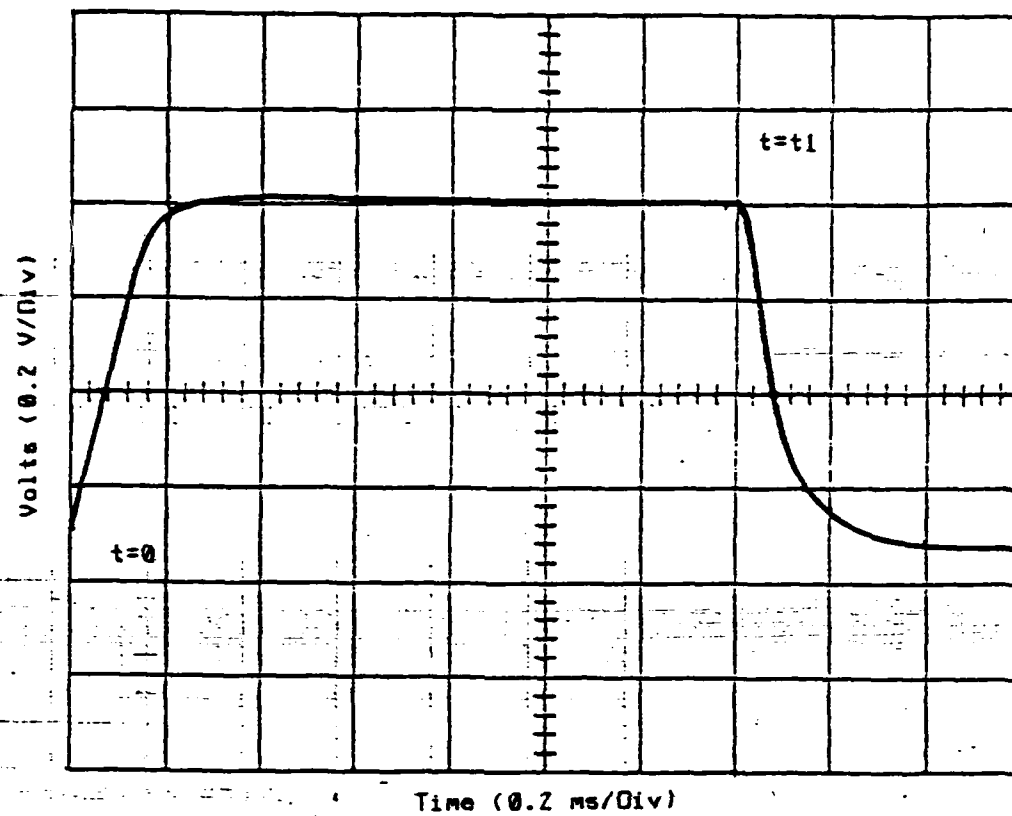


Fig. C-2 Oscilloscope Trace of Paddle
Eclipsing Electric Eye.

APPENDIX D

Solenoid Torque and Dynamic Analysis

The goal of this design. The goal of this design was to shut the sample trap in about 1 millisecond (ms). At this speed, a particle traveling at 10 meters per second (m/s) would travel 1 cm or approximately 11 % of the sample trap length. A velocity of 10 m/s is at the upper limit of the particle velocity distribution and would account for only a small percentage of the particles ejected by the bed. The majority of the particles, for the fluidization conditions used in the bed, have an average ejection velocity of 1-2 m/s, based on data from George and Grace [8].

TORQUE ANALYSIS

To determine the minimum required torque output of the solenoid, two analysis were performed. The first analysis calculates an average torque required to produce the desired velocity. The second analysis uses the torque data from the selected solenoid and calculates the expected closure time and swing time for the paddle arms.

First Analysis

To close the sample trap in 1 ms, the angular velocity of the paddles at closure can be calculated as:

$$u = \frac{W_2}{R t_2} \quad (D.1)$$

where: u = Angular velocity of paddles

W_2 = Width of sample trap

R = Paddle pivot to sample trap distance

t_2 = Closure time of sample trap

Using the values of $W_2 = 0.00197$ m, $R = 0.0413$ m, and $t_2 = 1$ ms,

equation (D.1) results in an angular velocity of 47.70 rad/sec.

The radial acceleration required to attain this velocity through a deflection of $\pi/4$ radians (45 Deg), is calculated by:

$$a = \frac{u^2}{2 \theta} \quad (D.2)$$

where: a = Angular acceleration of paddles

u = Angular velocity of paddles

θ = Angular deflection of paddles

Using the result of equation D1 and $\theta = \pi/4$ radians, equation D2

gives the required angular acceleration of the paddles as 1448.5

rad/s/s. Combining this result with the result for the total mass moment of inertia from Appendix A, the required average torque output of the solenoid can be calculated as:

$$T = I a \quad (D3)$$

where: a = Angular acceleration = Angular acceleration of paddles
 I = Mass moment of inertia
 T = Required solenoid torque

The resultant value for the torque (T) is 0.87 N m (7.7 Lbf in).

A geometric average of the selected solenoid's torque output, as shown in Fig. D-1a, indicates an average of 1.0 N m (8.8 Lbf in).

Therefore, the selected solenoid has sufficient torque output to achieve the desired paddle velocity.

SECOND ANALYSIS

For the second analysis, it will be assumed that the torque output of the selected solenoid can be modeled as a linear spring. Fig. D-1b shows the torque output of the solenoid as a function of angular displacement. From Fig. D-1b, a spring constant of $k = 0.72 \text{ N m/rad}$ (0.11 Lbf in/deg) can be used to approximate the torque curve. The spring constant is derived from the slope of the torque-angular displacement curve.

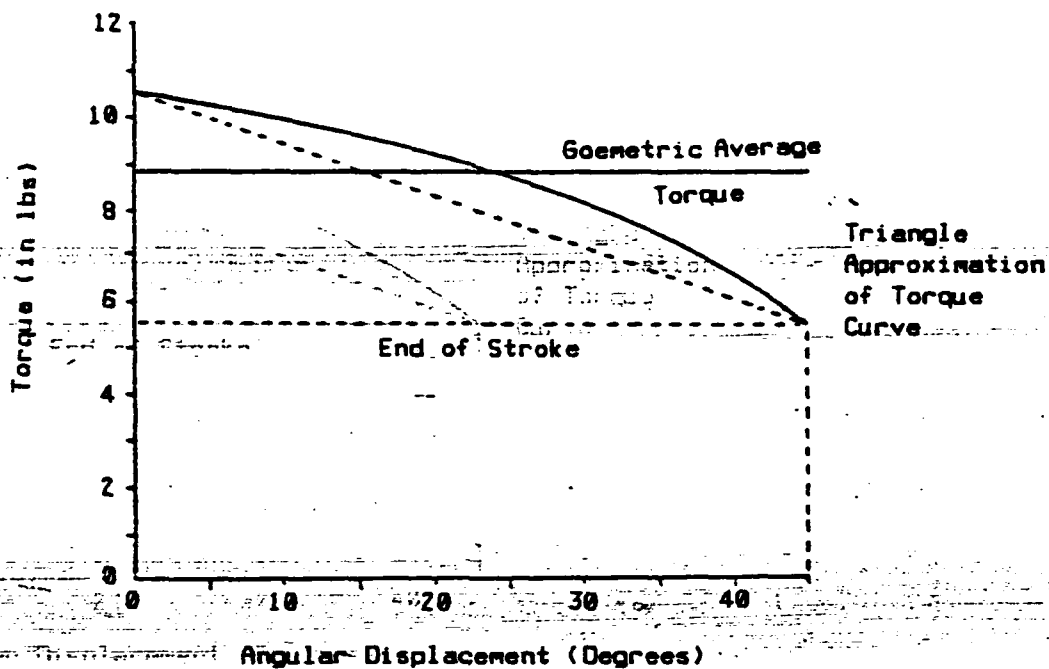


Fig. D-1a Torque Output of Rotary Solenoid Showing Triangle Approximation.

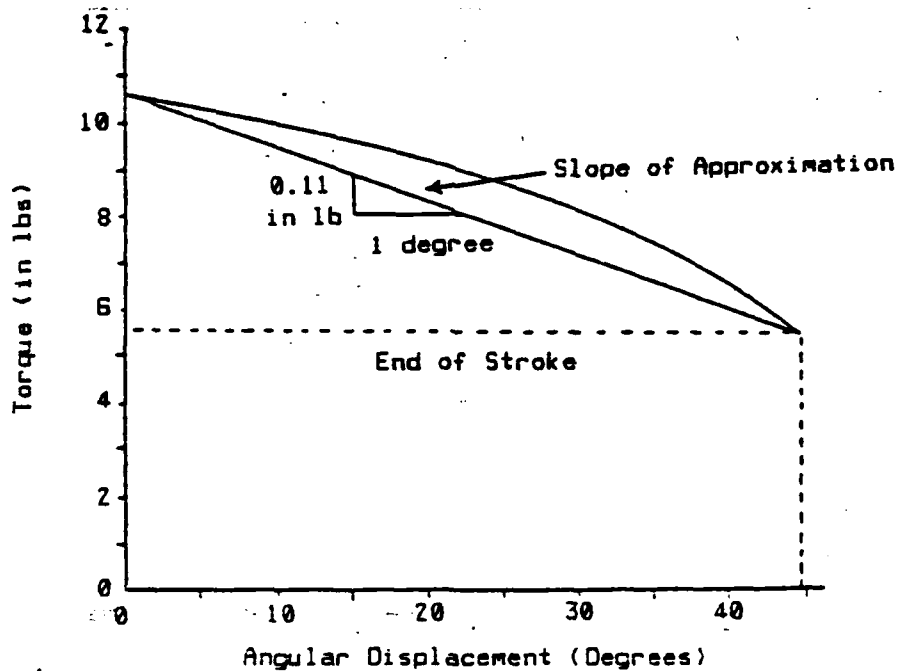


Fig. D-1b Torque Output of Rotary Solenoid Showing Slope of Approximation Curve Used to Determine Spring Constant.

The system can then be modeled as a simple rotational mass - spring system. The differential equation of motion, general solution, and boundary conditions are:

$$\text{Diff Eqn:} \quad I \ddot{\theta} + k \theta = 0 \quad (D.4a)$$

$$\text{Gen. Soln:} \quad \theta = C1 \sin(\omega t) + C2 \cos(\omega t) \quad (D.4b)$$

$$\text{where:} \quad \omega^2 = \frac{k}{I}$$

$$\text{b.c.:} \quad \begin{array}{ll} 1) & t = 0: \quad \dot{\theta} = 0 \\ 2) & t = 0: \quad \theta = 1.65 \text{ rad} \end{array}$$

Solving equation (D.4b) using the given boundary equations, gives the following expressions for any angular displacement (θ) and angular velocity ($\dot{\theta}$):

$$\theta = 1.65 \cos(\omega t) \quad (D.5a)$$

$$\dot{\theta} = -1.65 \omega \sin(\omega t) \quad (D.5b)$$

Knowing that the solenoid stroke is $\pi/4$ radians, the total solenoid actuation time can be obtained from equation (D.5a) by setting $\theta = (1.65 - \pi/4)$. The total actuation time was determined to be 29.2 ms. Inserting this value for time into equation (D.5b), a rotational velocity of 48.6 rad/s was found. This velocity is very close to the desired velocity obtained from equation (D.1).

DYNAMIC ANALYSIS

The desire to determine whether the debris of a specific bubble has been trapped by the sampling device requires the determination of the total actuation time for the apparatus.

Knowing this value, the delay between the detection of a bubble and the closure of the sample trap can be determined, and hence, whether the particles from the detected bubble were within the vicinity of the trap.

Appendix C determined that the actual closure time for the sample trap was 1.44 ms. Using this value in equation (D.1), a rotational velocity at the end of the stroke of only 33.12 rad/sec is calculated. Because the mass moment of inertia for the solenoid was unknown in the beginning, the analysis ignored it. With the determination of the actual closure time in Appendix C, the total moment of inertia, including the solenoid can be approximated. By iterating equations (D.5a) and (D.5b) with $\dot{\theta} = 33.12$ radians/sec, a new inertia value of 1.27×10^{-3} kg m is determined. Using this inertia value in equation (D.5b), the total actuation time is 42.6 ms. This increase in actuation time of 13.5 ms is relatively close to the manufactures quoted actuation time for the solenoid of 12 ms and suggests that the values are within reason.

Table D.1 provides a summary of the results obtained from the dynamic analysis.

TABLE D.1

Mass moment of inertia:

| | |
|-------------|-------------------------------|
| Paddles (I) | 5.991 (-04) kg m ² |
| | 2.037 (00) lb in ² |

| | | |
|-------------------------|-------------------------|------------------------------|
| Paddles + Solenoid (It) | Paddles + Solenoid (It) | 1.27 (-03) kg m ² |
| | | 4.32 (00) lb in ² |

Closure time:

| | |
|------------------|---------|
| Sample trap (t2) | 1.44 ms |
|------------------|---------|

| | |
|------------------|---------|
| Total swing (t3) | 42.6 ms |
|------------------|---------|

Summary of dynamic analysis results.

APPENDIX E

Bed Particle Size Distribution Analysis

A sample of particles was obtained from the fluidized bed after the bed had been operating for several hours. Sample sizes, ranging from 1.2 to 2.8 kg, were then taken from the central area of the bed. Each sample was then sieved through a series of 14 US standard wire mesh sieves using a Tyler Industrial Products Model RX-24 portable sieve shaker for 30 minutes. The contents of each sieve was then weighed, using a Torsion Balance Co TORBAL scale, to an accuracy of 0.01 gram. The resulting average particle size distribution is listed in Table E.1 and shown in fig. E-1.

TABLE E.1

| US Standard Seive No. | Seive Size um | Weight In Seive grams | Percent of Total Sample | Cumulative Percent |
|-----------------------------|---------------------|-----------------------------|-------------------------------|-----------------------|
| 18 | 1000 | 8.49 | 0.31 | 0.31 |
| 20 | 850 | 24.60 | 0.90 | 1.21 |
| 30 | 600 | 101.96 | 3.73 | 4.95 |
| 35 | 500 | 110.85 | 4.06 | 9.01 |
| 45 | 355 | 176.35 | 6.46 | 15.46 |
| 50 | 297 | 430.77 | 15.78 | 31.24 |
| 60 | 250 | 385.59 | 14.12 | 45.36 |
| 70 | 212 | 395.32 | 14.48 | 59.84 |
| 80 | 180 | 469.20 | 17.18 | 77.03 |
| 100 | 149 | 339.93 | 12.45 | 89.48 |
| 120 | 125 | 125.01 | 4.58 | 94.06 |
| 140 | 106 | 109.45 | 4.01 | 98.06 |
| 170 | 90 | 46.67 | 1.71 | 99.77 |
| 200 | 75 | 5.91 | 0.22 | 99.99 |
| | <75 | 0.30 | 0.01 | 100.00 |

Particle Specific Gravity = 8.1

Average particle size distribution of bed material in grams
and percentage of total weight using sieve analysis.

APPENDIX F

Mean Bed Flow Velocity Determination

To determine the mean velocity of air flowing through the bed, the ASME report on fluid meters [17] was used. Based on this paper, equation (F.1) was used for determining the mass flow rate of air through the bed.

$$W = 0.099702 (K Y F d^2) (\rho dP)^{1/2} \quad (F.1)$$

where:

- W = Mass flow rate (lbm/sec)
- d = Orifice diameter (inches)
- K = Flow coefficient
- F = Thermal expansion factor (1 for air)
- Y = Expansion factor
- dP = Differential pressure (inches water)
- ρ = Density of air (ahead of orifice)

The flow coefficient (K) is a function of Reynold's number, the orifice diameter (d), and the pipe diameter (D). For the pressure tap configuration used in the MIT atmospheric fluidized bed (1-D / 1/2-D) the flow coefficient is calculated using equation (F.2).

$$K = K_o + \frac{1000 b}{\sqrt{B} Re} \quad (F.2)$$

where:

Re = Reynolds No.

B = d/D = (orifice dia / pipe dia)

$$K_o = (0.6014 - 0.01352 D^{-1/4}) \\ + (0.3760 + 0.07257 D^{-1/4}) \\ \left(\frac{0.00025}{D^2 B^2 + 0.00025 D} + B^4 + 1.5 B^{16} \right)$$

$$b = (0.0002 + \frac{0.0011}{D}) \\ + (0.0038 + \frac{0.0004}{D}) \\ (B^2 + (16.5 + 5 D) B^{16})$$

The expansion factor (Y) is determined from equation (F.3) and is a function of the diameter ratio (B), the ratio of specific heats (s), and the ratio of the differential pressure to inlet pressure.

$$Y = 1 - (0.410 + 0.350 B^4) \frac{dP}{P_1 s} \quad (F.3)$$

where:

P₁ = Inlet pressure

s = Ratio of specific heats (1.4 for air)

Mass flow rate is a function of velocity, and therefore, by definition a function of Reynold's number. Equation (F.4) is used to determine mass flow rate as a function of viscosity and Reynold's number.

$$W = \frac{u D^2}{C Re} \quad (F.4)$$

where :

u = Absolute viscosity (lbm/ft sec)
 C = Constant (15.28)

This requires that the solutions of equation (F.1) and equation (F.4) be iterated until the Reynold's numbers converge. The determination of mean air velocity is obtained from the mass flow rate (W) using equation (F.5).

$$V = \frac{W}{\rho A} \quad (F.5)$$

where:

ρ = Density of air (lbm/ft³)
 A = Area of bed (ft²)

To perform these calculations, a computer program was used. The program (APPENDIX G) is written in HP BASIC 2.0 for running on an HP 9816 series 200 micro-computer. Convergence usually required four to seven iterations and should be correct to within 0.5%.

APPENDIX G

This Appendix lists the BASIC computer program used to calculate mean bed velocity as discussed in Appendix F. It is written in HP BASIC 2.0.

```

10      !.....MAIN Program.....
20      ! Metering of gases by means of the ASME square-edged orifice with
30      ! 1-D 1/2-D taps. Reference Fluid Meters Their Theory and
40      ! Application, ASME Report 6th edition, ASME New York, NY, 1971
50      ! Program must be altered for Orifice diameter other than 7.071 in
60      ! and pipe diameter other than 10.02 in. (see line 130)
70      !
80      !
90      !
100     INTEGER Answer
110     REAL D1,D2,W,K,Y1,P1,P1a,T1,S,P_del,Beta,Area_bed,Vmu,Reynolds_no,Rho,Rho1
,P1a,Velocity
120     DIM Homes(2),Clears(2)
130     DATA 7.071,10.02,1.4,11.511,50000.,76.
140     READ D2,D1,S,Area_bed,Reynolds_no,P1a
150     Clears=CHRS(255)&CHRS(75)                ! CLEAR screen
160     Homes=CHRS(255)&CHRS(84)                  ! HOME screen
170     !
180     ! Input variables
190     !
200     INPUT "Enter static pressure P1 (cm Hg): ",P1
210     INPUT "Enter pressure drop dP (inches water): ",P_del
220     INPUT "Enter air temperature (Degrees F): ",T1
230     !
240     ! Compute data
250     !
260     OUTPUT 2:Homes:                          ! Home display
270     OUTPUT 2:Clears:                        ! Clear display
280     Beta=D2/D1                              ! Calculate beta
290     P1a=P1+P1a                              ! Absolute pressure
300     P1=(P1a)/2.54                          ! Change to inches
310     T2=T1+459.67                          ! Convert to R
320     Rho=FNDensity(P1a,T2)                  ! Air density bed
330     Rho1=FNDensity(P1a,T2)                 ! Air density upstream
340     Vmu=FNViscosity(T2)                   ! Air viscosity
350     Y1=FNExpan(Beta,P1,S,P_del)           ! Expansion factor Y
360     K=FNFlow_coeff(Reynolds_no,Beta,D1)    ! Flow coefficient K
370     W=FNMass_flow(D2,K,Y1,Rho1,P_del)     ! Mass flow rate
380     Rd=FNReyn(W,Vmu,D2)                   ! Reynolds # calculated
390     IF ABS(Rd-Reynolds_no)>>1. THEN         ! Check accuracy
400         Reynolds_no=Rd
410         GOTO 350
420     END IF
430     Velocity=W/(Rho*Area_bed)              ! Velocity calculation
440     PRINT "Velocity= ":Velocity:" ft/s"     ! Output results
450     INPUT "Enter (1) to continue, (0) to stop",Answer
460     IF Answer=0 THEN STOP
470     IF Answer<>1 THEN
480         PRINT "Value must be either 1 or 0: try again"
490         GOTO 450
500     END IF
510     GOTO 150
520     END
530     !
540     ! End MAIN.....Begin FUNCTIONS
550     !
560     DEF FNExpan(Beta,P1,S,P_del)            ! Expansion factor Y
570         Hold=P_del/(P1-S*13.5955)
580         Y=1-(.41+.35*Beta^4)*Hold
590         RETURN Y

```

```

600  FNEND
610  !
620  !
630  DEF FNFlow_coeff(Reynolds_no,Beta,D1)           ! Flow coefficient K
640      Ko=.6014-.01352*01^(-.25)+(.376+.37257*01^(-.25))*(.00025/(01*01*Beta*Be
ta+.00025*01))+Beta^4+1.5*Beta^16)
650      B=.0002+.0011/01+ (.0038+.0004/01)*(Beta*Beta+(16.5+5*01)*Beta^16)
660      K=Ko+1000*B/SQR(Beta*Reynolds_no)
670      RETURN K
680  FNEND
690  !
700  !
710  DEF FNMass_flow(D2,K,Y1,Rho1,P_del)             ! Mass flow rate W
720      W=.099702*D2*D2*K*Y1*SQR(Rho1*P_del)
730      RETURN W
740  FNEND
750  !
760  !
770  DEF FNRsyn(W,Umu,D2)                             ! Reynolds # calculated
780      Rd=15.28*W/(Umu*D2)
790      RETURN Rd
800  FNEND
810  !
820  !
830  DEF FNDensity(Patm,T2)                           ! Calculate air density
840      Rho=.522406*Patm/T2
850      RETURN Rho
860  FNEND
870  !
880  !
890  DEF FNViscosity(T2)                               ! Calculate air viscosity
900      Umu=7.303E-7*T2^1.5/(T2+198.6)
910      RETURN Umu
920  FNEND

```

APPENDIX H

This Appendix contains the parts list for the sampling system in three tables. Table H.1 is a list of components for the sampling apparatus. Table H.2 is a list of components for the electrical circuit while Table H.3 is for the vacuum system.

Table H.1

| Item No. | Component | Description |
|----------|-------------------------------|--|
| 1 | Solenoid | LEDEX Size SS 45 Degree Right Hand Stroke Rotary Solenoid Part No. S-8204-029 LEDEX Inc. 801 Scholz Dr, P.O. Box 427 Vandalia, Oh 45377 (513) 898-3621 |
| 2 | Paddle | Foam, Basswood epoxy laminate with Maple mounting blocks 0.5 X 1.2 X 11.5 inches |
| 3 | Interface | Aluminum Cylinders with set screw fastener. R= 0.675 in H= 1.5 in |
| 4 | Solenoid Mounting | Aluminum mounting plate 1/4 X 2.8 X 2.8 inches |
| 5 | Extension Bar | Aluminum bar 1/4 X 3/4 X 12.6 inches |
| 6 | Trap Mount | Aluminum Plate 1/4 X 1.1 X 1.5 inches |
| 7 | Sample Trap | 1/16 inch Aluminum plate Inside Dimensions: 0.5 X 1.5 X 3.5 inches |
| 8 | Vertical Mounting Slide | Aluminum bar 1/4 X 3/4 X 24 inches Adjustment holes drilled every 0.5 inch |
| 9 | Base Structure | Tripod Aluminum Structure |

List of components for sampling apparatus.

TABLE H.2

| Item No. | Component | Description |
|----------|-----------|---|
| 1 | B1 | Bridge rectifier assembly, Silicon, LEDEX Part No. 121011-001, includes arc suppressor in unit. |
| 2 | D1 | Arc Suppressor, not needed if above rectifier assembly used. LEDEX Part No. 122655-001 |
| 3 | M1 | Solenoid (see Table H.1) |
| 4 | R1 | Resistor, 2 Mohm, 1%, 2 Watt |
| 5 | R2 | Resistor, 100 kohm, 1%, 1 Watt |
| 6 | R3 | Resistor, 250 ohm, 10%, 50 Watt |
| 7 | S1 | Switch, SPST, Push Button, 10 A, 250 V |
| 8 | S2 | Switch, SPST, Toggle, 10 A, 250 V |

List of components for solenoid power supply.

TABLE H.3

| Item No. | Component | Description |
|----------|-----------|--|
| 1 | V1 | 3/8 inch Ball Valve |
| 2 | P1 | Eductor |
| 3 | F1 | Screen Filter, 320 um mesh |
| 4 | C1 | Sample Container, Small Plastic Bottle, 1 Pt |
| 5 | C2 | Sample Trap (see Table H.1) |
| 6 | L1 | 1/4 inch Polyflow Tubing |

List of components for vacuum system.

APPENDIX I

This Appendix contains a complete listing of all data obtained during this study. The data is arranged according to the distance of the trap height above the distributor.

DATA for Umf DETERMINATION

| Hb (inches) | P1 (cm Hg) | Pb (cm H2O) | dP (n H2O) | T (F) |
|----------------|---------------|----------------|---------------|----------|
| 10.75 | 7.2 | 51.9 | 1.805 | 62.0 |
| 10.75 | 6.8 | 50.9 | 1.517 | 62.0 |
| 10.25 | 6.2 | 49.1 | 0.932 | 62.0 |
| 9.75 | 6.0 | 48.8 | 0.772 | 62.0 |
| 9.50 | 5.6 | 47.5 | 0.515 | 62.0 |
| 9.25 | 5.1 | 44.9 | 0.335 | 62.5 |
| 8.75 | 4.8 | 42.9 | 0.265 | 63.0 |
| 8.50 | 4.5 | 39.9 | 0.177 | 63.0 |
| 8.50 | 4.0 | 39.5 | 0.125 | 63.5 |
| 8.50 | 3.7 | 33.9 | 0.107 | 64.0 |
| 8.50 | 3.5 | 32.0 | 0.094 | 64.0 |
| 8.50 | 3.3 | 30.1 | 0.084 | 64.0 |
| 8.50 | 2.4 | 22.3 | 0.043 | 64.5 |
| 8.50 | 2.0 | 18.5 | 0.027 | 65.0 |
| 8.50 | 1.6 | 14.6 | 0.017 | 65.0 |

Trap Height above Distributor: cm (in) = 30.96 (12.19)
 Bed Height above Distributor: cm (in) = 25.4 (10)
 Trap Height above bed surface: cm (in) = 5.56 (2.19)
 P1: cm Hg (in Hg) = 5.8 (2.28)
 dP: cm water (in water) = 1.234 (0.486)
 Temp: C (F) = 19.5 (67.0)

SAMP # Weight of Sample
(grams)

| | |
|----|------|
| 1 | 3.16 |
| 2 | 2.06 |
| 3 | 1.88 |
| 4 | 2.43 |
| 5 | 2.48 |
| 6 | 2.10 |
| 7 | 1.84 |
| 8 | 2.67 |
| 9 | 2.57 |
| 10 | 2.16 |
| 11 | 2.16 |
| 12 | 1.03 |
| 13 | 2.46 |
| 14 | 1.13 |
| 15 | 1.21 |

AVG = 2.09 grams
 STN DV = 0.60 grams

Trap Height above Distributor: cm (in) = 30.96 (12.19)
 Bed Height above Distributor: cm (in) = 26.67 (10.5)
 Trap Height above bed surface: cm (in) = 4.29 (1.69)
 P1: cm Hg (in Hg) = 6.8 (2.68)
 dP: cm water (in water) = 1.887 (0.743)
 Temp: C (F) = 18 (64.5)

SAMP # Weight of Sample
(grams)

| | |
|----|------|
| 16 | 7.72 |
| 17 | 9.12 |
| 18 | 3.83 |
| 19 | 4.04 |
| 20 | 5.66 |
| 21 | 3.08 |
| 22 | 8.86 |
| 23 | 4.60 |
| 24 | 6.55 |
| 25 | 5.84 |

AVG = 5.96 grams
 STN DV = 2.12 grams

Trap Height above Distributor: cm (in) = 37.31 (14.69)
 Bed Height above Distributor: cm (in) = 25.4 (10)
 Trap Height above bed surface: cm (in) = 11.91 (4.69)
 P1: cm Hg (in Hg) = 5.8 (2.28)
 dP: cm water (in water) = 1.201 (0.473)
 Temp: C (F) = 20.5 (69.0)

| SAMP # | Weight of Sample (grams) | |
|--------|-----------------------------|---------------------|
| 26 | 0.62 | |
| 27 | 0.55 | |
| 28 | 0.54 | |
| 29 | 0.64 | |
| 30 | 0.76 | |
| 31 | 0.58 | |
| 32 | 0.61 | |
| 33 | 0.47 | |
| 34 | 0.85 | AVG = 0.62 grams |
| 35 | 0.61 | STN DV = 0.11 grams |

Trap Height above Distributor: cm (in) = 37.31 (14.69)
 Bed Height above Distributor: cm (in) = 26.67 (10.5)
 Trap Height above bed surface: cm (in) = 10.64 (4.19)
 P1: cm Hg (in Hg) = 6.3 (2.28)
 dP: cm water (in water) = 1.897 (0.747)
 Temp: C (F) = 19 (66.0)

| SAMP # | Weight of Sample (grams) | |
|--------|-----------------------------|---------------------|
| 36 | 2.87 | |
| 37 | 1.42 | |
| 38 | 1.89 | |
| 39 | 1.34 | |
| 40 | 1.18 | |
| 41 | 1.52 | |
| 42 | 1.57 | |
| 43 | 1.68 | |
| 44 | 1.56 | AVG = 1.66 grams |
| 45 | 1.57 | STN DV = 0.46 grams |

Trap Height above Distributor: cm (in) = 37.31 (14.69)
 Bed Height above Distributor: cm (in) = 27.94 (11.0)
 Trap Height above bed surface: cm (in) = 9.37 (3.69)
 P1: cm Hg (in Hg) = 6.8 (2.68)
 dP: cm water (in water) = 1.887 (0.743)
 Temp: C (F) = 19 (66.0)

SAMP # Weight of Sample
 (grams)

| | | | |
|----|------|--------|--------------|
| 46 | 4.32 | | |
| 47 | 2.48 | | |
| 48 | 3.12 | | |
| 49 | 2.83 | | |
| 50 | 4.46 | | |
| 51 | 2.37 | | |
| 52 | 4.46 | | |
| 53 | 4.95 | | |
| 54 | 4.15 | AVG | = 3.61 grams |
| 55 | 2.96 | STN DV | = 0.95 grams |

TRAP HEIGHT = 20.25 in

| Height of Pressure Tap above Distributor (inches) | Pressure for Samples 66-75 (cm H ₂ O) | Pressure for Samples 86-95 (cm H ₂ O) | Pressure for Samples 56-65 (cm H ₂ O) | Pressure for Samples 76-85 (cm H ₂ O) |
|---|--|--|--|--|
| 1.6 | 52.9 | 54.0 | 56.1 | 58.5 |
| 2.6 | 48.8 | 49.8 | 51.7 | 52.8 |
| 3.6 | 40.6 | 41.3 | 43.8 | 44.7 |
| 4.6 | 34.9 | 35.8 | 38.9 | 40.0 |
| 5.6 | 27.8 | 29.7 | 32.6 | 33.6 |
| 6.6 | 21.2 | 22.3 | 25.5 | 27.6 |
| 7.6 | 14.6 | 16.1 | 19.1 | 20.7 |
| 8.6 | 8.3 | 9.7 | 12.5 | 14.8 |
| 9.6 | 2.2 | 3.5 | 6.4 | 8.5 |
| 10.6 | 0.0 | 0.1 | 1.5 | 2.4 |
| 11.6 | 0.0 | 0.0 | 0.0 | 0.3 |
| 12.6 | 0.0 | 0.0 | 0.0 | 0.0 |
| 13.6 | 0.0 | 0.0 | 0.0 | 0.0 |
| 14.6 | 0.0 | 0.0 | 0.0 | 0.0 |

TRAP HEIGHT = 23.25 in

| Height of Pressure Tap above Distributor (inches) | Pressure for Samples 206-215 (cm H ₂ O) | Pressure for Samples 196-205 (cm H ₂ O) | Pressure for Samples 186-195 (cm H ₂ O) | Pressure for Samples 176-185 (cm H ₂ O) |
|---|--|--|--|--|
| 1.6 | 52.0 | 53.4 | 56.3 | 57.7 |
| 2.6 | 48.9 | 49.6 | 51.8 | 52.2 |
| 3.6 | 40.7 | 41.5 | 43.6 | 44.7 |
| 4.6 | 34.7 | 35.8 | 38.8 | 40.0 |
| 5.6 | 28.3 | 29.3 | 32.0 | 33.3 |
| 6.6 | 21.5 | 22.9 | 25.6 | 26.6 |
| 7.6 | 14.9 | 16.6 | 18.8 | 20.3 |
| 8.6 | 8.4 | 9.8 | 12.9 | 13.8 |
| 9.6 | 2.2 | 3.3 | 6.2 | 7.5 |
| 10.6 | 0.0 | 0.1 | 1.3 | 2.9 |
| 11.6 | 0.0 | 0.0 | 0.0 | 0.3 |
| 12.6 | 0.0 | 0.0 | 0.0 | 0.0 |
| 13.6 | 0.0 | 0.0 | 0.0 | 0.0 |
| 14.6 | 0.0 | 0.0 | 0.0 | 0.0 |

Trap Height above Distributor: cm (in) = 51.44 (20.25)
 Bed Height above Distributor: cm (in) = 29.21 (11.5)
 Trap Height above bed surface: cm (in) = 22.23 (8.75)
 Static Bed Height: cm (in) = 22.56 (8.88)
 PI: cm Hg (in Hg) = 8.3 (3.21)
 dP: cm water (in water) = 6.985 (2.75)
 Temp: C (F) = 16.5 (62.0)

SAMP # Weight of Sample
(grams)

| | | | |
|----|------|--------|--------------|
| 76 | 1.47 | | |
| 77 | 1.35 | | |
| 78 | 1.24 | | |
| 79 | 1.29 | | |
| 80 | 0.74 | | |
| 81 | 1.38 | | |
| 82 | 1.38 | | |
| 83 | 1.47 | | |
| 84 | 1.58 | AVG | = 1.32 grams |
| 85 | 1.33 | STN DV | = 0.23 grams |

Trap Height above Distributor: cm (in) = 51.44 (20.25)
 Bed Height above Distributor: cm (in) = 27.31 (10.75)
 Trap Height above bed surface: cm (in) = 24.13 (9.5)
 Static Bed Height: cm (in) = 22.56 (8.88)
 PI: cm Hg (in Hg) = 7.3 (2.87)
 dP: cm water (in water) = 4.910 (1.933)
 Temp: C (F) = 16.5 (62.0)

SAMP # Weight of Sample
(grams)

| | | | |
|----|------|--------|--------------|
| 56 | 0.95 | | |
| 57 | 0.61 | | |
| 58 | 1.83 | | |
| 59 | 0.84 | | |
| 60 | 1.02 | | |
| 61 | 0.76 | | |
| 62 | 0.67 | | |
| 63 | 1.06 | | |
| 64 | 0.60 | AVG | = 0.92 grams |
| 65 | 0.88 | STN DV | = 0.36 grams |

Trap Height above Distributor: cm (in) = 51.44 (20.25)
 Bed Height above Distributor: cm (in) = 26.67 (10.5)
 Trap Height above bed surface: cm (in) = 24.76 (9.75)
 Static Bed Height: cm (in) = 22.56 (8.88)
 P1: cm Hg (in Hg) = 6.5 (2.56)
 dP: cm water (in water) = 3.261 (1.284)
 Temp: C (F) = 16 (61.0)

SAMP # Weight of Sample
(grams)

| | | | |
|----|------|--------|--------------|
| 86 | 0.07 | | |
| 87 | 0.08 | | |
| 88 | 0.17 | | |
| 89 | 0.04 | | |
| 90 | 0.08 | | |
| 91 | 0.04 | | |
| 92 | 0.07 | | |
| 93 | 0.13 | | |
| 94 | 0.07 | AVG | = 0.09 grams |
| 95 | 0.17 | STN DV | = 0.05 grams |

Trap Height above Distributor: cm (in) = 51.44 (20.25)
 Bed Height above Distributor: cm (in) = 25.4 (10.0)
 Trap Height above bed surface: cm (in) = 26.03 (10.25)
 Static Bed Height: cm (in) = 22.56 (8.88)
 P1: cm Hg (in Hg) = 6.2 (2.44)
 dP: cm water (in water) = 2.581 (1.016)
 Temp: C (F) = 17 (63.0)

SAMP # Weight of Sample
(grams)

| | | | |
|----|------|--------|--------------|
| 66 | 0.05 | | |
| 67 | 0.15 | | |
| 68 | 0.14 | | |
| 69 | 0.07 | | |
| 70 | 0.11 | | |
| 71 | 0.10 | | |
| 72 | 0.18 | | |
| 73 | 0.08 | | |
| 74 | 0.11 | AVG | = 0.12 grams |
| 75 | 0.16 | STN DV | = 0.04 grams |

TRAP HEIGHT = 16.12 in

| Height of Pressure Tap above Distributor (inches) | Pressure for Samples 106-115 (cm H ₂ O) | Pressure for Samples 126-135 (cm H ₂ O) | Pressure for Samples 96-105 (cm H ₂ O) | Pressure for Samples 116-125 (cm H ₂ O) |
|---|--|--|---|--|
| 1.6 | 52.6 | 54.4 | 55.6 | 58.5 |
| 2.6 | 48.7 | 49.9 | 51.3 | 52.9 |
| 3.6 | 40.3 | 41.8 | 43.3 | 44.4 |
| 4.6 | 34.6 | 35.9 | 37.9 | 39.6 |
| 5.6 | 27.9 | 29.2 | 31.3 | 33.9 |
| 6.6 | 20.6 | 22.8 | 25.2 | 27.1 |
| 7.6 | 13.8 | 15.5 | 18.9 | 20.6 |
| 8.6 | 7.8 | 9.4 | 12.3 | 14.6 |
| 9.6 | 1.8 | 3.2 | 5.3 | 7.6 |
| 10.6 | 0.0 | 0.3 | 0.9 | 2.5 |
| 11.6 | 0.0 | 0.0 | 0.0 | 0.3 |
| 12.6 | 0.0 | 0.0 | 0.0 | 0.0 |
| 13.6 | 0.0 | 0.0 | 0.0 | 0.0 |
| 14.6 | 0.0 | 0.0 | 0.0 | 0.0 |

TRAP HEIGHT = 18.25 in

| Height of Pressure Tap above Distributor (inches) | Pressure for Samples 146-155 (cm H ₂ O) | Pressure for Samples 136-145 (cm H ₂ O) | Pressure for Samples 156-165 (cm H ₂ O) | Pressure for Samples 166-175 (cm H ₂ O) |
|---|--|--|--|--|
| 1.6 | 52.7 | 54.3 | 55.8 | 57.9 |
| 2.6 | 49.0 | 49.9 | 51.5 | 52.6 |
| 3.6 | 41.0 | 41.6 | 43.3 | 44.9 |
| 4.6 | 34.6 | 36.1 | 38.1 | 39.9 |
| 5.6 | 28.0 | 29.3 | 31.6 | 33.5 |
| 6.6 | 21.5 | 22.5 | 24.9 | 26.6 |
| 7.6 | 14.9 | 15.8 | 18.8 | 20.7 |
| 8.6 | 8.5 | 9.8 | 12.2 | 14.5 |
| 9.6 | 2.4 | 3.4 | 6.0 | 7.8 |
| 10.6 | 0.0 | 0.1 | 0.9 | 2.5 |
| 11.6 | 0.0 | 0.0 | 0.0 | 0.3 |
| 12.6 | 0.0 | 0.0 | 0.0 | 0.0 |
| 13.6 | 0.0 | 0.0 | 0.0 | 0.0 |
| 14.6 | 0.0 | 0.0 | 0.0 | 0.0 |

| | | |
|--|---------|---------|
| Trap Height above Distributor: cm (in) | = 40.95 | (16.12) |
| Bed Height above Distributor: cm (in) | = 28.58 | (11.25) |
| Trap Height above bed surface: cm (in) | = 12.37 | (4.88) |
| Static Bed Height: cm (in) | = 22.56 | (8.88) |
| P1: cm Hg (in Hg) | = 8.0 | (3.15) |
| dP: cm water (in water) | = 6.858 | (2.7) |
| Temp: C (F) | = 16 | (61.0) |

| SAMP # | Weight of Sample (grams) |
|--------|-----------------------------|
|--------|-----------------------------|

| | | |
|-----|------|---------------------|
| 116 | 4.18 | |
| 117 | 3.03 | |
| 118 | 2.32 | |
| 119 | 1.47 | |
| 120 | 2.34 | |
| 121 | 2.64 | |
| 122 | 1.73 | |
| 123 | 2.12 | |
| 124 | 1.96 | AVG = 2.41 grams |
| 125 | 2.38 | STN DV = 0.76 grams |

| | | |
|--|---------|---------|
| Trap Height above Distributor: cm (in) | = 40.95 | (16.12) |
| Bed Height above Distributor: cm (in) | = 27.30 | (10.75) |
| Trap Height above bed surface: cm (in) | = 13.65 | (5.38) |
| Static Bed Height: cm (in) | = 22.56 | (8.88) |
| P1: cm Hg (in Hg) | = 7.4 | (2.91) |
| dP: cm water (in water) | = 4.808 | (1.893) |
| Temp: C (F) | = 16 | (61.0) |

| SAMP # | Weight of Sample (grams) |
|--------|-----------------------------|
|--------|-----------------------------|

| | | |
|-----|------|---------------------|
| 96 | 1.33 | |
| 97 | 0.81 | |
| 98 | 1.37 | |
| 99 | 1.56 | |
| 100 | 1.42 | |
| 101 | 1.48 | |
| 102 | 1.27 | |
| 103 | 2.05 | |
| 104 | 1.21 | AVG = 1.36 grams |
| 105 | 1.11 | STN DV = 0.32 grams |

3/3

AD-A159 010 A DETERMINATION OF PARTICLE DENSITY DISTRIBUTIONS ABOVE 3/3
FLUIDIZED BEDS(II) MASSACHUSETTS INST OF TECH CAMBRIDGE

UNCLASSIFIED DEPT OF OCEAN ENGINEERING G A FIFER MAR 83
N66314-70-A-0073 F/G 14/2 NL

UNCLASSIFIED DEPT OF OCEAN ENGINEERING G A FIFER MAR 83
N66314-70-A-0073 F/G 14/2 NL

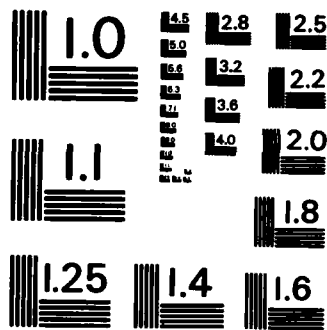
UNCLASSIFIED DEPT OF OCEAN ENGINEERING G A FIFER MAR 83 N66314-70-A-0073 F/G 14/2 NL

UNCLASSIFIED DEPT OF OCEAN ENGINEERING G A FIFER MAR 83
N66314-70-A-0073 F/G 14/2 NL

END

FILMED

DTIC



Trap Height above Distributor: cm (in) = 40.95 (16.12)
 Bed Height above Distributor: cm (in) = 26.67 (10.5)
 Trap Height above bed surface: cm (in) = 14.28 (5.62)
 Static Bed Height: cm (in) = 22.56 (8.88)
 P1: cm Hg (in Hg) = 6.6 (2.60)
 dP: cm water (in water) = 3.259 (1.283)
 Temp: C (F) = 16 (61.0)

SAMP # Weight of Sample
(grams)

| | | | |
|-----|------|------|---------------------|
| | 126 | 0.36 | |
| | 127 | 0.31 | |
| 128 | 0.21 | 0.21 | |
| 129 | 0.27 | 0.27 | |
| | 130 | 0.18 | |
| | 131 | 0.37 | |
| | 132 | 0.34 | |
| | 133 | 0.29 | |
| | 134 | 0.34 | AVG = 0.28 grams |
| | 135 | 0.16 | STN DV = 0.08 grams |

Trap Height above Distributor: cm (in) = 40.95 (16.12)
 Bed Height above Distributor: cm (in) = 26.04 (10.25)
 Trap Height above bed surface: cm (in) = 14.91 (5.88)
 Static Bed Height: cm (in) = 22.56 (8.88)
 P1: cm Hg (in Hg) = 6.3 (2.48)
 dP: cm water (in water) = 2.591 (1.020)
 Temp: C (F) = 16 (61.0)

SAMP # Weight of Sample
(grams)

| | | |
|-----|------|---------------------|
| 106 | 0.38 | |
| 107 | 0.12 | |
| 108 | 0.15 | |
| 109 | 0.17 | |
| 110 | 0.13 | |
| 111 | 0.18 | |
| 112 | 0.56 | |
| 113 | 0.05 | |
| 114 | 0.18 | AVG = 0.22 grams |
| 115 | 0.24 | STN DV = 0.15 grams |

Trap Height above Distributor: cm (in) = 46.36 (18.25)
 Bed Height above Distributor: cm (in) = 28.58 (11.25)
 Trap Height above bed surface: cm (in) = 17.78 (7.00)
 Static Bed Height: cm (in) = 22.56 (8.88)
 PI: cm Hg (in Hg) = 8.1 (3.19)
 dP: cm water (in water) = 6.858 (2.7)
 Temp: C (F) = 16 (61.0)

SAMP # Weight of Sample
 (grams)

| | | | |
|-----|------|--------|--------------|
| 166 | 1.13 | | |
| 167 | 1.18 | | |
| 168 | 1.34 | | |
| 169 | 0.93 | | |
| 170 | 0.88 | | |
| 171 | 1.01 | | |
| 172 | 1.20 | | |
| 173 | 1.15 | | |
| 174 | 1.08 | AVG | = 1.08 grams |
| 175 | 0.85 | STN DV | = 0.16 grams |

Trap Height above Distributor: cm (in) = 46.36 (18.25)
 Bed Height above Distributor: cm (in) = 27.30 (10.75)
 Trap Height above bed surface: cm (in) = 19.06 (7.5)
 Static Bed Height: cm (in) = 22.56 (8.88)
 PI: cm Hg (in Hg) = 7.3 (2.87)
 dP: cm water (in water) = 4.808 (1.893)
 Temp: C (F) = 16 (61.0)

SAMP # Weight of Sample
 (grams)

| | | | |
|-----|------|--------|--------------|
| 156 | 0.64 | | |
| 157 | 0.48 | | |
| 158 | 0.78 | | |
| 159 | 0.58 | | |
| 160 | 0.44 | | |
| 161 | 0.58 | | |
| 162 | 0.83 | | |
| 163 | 0.57 | | |
| 164 | 0.52 | AVG | = 0.60 grams |
| 165 | 0.62 | STN DV | = 0.12 grams |

Trap Height above Distributor: cm (in) = 46.36 (18.25)
 Bed Height above Distributor: cm (in) = 26.67 (10.5)
 Trap Height above bed surface: cm (in) = 19.69 (7.75)
 Static Bed Height: cm (in) = 22.56 (8.88)
 P1: cm Hg (in Hg) = 6.6 (2.60)
 dP: cm water (in water) = 3.244 (1.277)
 Temp: C (F) = 16.5 (62.0)

| SAMP # | Weight of Sample (grams) |
|--------|-----------------------------|
|--------|-----------------------------|

| | |
|---------------------|------|
| 136 | 0.03 |
| 137 | 0.13 |
| 138 | 0.06 |
| 139 | 0.05 |
| 140 | 0.07 |
| 141 | 0.06 |
| 142 | 0.05 |
| 143 | 0.05 |
| 144 | 0.11 |
| 145 | 0.14 |
| AVG = 0.08 grams | |
| STN DV = 0.04 grams | |

Trap Height above Distributor: cm (in) = 46.36 (18.25)
 Bed Height above Distributor: cm (in) = 26.04 (10.25)
 Trap Height above bed surface: cm (in) = 20.32 (8.00)
 Static Bed Height: cm (in) = 22.56 (8.88)
 P1: cm Hg (in Hg) = 6.3 (2.48)
 dP: cm water (in water) = 2.631 (1.036)
 Temp: C (F) = 16.5 (62.0)

| SAMP # | Weight of Sample (grams) |
|--------|-----------------------------|
|--------|-----------------------------|

| | |
|---------------------|------|
| 146 | 0.01 |
| 147 | 0.01 |
| 148 | 0.02 |
| 149 | 0.02 |
| 150 | 0.03 |
| 151 | 0.02 |
| 152 | 0.01 |
| 153 | 0.01 |
| 154 | 0.02 |
| 155 | 0.05 |
| AVG = 0.02 grams | |
| STN DV = 0.01 grams | |

Trap Height above Distributor: cm (in) = 59.06 (23.25)
 Bed Height above Distributor: cm (in) = 27.94 (11.00)
 Trap Height above bed surface: cm (in) = 31.12 (12.25)
 Static Bed Height: cm (in) = 22.56 (8.88)
 P1: cm Hg (in Hg) = 8.2 (3.23)
 dP: cm water (in water) = 6.858 (2.7)
 Temp: C (F) = 16.5 (62.0)

SAMP # Weight of Sample
 (grams)

| | | | |
|-----|------|--------|--------------|
| 176 | 0.32 | | |
| 177 | 0.22 | | |
| 178 | 0.24 | | |
| 179 | 0.52 | | |
| 180 | 0.31 | | |
| 181 | 0.42 | | |
| 182 | 0.34 | | |
| 183 | 0.31 | | |
| 184 | 0.23 | AVG | = 0.31 grams |
| 185 | 0.21 | STN DV | = 0.10 grams |

Trap Height above Distributor: cm (in) = 59.06 (23.25)
 Bed Height above Distributor: cm (in) = 27.18 (10.70)
 Trap Height above bed surface: cm (in) = 31.76 (12.50)
 Static Bed Height: cm (in) = 22.56 (8.88)
 P1: cm Hg (in Hg) = 7.3 (2.87)
 dP: cm water (in water) = 4.813 (1.895)
 Temp: C (F) = 16 (61.0)

SAMP # Weight of Sample
 (grams)

| | | | |
|-----|------|--------|--------------|
| 186 | 0.25 | | |
| 187 | 0.17 | | |
| 188 | 0.14 | | |
| 189 | 0.17 | | |
| 190 | 0.12 | | |
| 191 | 0.23 | | |
| 192 | 0.16 | | |
| 193 | 0.25 | | |
| 194 | 0.18 | AVG | = 0.18 grams |
| 195 | 0.17 | STN DV | = 0.04 grams |

| | |
|--|-----------------|
| Trap Height above Distributor: cm (in) | = 59.06 (23.25) |
| Bed Height above Distributor: cm (in) | = 26.67 (10.50) |
| Trap Height above bed surface: cm (in) | = 32.39 (12.75) |
| Static Bed Height: cm (in) | = 22.56 (8.88) |
| P1: cm Hg (in Hg) | = 6.5 (2.56) |
| dP: cm water (in water) | = 3.236 (1.274) |
| Temp: C (F) | = 16 (61.0) |

SAMP # Weight of Sample
(grams)

| | | |
|-----|------|---------------------|
| 196 | 0.05 | |
| 197 | 0.07 | |
| 198 | 0.07 | |
| 199 | 0.04 | |
| 200 | 0.06 | |
| 201 | 0.09 | |
| 202 | 0.04 | |
| 203 | 0.07 | |
| 204 | 0.06 | AVG = 0.06 grams |
| 205 | 0.06 | STN DV = 0.02 grams |

| | |
|--|-----------------|
| Trap Height above Distributor: cm (in) | = 59.06 (23.25) |
| Bed Height above Distributor: cm (in) | = 26.04 (10.25) |
| Trap Height above bed surface: cm (in) | = 33.02 (13.00) |
| Static Bed Height: cm (in) | = 22.56 (8.88) |
| P1: cm Hg (in Hg) | = 6.3 (2.48) |
| dP: cm water (in water) | = 2.619 (1.031) |
| Temp: C (F) | = 16 (61.0) |

SAMP # Weight of Sample
(grams)

| | | |
|-----|------|----------------------|
| 206 | 0.01 | |
| 207 | 0.02 | |
| 208 | 0.01 | |
| 209 | 0.01 | |
| 210 | 0.01 | |
| 211 | 0.01 | |
| 212 | 0.01 | |
| 213 | 0.02 | |
| 214 | 0.01 | AVG = 0.01 grams |
| 215 | 0.01 | STN DV = 0.004 grams |

TRAP HEIGHT = 12.75 in

| Height of Pressure Tap above Distributor (inches) | Pressure for Samples 256-265 (cm H ₂ O) | Pressure for Samples 266-275 (cm H ₂ O) | Pressure for Samples 276-285 (cm H ₂ O) | Pressure for Samples 286-295 (cm H ₂ O) |
|---|--|--|--|--|
| 1.6 | 53.7 | 54.8 | 57.2 | 58.8 |
| 2.6 | 48.5 | 49.9 | 51.7 | 53.2 |
| 3.6 | 40.8 | 42.1 | 44.4 | 45.8 |
| 4.6 | 34.9 | 35.7 | 38.7 | 40.4 |
| 5.6 | 28.1 | 29.7 | 32.5 | 34.0 |
| 6.6 | 21.6 | 23.8 | 26.1 | 27.8 |
| 7.6 | 14.7 | 17.2 | 19.1 | 21.6 |
| 8.6 | 8.1 | 10.7 | 13.5 | 16.2 |
| 9.6 | 2.1 | 4.5 | 6.8 | 9.5 |
| 10.6 | 0.0 | 0.5 | 1.6 | 3.7 |
| 11.6 | 0.0 | 0.0 | 0.0 | 0.7 |
| 12.6 | 0.0 | 0.0 | 0.0 | 0.0 |
| 13.6 | 0.0 | 0.0 | 0.0 | 0.0 |
| 14.6 | 0.0 | 0.0 | 0.0 | 0.0 |

TRAP HEIGHT = 14.25 in

| Height of Pressure Tap above Distributor (inches) | Pressure for Samples 216-225 (cm H ₂ O) | Pressure for Samples 226-235 (cm H ₂ O) | Pressure for Samples 236-245 (cm H ₂ O) | Pressure for Samples 246-255 (cm H ₂ O) |
|---|--|--|--|--|
| 1.6 | 52.2 | 53.4 | 56.4 | 58.0 |
| 2.6 | 48.7 | 49.7 | 51.6 | 52.7 |
| 3.6 | 40.9 | 42.3 | 43.9 | 45.3 |
| 4.6 | 34.7 | 36.1 | 38.2 | 40.2 |
| 5.6 | 27.9 | 29.5 | 31.2 | 34.1 |
| 6.6 | 20.6 | 23.0 | 25.7 | 27.7 |
| 7.6 | 14.9 | 16.9 | 18.9 | 21.3 |
| 8.6 | 8.6 | 10.7 | 13.4 | 14.4 |
| 9.6 | 2.5 | 3.7 | 6.5 | 8.9 |
| 10.6 | 0.0 | 0.3 | 1.2 | 3.1 |
| 11.6 | 0.0 | 0.0 | 0.0 | 0.0 |
| 12.6 | 0.0 | 0.0 | 0.0 | 0.0 |
| 13.6 | 0.0 | 0.0 | 0.0 | 0.0 |
| 14.6 | 0.0 | 0.0 | 0.0 | 0.0 |

| | | |
|--|---------|---------|
| Trap Height above Distributor: cm (in) | = 36.20 | (14.25) |
| Bed Height above Distributor: cm (in) | = 28.58 | (11.25) |
| Trap Height above bed surface: cm (in) | = 7.62 | (3.00) |
| Static Bed Height: cm (in) | = 22.56 | (8.88) |
| P1: cm Hg (in Hg) | = 8.2 | (3.23) |
| dP: cm water (in water) | = 6.98 | (2.75) |
| Temp: C (F) | = 16.5 | (62.0) |

| SAMP # | Weight of Sample (grams) |
|--------|-----------------------------|
|--------|-----------------------------|

| | |
|-----|-------|
| 246 | 3.34 |
| 247 | 5.36 |
| 248 | 4.64 |
| 249 | 5.71 |
| 250 | 4.17 |
| 251 | 4.33 |
| 252 | 4.55 |
| 253 | 4.33 |
| 254 | *8.44 |
| 255 | 3.90 |

AVG = 4.48 grams
STN DV = 0.72 grams

* value not used in computing average.

| | | |
|--|---------|---------|
| Trap Height above Distributor: cm (in) | = 36.20 | (14.25) |
| Bed Height above Distributor: cm (in) | = 27.30 | (10.75) |
| Trap Height above bed surface: cm (in) | = 8.90 | (3.50) |
| Static Bed Height: cm (in) | = 22.56 | (8.88) |
| P1: cm Hg (in Hg) | = 7.3 | (2.87) |
| dP: cm water (in water) | = 4.768 | (1.877) |
| Temp: C (F) | = 16.5 | (62.0) |

| SAMP # | Weight of Sample (grams) |
|--------|-----------------------------|
|--------|-----------------------------|

| | |
|-----|------|
| 236 | 1.55 |
| 237 | 1.88 |
| 238 | 1.92 |
| 239 | 1.80 |
| 240 | 1.69 |
| 241 | 2.05 |
| 242 | 1.84 |
| 243 | 1.80 |
| 244 | 1.87 |
| 245 | 2.38 |

AVG = 1.88 grams
STN DV = 0.22 grams

| | | |
|--------------------------------|---------------------|-----------------|
| Trap Height above Distributor: | cm (in) | = 36.20 (14.25) |
| Bed Height above Distributor: | cm (in) | = 26.67 (10.50) |
| Trap Height above bed surface: | cm (in) | = 9.53 (3.75) |
| Static Bed Height: | cm (in) | = 22.56 (8.88) |
| P1: | cm Hg (in Hg) | = 6.6 (2.60) |
| dP: | cm water (in water) | = 3.218 (1.267) |
| Temp: | C (F) | = 16.5 (62.0) |

| SAMP # | Weight of Sample (grams) | | |
|--------|-----------------------------|--------|--------------|
| 226 | 0.93 | | |
| 227 | 0.68 | | |
| 228 | 0.61 | | |
| 229 | 0.56 | | |
| 230 | 0.81 | | |
| 231 | 0.52 | | |
| 232 | 0.38 | | |
| 233 | 0.57 | | |
| 234 | 0.75 | AVG | = 0.62 grams |
| 235 | 0.44 | STN DV | = 0.17 grams |

| | | |
|--------------------------------|---------------------|-----------------|
| Trap Height above Distributor: | cm (in) | = 36.20 (14.25) |
| Bed Height above Distributor: | cm (in) | = 26.04 (10.25) |
| Trap Height above bed surface: | cm (in) | = 10.16 (4.00) |
| Static Bed Height: | cm (in) | = 22.56 (8.88) |
| P1: | cm Hg (in Hg) | = 6.3 (2.48) |
| dP: | cm water (in water) | = 2.624 (1.033) |
| Temp: | C (F) | = 16.5 (62.0) |

| SAMP # | Weight of Sample (grams) | | |
|--------|-----------------------------|--------|--------------|
| 216 | 0.32 | | |
| 217 | 0.35 | | |
| 218 | 0.36 | | |
| 219 | 0.30 | | |
| 220 | 0.32 | | |
| 221 | 0.35 | | |
| 222 | 0.24 | | |
| 223 | 0.30 | | |
| 224 | 0.34 | AVG | = 0.32 grams |
| 225 | 0.30 | STN DV | = 0.04 grams |

| | | |
|--|---------|---------|
| Trap Height above Distributor: cm (in) | = 32.39 | (12.75) |
| Bed Height above Distributor: cm (in) | = 28.58 | (11.25) |
| Trap Height above bed surface: cm (in) | = 3.81 | (1.50) |
| Static Bed Height: cm (in) | = 22.56 | (8.88) |
| P1: cm Hg (in Hg) | = 8.1 | (3.19) |
| dP: cm water (in water) | = 6.985 | (2.75) |
| Temp: C (F) | = 17. | (63.0) |

| SAMP # | Weight of Sample (grams) | | |
|--------|-----------------------------|--------|--------------|
| 286 | 6.55 | | |
| 287 | 7.51 | | |
| 288 | 7.46 | | |
| 289 | 8.05 | | |
| 290 | 6.92 | | |
| 291 | 7.38 | | |
| 292 | 7.23 | | |
| 293 | 7.65 | | |
| 294 | 7.04 | AVG | = 7.22 grams |
| 295 | 6.38 | STN DV | = 0.51 grams |

| | | |
|--|---------|---------|
| Trap Height above Distributor: cm (in) | = 32.39 | (12.75) |
| Bed Height above Distributor: cm (in) | = 27.30 | (10.75) |
| Trap Height above bed surface: cm (in) | = 5.09 | (2.00) |
| Static Bed Height: cm (in) | = 22.56 | (8.88) |
| P1: cm Hg (in Hg) | = 7.3 | (2.87) |
| dP: cm water (in water) | = 4.836 | (1.904) |
| Temp: C (F) | = 17 | (63.0) |

| SAMP # | Weight of Sample (grams) | | |
|--------|-----------------------------|--------|--------------|
| 276 | 2.44 | | |
| 277 | 3.77 | | |
| 278 | 3.53 | | |
| 279 | 4.04 | | |
| 280 | 4.56 | | |
| 281 | 3.81 | | |
| 282 | 4.55 | | |
| 283 | 5.60 | | |
| 284 | 5.75 | AVG | = 4.35 grams |
| 285 | 5.49 | STN DV | = 1.05 grams |

Trap Height above Distributor: cm (in) = 32.39 (12.75)
 Bed Height above Distributor: cm (in) = 26.67 (10.5)
 Trap Height above bed surface: cm (in) = 5.72 (2.25)
 Static Bed Height: cm (in) = 22.56 (8.88)
 P1: cm Hg (in Hg) = 6.6 (2.60)
 dP: cm water (in water) = 3.269 (1.287)
 Temp: C (F) = 16.5 (62.0)

| SAMP # | Weight of Sample (grams) | |
|--------|-----------------------------|---------------------|
| 266 | 0.74 | |
| 267 | 1.80 | |
| 268 | 1.17 | |
| 269 | 1.17 | |
| 270 | 1.87 | |
| 271 | 1.15 | |
| 272 | 1.58 | |
| 273 | 1.03 | |
| 274 | 1.00 | AVG = 1.31 grams |
| 275 | 1.56 | STN DV = 0.37 grams |

Trap Height above Distributor: cm (in) = 32.39 (12.75)
 Bed Height above Distributor: cm (in) = 26.04 (10.25)
 Trap Height above bed surface: cm (in) = 6.35 (2.50)
 Static Bed Height: cm (in) = 22.56 (8.88)
 P1: cm Hg (in Hg) = 6.3 (2.48)
 dP: cm water (in water) = 2.604 (1.025)
 Temp: C (F) = 16.5 (62.0)

| SAMP # | Weight of Sample (grams) | |
|--------|-----------------------------|---------------------|
| 256 | 0.50 | |
| 257 | 0.76 | |
| 258 | 0.67 | |
| 259 | 0.51 | |
| 260 | 0.54 | |
| 261 | 0.68 | |
| 262 | 0.47 | |
| 263 | 0.65 | |
| 264 | 0.61 | AVG = 0.63 grams |
| 265 | 0.87 | STN DV = 0.13 grams |

APPENDIX J

This Appendix contains the output from the image analyzer.

The output is arranged in the following order.

1. Bed distribution
2. 4 cm freeboard height
3. 8 cm freeboard height
4. 12 cm freeboard height
5. 18 cm freeboard height
6. 22 cm freeboard height
7. 31 cm freeboard height

Each of the distributions at a given bed height applies only to the $U_0/U_{mf} = 3.81$ condition. For each of the seven image analyzer outputs listed, the following three formats are used.

1. Histogram of absolute particle frequency vs particle diameter.
2. Cumulative percentage plot of particle size distribution.
3. Table listing of the above data.

The dashed line on both the bar graphs and on the cumulative percentage plots represent the Gaussian distributions which fit the given set of data. This Gaussian distribution should be used only as a rough estimate of the data because the analysis included "particles" less than 70 microns. By viewing a blank slide with only the tape applied, these "particles" were confirmed to be bubbles and dirt entrapped in the adhesive on the tape used to hold the sample particles in place.

ABS. FREQUENCY

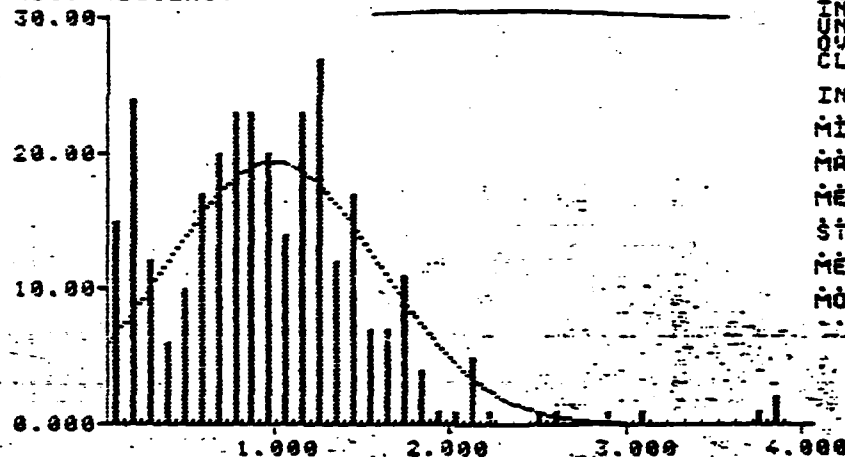


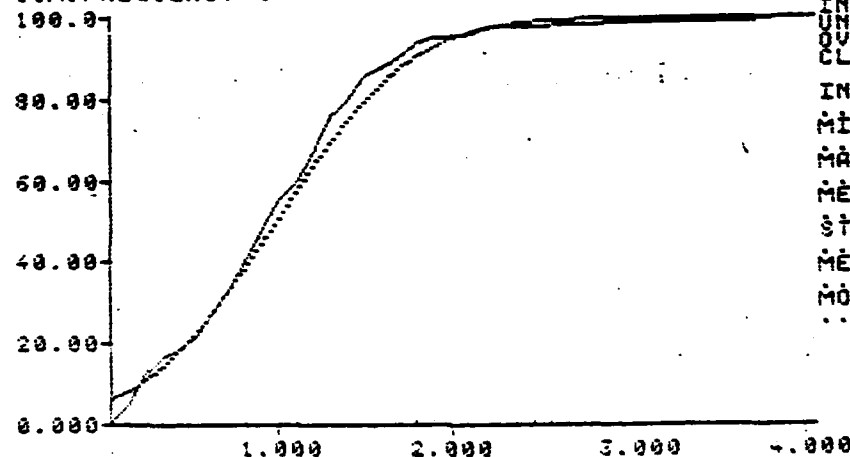
Image Analyzer Output
Bed Particle Distribution

COUNTS 397
IN RANGE 307
UNDERFLOW 0
OVERFLOW 0
CLASS SIZE 40

INTERVAL 0.94651E-01
MINIMUM 0.489774E-01
MAXIMUM 0.90758
MEAN 0.983512
ST. DEV. 0.608569
MEDIAN 0.934044
MODE 1.23768

OCIRCLE

CUM. FREQUENCY %



COUNTS 397
IN RANGE 307
UNDERFLOW 0
OVERFLOW 0
CLASS SIZE 40

INTERVAL 0.94651E-01
MINIMUM 0.489774E-01
MAXIMUM 0.90758
MEAN 0.983512
ST. DEV. 0.608569
MEDIAN 0.934044
MODE 1.23768

OCIRCLE

Image Analyzer Output
Bed Particle Distribution

CLASSIFICATION LIST FOR DCIRCLE IN CHANNELS 1

| UNDERFLOW 0 | | OVERFLOW 0 | | | | | |
|-------------|------------|------------|-----|------|-------------------------|--------|----------|
| CLASS | FROM | TO | ABS | REL | FREQUENCIES CUM. ABS | REL | CUM. REL |
| 1 | .48977E-01 | .14344 | 13. | 4.89 | 13. | 4.89 | 2 |
| 2 | .14344 | .24191 | 24. | 7.82 | 39. | 12.70 | 2 |
| 3 | .24191 | .33837 | 12. | 3.91 | 51. | 16.61 | 2 |
| 4 | .33837 | .43484 | 6. | 1.95 | 57. | 18.57 | 2 |
| 5 | .43484 | .53130 | 10. | 3.26 | 67. | 21.82 | 2 |
| 6 | .53130 | .62777 | 17. | 5.34 | 84. | 27.36 | 2 |
| 7 | .62777 | .72423 | 20. | 6.51 | 104. | 33.88 | 2 |
| 8 | .72423 | .82070 | 23. | 7.49 | 127. | 41.37 | 2 |
| 9 | .82070 | .91716 | 23. | 7.49 | 150. | 48.86 | 2 |
| 10 | .91716 | 1.0136 | 20. | 6.51 | 170. | 55.37 | 2 |
| 11 | 1.0136 | 1.1101 | 14. | 4.56 | 184. | 59.93 | 2 |
| 12 | 1.1101 | 1.2066 | 23. | 7.49 | 207. | 67.43 | 2 |
| 13 | 1.2066 | 1.3030 | 27. | 8.79 | 234. | 76.22 | 2 |
| 14 | 1.3030 | 1.3995 | 12. | 3.91 | 246. | 80.13 | 2 |
| 15 | 1.3995 | 1.4960 | 17. | 5.34 | 263. | 85.67 | 2 |
| 16 | 1.4960 | 1.5924 | 7. | 2.28 | 270. | 87.95 | 2 |
| 17 | 1.5924 | 1.6889 | 7. | 2.28 | 277. | 90.23 | 2 |
| 18 | 1.6889 | 1.7853 | 11. | 3.58 | 288. | 93.81 | 2 |
| 19 | 1.7853 | 1.8818 | 4. | 1.30 | 292. | 95.11 | 2 |
| 20 | 1.8818 | 1.9783 | 1. | .33 | 293. | 95.44 | 2 |
| 21 | 1.9783 | 2.0747 | 1. | .33 | 294. | 95.77 | 2 |
| 22 | 2.0747 | 2.1712 | 3. | 1.63 | 299. | 97.39 | 2 |
| 23 | 2.1712 | 2.2677 | 1. | .33 | 300. | 97.72 | 2 |
| 24 | 2.2677 | 2.3641 | 0. | 0.00 | 300. | 97.72 | 2 |
| 25 | 2.3641 | 2.4606 | 0. | 0.00 | 300. | 97.72 | 2 |
| 26 | 2.4606 | 2.5571 | 1. | .33 | 301. | 98.05 | 2 |
| 27 | 2.5571 | 2.6535 | 1. | .33 | 302. | 98.37 | 2 |
| 28 | 2.6535 | 2.7500 | 0. | 0.00 | 302. | 98.37 | 2 |
| 29 | 2.7500 | 2.8465 | 0. | 0.00 | 302. | 98.37 | 2 |
| 30 | 2.8465 | 2.9429 | 1. | .33 | 303. | 98.70 | 2 |
| 31 | 2.9429 | 3.0394 | 0. | 0.00 | 303. | 98.70 | 2 |
| 32 | 3.0394 | 3.1359 | 1. | .33 | 304. | 99.02 | 2 |
| 33 | 3.1359 | 3.2323 | 0. | 0.00 | 304. | 99.02 | 2 |
| 34 | 3.2323 | 3.3288 | 0. | 0.00 | 304. | 99.02 | 2 |
| 35 | 3.3288 | 3.4253 | 0. | 0.00 | 304. | 99.02 | 2 |
| 36 | 3.4253 | 3.5217 | 0. | 0.00 | 304. | 99.02 | 2 |
| 37 | 3.5217 | 3.6182 | 0. | 0.00 | 304. | 99.02 | 2 |
| 38 | 3.6182 | 3.7147 | 0. | 0.00 | 304. | 99.02 | 2 |
| 39 | 3.7147 | 3.8111 | 1. | .33 | 305. | 99.35 | 2 |
| 40 | 3.8111 | 3.9076 | 2. | .65 | 307. | 100.00 | 2 |

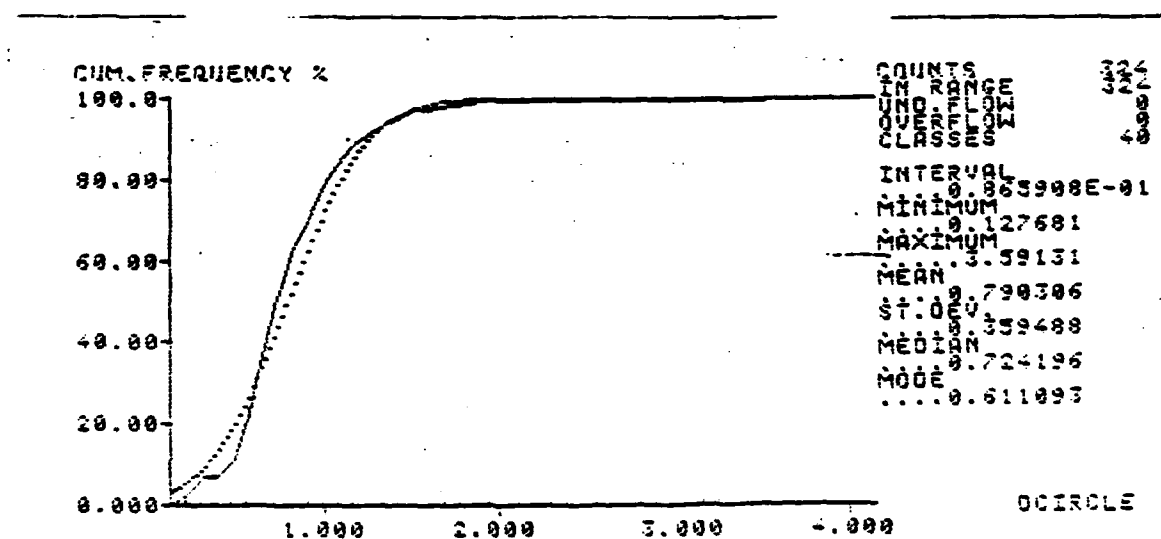
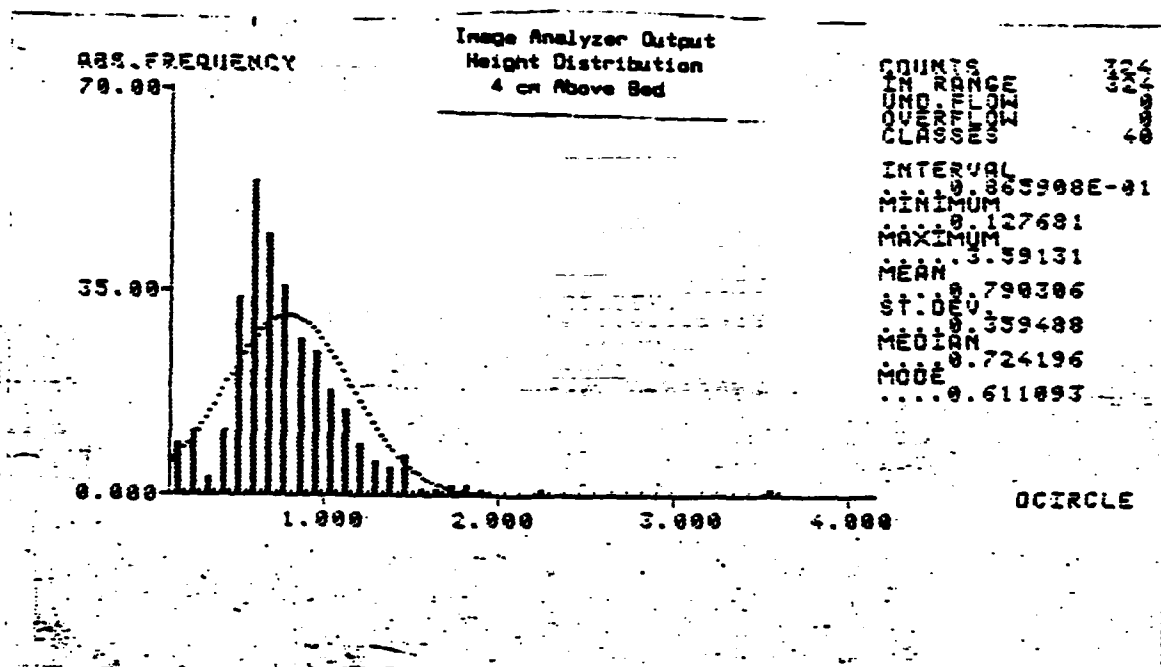


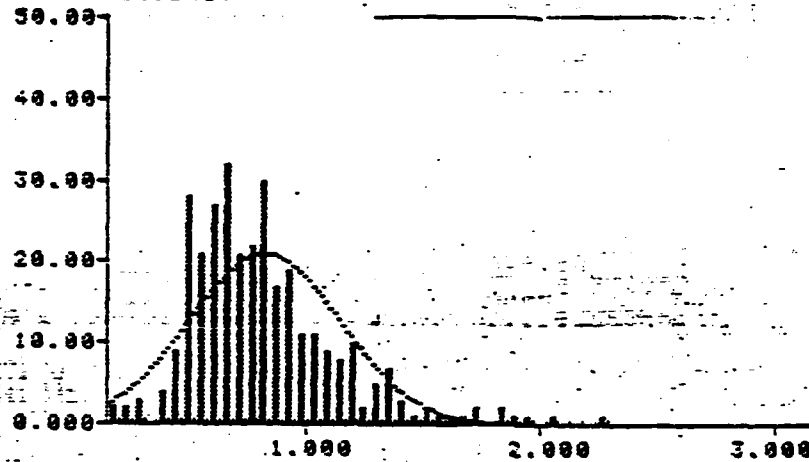
Image Analyzer Output
Height Distribution
4 cm Above Bed

CLASSIFICATION LIST FOR OCIRCLE IN CHANNELS 1

| UNDERFLOW 0 | | OVERFLOW 0 | | | | | |
|-------------|--------|------------|-----|---------|-------------------------|----------|---|
| CLASS | FROM | TO | ABS | REL | FREQUENCIES CUM. ABS | CUM. REL | |
| 1 | .12769 | .21427 | 9. | 2.78 % | 9. | 2.78 % | X |
| 2 | .21427 | .30086 | 11. | 3.40 % | 20. | 6.17 % | X |
| 3 | .30086 | .38745 | 3. | .93 % | 23. | 7.10 % | X |
| 4 | .38745 | .47404 | 11. | 3.40 % | 34. | 10.49 % | X |
| 5 | .47404 | .56064 | 34. | 10.49 % | 68. | 20.99 % | X |
| 6 | .56064 | .64723 | 54. | 16.67 % | 122. | 37.65 % | X |
| 7 | .64723 | .73382 | 45. | 13.89 % | 167. | 51.54 % | X |
| 8 | .73382 | .82041 | 36. | 11.11 % | 203. | 62.65 % | X |
| 9 | .82041 | .90700 | 27. | 8.33 % | 230. | 70.99 % | X |
| 10 | .90700 | .99359 | 23. | 7.72 % | 253. | 78.70 % | X |
| 11 | .99359 | 1.0802 | 18. | 5.56 % | 273. | 84.26 % | X |
| 12 | 1.0802 | 1.1668 | 13. | 4.63 % | 288. | 88.89 % | X |
| 13 | 1.1668 | 1.2534 | 9. | 2.78 % | 297. | 91.67 % | X |
| 14 | 1.2534 | 1.3400 | 6. | 1.85 % | 303. | 93.52 % | X |
| 15 | 1.3400 | 1.4265 | 5. | 1.54 % | 308. | 95.06 % | X |
| 16 | 1.4265 | 1.5131 | 7. | 2.16 % | 315. | 97.22 % | X |
| 17 | 1.5131 | 1.5997 | 1. | .31 % | 316. | 97.53 % | X |
| 18 | 1.5997 | 1.6863 | 1. | .31 % | 317. | 97.84 % | X |
| 19 | 1.6863 | 1.7729 | 2. | .62 % | 319. | 98.46 % | X |
| 20 | 1.7729 | 1.8595 | 2. | .62 % | 321. | 99.07 % | X |
| 21 | 1.8595 | 1.9461 | 1. | .31 % | 322. | 99.38 % | X |
| 22 | 1.9461 | 2.0327 | 0. | 0.00 % | 322. | 99.38 % | X |
| 23 | 2.0327 | 2.1193 | 0. | 0.00 % | 322. | 99.38 % | X |
| 24 | 2.1193 | 2.2059 | 0. | 0.00 % | 322. | 99.38 % | X |
| 25 | 2.2059 | 2.2925 | 1. | .31 % | 323. | 99.69 % | X |
| 26 | 2.2925 | 2.3790 | 0. | 0.00 % | 323. | 99.69 % | X |
| 27 | 2.3790 | 2.4656 | 0. | 0.00 % | 323. | 99.69 % | X |
| 28 | 2.4656 | 2.5522 | 0. | 0.00 % | 323. | 99.69 % | X |
| 29 | 2.5522 | 2.6388 | 0. | 0.00 % | 323. | 99.69 % | X |
| 30 | 2.6388 | 2.7254 | 0. | 0.00 % | 323. | 99.69 % | X |
| 31 | 2.7254 | 2.8120 | 0. | 0.00 % | 323. | 99.69 % | X |
| 32 | 2.8120 | 2.8986 | 0. | 0.00 % | 323. | 99.69 % | X |
| 33 | 2.8986 | 2.9852 | 0. | 0.00 % | 323. | 99.69 % | X |
| 34 | 2.9852 | 3.0718 | 0. | 0.00 % | 323. | 99.69 % | X |
| 35 | 3.0718 | 3.1584 | 0. | 0.00 % | 323. | 99.69 % | X |
| 36 | 3.1584 | 3.2449 | 0. | 0.00 % | 323. | 99.69 % | X |
| 37 | 3.2449 | 3.3315 | 0. | 0.00 % | 323. | 99.69 % | X |
| 38 | 3.3315 | 3.4181 | 0. | 0.00 % | 323. | 99.69 % | X |
| 39 | 3.4181 | 3.5047 | 0. | 0.00 % | 323. | 99.69 % | X |
| 40 | 3.5047 | 3.5913 | 1. | .31 % | 324. | 100.00 % | X |

Image Analyzer Output
Height Distribution
8 cm Above Bed

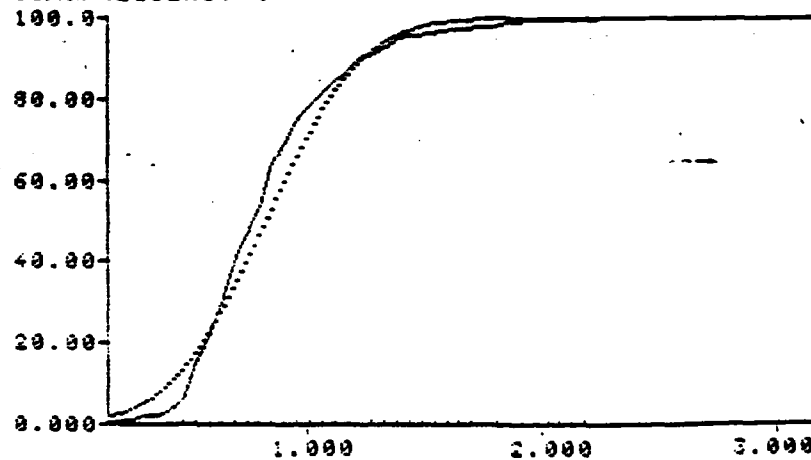
ABS. FREQUENCY



COUNTS 317
IN RANGE 317
OVERLAP 0
CLASSES 40
INTERVAL 0.35681E-01
MINIMUM 0.148672
MAXIMUM 2.29139
MEAN 0.816218
ST. DEV 0.322185
MEDIAN 0.761852
MODE 0.653551

OCIRCLE

CUM. FREQUENCY 2



COUNTS 317
IN RANGE 317
OVERLAP 0
CLASSES 40
INTERVAL 0.35681E-01
MINIMUM 0.148672
MAXIMUM 2.29139
MEAN 0.816218
ST. DEV 0.322185
MEDIAN 0.761852
MODE 0.653551

OCIRCLE

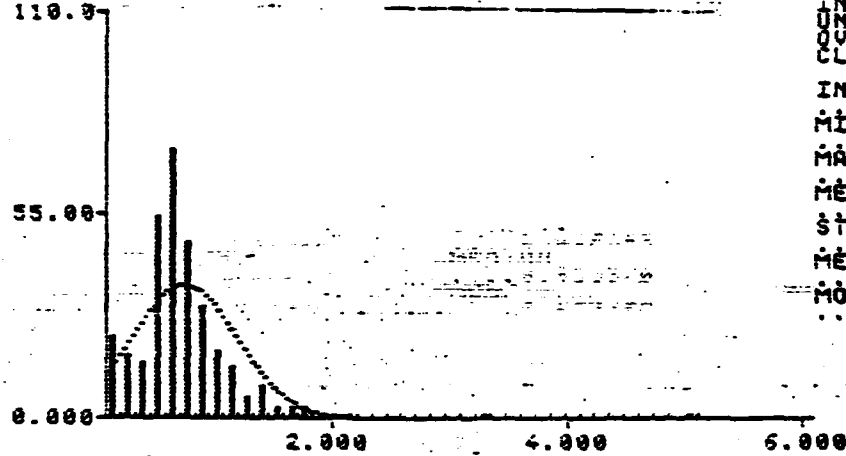
Image Analyzer Output
Height Distribution
8 cm Above Bed

CLASSIFICATION LIST FOR DCIRCLE IN CHANNELS 1

| UNDERFLOW | | OVERFLOW | | | | | |
|-----------|--------|----------|-----|-------|-------------------------|----------|---|
| CLASS | FROM | TO | ABS | REL | FREQUENCIES CUM. ABS | CUM. REL | |
| 1 | .14867 | .28224 | 2. | .63 | 2. | .63 | % |
| 2 | .28224 | .25381 | 2. | .63 | 4. | 1.26 | % |
| 3 | .25381 | .38938 | 3. | .95 | 7. | 2.21 | % |
| 4 | .38938 | .36294 | 8. | 8.00 | 7. | 2.21 | % |
| 5 | .36294 | .41631 | 4. | 1.26 | 11. | 3.47 | % |
| 6 | .41631 | .47008 | 9. | 2.84 | 20. | 6.31 | % |
| 7 | .47008 | .52363 | 20. | 8.83 | 48. | 15.14 | % |
| 8 | .52363 | .57722 | 21. | 6.62 | 69. | 21.77 | % |
| 9 | .57722 | .63078 | 27. | 8.52 | 96. | 30.28 | % |
| 10 | .63078 | .68433 | 32. | 10.89 | 128. | 40.38 | % |
| 11 | .68433 | .73792 | 21. | 6.62 | 149. | 47.00 | % |
| 12 | .73792 | .79149 | 22. | 6.94 | 171. | 53.94 | % |
| 13 | .79149 | .84506 | 30. | 9.46 | 201. | 63.41 | % |
| 14 | .84506 | .89863 | 17. | 5.36 | 218. | 68.77 | % |
| 15 | .89863 | .95219 | 19. | 5.99 | 237. | 74.76 | % |
| 16 | .95219 | 1.0058 | 11. | 3.47 | 248. | 78.23 | % |
| 17 | 1.0058 | 1.0593 | 11. | 3.47 | 259. | 81.70 | % |
| 18 | 1.0593 | 1.1129 | 9. | 2.84 | 268. | 84.54 | % |
| 19 | 1.1129 | 1.1663 | 8. | 2.52 | 276. | 87.07 | % |
| 20 | 1.1663 | 1.2200 | 10. | 3.15 | 286. | 90.22 | % |
| 21 | 1.2200 | 1.2736 | 2. | .63 | 288. | 90.85 | % |
| 22 | 1.2736 | 1.3272 | 3. | 1.58 | 293. | 92.43 | % |
| 23 | 1.3272 | 1.3807 | 7. | 2.21 | 300. | 94.64 | % |
| 24 | 1.3807 | 1.4343 | 3. | .95 | 303. | 95.58 | % |
| 25 | 1.4343 | 1.4879 | 1. | .32 | 304. | 95.90 | % |
| 26 | 1.4879 | 1.5414 | 2. | .63 | 306. | 96.53 | % |
| 27 | 1.5414 | 1.5950 | 1. | .32 | 307. | 96.85 | % |
| 28 | 1.5950 | 1.6486 | 1. | .32 | 308. | 97.16 | % |
| 29 | 1.6486 | 1.7021 | 1. | .32 | 309. | 97.48 | % |
| 30 | 1.7021 | 1.7557 | 2. | .63 | 311. | 98.11 | % |
| 31 | 1.7557 | 1.8093 | 0. | 0.00 | 311. | 98.11 | % |
| 32 | 1.8093 | 1.8628 | 2. | .63 | 313. | 98.74 | % |
| 33 | 1.8628 | 1.9164 | 1. | .32 | 314. | 99.05 | % |
| 34 | 1.9164 | 1.9700 | 1. | .32 | 315. | 99.37 | % |
| 35 | 1.9700 | 2.0236 | 0. | 0.00 | 315. | 99.37 | % |
| 36 | 2.0236 | 2.0771 | 1. | .32 | 316. | 99.68 | % |
| 37 | 2.0771 | 2.1307 | 0. | 0.00 | 316. | 99.68 | % |
| 38 | 2.1307 | 2.1843 | 0. | 0.00 | 316. | 99.68 | % |
| 39 | 2.1843 | 2.2378 | 0. | 0.00 | 316. | 99.68 | % |
| 40 | 2.2378 | 2.2914 | 1. | .32 | 317. | 100.00 | % |

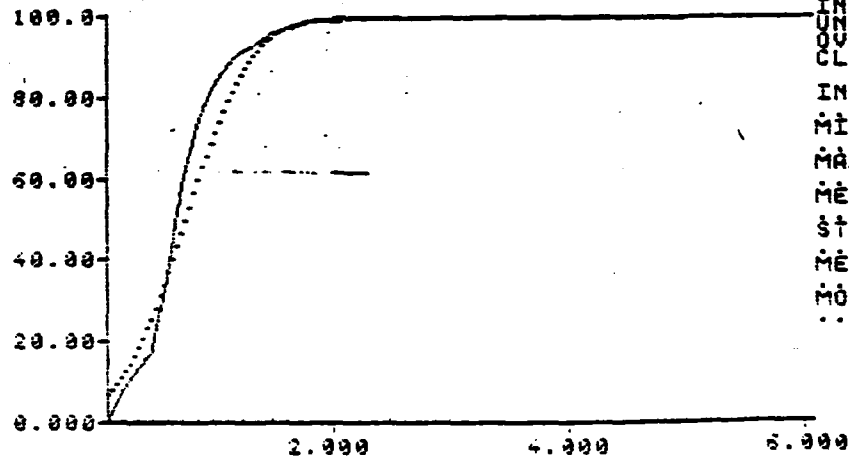
Image Analyzer Output
Height Distribution
12 cm Above Bed

ABS. FREQUENCY



COUNTS 329
IN RANGE 248
OVERFLOW 81
CLASSES 4
INTERVAL 0.126249
MINIMUM 0.621736E-01
MAXIMUM 0.311212
MEAN 0.719992
ST. DEV 0.246468
MEDIAN 0.655370
MODE 0.625272

CUM. FREQUENCY %



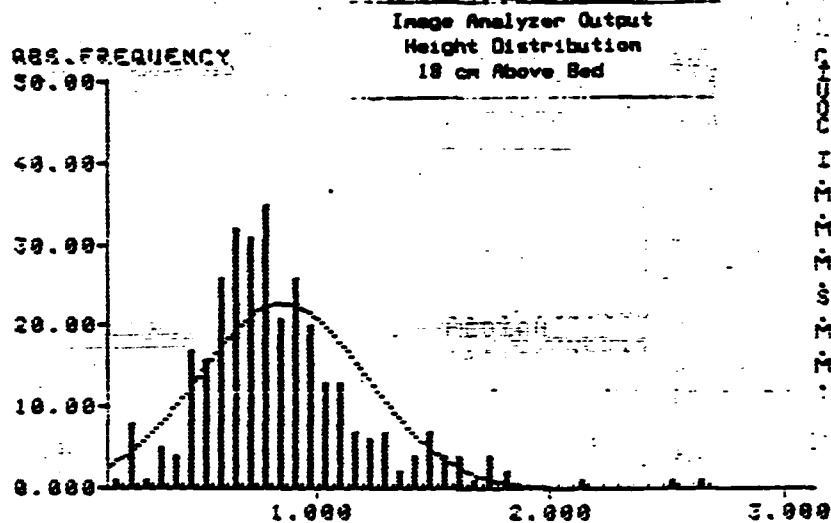
COUNTS 329
IN RANGE 248
OVERFLOW 81
CLASSES 4
INTERVAL 0.126249
MINIMUM 0.621736E-01
MAXIMUM 0.311212
MEAN 0.719992
ST. DEV 0.246468
MEDIAN 0.655370
MODE 0.625272

Image Analyzer Output
Height Distribution
12 cm Above Bed

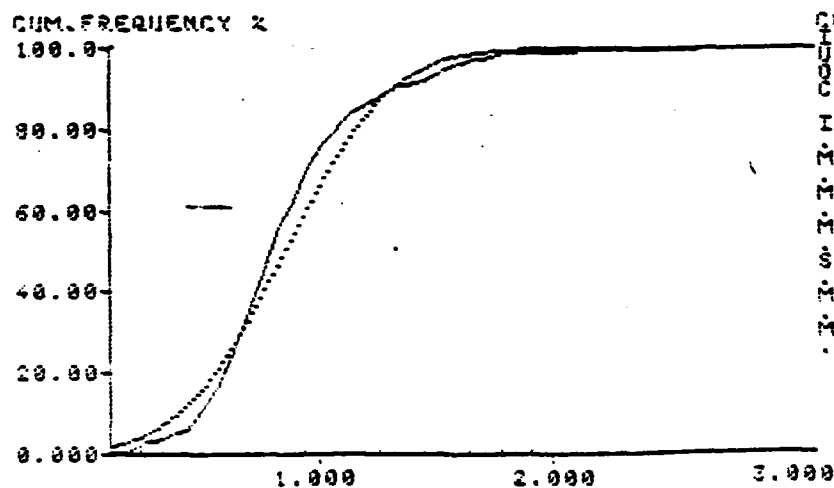
CLASSIFICATION LIST FOR DCIRCLE IN CHANNELS 1

UNDERFLOW 0 OVERFLOW 0

| CLASS | FROM | TO | ABS | REL | FREQUENCIES CUR. ABS | CUM. REL |
|-------|------------|--------|-----|-------|-------------------------|----------|
| 1 | .62174E-01 | .18842 | 22. | 6.87 | 22. | 6.87 |
| 2 | .18842 | .31467 | 17. | 5.31 | 39. | 12.19 |
| 3 | .31467 | .44092 | 15. | 4.69 | 54. | 16.87 |
| 4 | .44092 | .56717 | 55. | 17.19 | 109. | 34.06 |
| 5 | .56717 | .69342 | 73. | 22.81 | 182. | 56.87 |
| 6 | .69342 | .81967 | 48. | 15.00 | 230. | 71.87 |
| 7 | .81967 | .94591 | 38. | 9.37 | 268. | 81.25 |
| 8 | .94591 | 1.0722 | 18. | 5.62 | 278. | 86.87 |
| 9 | 1.0722 | 1.1984 | 14. | 4.37 | 292. | 91.25 |
| 10 | 1.1984 | 1.3247 | 6. | 1.87 | 298. | 93.12 |
| 11 | 1.3247 | 1.4509 | 9. | 2.81 | 307. | 95.94 |
| 12 | 1.4509 | 1.5772 | 3. | .94 | 310. | 96.87 |
| 13 | 1.5772 | 1.7034 | 3. | .94 | 313. | 97.81 |
| 14 | 1.7034 | 1.8297 | 3. | .94 | 316. | 98.75 |
| 15 | 1.8297 | 1.9559 | 0. | 0.00 | 316. | 98.75 |
| 16 | 1.9559 | 2.0822 | 1. | .31 | 317. | 99.06 |
| 17 | 2.0822 | 2.2084 | 1. | .31 | 318. | 99.37 |
| 18 | 2.2084 | 2.3347 | 0. | 0.00 | 318. | 99.37 |
| 19 | 2.3347 | 2.4609 | 0. | 0.00 | 318. | 99.37 |
| 20 | 2.4609 | 2.5871 | 0. | 0.00 | 318. | 99.37 |
| 21 | 2.5871 | 2.7134 | 0. | 0.00 | 318. | 99.37 |
| 22 | 2.7134 | 2.8396 | 0. | 0.00 | 318. | 99.37 |
| 23 | 2.8396 | 2.9659 | 0. | 0.00 | 318. | 99.37 |
| 24 | 2.9659 | 3.0921 | 0. | 0.00 | 318. | 99.37 |
| 25 | 3.0921 | 3.2184 | 0. | 0.00 | 318. | 99.37 |
| 26 | 3.2184 | 3.3446 | 1. | .31 | 319. | 99.69 |
| 27 | 3.3446 | 3.4709 | 0. | 0.00 | 319. | 99.69 |
| 28 | 3.4709 | 3.5971 | 0. | 0.00 | 319. | 99.69 |
| 29 | 3.5971 | 3.7234 | 0. | 0.00 | 319. | 99.69 |
| 30 | 3.7234 | 3.8496 | 0. | 0.00 | 319. | 99.69 |
| 31 | 3.8496 | 3.9759 | 0. | 0.00 | 319. | 99.69 |
| 32 | 3.9759 | 4.1021 | 0. | 0.00 | 319. | 99.69 |
| 33 | 4.1021 | 4.2284 | 0. | 0.00 | 319. | 99.69 |
| 34 | 4.2284 | 4.3546 | 0. | 0.00 | 319. | 99.69 |
| 35 | 4.3546 | 4.4809 | 0. | 0.00 | 319. | 99.69 |
| 36 | 4.4809 | 4.6071 | 0. | 0.00 | 319. | 99.69 |
| 37 | 4.6071 | 4.7334 | 0. | 0.00 | 319. | 99.69 |
| 38 | 4.7334 | 4.8596 | 0. | 0.00 | 319. | 99.69 |
| 39 | 4.8596 | 4.9859 | 0. | 0.00 | 319. | 99.69 |
| 40 | 4.9859 | 5.1121 | 1. | .31 | 320. | 100.00 |



COUNTS 329
IN RANGE 329
UNDERFLOW 0
OVERFLOW 0
CLASSES 40
INTERVAL 0.01792E-01
MINIMUM 0.110281
MAXIMUM 2.67745
MEAN 0.851830
ST. DEV. 0.359383
MEDIAN 0.786914
MODE 0.776786



COUNTS 329
IN RANGE 329
UNDERFLOW 0
OVERFLOW 0
CLASSES 40
INTERVAL 0.01792E-01
MINIMUM 0.110281
MAXIMUM 2.67745
MEAN 0.851830
ST. DEV. 0.359383
MEDIAN 0.786914
MODE 0.776786

Image Analyzer Output
Height Distribution
18 cm Above Bed

CLASSIFICATION LIST FOR DCIRCLE IN CHANNELS

| UNDERFLOW | | OVERFLOW | | | | | |
|-----------|--------|----------|-----|-------|-------------------------|----------|---|
| CLASS | FROM | TO | ABS | REL | FREQUENCIES CUM. ABS | CUM. REL | |
| 1 | .11828 | .17446 | 1. | .31 | 1. | .31 | % |
| 2 | .17446 | .23864 | 8. | 2.58 | 9. | 2.81 | % |
| 3 | .23864 | .30282 | 1. | .31 | 10. | 3.12 | % |
| 4 | .30282 | .36700 | 5. | 1.56 | 15. | 4.69 | % |
| 5 | .36700 | .43118 | 4. | 1.23 | 19. | 5.94 | % |
| 6 | .43118 | .49536 | 17. | 5.31 | 36. | 11.25 | % |
| 7 | .49536 | .55954 | 16. | 5.00 | 52. | 16.25 | % |
| 8 | .55954 | .62372 | 26. | 8.12 | 78. | 24.37 | % |
| 9 | .62372 | .68789 | 32. | 10.00 | 110. | 34.37 | % |
| 10 | .68789 | .75207 | 31. | 9.69 | 141. | 44.06 | % |
| 11 | .75207 | .81625 | 33. | 10.34 | 176. | 54.40 | % |
| 12 | .81625 | .88043 | 21. | 6.56 | 197. | 61.56 | % |
| 13 | .88043 | .94461 | 26. | 8.12 | 223. | 69.69 | % |
| 14 | .94461 | 1.0088 | 20. | 6.23 | 243. | 75.94 | % |
| 15 | 1.0088 | 1.0730 | 13. | 4.06 | 256. | 80.00 | % |
| 16 | 1.0730 | 1.1371 | 13. | 4.06 | 269. | 84.06 | % |
| 17 | 1.1371 | 1.2013 | 7. | 2.19 | 276. | 86.25 | % |
| 18 | 1.2013 | 1.2655 | 6. | 1.87 | 282. | 88.12 | % |
| 19 | 1.2655 | 1.3297 | 7. | 2.19 | 289. | 90.31 | % |
| 20 | 1.3297 | 1.3939 | 2. | .63 | 291. | 90.94 | % |
| 21 | 1.3939 | 1.4580 | 4. | 1.23 | 295. | 92.19 | % |
| 22 | 1.4580 | 1.5222 | 7. | 2.19 | 302. | 94.37 | % |
| 23 | 1.5222 | 1.5864 | 4. | 1.23 | 306. | 95.62 | % |
| 24 | 1.5864 | 1.6506 | 4. | 1.23 | 310. | 96.87 | % |
| 25 | 1.6506 | 1.7148 | 1. | .31 | 311. | 97.19 | % |
| 26 | 1.7148 | 1.7789 | 4. | 1.23 | 315. | 98.44 | % |
| 27 | 1.7789 | 1.8431 | 2. | .63 | 317. | 99.06 | % |
| 28 | 1.8431 | 1.9073 | 0. | 0.00 | 317. | 99.06 | % |
| 29 | 1.9073 | 1.9715 | 0. | 0.00 | 317. | 99.06 | % |
| 30 | 1.9715 | 2.0357 | 0. | 0.00 | 317. | 99.06 | % |
| 31 | 2.0357 | 2.0998 | 0. | 0.00 | 317. | 99.06 | % |
| 32 | 2.0998 | 2.1640 | 1. | .31 | 318. | 99.37 | % |
| 33 | 2.1640 | 2.2282 | 0. | 0.00 | 318. | 99.37 | % |
| 34 | 2.2282 | 2.2924 | 0. | 0.00 | 318. | 99.37 | % |
| 35 | 2.2924 | 2.3566 | 0. | 0.00 | 318. | 99.37 | % |
| 36 | 2.3566 | 2.4207 | 0. | 0.00 | 318. | 99.37 | % |
| 37 | 2.4207 | 2.4849 | 0. | 0.00 | 318. | 99.37 | % |
| 38 | 2.4849 | 2.5491 | 1. | .31 | 319. | 99.69 | % |
| 39 | 2.5491 | 2.6133 | 0. | 0.00 | 319. | 99.69 | % |
| 40 | 2.6133 | 2.6774 | 1. | .31 | 320. | 100.00 | % |

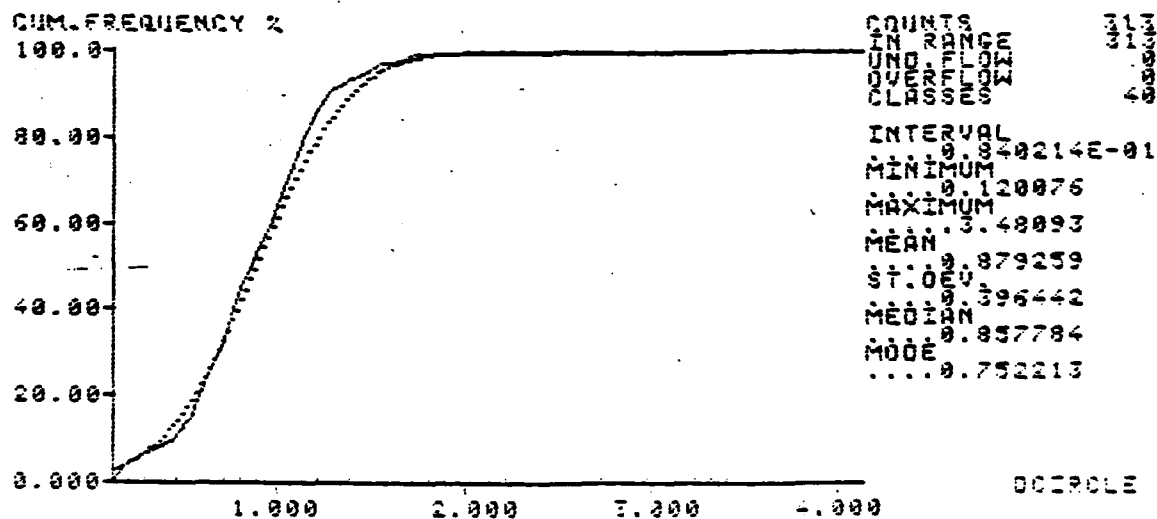
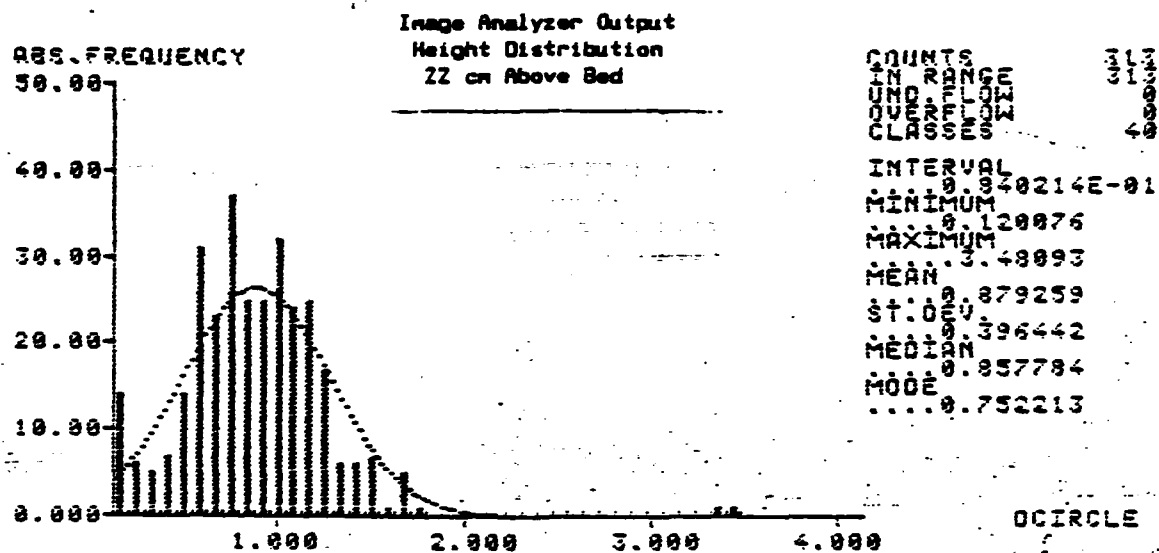


Image Analyzer Output
Height Distribution
22 cm Above Bed

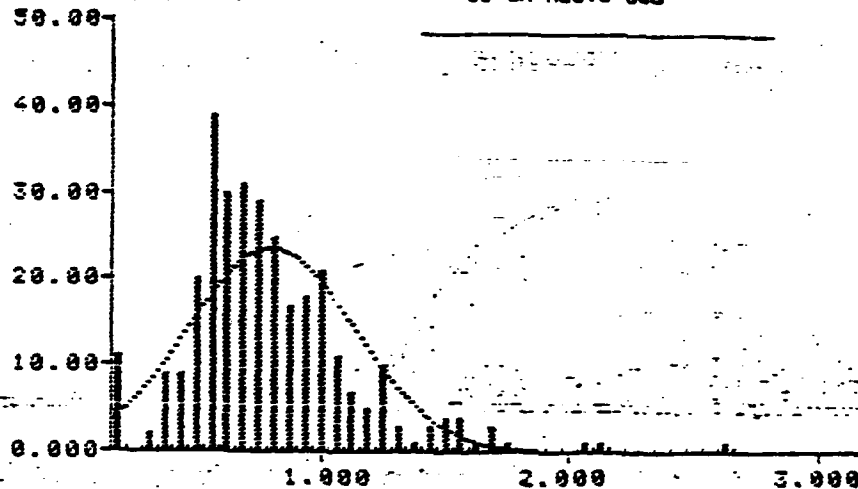
CLASSIFICATION LIST FOR DOOR IN CHANNELS 1

UNDERFLOW 0 OVERFLOW 0

| CLASS | FROM | TO | ABS | REL | FREQUENCIES CUM. ABS | CUM. REL |
|-------|--------|--------|-----|---------|-------------------------|----------|
| 1 | .12888 | .28418 | 14. | 4.47 % | 14. | 4.47 % |
| 2 | .28418 | .28812 | 6. | 1.92 % | 20. | 6.39 % |
| 3 | .28812 | .37214 | 5. | 1.60 % | 25. | 7.99 % |
| 4 | .37214 | .45616 | 7. | 2.24 % | 32. | 10.22 % |
| 5 | .45616 | .54018 | 14. | 4.47 % | 46. | 14.70 % |
| 6 | .54018 | .62420 | 31. | 9.90 % | 77. | 24.60 % |
| 7 | .62420 | .70823 | 22. | 7.35 % | 100. | 31.95 % |
| 8 | .70823 | .79225 | 37. | 11.82 % | 137. | 43.77 % |
| 9 | .79225 | .87627 | 25. | 7.99 % | 162. | 51.76 % |
| 10 | .87627 | .96029 | 25. | 7.99 % | 187. | 59.74 % |
| 11 | .96029 | 1.0443 | 32. | 10.22 % | 219. | 69.97 % |
| 12 | 1.0443 | 1.1283 | 24. | 7.67 % | 243. | 77.64 % |
| 13 | 1.1283 | 1.2124 | 25. | 7.99 % | 268. | 85.62 % |
| 14 | 1.2124 | 1.2964 | 17. | 5.43 % | 285. | 91.05 % |
| 15 | 1.2964 | 1.3804 | 6. | 1.92 % | 291. | 92.97 % |
| 16 | 1.3804 | 1.4644 | 6. | 1.92 % | 297. | 94.89 % |
| 17 | 1.4644 | 1.5484 | 7. | 2.24 % | 304. | 97.12 % |
| 18 | 1.5484 | 1.6325 | 1. | .32 % | 305. | 97.44 % |
| 19 | 1.6325 | 1.7165 | 1. | 1.60 % | 310. | 99.04 % |
| 20 | 1.7165 | 1.8005 | 1. | .32 % | 311. | 99.36 % |
| 21 | 1.8005 | 1.8845 | 0. | 0.00 % | 311. | 99.36 % |
| 22 | 1.8845 | 1.9685 | 0. | 0.00 % | 311. | 99.36 % |
| 23 | 1.9685 | 2.0526 | 0. | 0.00 % | 311. | 99.36 % |
| 24 | 2.0526 | 2.1366 | 0. | 0.00 % | 311. | 99.36 % |
| 25 | 2.1366 | 2.2206 | 0. | 0.00 % | 311. | 99.36 % |
| 26 | 2.2206 | 2.3046 | 0. | 0.00 % | 311. | 99.36 % |
| 27 | 2.3046 | 2.3887 | 0. | 0.00 % | 311. | 99.36 % |
| 28 | 2.3887 | 2.4727 | 0. | 0.00 % | 311. | 99.36 % |
| 29 | 2.4727 | 2.5567 | 0. | 0.00 % | 311. | 99.36 % |
| 30 | 2.5567 | 2.6407 | 0. | 0.00 % | 311. | 99.36 % |
| 31 | 2.6407 | 2.7247 | 0. | 0.00 % | 311. | 99.36 % |
| 32 | 2.7247 | 2.8088 | 0. | 0.00 % | 311. | 99.36 % |
| 33 | 2.8088 | 2.8928 | 0. | 0.00 % | 311. | 99.36 % |
| 34 | 2.8928 | 2.9768 | 0. | 0.00 % | 311. | 99.36 % |
| 35 | 2.9768 | 3.0608 | 0. | 0.00 % | 311. | 99.36 % |
| 36 | 3.0608 | 3.1448 | 0. | 0.00 % | 311. | 99.36 % |
| 37 | 3.1448 | 3.2289 | 0. | 0.00 % | 311. | 99.36 % |
| 38 | 3.2289 | 3.3129 | 0. | 0.00 % | 311. | 99.36 % |
| 39 | 3.3129 | 3.3969 | 1. | .32 % | 312. | 99.68 % |
| 40 | 3.3969 | 3.4809 | 1. | .32 % | 313. | 100.00 % |

Image Analyzer Output
Height Distribution
31 cm Above Bed

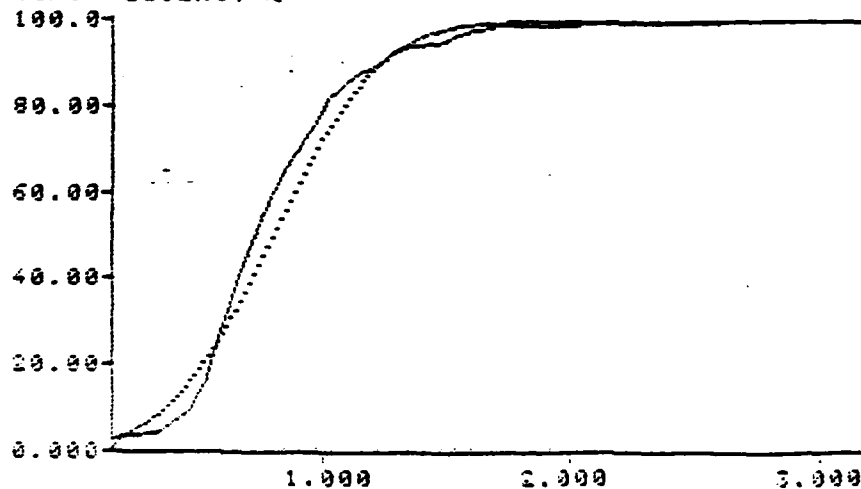
ABS. FREQUENCY



COUNTS 317
IN 317
UND 317
OVR 317
CLASS 317
INTERVAL 6.25072E-01
MINIMUM 0.154962
MAXIMUM 2.63925
MEAN 0.795639
ST. DEV 0.333608
MEDIAN 0.734619
MODE 0.568944

OCIRCLE

CUM. FREQUENCY 2



COUNTS 317
IN 317
UND 317
OVR 317
CLASS 317
INTERVAL 6.25072E-01
MINIMUM 0.154962
MAXIMUM 2.63925
MEAN 0.795639
ST. DEV 0.333608
MEDIAN 0.734619
MODE 0.568944

OCIRCLE

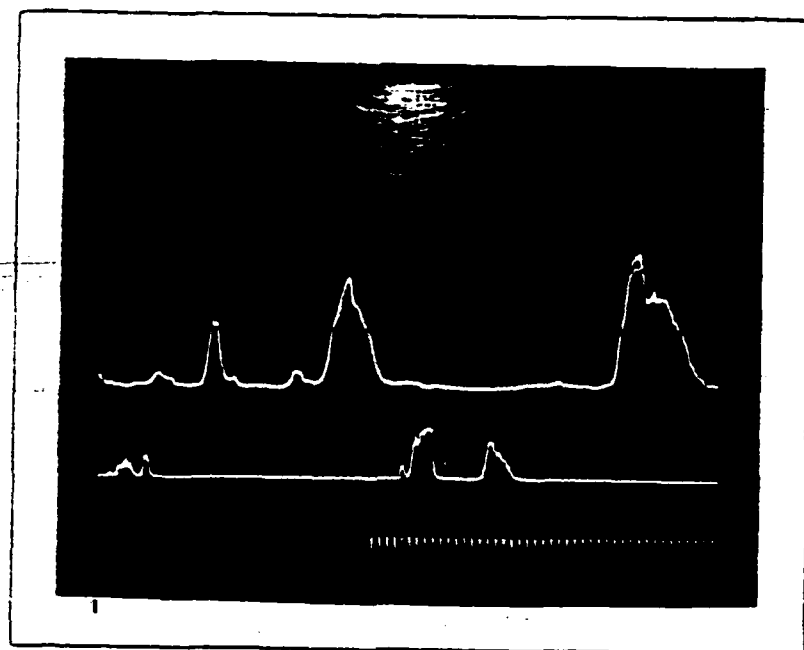
Image Analyzer Output
Height Distribution
31 cm Above Bed

CLASSIFICATION LIST FOR DITCH IN CHANNELS 1

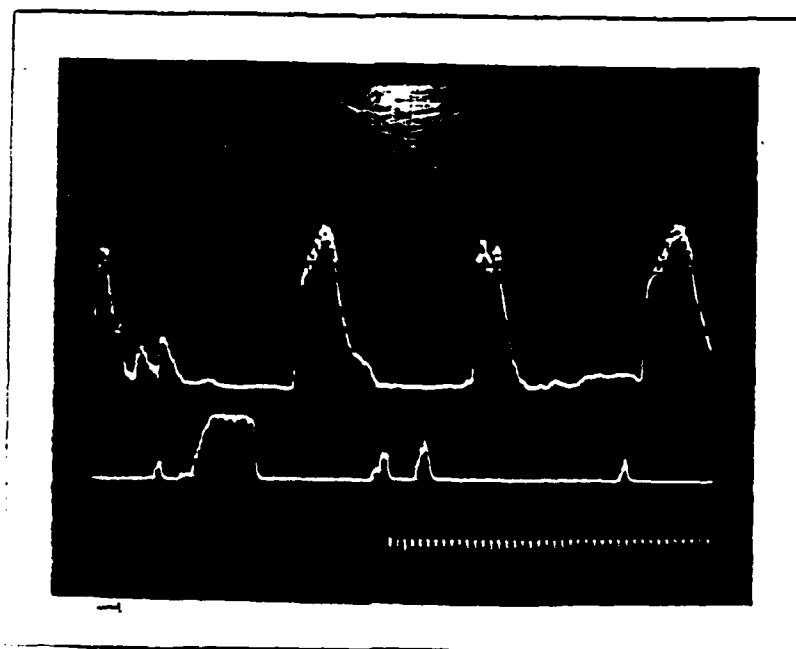
| UNDERFLOW | 0 | OVERFLOW | 0 | | | | | | |
|-----------|--------|----------|---|-----|-------|-------------|------|--------|----------|
| CLASS | FROM | TO | | ABS | REL | FREQUENCIES | CUM. | ABS | CUM. REL |
| | .15496 | .21757 | | 11. | 3.47 | 2 | 11. | 3.47 | 2 |
| | .21757 | .28018 | | 9. | 8.00 | 2 | 11. | 3.47 | 2 |
| | .28018 | .34278 | | 2. | 5.53 | 2 | 13. | 4.10 | 2 |
| | .34278 | .40539 | | 9. | 2.84 | 2 | 22. | 6.94 | 2 |
| | .40539 | .46800 | | 9. | 2.84 | 2 | 31. | 9.78 | 2 |
| | .46800 | .53061 | | 29. | 5.51 | 2 | 51. | 16.09 | 2 |
| | .53061 | .59321 | | 39. | 12.30 | 2 | 90. | 28.39 | 2 |
| | .59321 | .65582 | | 39. | 9.46 | 2 | 129. | 37.85 | 2 |
| | .65582 | .71843 | | 31. | 9.78 | 2 | 151. | 47.63 | 2 |
| | .71843 | .78103 | | 29. | 9.15 | 2 | 180. | 56.78 | 2 |
| | .78103 | .84364 | | 25. | 7.89 | 2 | 205. | 64.67 | 2 |
| | .84364 | .90625 | | 17. | 5.53 | 2 | 222. | 70.20 | 2 |
| | .90625 | .96886 | | 13. | 5.68 | 2 | 249. | 75.71 | 2 |
| | .96886 | 1.0315 | | 21. | 8.62 | 2 | 261. | 82.33 | 2 |
| | 1.0315 | 1.0941 | | 11. | 6.47 | 2 | 272. | 85.80 | 2 |
| | 1.0941 | 1.1567 | | 7. | 2.24 | 2 | 279. | 88.04 | 2 |
| | 1.1567 | 1.2193 | | 5. | 1.58 | 2 | 284. | 89.62 | 2 |
| | 1.2193 | 1.2819 | | 18. | 6.15 | 2 | 294. | 92.76 | 2 |
| | 1.2819 | 1.3445 | | 3. | 9.5 | 2 | 297. | 93.69 | 2 |
| | 1.3445 | 1.4071 | | 1. | 3.2 | 2 | 298. | 94.81 | 2 |
| | 1.4071 | 1.4697 | | 3. | 9.5 | 2 | 301. | 94.95 | 2 |
| | 1.4697 | 1.5323 | | 4. | 1.26 | 2 | 305. | 96.21 | 2 |
| | 1.5323 | 1.5949 | | 4. | 1.26 | 2 | 309. | 97.48 | 2 |
| | 1.5949 | 1.6575 | | 1. | 3.2 | 2 | 310. | 97.79 | 2 |
| | 1.6575 | 1.7201 | | 3. | 9.5 | 2 | 313. | 98.74 | 2 |
| | 1.7201 | 1.7828 | | 1. | 3.2 | 2 | 314. | 99.05 | 2 |
| | 1.7828 | 1.8454 | | 0. | 0.00 | 2 | 314. | 99.05 | 2 |
| | 1.8454 | 1.9080 | | 0. | 0.00 | 2 | 314. | 99.05 | 2 |
| | 1.9080 | 1.9706 | | 0. | 0.00 | 2 | 314. | 99.05 | 2 |
| | 1.9706 | 2.0332 | | 0. | 0.00 | 2 | 314. | 99.05 | 2 |
| | 2.0332 | 2.0958 | | 1. | 3.2 | 2 | 315. | 99.37 | 2 |
| | 2.0958 | 2.1584 | | 1. | 3.2 | 2 | 316. | 99.68 | 2 |
| | 2.1584 | 2.2210 | | 0. | 0.00 | 2 | 316. | 99.68 | 2 |
| | 2.2210 | 2.2836 | | 0. | 0.00 | 2 | 316. | 99.68 | 2 |
| | 2.2836 | 2.3462 | | 0. | 0.00 | 2 | 316. | 99.68 | 2 |
| | 2.3462 | 2.4088 | | 0. | 0.00 | 2 | 316. | 99.68 | 2 |
| | 2.4088 | 2.4714 | | 0. | 0.00 | 2 | 316. | 99.68 | 2 |
| | 2.4714 | 2.5340 | | 0. | 0.00 | 2 | 316. | 99.68 | 2 |
| | 2.5340 | 2.5966 | | 0. | 0.00 | 2 | 316. | 99.68 | 2 |
| | 2.5966 | 2.6593 | | 1. | 3.2 | 2 | 317. | 100.00 | 2 |

APPENDIX K

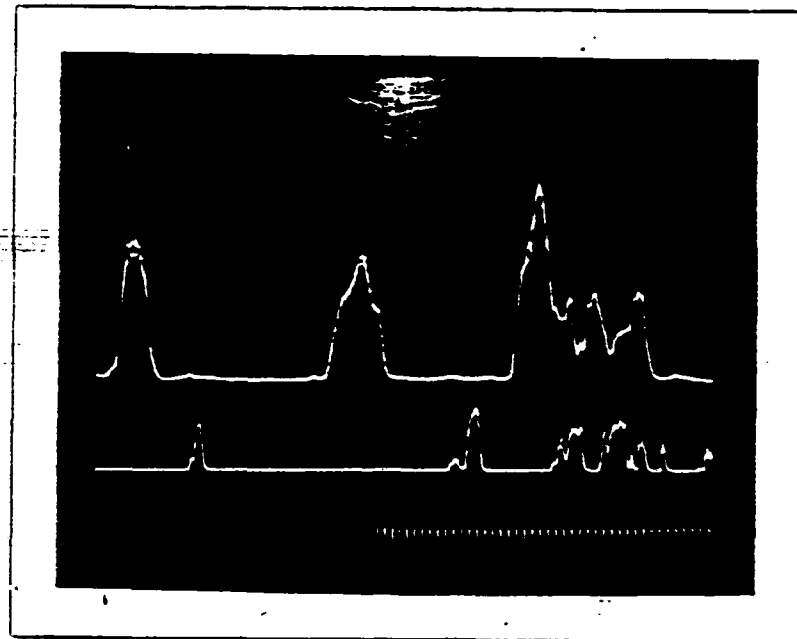
This Appendix contains the photographs of the oscilloscope traces obtained while sampling. Each of the pictures is labeled with the sample number for which it represents.



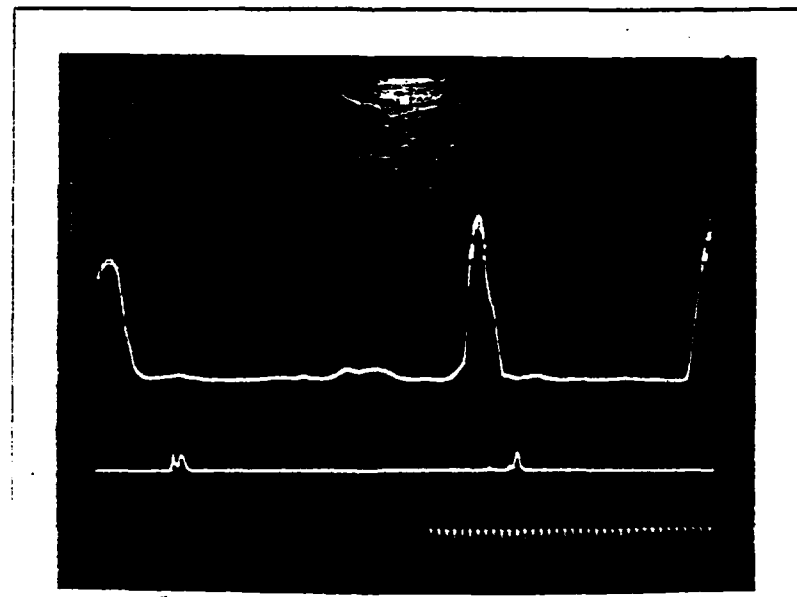
Oscilloscope Trace for Sample Number 56



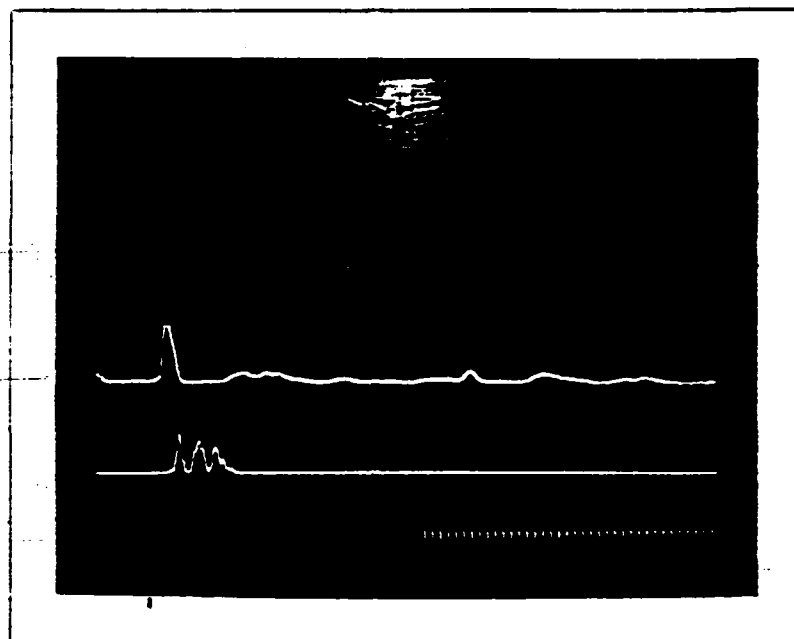
Oscilloscope Trace for Sample Number 57



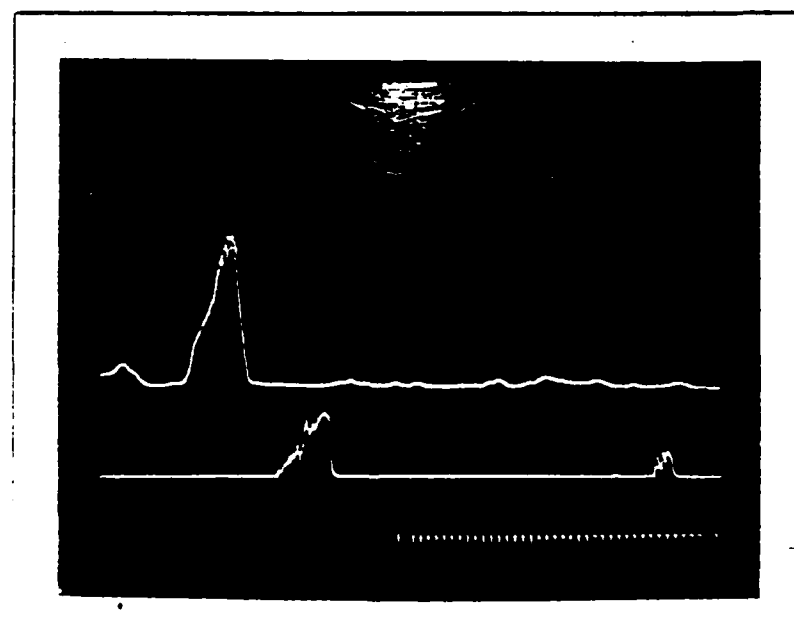
Oscilloscope Trace for Sample Number 58



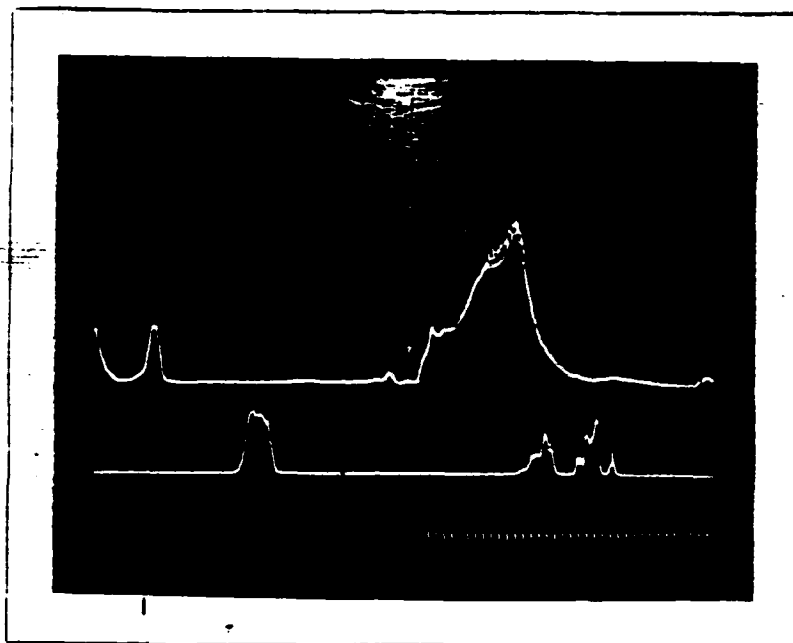
Oscilloscope Trace for Sample Number 59



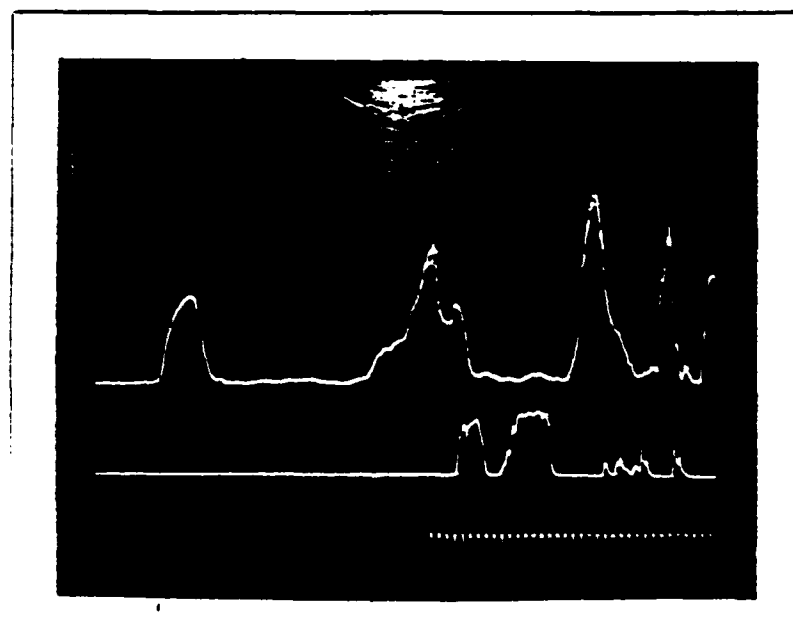
Oscilloscope Trace for Sample Number 60



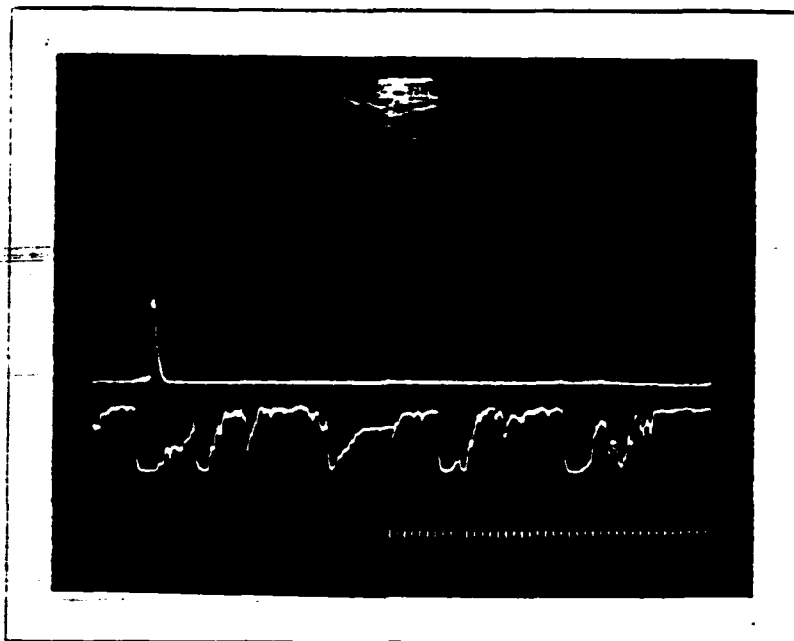
Oscilloscope Trace for Sample Number 62



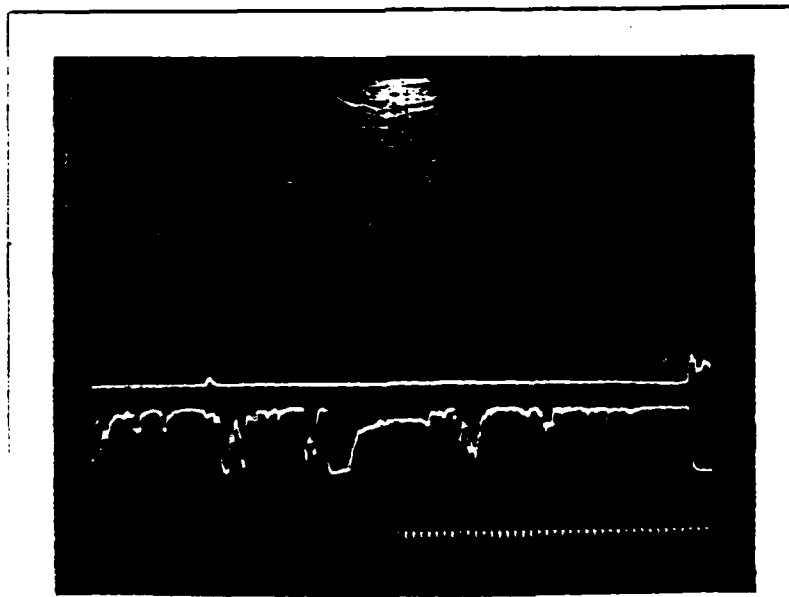
Oscilloscope Trace for Sample Number 63



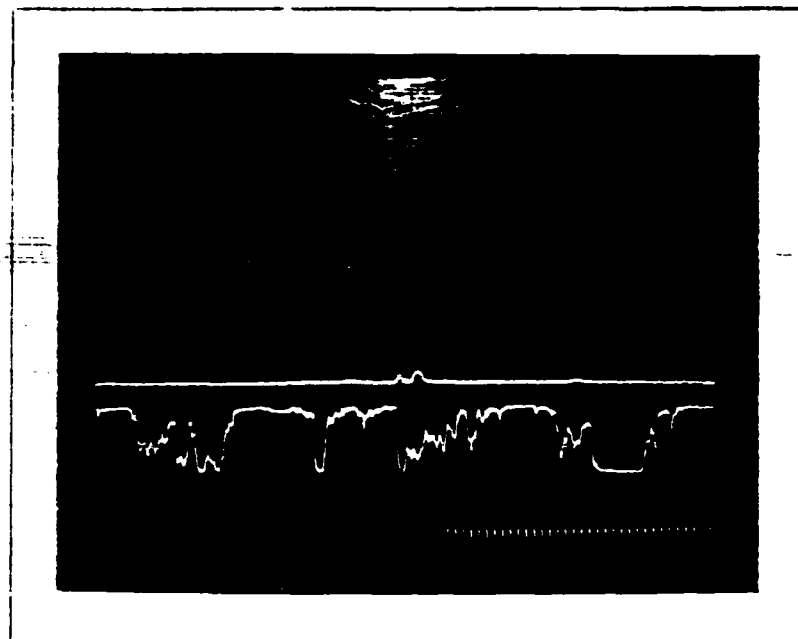
Oscilloscope Trace for Sample Number 64



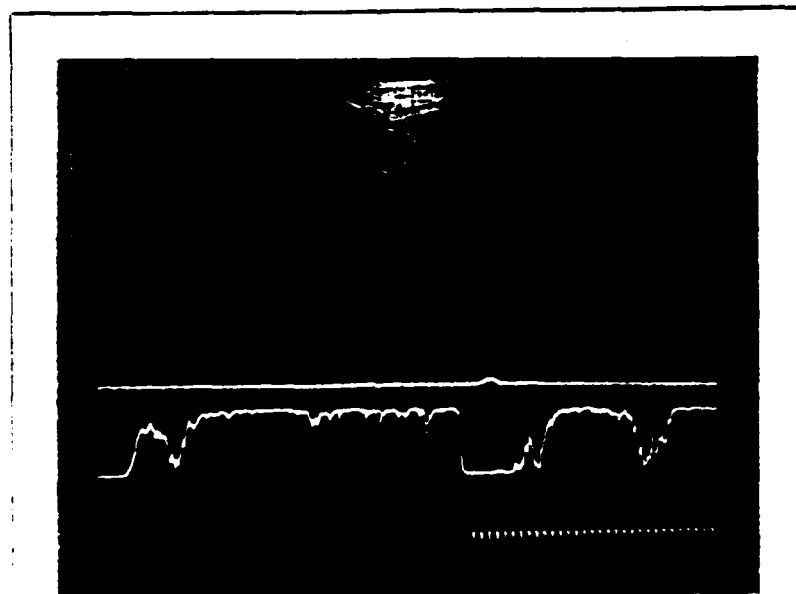
Oscilloscope Trace for Sample Number 66



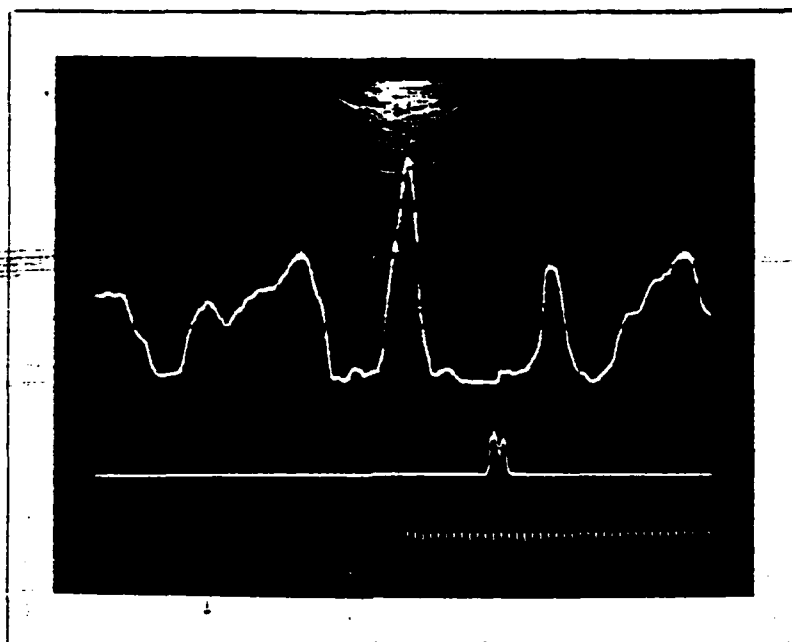
Oscilloscope Trace for Sample Number 67



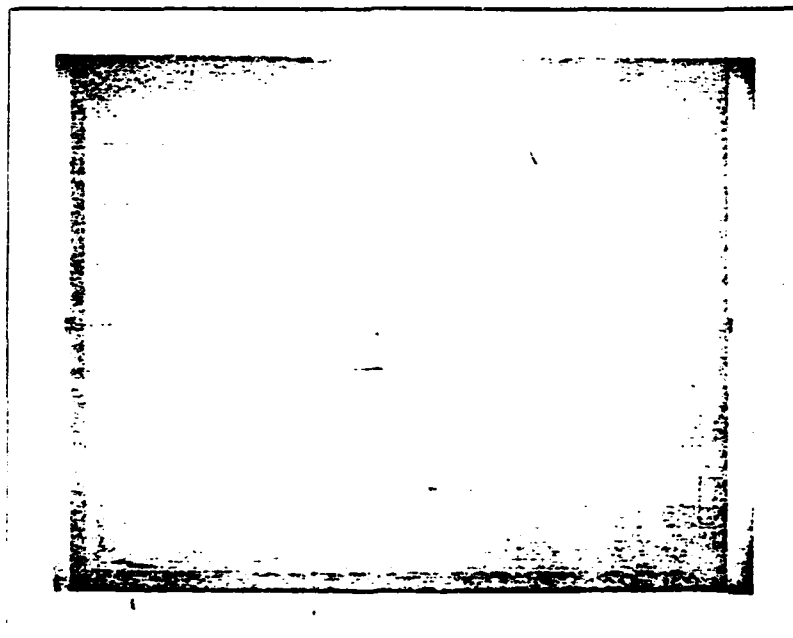
Oscilloscope Trace for Sample Number 69



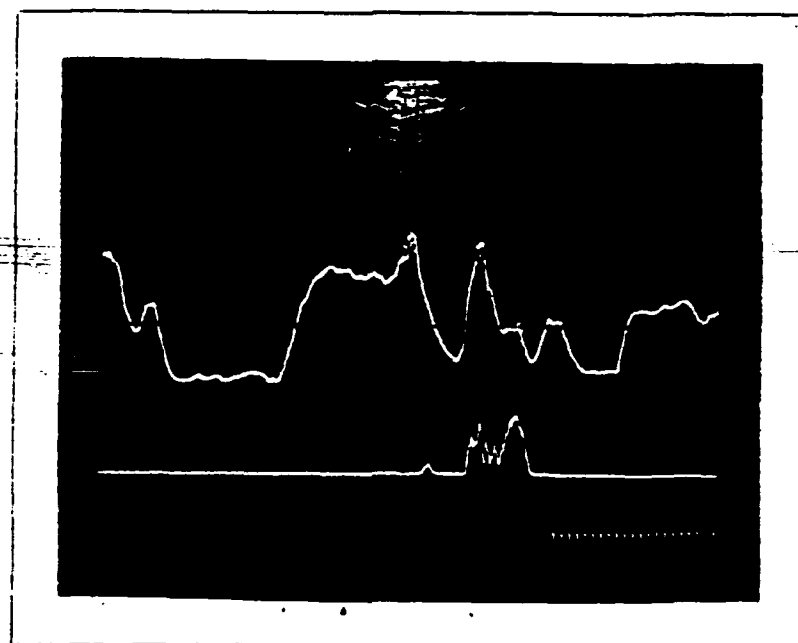
Oscilloscope Trace for Sample Number 70



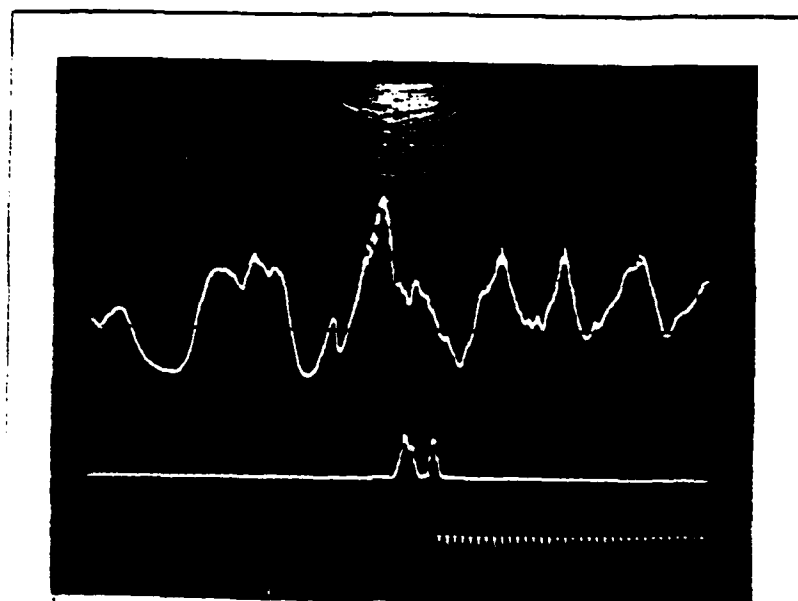
Oscilloscope Trace for Sample Number 77



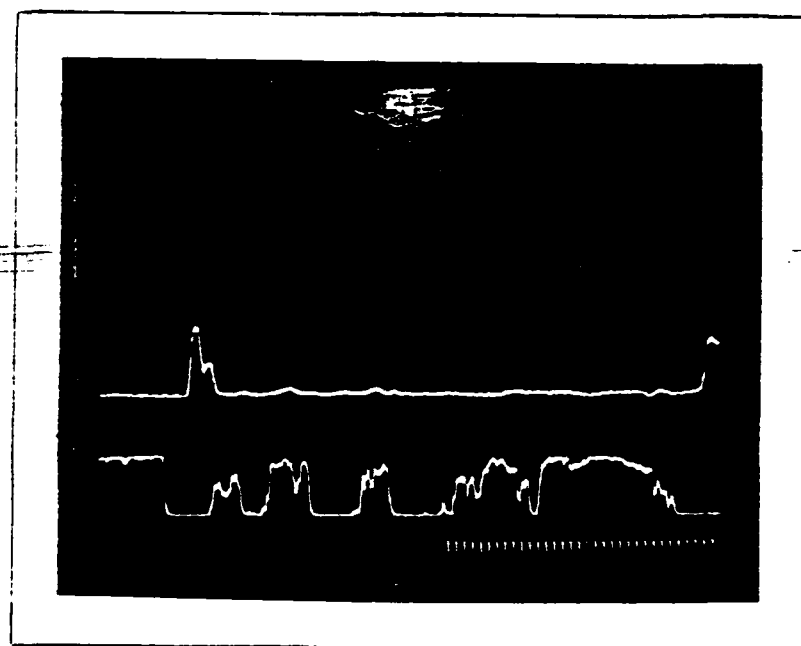
Oscilloscope Trace for Sample Number 79



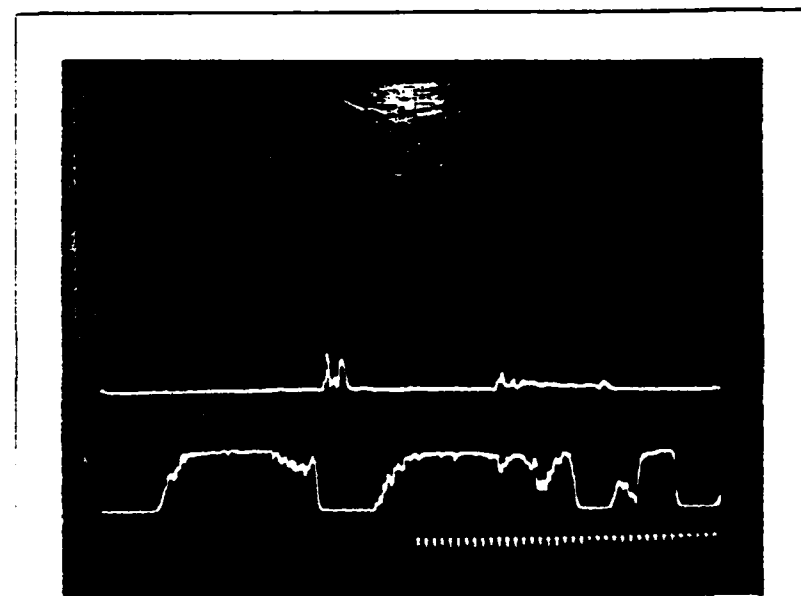
Oscilloscope Trace for Sample Number 83



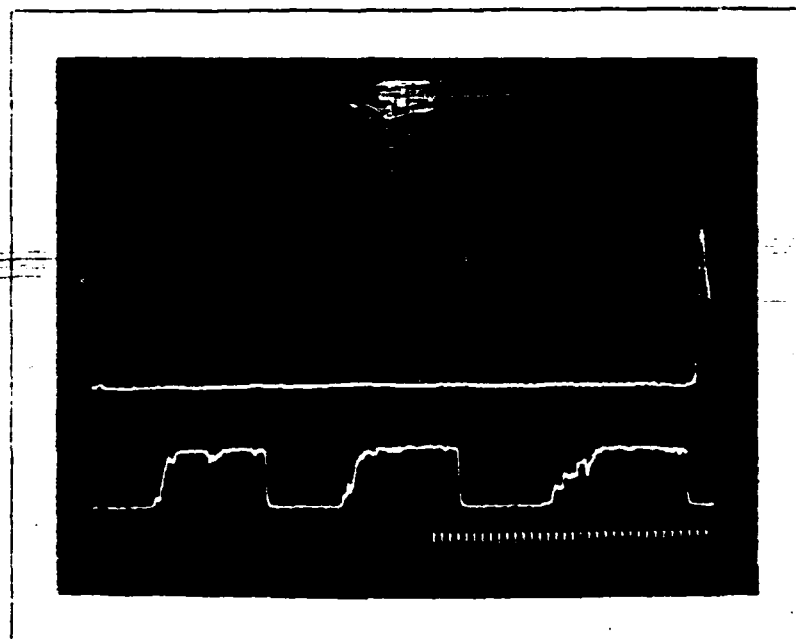
Oscilloscope Trace for Sample Number 84



Oscilloscope Trace for Sample Number 86



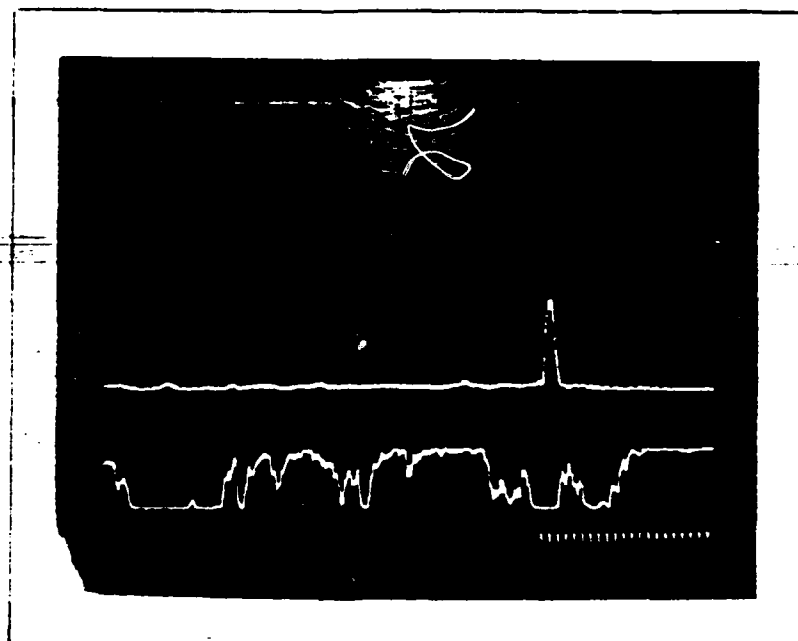
Oscilloscope Trace for Sample Number 88



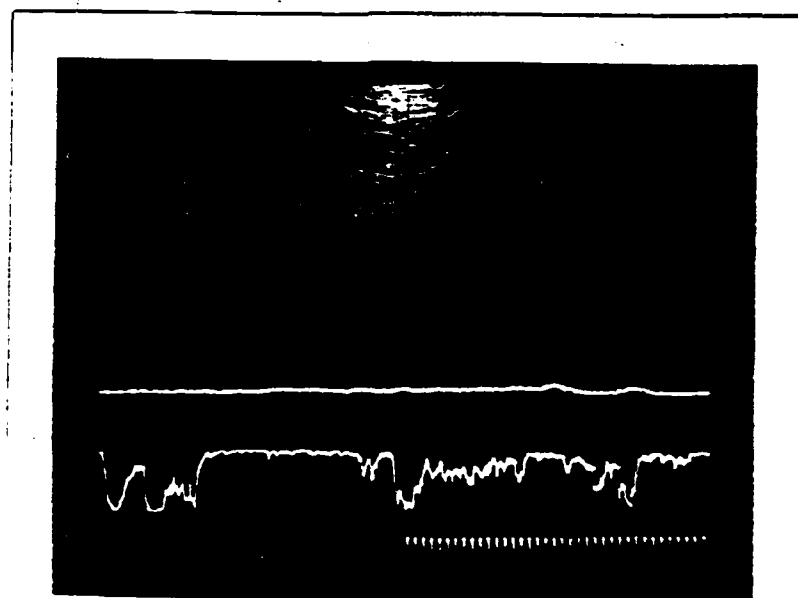
Oscilloscope Trace for Sample Number 89



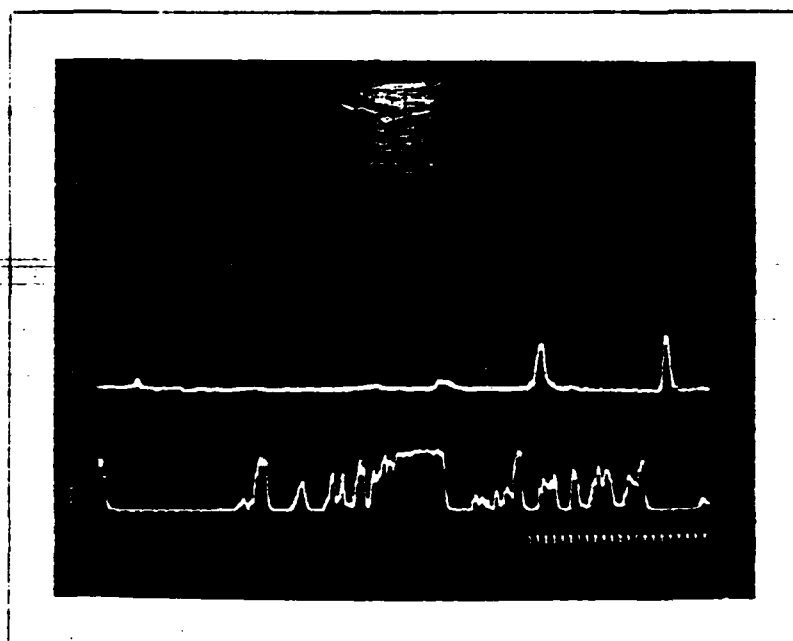
Oscilloscope Trace for Sample Number 90



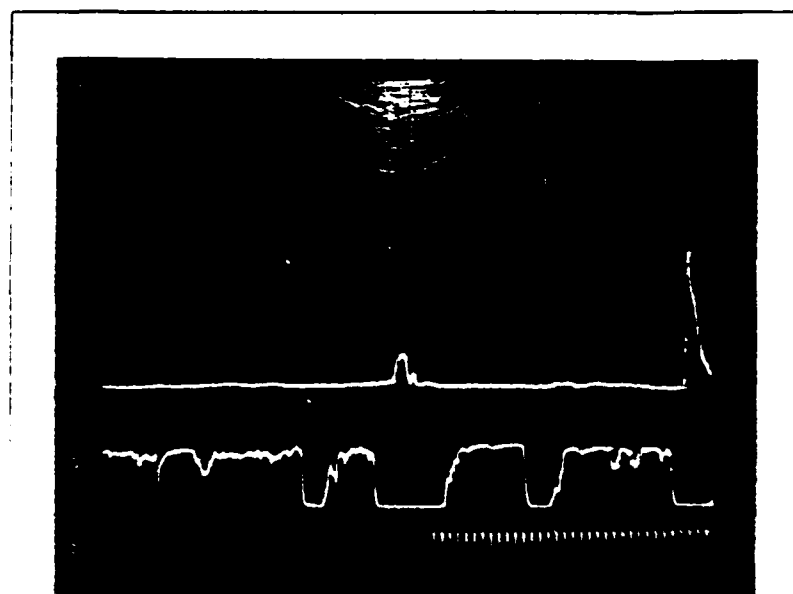
Oscilloscope Trace for Sample Number 92



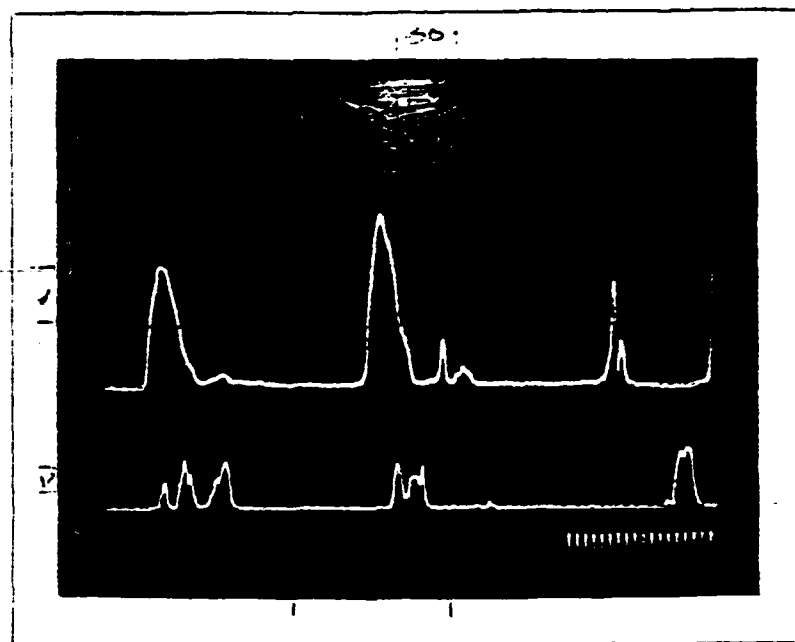
Oscilloscope Trace for Sample Number 93



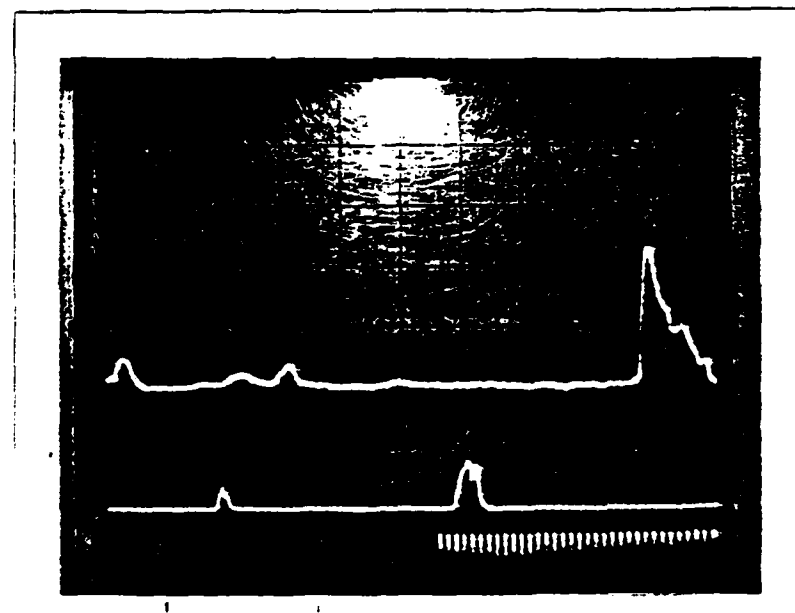
Oscilloscope Trace for Sample Number 94



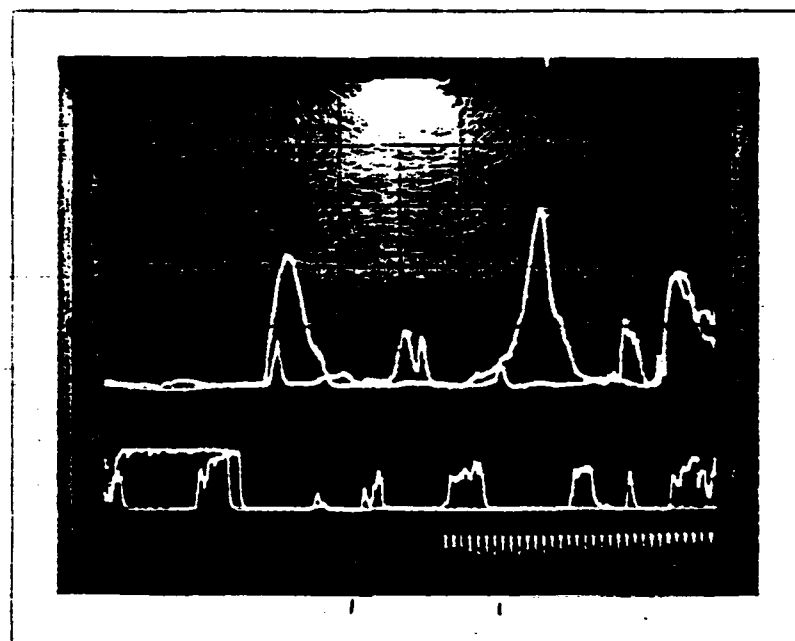
Oscilloscope Trace for Sample Number 95



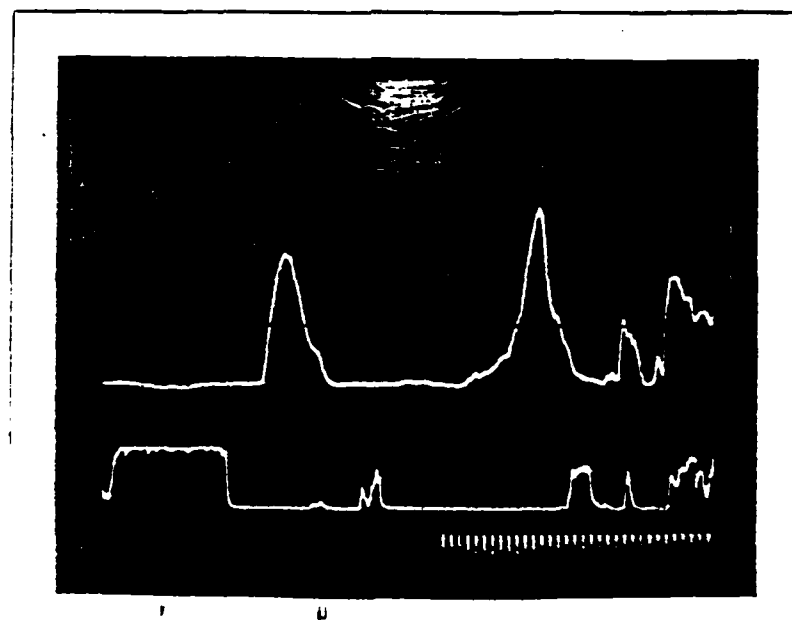
Oscilloscope Trace for Sample Number 96



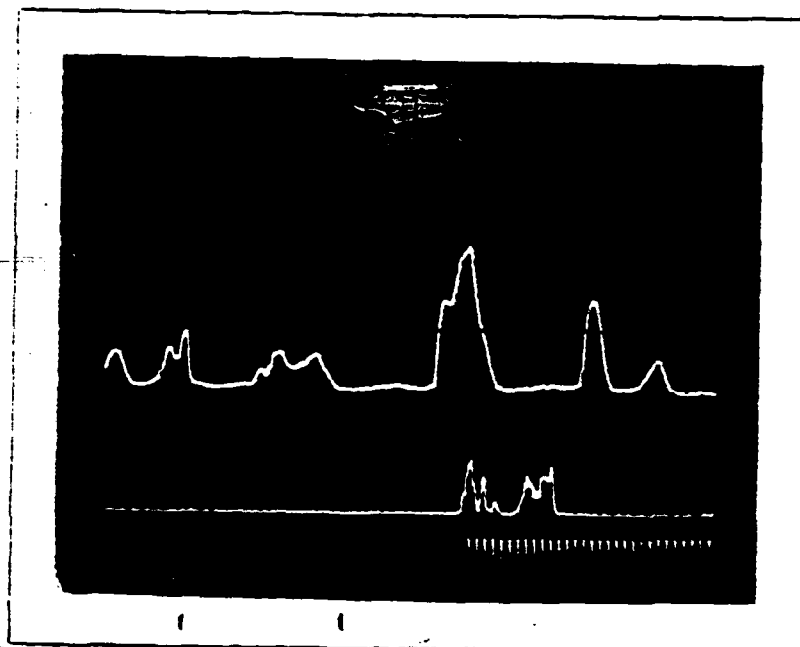
Oscilloscope Trace for Sample Number 97



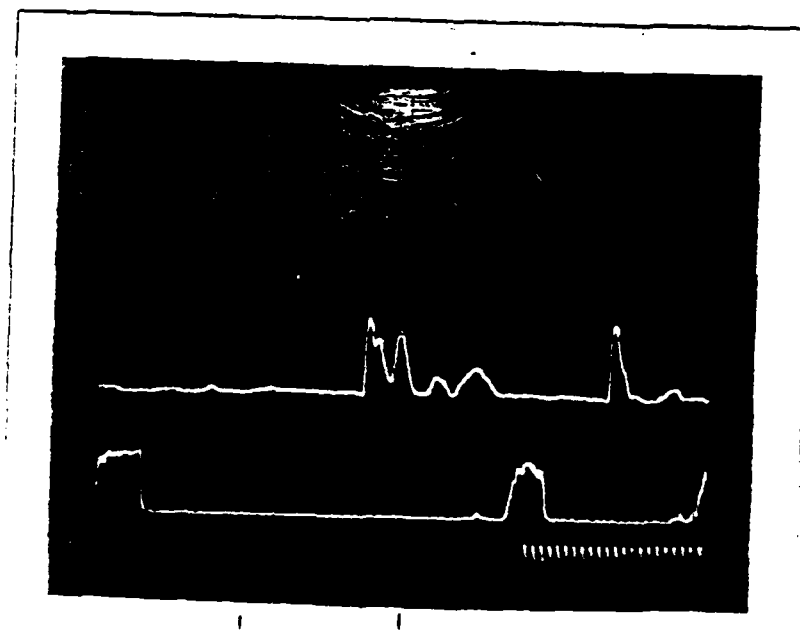
Oscilloscope Trace for Sample Number 98



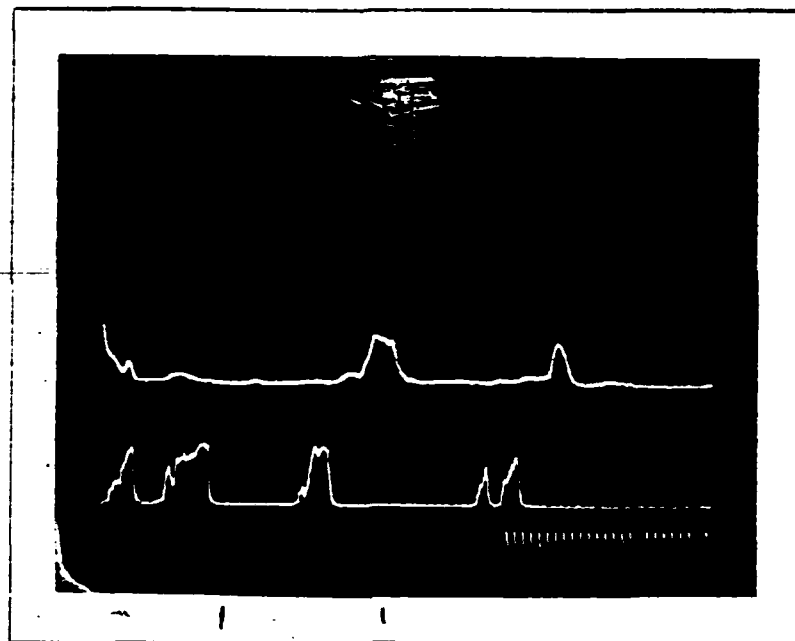
Oscilloscope Trace for Sample Number 99



Oscilloscope Trace for Sample Number 100



Oscilloscope Trace for Sample Number 101



Oscilloscope Trace for Sample Number 102

APPENDIX L

This Appendix contains a complete listing of the particle trajectory computer model used in this research. In addition, an in depth program description and flow diagram is included.

Model Computer Program

This section describes the computer program listed in Appendix K. To assist in understanding the program logic, the program itself contains numerous comment statements. The program consists of a main program and seven (7) subroutines. The main program controls the input of parameters, trajectory calculations, and output selections. The subroutines control the actual data output in either table form or graphics. The following is an in-depth description of the program:

| Lines | Description |
|---------|--|
| 50-150 | This section is used to explicitly define the major variables used within the program. The large arrays are defined in common block form to save memory. Constants used in the program are also defined. |
| 190-610 | <p>This section is used to input variable data to the program. Three options exist for the bed particle distribution input:</p> <ol style="list-style-type: none">1) The default condition sets the quantity of each particle to unity. This option is generally used when a height determination is required or being sought after.2) The particle number option allows the entry of bed distribution by the number of particles present in each diameter range. This is used when data from the image analyzer was being used.3) The last option is used when the particle size distribution is determined from a sieve analysis and the data is measured in grams mass. The program will then determine the |

particle number density based on the assumption that the particles are spherical.

650-690 These lines convert the velocity input values from Ft/s to m/s.

700-710 Determine the slope of the triangular jet using the input amplitude and duration.

720-800 Initialize the data arrays to zero (0).

810-1660 This section calculates the trajectory for each diameter particle. This WHILE condition contains the following 8 subsections.

820-840 Initialize the height of the particle to pass the first WHILE statement. Calculate the particle diameter to be used.

850-1340 Calculate the particles trajectory parameters while the particle is above the bed surface. This DO loop contains the following 6 subsections.

860-940 If the elapsed time since the particle left the bed is less than the jet duration time, the add the jet velocity to U_0 .

950-990 Calculates the relative velocity of the air with respect to the particle. Determine the sign of the drag force.

1010-1060 Calculate Reynold's number.

1100-1170 Calculate the drag on the particle and then determine the particles new velocity and position.

1180-1220 If the particles velocity is positive, record the new max height and elapsed time.

1230-1320. Add 1 count to the probability array in the storage position representing the particles height/2. By using the DIV statement, a height window (dH) of 2 cm is created.

1350-1370 Change all heights from Ft/s to m/s

1380-1430 Multiply probability distribution by bed distribution weighting factor.

1440-1500 Determine the maximum value and normalize

the data such that the maximum is 100.

| | |
|-----------|--|
| 1510-1560 | Calculate the particle entrainment by summing the total volume of each particle distribution at a given height. |
| 1570-1660 | Normalize the entrainment data to 100 and calculate the ln value if not equal to zero. |
| 1700-1820 | Display output menu. |
| 1830-2210 | Controls the selected output. |
| 2220 | End of MAIN program |
| 2260-2520 | Sub Display_Data is used to list input parameters used and the maximum height attained by each diameter particle. |
| 2560-3930 | Sub Display_graphics controls the processing and output of graphic information. This subprogram contains the following 4 sections. |
| 2640-3120 | Performs scaling for determining graphic dimensions and limits. |
| 3130-3240 | Creates graphic display and labels the X and Y axis. |
| 3250-3830 | Controls the plotting of selected graphic output. |
| 3840-3920 | Prints hard copy. |
| 3980-4130 | Function routine for determining scaling factor for graphic display. |
| 4180-4280 | Finds the limit of data within an INTEGER array to limit the X axis on a plot to the range in which the Y values are non-zero. |
| 4330-4460 | Determines the maximum value stored in an INTEGER array. |
| 4510-4640 | Same as 4330-4460 except for REAL array. |
| 4690-4770 | Same as 4180-4280 except for REAL array. |

END of PROGRAM

```

10  !.....MAIN Program.....
20  !
30  !
40  !
50  OPTION BASE 1
60  INTEGER Answer,Specify,Point,View,Bed_min,I
70  REAL Uo,Uo0,Uj,Del_t,Part_height,Slope,Jet_t,Jt
80  COM INTEGER Distribution(50,80);Distrib_density(50,80),REAL Height(2,50),3
ed_particle(50),Entrainment(2,80)
90  DIM Homes(2),Clears(2)
100 Clears=CHRS(255)&CHRS(75)          ! CLEAR SCR key
110 Homes=CHRS(255)&CHRS(84)           ! HOME key
120 Viscosity_kin=1.486E-5             ! air, m^2/s
130 Density_air=1.201                  ! kg/m^3
140 Density_part=7.85E+3               ! kg/m^3
150 Gravity=9.80665                   ! m/s^2
160 !
170 ! Input variables
180 !
190 PRINTER IS 1                       ! Output to CRT
200 INPUT "Enter mean air velocity Uo (Ft/s): ",Uo
210 INPUT "Enter amplitude of jet velocity (Ft/s): ",Uj
220 INPUT "Enter initial particle velocity Uo0 (Ft/s): ",Uo0
230 INPUT "Enter duration of jet (s): ",Jet_t
240 INPUT "Enter time increment for iteration (s): ",Del_t
250 INPUT "Do you desire to input the bed particle distribution (1 yes,0 no):"
,Answer
260 IF Answer=0 THEN                   ! Bed dist not wanted
270   FOR I=1 TO 50                   ! Set bed dist to 1
280     Bed_particle(I)=1.
290   NEXT I
300 ELSE
310   IF Answer=1 THEN                 ! Bed dist wanted
320     INPUT "Input will be: weight in grams (1) or number (2): ",Specify
330     IF Specify=1 OR Specify=2 THEN
340       PRINT "Enter data for each diameter"          ! Enter gram or 3
350       Min_bed=1
360       FOR I=1 TO 50                                ! Each diameter
370         PRINT "D= ":I*10+70:" um"
380         INPUT Bed_particle(I)
390         IF Bed_particle(I)<Bed_particle(Min_bed) THEN Min_bed=I
400       NEXT I
410       IF Specify=1 THEN                             ! If weight entry
420         FOR I=1 TO 50                                ! Calculate z
430           Bed_particle(I)=5*Bed_particle(I)/(PI*(I*10+70)^3*Density_part)
440           IF Bed_particle(I)<Bed_particle(Min_bed) THEN Min_bed=I
450         NEXT I
460       END IF
470     ELSE
480       GOTO 320
490     END IF
500   ELSE
510     GOTO 250
520   END IF
530 END IF
540 Max_bed=1
550 FOR I=1 TO 50                                ! Find largest z
560   IF Bed_particle(I)>Bed_particle(Max_bed) THEN Max_bed=I

```

```

570 NEXT I
580 Max_value=100/Bed_particle(Max_bed)           ! determine scaler
590 FOR I=1 TO 50                                ! Scale data max=100
600     Bed_particle(I)=Bed_particle(I)*Max_value
610 NEXT I
620 !
630 ! Compute data
640 !
650 U1=Uo
660 Up1=Upol
670 Uo=Uo*.3048                                  ! Change to m/s
680 Upol=Upol*.3048
690 Uj1=Uj*.3048
700 IF Jet_t=0 THEN Jet_t=1
710 Slope=2.*Uj1/Jet_t                          ! Triangle jet pulse
720 FOR I=1 TO 50
730     Height(1,I)=0.                            ! Zero height array
740     Height(2,I)=0.                            ! Zero number array
750     FOR J=1 TO 90
760         Distribution(I,J)=0.                  ! Zero dist array
770         Entrainment(1,J)=0.                  ! Zero entrain array
780         Entrainment(2,J)=0.
790     NEXT J
800 NEXT I
810 FOR I=1 TO 50                                ! For each particle
820     Part_height=.000001                      ! Set for WHILE state.
830     Upo=Upol                                  ! Initial U constant
840     Diameter_part=(I+7)*1.0E-5               ! Particle Dia um
850     WHILE Part_height>0
860         Jt=Jet_t/2.
870         Time_now=Height(2,I)*Del_t           ! Time of part flight
880         IF Time_now<Jet_t THEN               ! part in jet?
890             IF Height(2,I)*Del_t<Jt THEN     ! 1st half of jet
900                 Uo=Uo+Slope*Height(2,I)*Del_t
910             ELSE
920                 Uo=Uo+Uj1-Slope*Height(2,I)*Del_t ! 2nd half of jet
930             END IF
940         END IF
950         Relative_vel=Uo-Upo                   ! Rel V seen by part
960         Sign=1                                ! Set sign positive
970         IF Relative_vel<0 THEN                ! Is V negative?
980             Sign=-1                          ! Set sign negative
990         END IF
1000        !                                     Calculate Re
1010        Reynolds_no=Relative_vel*Diameter_part/Viscosity_kin
1020        Reynolds_no=ABS(Reynolds_no)
1030        IF Reynolds_no=0. THEN
1040            Acceleration=-Gravity
1050            GOTO 1150
1060        END IF
1070        !                                     Calculate drag
1080        ! Uses data correlation for drag coefficient good for Re<1E5
1090        !
1100        Drag_coeff=24/Reynolds_no+6/(1+SQR(Reynolds_no))+.4
1110        Drag=Sign*Drag_coeff*Density_air*Relative_vel*Relative_vel*PI*Diameter
_part*Diameter_part/8
1120        !                                     Calculate acceleration
1130        Acceleration=Drag/(Density_part*PI*Diameter_part*3/6)-Gravity
1140        !                                     Calculate del velocity
1150        Velocity=Upo+Acceleration*Del_t

```

```

1160      !                                     Calculate new position
1170      Part_height=Part_height+(Velocity+Upo)*Del_t/2
1180      IF Upo>0 THEN                                     ! Part still rising?
1190          Height(1,I)=Part_height                     ! Save position
1200          Height(2,I)=Height(2,I)+1                   ! Inc t for max rise
1210      END IF
1220      Upo=Velocity                                     ! Set new V for next inc
1230      Point=(100*Part_height)/DIV 2                   ! 2 cm wide storage bins
1240      IF Point>79 THEN                                  ! Set default for fatal
1250          Point=79
1260      END IF
1270      IF Point<=0 THEN                                  ! Set default for fatal
1280          Point=0
1290      END IF
1300      PRINT I,Point                                     ! Indicate comp working
1310      ! Save 3 times part in height bin
1320      Distribution(I,Point+1)=Distribution(I,Point+1)+1
1330  END WHILE
1340  NEXT I
1350  FOR I=1 TO 50
1360      Height(1,I)=Height(1,I)*100                     ! Change to cm
1370  NEXT I
1380  FOR I=1 TO 50
1390      Value=Bed_particle(I)                             ! Part size weight factor from bed dist
1400      FOR J=1 TO 80
1410          Distrib_density(I,J)=Distribution(I,J)*Value ! Weight dist values
1420      NEXT J
1430  NEXT I
1440  Max_dist=FNMax_int(Distrib_density(*),50,80)         ! Find max value
1450  Factor=100./Max_dist                                  ! Scale for 100 max
1460  FOR I=1 TO 50
1470      FOR J=1 TO 80
1480          Distrib_density(I,J)=Distrib_density(I,J)*Factor ! Scale values
1490      NEXT J
1500  NEXT I
1510  FOR I=1 TO 50      ! Mass density/unit area   at height above bed
1520      Volume=PI*((I+7)/1000)^3/6                 ! Volume Cu cm
1530      FOR J=1 TO 80
1540          Entrainment(1,J)=Entrainment(1,J)+Volume*Distrib_density(I,J)
1550      NEXT J
1560  NEXT I
1570  Max_entrain=1
1580  FOR I=1 TO 80
1590      IF Entrainment(1,I)>Entrainment(1,Max_entrain) THEN Max_entrain=I ! Find maximum
1600  NEXT I
1610  Factor=100/Entrainment(1,Max_entrain)             ! Normalize to 100
1620  FOR I=1 TO 80
1630      Entrainment(1,I)=Entrainment(1,I)*Factor
1640      IF Entrainment(1,I)<=0. THEN 1650
1650      Entrainment(2,I)=LOG(Entrainment(1,I))
1660  NEXT I
1670  !
1680  ! Output Control Section
1690  !
1700  PRINTER IS :                                         ! Output to CRT
1710  PRINT USING "9,3/"
1720  PRINT "1)   Display height vs diameter data"
1730  PRINT "2)   Display height vs diameter graph"
1740  PRINT "3)   Display density vs height as function of dia graph"
1750  PRINT "4)   Display density vs diameter as a function of height graph"

```



```

1760 PRINT "5)      Display same as 3 but with bed density"
1770 PRINT "5)      Display same as 4 but with bed density"
1780 PRINT "7)      Display density vs diameter of bed mass"
1790 PRINT "8)      Display entrainment density above bed"
1800 PRINT "9)      Display Ln entrainment density above bed"
1810 PRINT "10)     EXIT PROGRAM"
1820 INPUT "Enter number of desired display: ",Answer
1830 SELECT Answer
1840   CASE =1
1850     CALL Display_data(U1,U01,Uj,Jet_t,Del_t,Homes,Clears)
1860   CASE =2
1870     CALL Display_graph(Clears,Homes,Answer,View)
1880   CASE =3
1890     INPUT "Enter particle size to be viewed (80-570 um)(0 for all): ",View
1900     IF View=0 THEN 1920
1910     IF View<80 OR View>570 THEN 1890
1920     View=(View DIV 10)-7
1930     CALL Display_graph(Clears,Homes,Answer,View)
1940   CASE =4
1950     INPUT "Enter desired height above bed surface (0-158 cm): ",View
1960     IF View<0 OR View>158 THEN 1950
1970     View=(View DIV 2)+1
1980     CALL Display_graph(Clears,Homes,Answer,View)
1990   CASE =5
2000     INPUT "Enter particle size to be viewed (80-570 um)(0 for all): ",View
2010     IF View=0 THEN 2030
2020     IF View<80 OR View>570 THEN 2000
2030     View=(View DIV 10)-7
2040     CALL Display_graph(Clears,Homes,Answer,View)
2050   CASE =6
2060     INPUT "Enter desired height above bed surface (0-158 cm): ",View
2070     IF View<0 OR View>158 THEN 2060
2080     View=(View DIV 2)+1
2090     CALL Display_graph(Clears,Homes,Answer,View)
2100   CASE =7
2110     CALL Display_graph(Clears,Homes,Answer,View)
2120   CASE =8
2130     CALL Display_graph(Clears,Homes,Answer,View)
2140   CASE =9
2150     CALL Display_graph(Clears,Homes,Answer,View)
2160   CASE =10
2170     STOP
2180   CASE ELSE
2190     GOTO 1820
2200 END SELECT
2210 GOTO 1700
2220 END
2230 !
2240 !
2250 !
2250 ! Sub used to list input parameters and max height at time t per diameter
2270 SUB Display_data(U1,U01,Uj,Jet_t,Del_t,Homes,Clears)
2290 DIM INTEGER Distribution(*),Distrib_density(*),REAL height(*),Bed_particle
2290   Entrainment(*)
2290   OUTPUT 2:Homes:           ! Home and Clear screen
2300   OUTPUT 2:Clears:
2310   !                           Print output
2320   PRINT "                               cm/s"
2330   PRINT "Mean Bed Velocity="          "U1=30.48
2340   PRINT "Initial Particle Velocity="  "U01=30.48

```

```

2350 PRINT "Peak Jet Velocity="      ":Uj=30.48
2360 PRINT "Gas Jet Duration="      ":Jet_t
2370 PRINT
2380 PRINT "  Diameter", "  Height", "  Time", "  Diameter": "  Height": "
Time"
2390 PRINT "    um", "    cm ", " seconds", "    um", "    cm", "    seconds
"
2400 PRINT
2410 FOR I=1 TO 50 STEP 2
2420 PRINT USING "2(SX,3D,SX,3D.0,SX,0.000,SX)":(I+7)*10,Height(1,I),Height(2
,I)*0el_t,(I+8)*10,Height(1,I+1),Height(2,I+1)*0el_t
2430 NEXT I
2440 PRINTER IS 1
2450 INPUT "Print hard copy? (1)= yes, (0)= no: ",Answer
2460 IF Answer=1 THEN
2470 PRINTER IS 701
2480 GOTO 2320
2490 ELSE
2500 IF Answer<>0 THEN 2450
2510 END IF
2520 SUBEND
2530 !
2540 !
2550 !
2560 ! Sub used to control graphics outout of data
2570 SUB Display_graph(Clears,Homes,INTEGER Data_set,View)
2580 COM INTEGER Distribution(*),Distrib_density(*),REAL Height(*),Bed_particle
(*),Entrainment(*)
2590 REAL Xmax,Ymax,Xtick,Ytick,Xmin,Ymin
2600 OUTPUT 2:Homes:
2610 OUTPUT 2:Clears:
2620 GINIT ! Initialize graphics
2630 GRAPHICS ON
2640 SELECT Data_set ! Scale plot routines
2650 CASE =2
2660 Xmax=600.
2670 Ymax=FNMax_real(Height(*),1,50)
2680 Xtick=50.
2690 Ytick=FNScale(Ymax)
2700 CASE =3
2710 Ymax=FNMax_int(Distribution(*),50,80)
2720 Xmax=FNData_limit(Distribution(*),50,80)
2730 Xtick=FNScale(Xmax)
2740 Ytick=FNScale(Ymax)
2750 CASE =4
2760 Xmax=500.
2770 Ymax=FNMax_int(Distribution(*),50,80)
2780 Xtick=50.
2790 Ytick=FNScale(Ymax)
2800 CASE =5
2810 Xmax=FNData_limit(Distrib_density(*),50,90)
2820 Ymax=100.
2830 Xtick=FNScale(Xmax)
2840 Ytick=FNScale(Ymax)
2850 CASE =6
2860 Xmax=600.
2870 Ymax=FNMax_int(Distrib_density(*),50,90)
2880 Xtick=50.
2890 Ytick=FNScale(Ymax)
2900 CASE =7

```

```

2910     Xmax=500.
2920     Ymax=100.
2930     Xtick=50.
2940     Ytick=10
2950     CASE =0
2950         Xmax=FNDData_limitr(Entrainment(+),1,80)
2970         Ymax=100.
2980         Xtick=FNScale(Xmax)
2990         Ytick=10.
3000     CASE =9
3010         Xmax=FNDData_limitr(Entrainment(+),1,80)
3020         Ymax=5.
3030         Ymin=-3.
3040         Xtick=FNScale(Xmax)
3050         Ytick=.5
3060         Y_axis=-2.5
3070         GOTO 3110
3080     END SELECT
3090     Y_axis=0.
3100     Ymin=-Ytick
3110     Xmin=-2.*Xtick
3120     X_axis=0.
3130     WINDOW Xmin,1.1*Xmax,Ymin,1.1*Ymax
3140     AXES Xtick,Ytick,X_axis,Y_axis
3150     LORG 6
3160     FOR I=X_axis TO Xmax STEP Xtick*2
3170         MOVE I,Y_axis
3180         LABEL I
3190     NEXT I
3200     LORG 8
3210     FOR I=Y_axis TO Ymax STEP Ytick
3220         MOVE X_axis,I
3230         LABEL I
3240     NEXT I
3250     SELECT Data_set
3250         CASE =2
3270             MOVE 80,Height(1,1)
3280             FOR I=2 TO 50
3290                 DRAW (I+7)*10,Height(1,I)
3300             NEXT I
3310         CASE =3
3320             Begin=View
3330             Finish=View
3340             IF View<0 THEN
3350                 Begin=1
3360                 Finish=50
3370             END IF
3380             FOR I=Begin TO Finish
3390                 MOVE 0,Distribution(I,1)
3400                 FOR J=1 TO Xmax/2
3410                     DRAW 2*J,Distribution(I,J)
3420                 NEXT J
3430             NEXT I
3440         CASE =4
3450             MOVE 80,Distribution(1,View)
3460             FOR I=2 TO 50
3470                 DRAW (I+7)*10,Distribution(I,View)
3480             NEXT I
3490         CASE =5
3500             Begin=View

```

```

! Set graphics scale
! Set graph axis
! Label X-axis

```

```

! Label Y-axis

```

```

! Plot data

```

```

! Plot all if<0

```

```

3510      Finish=View
3520      IF View<0 THEN                                ! Plot all if <0
3530          Begin=1
3540          Finish=50
3550      END IF
3560      FOR I=Begin TO Finish
3570          MOVE 0,Distrib_density(I,1)
3580          FOR J=1 TO Xmax/2
3590              DRAW 2*J,Distrib_density(I,J)
3600          NEXT J
3610      NEXT I
3620      CASE =5
3630          MOVE 80,Distrib_density(1,View)
3640          FOR I=2 TO 50
3650              DRAW (I+7)*10,Distrib_density(I,View)
3660          NEXT I
3670      CASE =7
3680          MOVE 80,Sed_particle(1)
3690          FOR I=2 TO 50
3700              DRAW (I+7)*10,Sed_particle(I)
3710          NEXT I
3720      CASE =8
3730          MOVE 0,Entrainment(1,1)
3740          FOR I=2 TO 80
3750              DRAW I*2,Entrainment(1,I)
3760          NEXT I
3770      CASE =9
3780          MOVE 0,Entrainment(2,1)
3790          FOR I=2 TO 80
3800              IF Entrainment(2,I)=0. THEN 3840
3810              DRAW I*2,Entrainment(2,I)
3820          NEXT I
3830      END SELECT
3840      INPUT "Print graph (1) yes, (0) no: ",Answer
3850      IF Answer=1 THEN
3860          DUMP DEVICE IS 701                                ! Dump to printer
3870          DUMP GRAPHICS
3880          GCLEAR
3890      ELSE
3900          IF Answer<>0 THEN 3840
3910      END IF
3920      GCLEAR
3930      SUBEND
3940      !
3950      !
3960      !
3970      ! Function determines graphics axis scaling
3980      DEF FNScale(Ymax)
3990      IF Ymax>100 THEN
4000          Tick=20.
4010      ELSE
4020          IF Ymax<=100 AND Ymax>20 THEN
4030              Tick=10.
4040          ELSE
4050              IF Ymax<=10 AND Ymax>4 THEN
4060                  Tick=2.
4070              ELSE
4080                  Tick=.5
4090              END IF
4100          END IF

```

```

4110 END IF
4120 RETURN Tick
4130 FNEND
4140 !
4150 !
4160 !
4170 ! Function determines max extent of data for X-axis limit
4180 DEF FNData_limit(INTEGER Data_1(*),Row_max,Col_max)
4190 Col=1
4200 REPEAT
4210   Sum=0.
4220   FOR I=1 TO Row_max
4230     Sum=Sum+Data_1(I,Col)
4240   NEXT I
4250   Col=Col+1
4260 UNTIL Sum=0 OR Col=Col_max-1
4270 RETURN Col+2
4280 FNEND
4290 !
4300 !
4310 !
4320 ! Function determines max value in integer array
4330 DEF FNMax_int(INTEGER Data_1(*),Row_max,Col_max)
4340 R_max=1
4350 C_max=1
4360 FOR I=1 TO Row_max
4370   FOR J=1 TO Col_max
4380     IF Data_1(I,J)>Data_1(R_max,C_max) THEN
4390       R_max=I
4400       C_max=J
4410     END IF
4420   NEXT J
4430 NEXT I
4440 Max=Data_1(R_max,C_max)
4450 RETURN Max
4460 FNEND
4470 !
4480 !
4490 !
4500 ! Function determines maximum value in real array
4510 DEF FNMax_real(Data_1(*),INTEGER Row_max,Col_max)
4520 R_max=1
4530 C_max=1
4540 FOR I=1 TO Row_max
4550   FOR J=1 TO Col_max
4560     IF Data_1(I,J)>Data_1(R_max,C_max) THEN
4570       R_max=I
4580       C_max=J
4590     END IF
4600   NEXT J
4610 NEXT I
4620 Max=Data_1(R_max,C_max)
4630 RETURN Max
4640 FNEND
4650 !
4660 !
4670 !
4680 ! Function determines max extent of data for X-axis limit
4690 DEF FNData_limitr(Data_1(*),Row,Col_max)
4700 Col=1

```

```
4710 IF Data_1(Row,Col)<=0 OR Col=Col_max THEN
4720   Limit=Col+2
4730   RETURN Limit
4740 END IF
4750 Col=Col+1
4760 GOTO 4710
4770 FNEND
```

APPENDIX M

This Appendix contains the calibration data for the anemometer probe. The calibration was conducted in a small wind tunnel using a pitot tube connected to a micromanometer capable of measuring pressures to within 0.001 ins. of water.

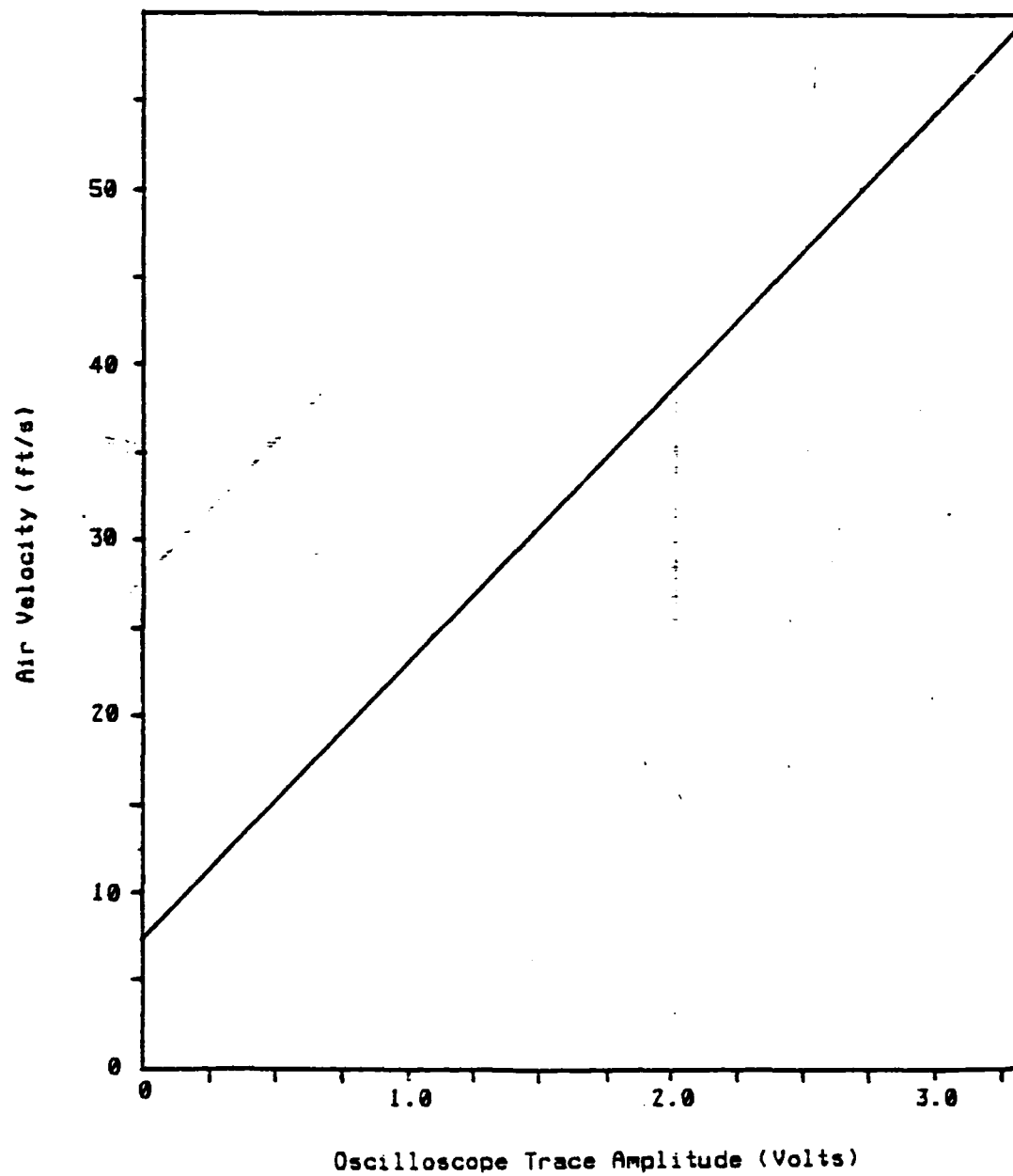


Fig. M-1 Calibration of Anemometer Probe.
Oscilloscope Voltage vs Air Velocity.

END

FILMED

11-85

DTIC